Università degli Studi di Pisa

Dipartimento di Scienze della Terra

Scuola di Dottorato di Ricerca in Scienze di Base Galileo Galilei
Programma di Scienze della Terra
XXIII Ciclo 2008 – 2010

Dissertazione Finale

Anna Coppola

Dendroclimatic analysis in the Adamello-Presanella Group (Central Italian Alps)

Tutore: *prof. Carlo Baroni*
Co-tutore: *dott. Giovanni Leonelli*

Referees: *prof.M. Pelfini*
prof. A. Carton

Direttore della Scuola
prof. Fabrizio Broglia

Presidente del Programma
prof. Roberto Santacroce

Table of contents

Abstract

Inter annual or inter decadal climate reconstructions in the subarctic region and in high-mountain environments suffer from the absence of suitable long instrumental climate records. Annual tree-rings, along with other annually resolved natural archives, are widely used as proxies in high resolution paleoclimatology.

A temperature signal-loss has been reported in tree-rings width and density records from several temperature-limited environments since the mid-20th century, revealing a decreasing attitude of tree-ring parameters in tracking increasing instrumental temperatures.

In this study we carried out a dendroclimatic analysis on a data set of five European larch ring-width chronologies in the Adamello-Presanella Group, in the Italian Central Alps. We intended to evaluate the dendroclimatic potential of the high-elevation conifer vegetation to be used as a climate proxy, assessing the stability over time of the climate/tree-ring growth relationship.

The dendroclimatic analysis was performed by means of correlation function and response function analysis, which allowed identifying climate parameters mainly involved in tree-rings growth. For capturing the dynamical variability of climate signal in the five tree-ring width chronologies, and to verify the stability over time of tree-rings/climate relationship, moving correlation function and moving response function analysis have been used. Moreover, to test the efficiency of the tree-rings dataset for climate reconstruction purposes, we conducted a reconstruction of JJ temperature for the 1596-2004 time period.

The analysis of climate/tree ring growth relationships, producing results that are consistent with the more recent dendroclimatic studies in the Alpine Region, confirmed the presence of a common climatic signal for conifers living at the timberline ecotone.

From the monthly climatic analysis a strong positive influence of early summer (JJ) temperatures on the tree growth emerged, with June mean temperature showing the highest positive correlation. Influence of mean monthly precipitation revealed to be quite irrelevant, although we found that the five chronologies are significantly negatively correlated to June mean precipitation.

European larch confirms in this study to be a highly climate-sensitive species, with summer temperature representing the main limitig factor at the treeline. Nevertheless, a temporal instability in growth/climate response is noticeable, that means a general decreasing trend in tree-rings climate sensitivity.

Non-stationary relationships with climatic parameters may cause some concerns in tree-ring based reconstructions, which usually presume a stable response of tree-rings to climate change. The reconstruction of 1595-2004 JJ mean temperatures we performed is statistically valuable, but shows higher proficiency in describing high frequency than low frequency early mean summer temperature changes.

Overall, a decreasing skill of European larch at the treeline in the Adamello-Presanella Group in tracking increasing instrumental temperatures appears. We also found that extremely warm conditions, such as the heat wave of summer 2003, do not produce a linear response on larch tree-ring growth. Moreover, from the moving correlation analysis emerged a probable effect of a growing season lengthening on larch tree-ring growth.

1 Introduction

Human society and all the biotic and abiotic systems are strictly linked each other and their relationships are influenced by natural environment conditions. Such conditions vary continuously over time and climate plays an evident strategic role in controlling their complex driving mechanisms.

It has been widely demonstrated that in recent times climate is rapidly changing, and that it has been changing in the past (Bradley & Jones, 1992; Bradley et al. 2003; Houghton et al 1990, 2001). For these reasons a more and more large interest has been addressed by the scientific community to investigate past natural climate variability.

Detailed reconstructions of past climate and past climate variability are important tasks both in natural and human sciences. Paleoclimatic researches provide strategic bases of knowledge from which estimate future climate scenarios, their geographical extent and frequency.

Inter annual or inter decadal climate reconstructions in the subarctic region and in high-mountain environments suffer from the lack of long instrumental climate records, often caused by the existence of a few proficient meteorological stations. It appears then clear how valuable could be the presence of natural archives such as annual tree-rings that, along with other annually resolved climate proxies, are often able to provide centennial to millennial climate-sensitive chronologies. Actually climatologists' interest has been recently widely turned to Dendrochronology and to the various possible applications of this Science in past climate reconstructions. The relationship of Dendrochronology with the broader field of Climatology has been then consolidated and tree-ring based reconstructions of climate are at present extensively cited in all the intergovernmental climate reports (IPCC 2001, 2007).

It is widely known that tree-rings have characteristics that make them excellent sources of paleoclimatic information. For their intrinsic structure and natural physiology, they actually operate as proxies of past climate variability: it is possible to date tree-rings at their precise calendar year with a very high degree of confidence, and it has been widely accepted a linear effective correlation between tree rings from extreme environments and climate variables (Fritts, 1976, Fritts et al. 1991; Hughes et al. 1982). Moreover, tree-ring variability often presents a common signal at a large (regional) scale and, year by year, thanks to the progressive increase in the number of accessible chronologies in databases, a larger network of tree-rings data is becoming effectively available worldwide.

Since the earlier Fritts' studies, and especially in recent decades, a rapid improvement of dendroclimatic methodologies and applications has been developed (Hughes et al., 1982; Schweingruber, 1988, 1996; Cook and Kairiukstis, 1990; Dean et al., 1996), leading to a wider use of tree rings in the reconstruction of diverse aspects of past climate at local, regional and global scale (e.g. Briffa et al. 1988a,b, 1992; Mann et al. 1998, 1999; Wilson & Luckman, 2002, 2003).

In the area of global climate change research, mountain and, specifically, alpine environments attract a wide interest. These environments actually include some of the more fragile ecosystems in the Earth, both for the presence of glacial systems suffering for the recent warming trend, and for the presence of numerous vegetal and animal endemism, that are currently changing their distribution and relative abundance (Carrer et al; 1998; Theurilliat & Guisan, 2001; Grace, 2002; Pauli et al. 2003; Grabherr et al 2010).

In recent studies a loss of climate sensitivity in conifer at higher latitudes has been detected (Briffa, et al. 1998a,c; Vaganov et al., 1999; Barber et al. 2000; Jacoby et al. 2000). In the European Alps evidences of a similar decrease in climate/tree-growth correlation was found for several conifer species at the upper treeline (Büntgen et al 2006a; Carrer et al., 1998; Carrer & Urbinati, 2006; Leonelli et al. 2009). This sensitivity change is problematic, but it does not seem to be a general feature over the entire Alpine Arch. Several authors developed dendroclimatic high-elevation proxy-based summer temperature reconstructions with tree-ring chronologies that expressed no sensitivity decrease in the recent period (Wilson & Topham, 2004; Frank & Esper 2005b, c; Büntgen et al. 2006b; Büntgen et al. 2008).

This study has the purpose to carry out a dendroclimatic analysis on a data set of five high-elevation temperature sensitive tree-ring chronologies, coming from five different sites of the Adamello-Presanella Group, in the Italian Central Alps.

The Adamello-Presanella Group is place to one of the largest glacial systems of the entire Alpine Arch and constitutes a well-defined unit within the Italian Central Alps, being separated from the surrounding mountain ranges from broad and deep valleys.

Due to the peculiar geographical characteristics of this Alpine Group, in this study we intend to explore the dendroclimatic potential of the present high elevation conifer tree vegetation to be used as a climate proxy, assessing the stability over time of the climate/tree-ring growth relationship.

2 Study area

The Adamello-Presanella Group lies in the Southern sector of the Central Italian Alps (Rhetian Alps, 45° 54'-46° 19' N; 10° 21'-10° 53' E), covers an area of more than 1100 Km^2 and hosts peaks exceeding 3500 m in elevation. The major peaks of the group are Cima Presanella (3557 m), Monte Adamello (3538 m) and Monte Carè Alto (3463 m) (Fig 2-1).

Other important massifs surround the Group: the Ortles-Cevedale Group to the North of the Val di Sole and Val Camonica, the Brenta dolomitic massif to the East of the Giudicarie Valley, and the Orobie Alps to the west of Val Camonica.

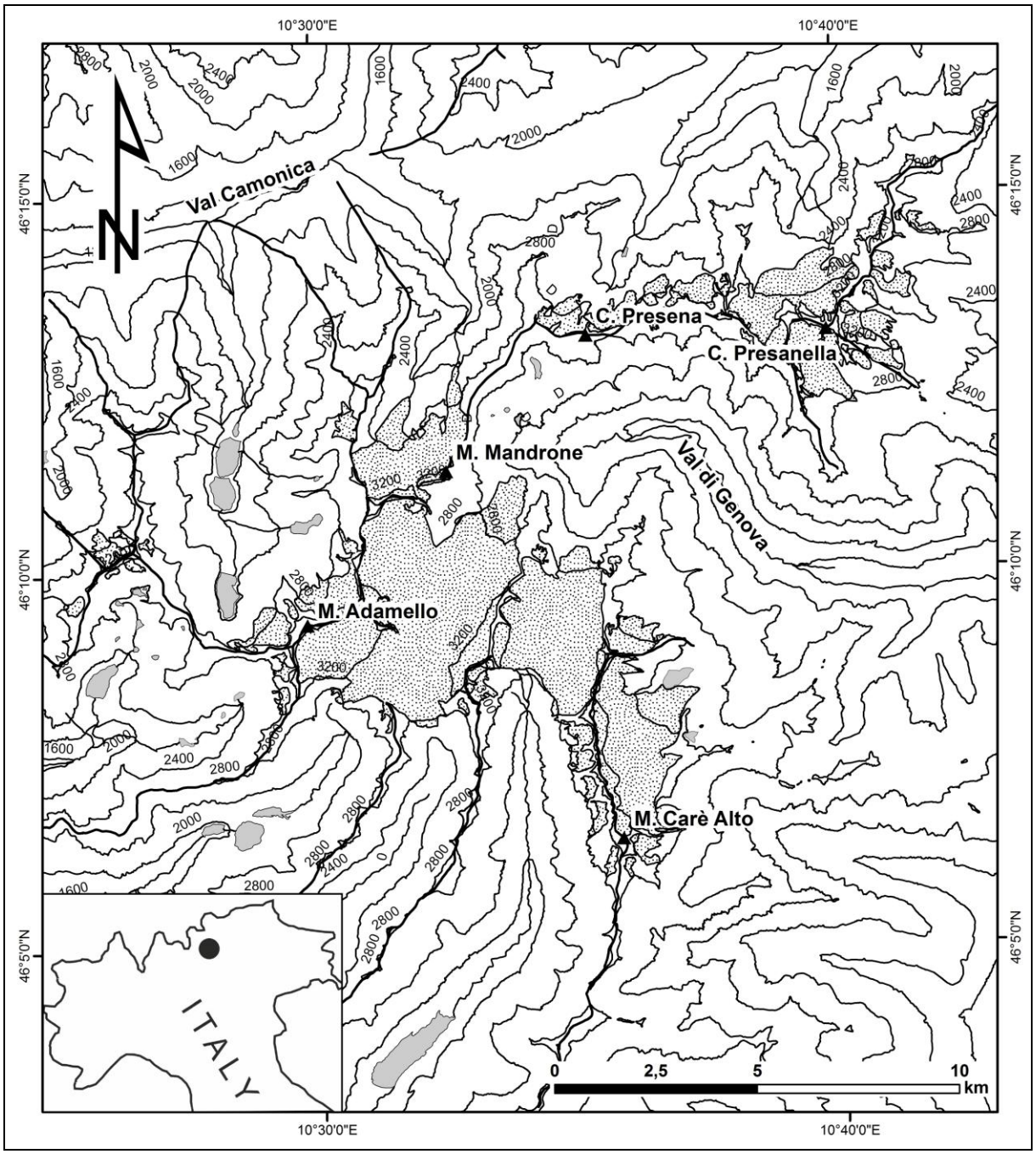

Fig.2-1Sketch map of the study area.

The Adamello-Presanella Group hosts about 100 glacial bodies, mostly lying in the northern and central sectors of the group; the Adamello Glacier, the widest glacier of the entire Italian Alps, develop on the summit area of the massif. The surface of the Adamello Glacier was 18,13 km^2 in 1983 (Baroni & Carton, 1996), reduced to 17,24 km^2 in 2003 (according to the analysis of the ASTER satellite image scanned on the 20th of June 2003; Ranzi et al. 2010). The glacialism is the morphogenetic phenomenon that most of all has contributed to the shaping of the landscape in the area. The numerous valleys descending from the central massif show a typical alpine morphology, with deep glacial troughs characterized by the succession of basins and steps, glacial shoulders, cirques, arêtes and horns (Fig. 2-3). In all the valleys glacial deposits of the major late glacial phases and of the LIA are present. Mass wasting and periglacial landforms are also common geomorphologic features scattered on the entire massif (Baroni et al., 2004).

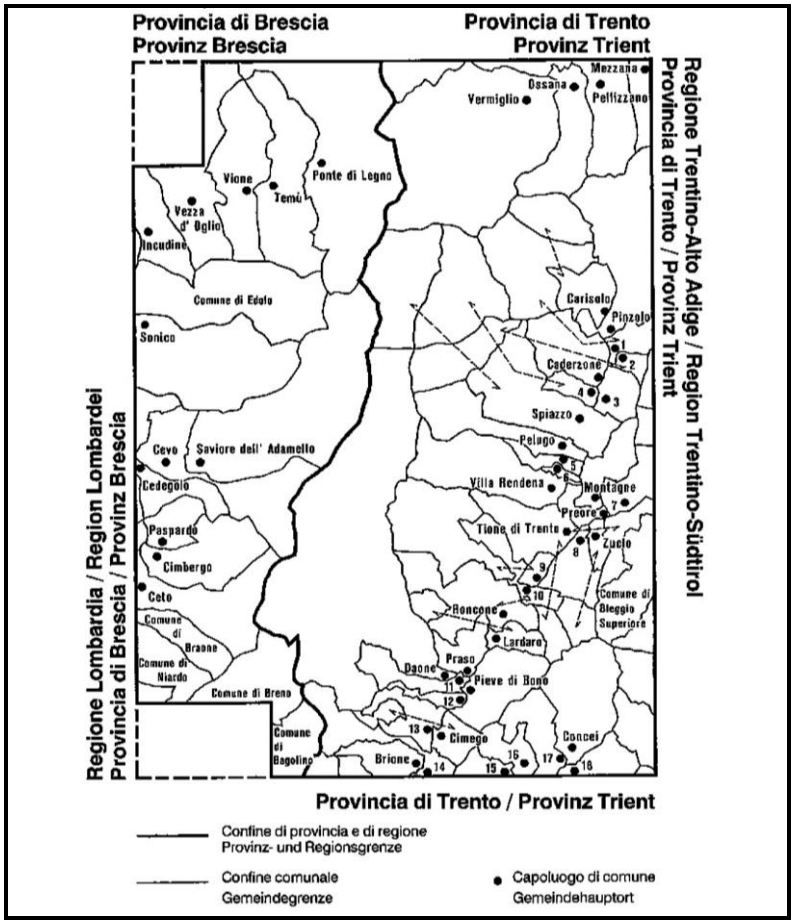

Fig. 2-2. Administrative borders in the study area. Map scale 1:500000. Kompass

The five sampling sites involved in this study are located at the heads of five different glacial valleys surrounding the Central Massif of the Adamello-Presanella Group. The five valleys are included into the territory of two adjacent Natural Parks, the Adamello-Brenta Natural Park and the Adamello Regional Park (Fig 2-2).

The former institution of the Adamello-Brenta Natural Park has been existed from 1967, but only in 1987 the institutive act was translated in laws focussed on the management and protection of the territory. It is the largest protected area of the Trentino region with an areal extension of 620,517 km^2. It includes the Adamello and Brenta mountain groups, divided by Val Rendena and bordered by Val di Non, Val di Sole and Valle delle Giudicarie. The Adamello Regional Park was instituted in 1983; it completely includes the Lombardy side of the Adamello-Presanella Group, in the North-Eastern part of the Brescia province. It extends for 510 Km^2 from the Tonale Pass to the Crocedomini Pass; the eastern side of its territory ends where Lombardy Region borders Trentino Region; westwards, its boundary is formed by the upper left side of the Oglio River, the fifth longest Italian river.

Fig. 2-3A panoramic view of the upper portion of Val di Fumo showing the typical U-shaped profile of the glacial valleys.

Geological lineaments

The Adamello-Presanella Group is mainly composed of volcanic rocks belonging to a large magmatic body, 670 km^2, the largest of Alpine age, commonly referred to as "the Adamello batholith" (Callegari 1983, 1985). The emplacement of the batholith occurred in several stages throughout a succession of diverse intrusive episodes, from Eocene to the upper

Oligocene in the late phase of Alpine orogeny. The different intrusive episodes were evidenced by radiometric analysis performed by means of the Rb/Sr and K/Ar methods on mica and amphiboles of the igneous rocks (Del Moro et al. 1985). Within the batholith it is possible to distinguish four minor plutonic bodies (Bianchi et al. 1970, Dal Piaz, 1973), which, from south to north, are referred to as: Re di Castello, 40-42 Ma; Adamello, 34-36 Ma; Avio, 32 - 34 Ma; Presanella, 29-33Ma, divided into smaller units (Fig.2-4). The batholith intruded into the metamorphic rocks of the pre-Permian crystalline basement and the overlying volcanic and Permian-Mesozoic sedimentary sequences, belonging to the Southern Alps. This sedimentary sequence originally formed the continuous coverage of the batholith, and then was dismantled by erosion.

The batholith is located in a wedge of continental crust in the Southern Alps bounded by the Tonale and the Giudicarie fault lines. These fault systems belong to the tectonic system named lineament "Insubrico" or "Periadriatico" (Oligocene Age) that separates the domain of the Southern Alps from the "Australpino Pennidico" domains to north. In particular, the Tonale line, direct-ESE OSO, is the tectonic boundary between the Southern Alps and the Austroalpine domain. The Giudicarie line directed NNE-SSW is situated within the Southern Alps and separate the Adamello block, and the Brenta Dolomites block (Callegari, 1983).

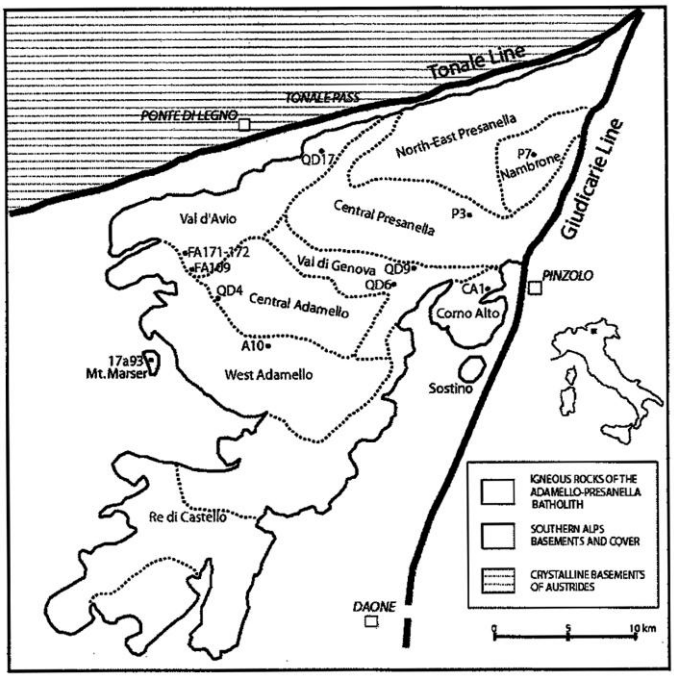

Fig. 2-4 Sketch map of the most important plutons of the Adamello batholiths (Mayer et al. 2003)

The emplacement of the diverse plutons yielded to thermometamorphic phenomena that produced a wide metamorphic contact aureole involving all the rocks around the batholith along a wide band of about 1-2 km (Bianchi & Dal Piaz 1940, 1948).

The most widely outcropping rocks are tonalite, granodiorite and quartz diorite; Tonalite is characterized by a felsic composition, with phaneritic texture. Feldspar is present as plagioclase (typically oligoclase or andesine) with 10% or less alkali feldspar. Quartz is present as more than 20% of the rock. Amphiboles and pyroxenes are common accessory minerals (Bianchi et al., 1970; Callegari & Dal Piaz, 1973).

Vegetation lineaments

The shift in elevation that spans from the about 400 m a.s.l. of valley floors to the 3557 m a.s.l. of Cima Presanella, affects the structure, composition and distribution of all the vegetational ecosystems of the studied valleys. In terms of vegetation, according to the classification published by Pignatti in 1979, these altitudes correspond to the vegetation belts named Sub Atlantic, Boreal, "alpica" and "nivale".

Beech (*Fagus sylvatica* L.), that is considered one of the most representative trees of the sub-atlantic belt is not widespread or nearly absent in the studied valleys, probably because, in most part of the region, spruce (*Picea abies* (L.) Karst.) has been preferred to beech in the past for economic reasons (Dalla Fior, 1963). The absence of beech in the intra-alpine areas is indeed a renowned characteristic of the Alpine landscape (Ozenda, 1985; Theurillat & Guisan, 2001).

The prevailing forest cover is composed by acidophilic association (*Vaccinio-Picetea*, Pignatti, 1995), that means a predominance of spruce, accompanied by a thick undergrowth of blueberry (*Vaccinium myrtillus* L., *Vaccinium vitis-idaea* L.) and saxifrage (*Saxifraga cuneifolia* L.*).* Above 1800 m a.s.l. *Larix decidua* Mill.-*Picea abies* L. open stands (*Vaccinio-Abietenion* Oberd. 1962) dominate the forest cover. Moving upward to higher altitudes, spruce commonly give way to open mixed association of larch and stone pine (*Larici-Pinetum cembrae* Ellenberg 1963) with an undergrowth usually poor of species.

The upper tree-limit is located at about 1900-2000 meters, but isolated trees reach territories up to 2200 meters. The upper tree limit can be framed in a large phytocoenoses that has been studied for the first time by Pallmann and Haftter in 1933, *Rhodoro vaccinietum*. This association is composed by ericaceous short shrubs (Rhododendron, Vaccinium, Loiseleuria, Erica), that can sometimes be associated with tall shrubs (*Pinus mugo* L.*)* or trees (*Picea abies* (L.) Karst., *Pinus cembra* L., *Larix decidua* Mill.*).* Vegetation is poor in species but consists of a large number of phytosociological types (Pignatti et al. 1988).

Above this belt, between the upper mountain forest and the alpine belt, the forest cover is replaced by some bush-like growth-forms, genetically determined to resist to windy and cold climate. This typical formation, often referred to with the German term *Krummholz* or *Krummholz belt* (Braun-Blanquet, 1964), is constituted by typical twisted postured species. Some of the predominant species of this formation in the Alps, and in our study area too, are green alder (*Alnus viridis* DC), juniper (*Juniperus nana* L.*),* rhododendron (*Rhododendron ferrugineum* L.), Salix (*Salix sp.)* (Pignatti, 1995).

At these altitudes it is still possible to find single specimens of larch, pine and spruce "advanced sentinels of the forest that would tend to rise, or survivor rear guard of the forest chased down by man for grazing lands "(transl. by G. Dalla Fior, 1963).

The dwarf shrub community *Loiseleurio Cetrarietum* is one of the dominating vegetation types immediately above the timberline (Grabherr, 1980) and is characterized by a dwarf shrub *Loinseleuria procumbens* (L.) Desv. (also known as *Mountain Azalea*), that is often associated with lichens (genera *Cladonia* and *Cetraria*) (Fig. 2-6).

Fig. 2-5 *Loiseleuria procumbes* (L.) Desv. forms herbaceous pillows on tonalite rock populated by lichens.

Above 2800-2900 meters, vegetation is dominated by alpine flora, pioneer vegetation consisting of lichens and bryophytes, and by various species with special adaptations to overcome the adversity of high mountains climate (Frattini, 1988).

At these altitudes on siliceous screes *Cerastium uniflorum* Desvío., *Soldanella pusilla* Baung., *Doronicum cluded (*All.*)* Tausch., *Geum reptans* L. and the glacier buttercup (*Ranunculus glacialis* L.) are some of the most common species (Figs. 2-6 and 2-7).

Fig. 2-6. *Ranunculus glacialis* L., 2570 m a.s.l.

Fig. 2-7 *Geum reptans* L., 2570 m a.s.l.

We will consider more in detail the taxonomic characteristics and areal distribution of the conifer species involved in this study.

Larix decidua Mill. *characteristics and distribution*

The name of this species, *Larix decidua,* derives from the Celtic "lar"(= fat, for the abundance of resin). It is a tall tree that can reach 50 m. height, with sparse foliage and gray, thick, deeply furrowed bark (Farjon, 1990). Its altitudinal distribution ranges from 400 m a.s.l. in the Southern Alps to 2500 m a.s.l. in the central Alps (Gafta & Pedrotti, 1998).

Larch is the only European deciduous conifer and usually has upright stems and a deep root system. At the treeline European larch often form mixed association with *Pinus cembra* L., while at lower altitudes, with typycally less precipitation rates, they are often associated with *Pinus sylvestris* L.

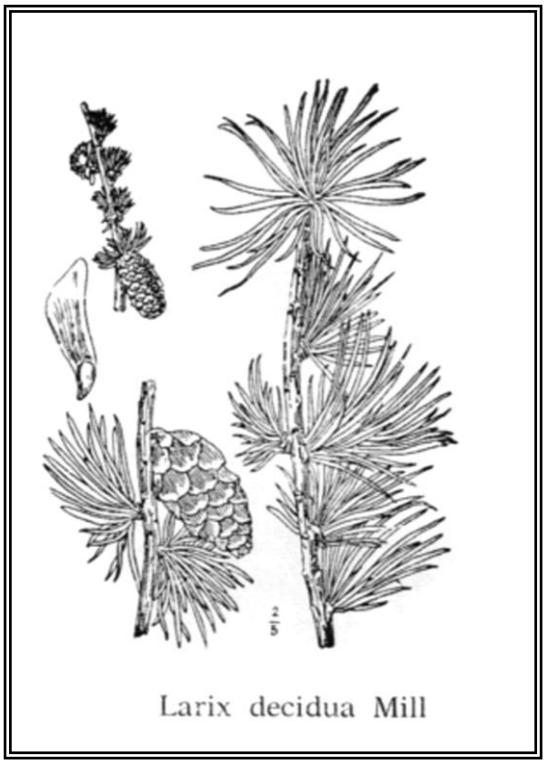

Fig. 2-8 Some anatomical characteristics of *Larix decidua* Mill Mod. from Dalla Fior, 1963.

It is a long-lived species, and in the subalpine belt it can reach an age of up to 1000 years. In cross-section annual rings appear easily discernible in the sequence of earlywood and latewood, as well as the transition between *duramen* to *alburnum* that is generally sharp, resin canals are bordered by 8-12 secretory cells with thin cell walls (Schweingruber, 1993).

Due to its clearly marked duramen, the extreme longevity, the high sensitivity to climate, its presence in high-elevation mountain sites and its behavior as a pioneer species on denuded areas, European larch exhibits a good attitude to dendrochronological investigations (Serre 1978, Tessier 1986, Nola 1994). However, the use of this species in dendroclimatic studies, especially in the western sector of the Alpine Arch, has been questioned due to the action performed by an insect, the larch budmoth (*Zeiraphera diniana* Gen., Lepidoptera, Tortricidae). These defoliator insects, causing the loss of needles, negatively influence tree growth, and consequently number and width of annual rings.

Other natural factors that cause growth disturbances to this species in the alpine environment are those that commonly play an important role in all the high-altitude forests (mainly wind, frost, snow accumulation, processes and geomorphologic phenomena such as landslides and avalanches). Human-induced actions strongly influenced the dynamics of larch

forests because of domestic livestock grazing, forestry and timber use (Ozenda, 1985, Gafta et al. 1998). Assuming that the distribution of larch in the Alpine region had a maximum expansion and abundance in the interglacial periods, at present times this species has considerably narrowed its distribution area. The origin of this regression can be ascribed to two main reasons: climatic variations and anthropogenic pressure.

Climatic changes have had, throughout the Geologic Ages, an important role in the evolution of this species distribution and also at present times, climate continuously exert its strong influence. This influence does not appear immediately obvious, because of the slow evolution and the long response times of wooden cenosis (Fernaroli 1936).

Human pressure has been considerably intensified over time and, in our study area too, this influence is revealed in more active forest exploitation in general, and in particular of larch trees because of their value as lumber. This intense human impact on natural alpine vegetation has persisted until about the mid 19th century, when agricultural abandonment, reflecting a post war trend, took place in Western Europe (MacDonald et al 2000; Tappeiner et al. 2003). The land abandonment consequent to the decline of alpine farming produced the recent (MCPFE, 2007) forest invasion into former summer pastures and grasslands.(Walther et al. 1986; Didier, 2001)

On land denuded of vegetation, larch is one of the few tree species that, thanks to its biological characteristics (frugality, heliophilia and colonization aptitude within the domain of maximum distribution), is easily able to settle and rebuild a unique forest cover in a short time (Fernaroli, 1936). Pure larch wood stands represent the initial phase of a secondary succession tending towards the climax association, representing the initial stage of a consequent ecological succession.

The first vegetational association of the succession is the *Laricetum pratosum* (Rübel). In this first phase, because of the characteristics of heliophilia of this species and of its associations, a large number of species can contribute to the establishment of the herbaceous undergrowth. Actually, the undergrowth in this phase is not composed by species specialized for this association but mostly by ubiquitous species (Fernaroli, 1936, Pignatti, 1995). Afterwards bush-shaped species (nanophanerophyte) begin to settle into the larch wood.

The shrubby undergrowth is initially non-specific, but, in a second time, only a few species expand. At the end of this phase, undergrowth is commonly mostly composed by the following shrub species: Alnus *viridis* L., Rhododendron *ferrugineum* L., *Vaccinium myrtillus* L., Rosa *sp.*, with a few other minor and mostly casual species (Fernaroli 1936, Dalla Fior 1963, Pignatti 1995)

Picea abies (L.) Karst. *characteristics and distribution*

Picea abies (L.) Karst. is an evergreen conifer with a shallow root system, its crown shape may widely vary. This variability is genetically and environmentally determined. Under optimal conditions, spruce can grow higher than 60 m, but in the mountain regions it usually reaches a height of about 20 m up to 30 m. In extreme conditions, like on windy hills, slopes and in avalanche channels or landslide sites with very thin soils, shapes and sizes can differ greatly from the norm (Dalla Fior, 1963; Farjon, 1990).

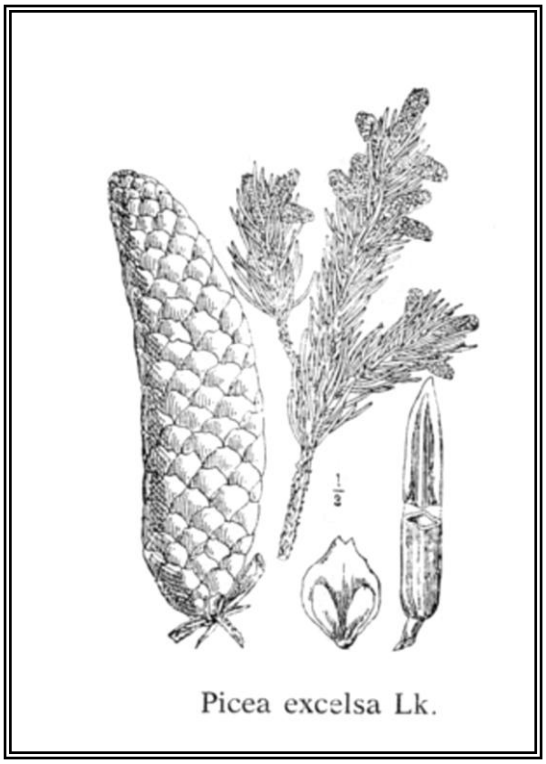

Fig. 2-9. Some anatomical characteristics of *Picea abies* (L.) Karst., here reported the old scientific denomination *Picea excelsa* L. mod from Dalla Fior , 1963.

In mountain regions and especially in the Northern hemisphere this species forms a clearly marked forest belt. At lower altitudes spruce is associated with beech, and in areas with low rainfall rates with *Pinus sylvestris* L. and *Pinus mugo* Turra. Thanks to the excellent technological properties of its wood, it has found wide applications in the industry, and it has been planted in many areas outside its natural range.

In cross section there is not a visible distinction between hardwood and sapwood and wood appears yellow-straw coloured with silk reflexes. The growth rings are easily discernible, with frequent resin ducts, and the latewood less intensely coloured than in larch (Schweingruber, 1993). The natural range of this species occupies most of the territory of the Trentino-Alto Adige region, except in the most oceanic area situated at its southern limit, however, because of the large extent of areas affected by forestry operations, it is difficult to distinguish natural and primitive stations (Fig.2-10). In particular, the Val d'Amola, Val di Ledro, Valle del Sarca, Val d'Adige, Val Ronchi and Vallarsa remain outside its natural range, which is almost complementary to the oak (*Quercus petraea* (Mattuschka) Liebl.) natural range (Gafta & Pedrotti, 1998).

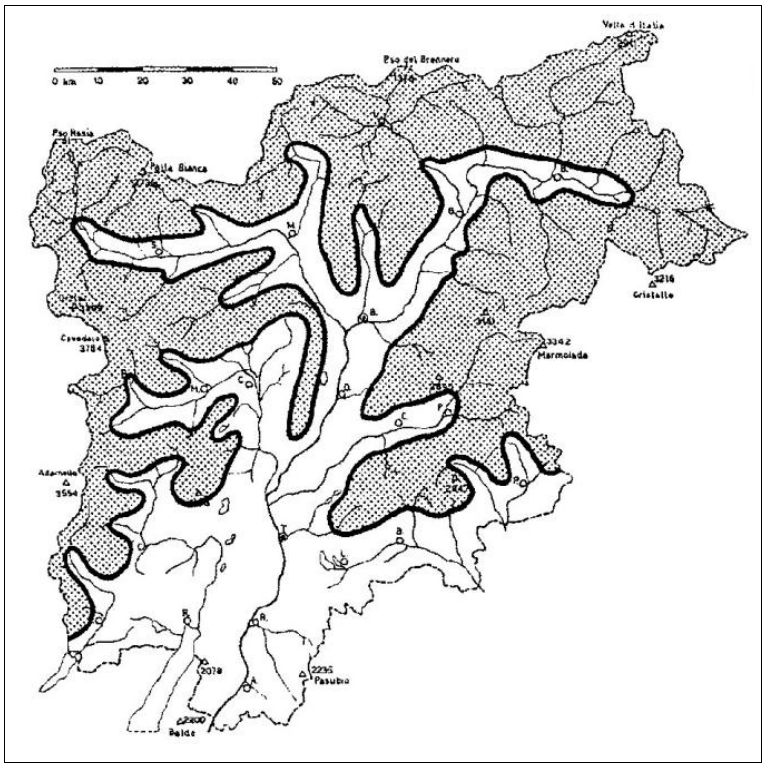

Fig. 2-10 Natural distribution of *Picea abies* (L.) Karst. in the Trentino-Alto Adige region (southern boundary) as reported in Gafta & Pedrotti., 1998

Fig. 2-11 *Larix decidua* Mill. (on the left side) and *Picea abies* (L) Karst. (on the right).

3 Materials and methods

Climate data

High-mountain areas are commonly poor in meteorological stations providing long and uninterrupted series of climate variables. Also in our study area there are not suitable long meteorological series coming from nearby high-elevation meteorological stations.

The only two meteorological stations located at an altitude > 1400 m a.s.l., that have recorded the longest climate data series in the area, are situated on the mountain pass named "Passo del Tonale" (1880 m a.s.l.). These two stations have registered data from 1987 to present, but the climatic series derived from these records are full of gaps with whole years missing (data from Meteotrentino http://www.meteotrentino.it/) (Tab. 3-1).

All the other available and examined stations in the area provide shorter and non continuous series. For instance, the "Cima Presena" Station, that is the station located at the highest elevation, 2730 m a.s.l., recorded data only for a very short time period, from January 1995 to December 2005. Furthermore, climate series coming from "Cima Presena" station present many gaps each year, except for 1999, the only one year with a complete and uninterrupted succession of data (data from Meteotrentino and from IASMA "Istituto Agrario San Michele all'Adige" http://www.meteotrentino.it/) (Tab.3-1).

Because of the poor quality and the short lengths of these instrumental climate data, we decided to refer in this study to the gridded data set provided by the HISTALP project (Auer et al 2007, Böhm et al. 2001, Böhm et al. 2009, http://www.zamg.ac.at/histalp). The HISTALP database consists of monthly homogenised records of temperature, pressure, precipitation, sunshine and cloudiness for the 'Greater Alpine Region' (GAR, 4–19 °E, 43–49 °N, 0–3500m a.s.l.). In this dataset the longest temperature and air pressure series extend back to 1760, precipitation to 1800, cloudiness to the 1840s and sunshine to the 1880s.

We used the gridded dataset of temperature and precipitation anomalies referred to the grid point 10°N, 46°E.

Monthly gridded temperature data span from 1760 to 2007 (247 years) and monthly gridded precipitation data from 1799 to 2003 (204 years). Temperature series are differentiated in temperatures recorded from high (>1400 m a.s.l.) and low (<1400m a.s.l.) altitude stations (Tab.3-2).

Temperature and precipitation anomalies refer to the Twentieth Century mean (1901-2000) and were derived only for homogenised data, both for the monthly temperature series (2004-11 release); and the monthly precipitation series (2004-2008 release) (Auer et al 2007).

	Passo Tonale 1	Passo Tonale 2	Val di Genova	Cima Presena	Lago d'Arno	Lago d'Avio	Lago Salarno	Pantano d'Avio	Malga Bissina	Malga Boazzo	Ponte Murandin	Rif. Agostini Pradalago	Torrente Arnò	Campo Carlo Magno
1978														
1979														
1980														
1981														
1982														
1983														
1984														
1985														
1986														
1987														
1988														
1989														
1990														
1991														
1992														
1993														
1994														
1995														
1996														
1997														
1998														
1999														
2000														
2001														
2002														
2003														
2004														
2005														
2006														
2007														
2008														

Tab. 3-1 Extension of historical temperature data series derived from high-elevation meteorological stations in the study area. Years with incomplete series are marked with a diagonal line.

Temperature		**Precipitation**
High >1400m a.s.l.	Low <1400m a.s.l.	1799-2003
1818-2007	1760-2007	

Tab. 3-2 Extension of temperature and precipitation data for the grid point 10° N, 46° E (HISTALP Dataset, Auer et al 2007)

Tree-ring data

Field collection and sampling strategy

This study is based on tree-ring cores and cross-sections collected during three different summer field trips carried on in 2005, 2007 and 2008.

The five sampling sites are located at the heads of five different glacial valleys surrounding the Central Massif of the Adamello-Presanella Group and are situated at the northern, western and southern sides of the Adamello-Presanella Group (Fig. 3-1, Tab. 3-3). The Italian names of these five valleys (used to indicate the five sampling sites in the following text) are Val Presanella, Val Presena, Val d'Avio, Val Malga and Val di Fumo.

In detail, Val Presanella, Val d'Avio and Val Presena are S-N oriented and are located on the northern side of the Massif, Val Malga has an EW orientation on the western side of the massif and Val di Fumo is NS oriented and located in southern side of the massif.

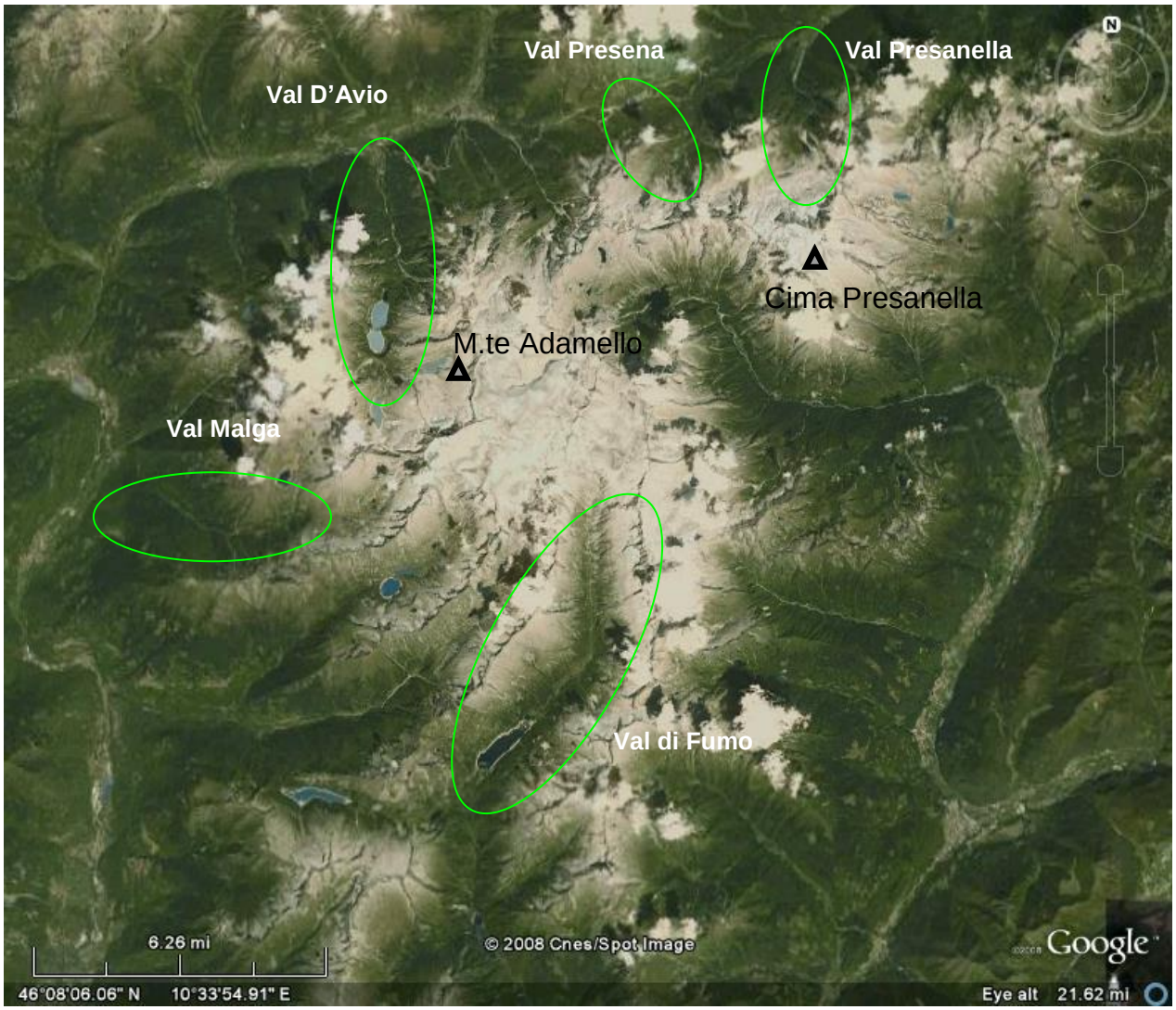

Fig. 3-1 spatial distribution of the five valleys where are located the five sampling sites.

The five sampling sites are mostly geobotanically homogeneous, with some minor differences, and the sampled trees are located close to the upper treeline, at an elevation range of 1980-2130 m a.s.l.

The alpine treeline is an extreme environment for plant life and has been demonstrated that plant growth at high-elevation sites is directly or indirectly limited by temperatures (Körner & Larcher 1988, Körner, 1998). Preferring for our purposes climatically-stressed sites, we chose these high-elevation sites for minimizing the non-climatic influences on tree growth, such as stand competition or insect-induced defoliation.

One of the main problems we met during the sampling campaigns was to find very old trees. The current vegetational composition at the tree line in our study area is affected by the natural and human-induced disturbances that have characterized these ecotones over the centuries (Anfodillo & Urbinati, 2001). Within the most recurrent disturbances in the study valleys, we especially found grazing and wood exploitation for charcoal and lumber production. Moreover, at the beginning of the last century, on the Adamello-Presanella area, the human impact on treeline was also determined by the fighting of World War I between the Italian and Austrian armies (Ronchi, Q., 1927; Viazzi, C. & Cavacicchi, 1996; Viazzi, C., 1981). More recently, the building of dams for hydroelectric power production (in Val d'Avio and in Val di Fumo) and the development of some ski tracks (in Val Presena) amplified human disturbance on the high-altitude natural environment.

At the present time the treeline population in the five sampling sites mainly consists of larch (*Larix decidua* Mill.) in pure or mixed formations with stone pine (*Pinus cembra* L.) in a variable percentage ("larici-cembretum" association, Pignatti et al. 1988, Pignatti, 1995). In Val Presanella and in Val Malga larch is associated to a limited number of Norway spruce (*Picea abies* (L.) Karst) (Figs 3-2 and 3-3).

Due to the purpose of this study, sampling has been performed in order to remove as much as possible non-climatic factors on tree growth (Cook & Kairiukstis, 1990).

In order to minimize possible effects of stand competition, only dominant and sparse trees with undisturbed canopies have been sampled. A special attention was given in choosing the correct trees, avoiding those plants showing external evidences of non-climatic growth disturbances, such as lightning scars, broken branches or crowns, buried stem bases.

Fig. 3-2 A view of the upper treeline in Val Presanella. The alpine hut (Rifugio Denza) is located at 2300m a.s.l.

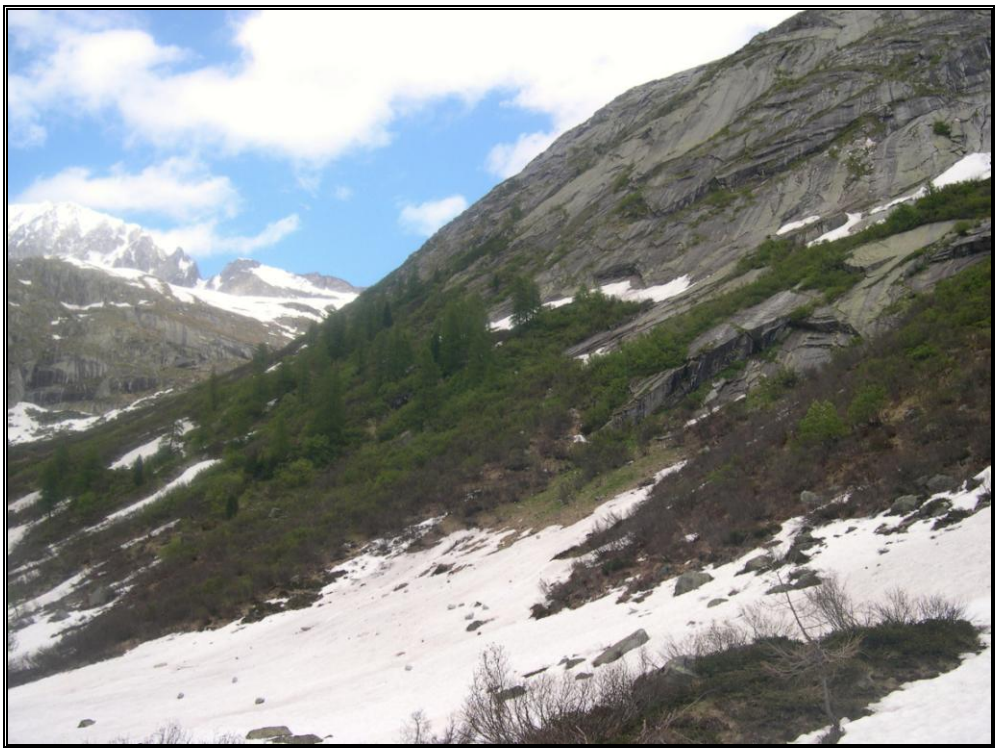

Fig. 3-3 A view of the upper tree-line in Val di Fumo. The upper sparse trees are located at about 2100 m a.s.l.

Site	Species	Mean altitude (m)	Latitude N	Longitude E
Avio	LaDe, PiCe	2150	46°10’	10°28’
Fumo	LaDe	1990	46°05’	10°34’
Presanella	LaDe, PcAb	1910	46°25’	10°65’
Presena	LaDe	2160	46°23’	10°60’
Malga	LaDe, PcAb	1850	46°07’	10°25’

Tab. 3-3 Site characteristics

At least two cores from opposite sides of each living tree were taken, following the standard sampling procedures (Stokes & Smiley, 1968). Cores were extracted using an increment borer at breast height (~ 1,30 m from the ground level), coring horizontally and at 90° with respect to the slope direction, in order to avoid possible compression wood (Fig 3-4).

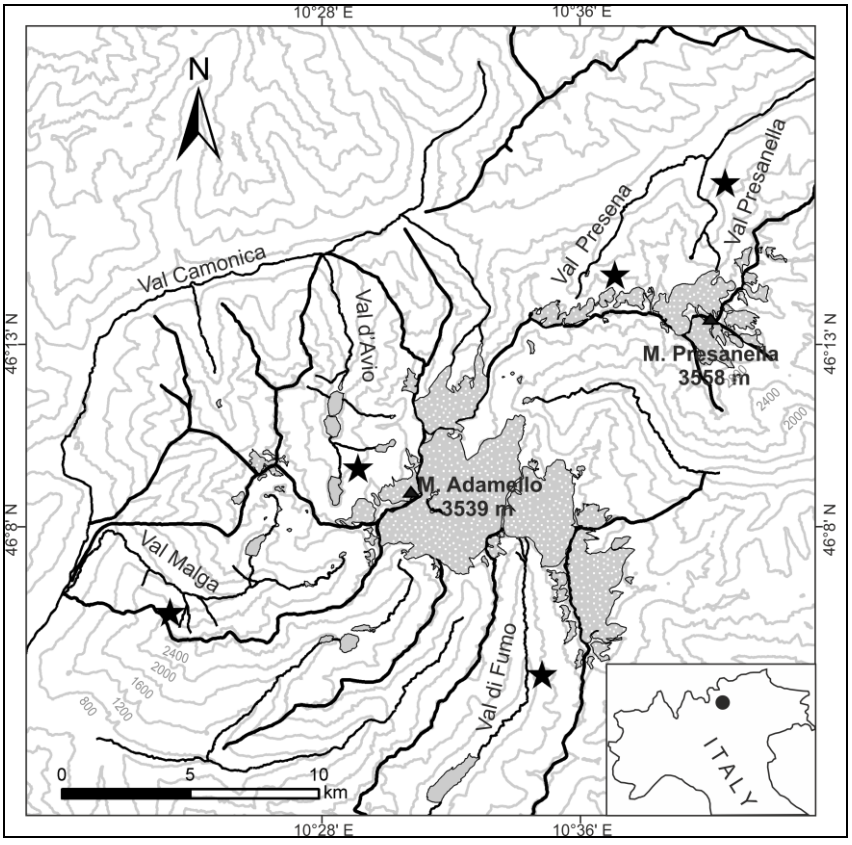

Fig. 3-4 Sketch map of the study area. Stars indicate sampling sites.

Fig. 3-5 An increment borer in a larch stem

All the cross-sections were taken by means of a chain saw. They all come from only one of the five sampling site (Val Presanella). The most part of the cross-sections have been sawn from uprooted trees found along three different snow-avalanche channels (Fig. 3-5).

Fig. 3-6 Two of the twenty-six cross-sections sawn by uprooted trees analysed and dated in this study, here shown as they were before of the sanding procedures.

Twelve cross-sections have been sawn from beams of nine isolated barns (locally named “maso” or “malga”), little rural alpine houses mainly used as stalls and haylofts. They are all located in Val Vermigliana, (Fig.3-6, 3-7 and 3-8) of which Val Presanella is a lateral valley. We want to explore the possibility to use these samples in order to improve the sample replication in the earlier part of the Presanella mean site chronologies. The use of historical materials in Dendroclimatic studies is usually avoided because of the uncertain provenance of

timbers utilized in historical buildings. Nevertheless, as reported in Wilson et al (2004) "in situations when it can be shown that historical timbers are locally derived from climate-sensitive stands, these records may have a considerable potential use in developing and extending dendroclimatic reconstructions". In our case some oral evidences testify that the provenance of timber used in the barns' construction is likely to be close to our sampling area.

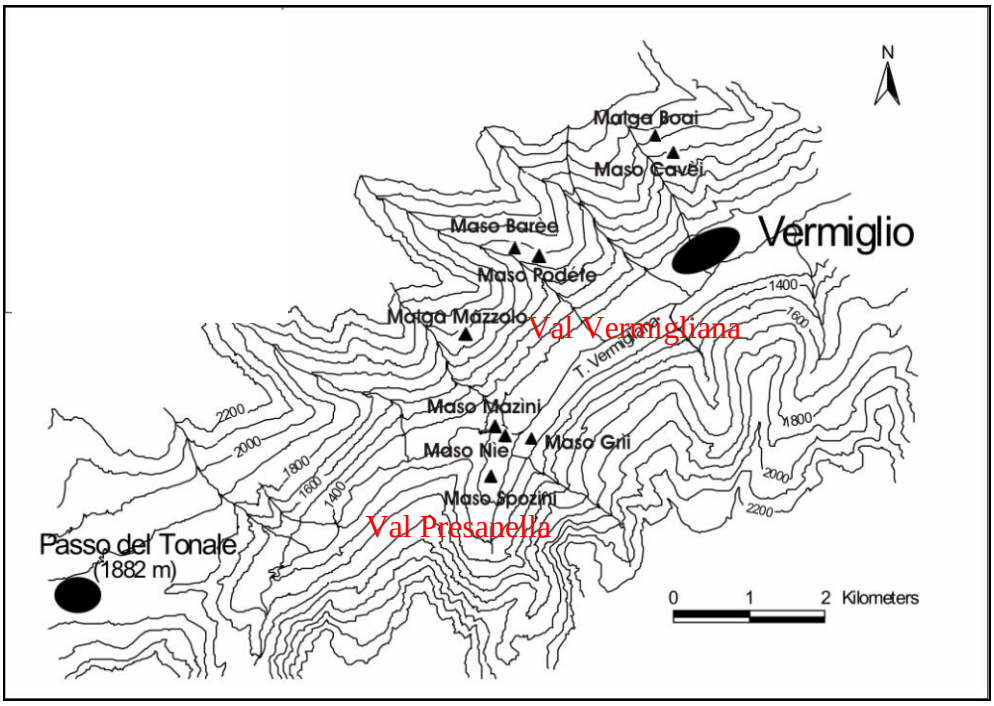

Fig. 3-7 Location of the sampled farmsteads

Fig. 3-8 "Maso Cavel", one of the sampled rural buildings.

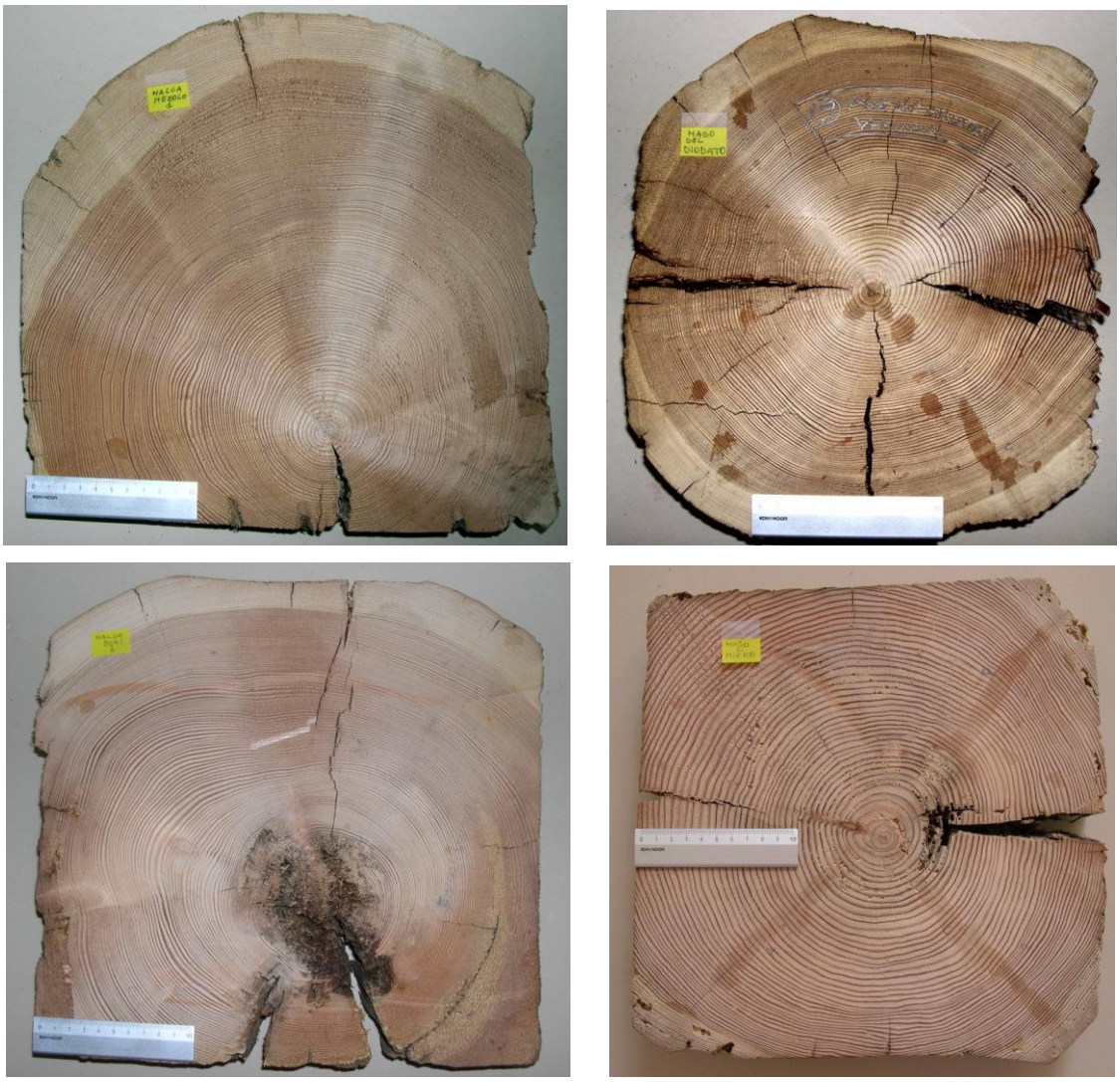

Fig. 3-9 Four of the twelve cross-section coming from farmstead's beams analysed and dated in this study.

The geographical position of each tree has been marked using a GPS (Global Position System) device and reported in a GIS database (Figs 3-10 to 3-14).

The tree-ring collection is constituted of 389 samples:

- 350 cores from 169 trees (Larix *decidua* Mill., Picea *abies* (L.) Karst and Pinus *cembra* L.)
- 38 cross-sections (Larix *decidua* Mill., 12 disks from historical material and 26 disks from uprooted trees).

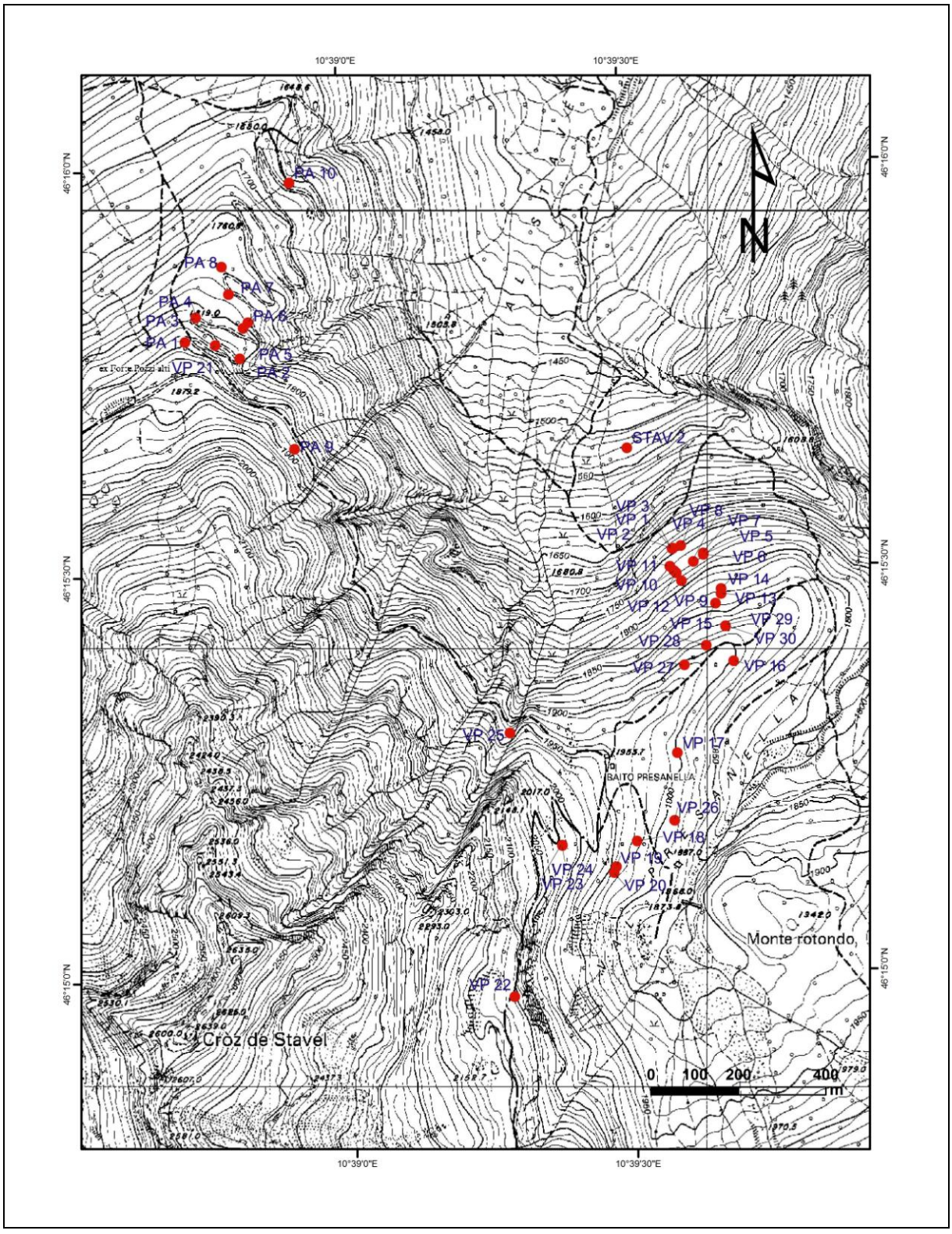

Fig. 3-10 Val Presanella. Location of the sampled trees.

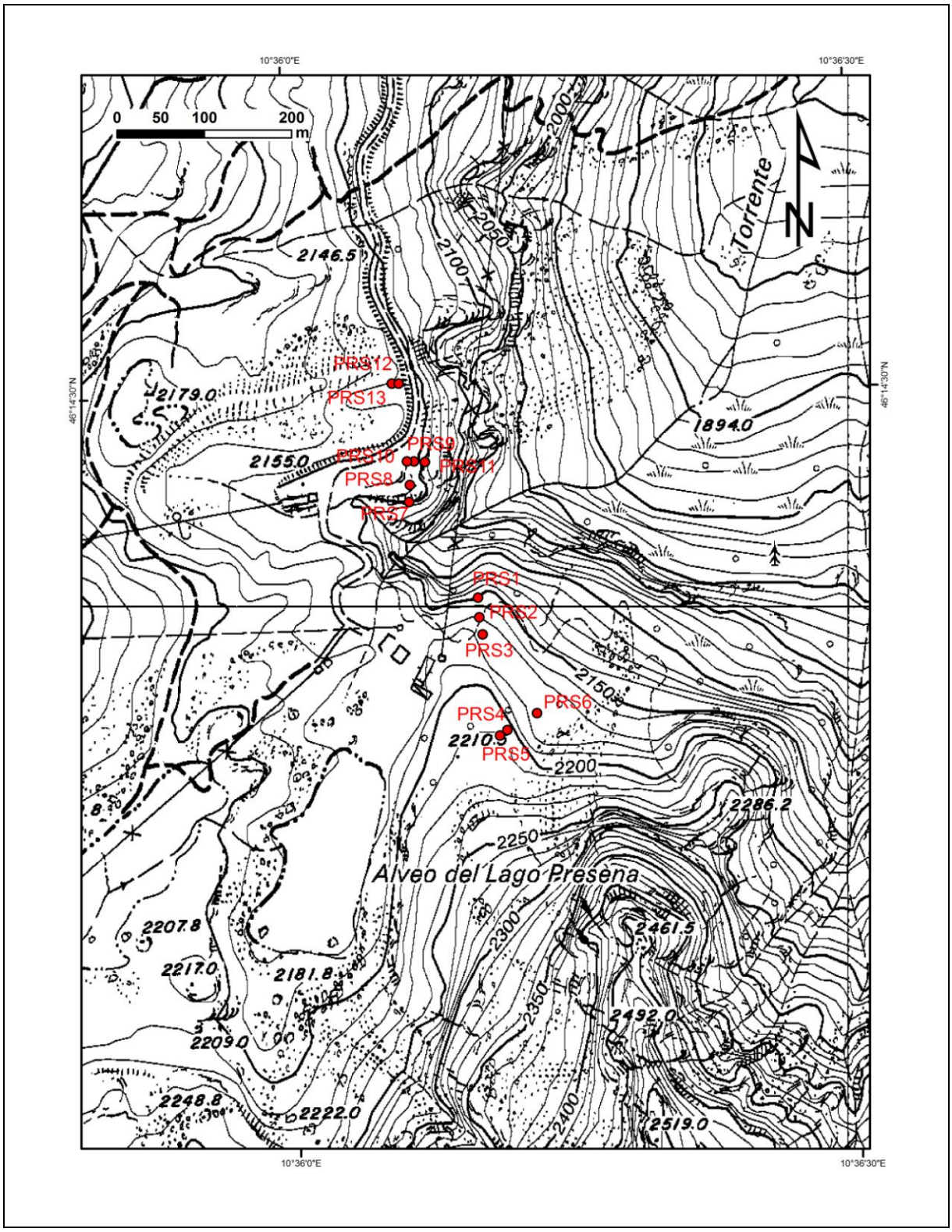

Fig. 3-11 Val Presena. Location of the sampled trees.

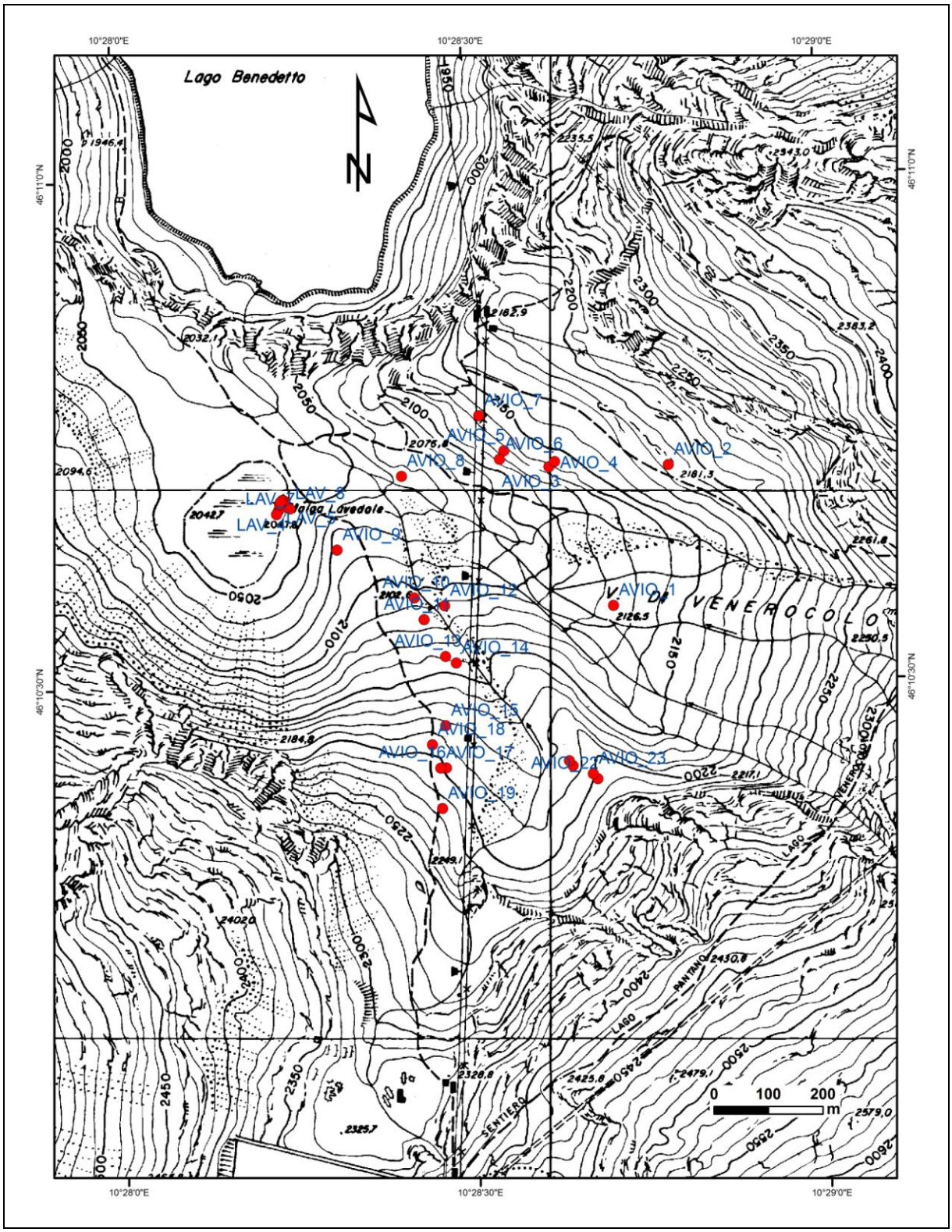

Fig. 3-12 Val d'Avio. Location of the sampled trees.

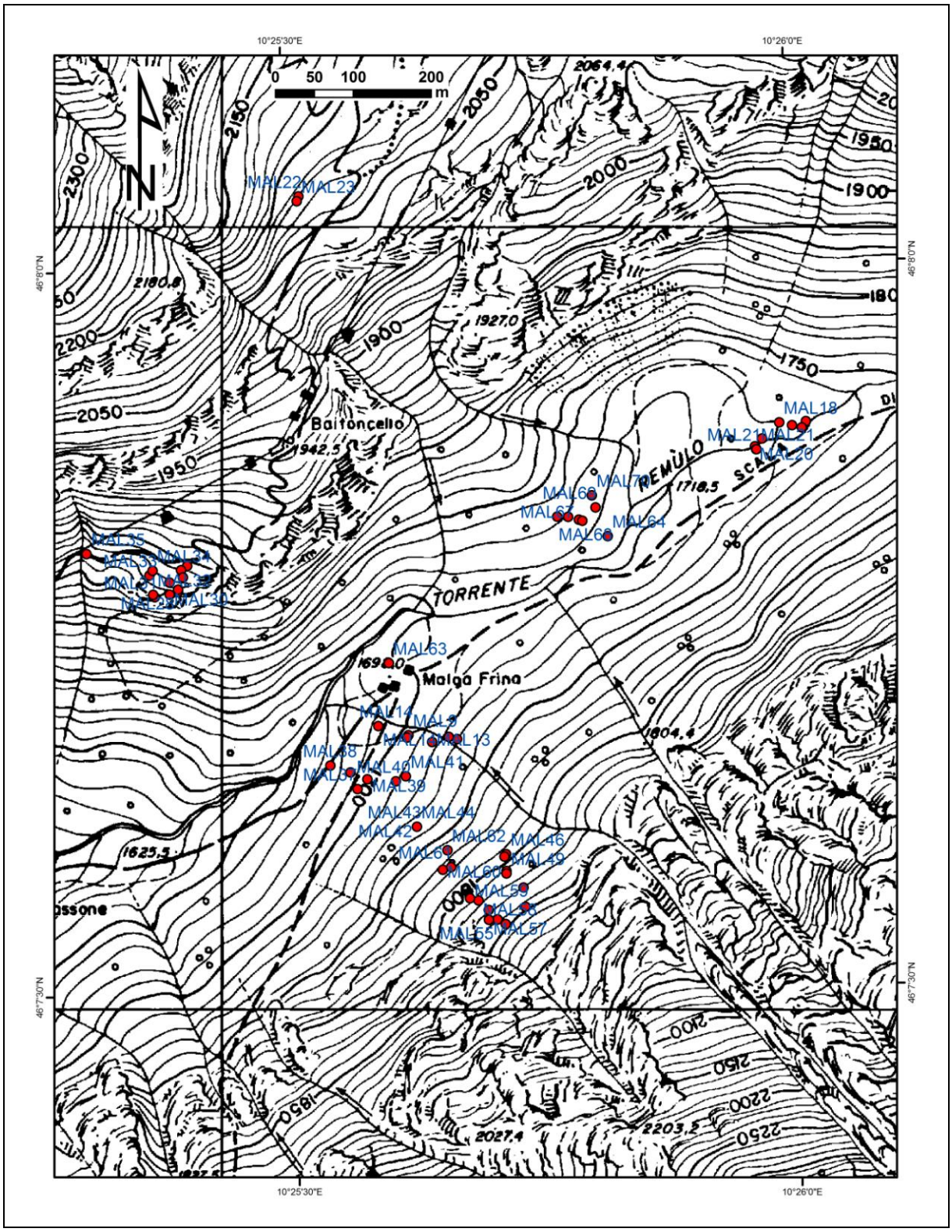

Fig. 3-13 Val Malga. Location of the sampled trees.

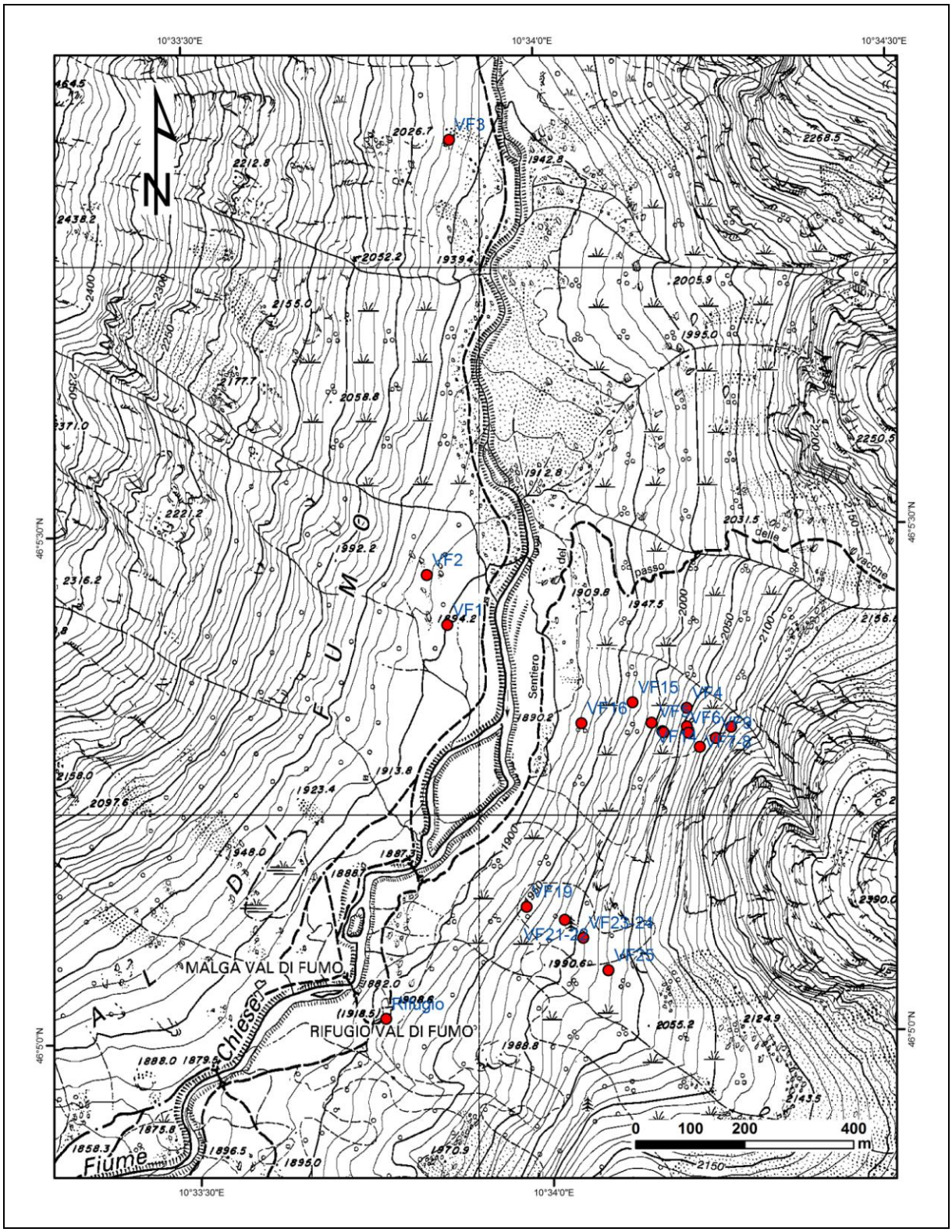

Fig. 3-14 Val di Fumo. Location of the sampled trees.

Samples preparation and tree-ring measurement

In the laboratory each core has been dried and mounted with vertical fibers on wooden supports. A transversal surface of the cores was then cut with a sharp cutter blade in order to make tree rings clearly visible (Ferguson, 1970; Pilcher, 1990).

The full disks surfaces were sanded with an electric belt sander on which were mounted sand papers of various grain sizes, from coarser to finer. The core surfaces were instead sanded by hand with simple sand paper of progressively finer grain sizes.

Tree-ring widths were measured with a precision of 0.01 mm using a LINTAB increment measuring table (RinnTec) associated with the program TSAP (Time Series Analysis Program, Rinn, 1996) (Fig. 3-15).

For each cross-section from three to four radii were measured, preferring undamaged directions and excluding those parts showing anatomical irregularities such as compression wood, suppressions, wound tissue, scars or knots.

When needed, the contrast between wide earlywood cells and small latewood cells was enhanced by rubbing chalk or water on the wood surface. Broken cores or cores with evident signs of mechanical disturbances were discarded.

Fig. 3-15 cores mounted on wooden supports ready for measuring and Lintab increment measuring table

Larch Bud Moth attacks correction

In the European Alps insect outbreaks are not so decisive in defining forest dynamics as in other forest ecosystems (e.g. the North-American conifer forests, Swetnam et al 1995, Swetnam & Lynch,1993). Nevertheless European larch trees are periodically severely affected by the attacks of a Lepidoptera, the gray larch bud moth (*Zeiraphera diniana*

Guénée, Lepidoptera: Tortricidae). *Zeiraphera diniana* (here referred to as LBM) is a foliage-feeding Lepidoptera that is widespread throughout the European Alps (Baltensweiler, 1985, Rolland et al 2001, Weber, 1997). The pullulations of this insect occur cyclically approximately every 8–9 years in the subalpine pure or mixed larch forests (Baltensweiler et al 1977; Baltensweiler and Fischlin 1988; Bjørnstad et al. 2002).

The effect of these attacks is the partial or complete defoliation of the trees, causing the production of an exceptionally narrow annual ring that sometimes is difficult to distinguish (Pignatelli & Bleuler 1988; Schweingruber, 1996).

For the current study, LBM effects are regarded to as noise and must be corrected in order to minimize the effects of non climatic (negative) outliers on the resulting mean site larch chronologies.

To detect years with LBM induced defoliation usually a comparison between host and non-host species is performed (Swetnam et al. 1985; Swetnam & Lynch 1993). Unfortunately, we had not non-host species to compare with larch in the whole sampling sites, because sampled spruces and stone pines, when present, were always younger than larch trees.

We identified years of LBM attacks with the simplest method, based on the accurate observation of the anatomical characteristics of the tree rings. Tree-ring features, as total ring-width or colour and thickness of latewood, are in fact important indicators of possible insect attacks and consequent tree defoliation (Filion et al. 1986; Pignatelli & Bleuler, 1988; Schweingruber et al. 1996; Liang et al. 1997). In our larch samples the typical growth pattern produced by LBM attacks was almost always clearly visible (Fig. 3-16).

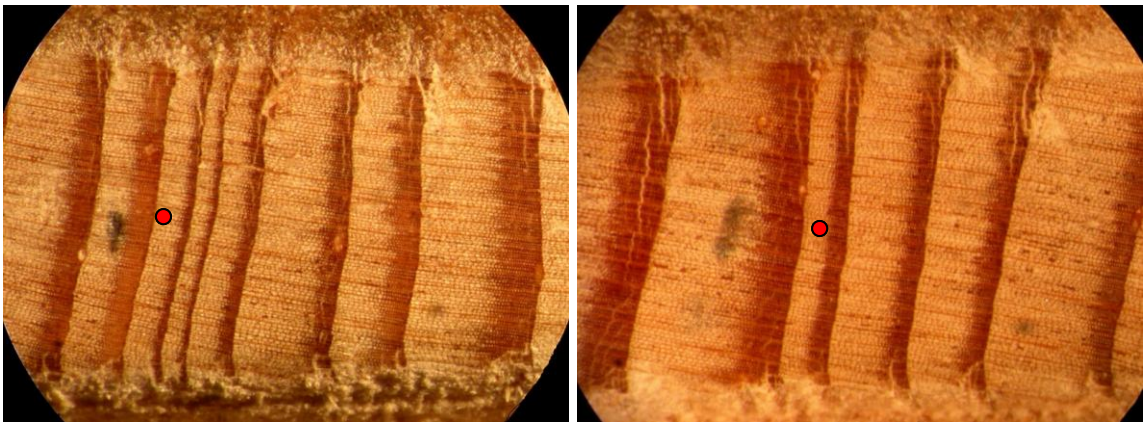

Fig. 3-16 tree-ring growth patterns produced by LBM attacks on two samples coming from the Val di Fumo site, the red dots indicate the year of defoliation.

To correct the low width values of the years of defoliation, we have followed Büntgen et al. 2006 (b). In detail, the affected rings width values were removed and substituted with a statistical estimate derived from the mean of the remaining unaffected rings.

Chronology development and statistics

The measured growth series coming from different radii of the same cross-section or from different cores of the same tree were visually and statistically cross-dated (Fritts, 1976, Fritts & Swetnam 1986) using the program TSAPwin. Once checked the correct dating and removed the possible measuring or dating errors, a mean growth series was calculated for each tree (Cook and Kairiukstis, 1990).

Two different statistical parameters were used to check out the correct cross-dating between the tree-ring series: *t*-values relating to correlation coefficient (Baillie & Pilcher, 1973) and the Gleichläufigkeit (GLK; year-to-year agreement between the interval trends of two time series; Schweingruber, 1988) computed by the TSAPwin software.

Only those time series longer than 100 year were used in the successive analysis and only the time series with a satisfying mean site correlation (GLK > 0,60) and t-values ($t > 2,5$) were retained for computing mean site chronologies.

To absolute dating the cross-sections coming from uprooted trees and historical material, the floating undated mean growth series were cross-dated against the dated tree-ring series of the living trees of the Val Presanella site (remember that all the dead material comes from that site).

The correct dating of the historical material has been further checked, cross-dating the floating mean series against four of the existing larch chronologies for the Alpine area, used as independent references: Eastern Alps (Italy, Bebber, 1990); Fodara Vedla (Italy, Hüsken, Schirmer, 1993), Obergurgl (Austria, Giertz, ITRDB, International Tree-Ring Data Base); Ötztal (Austria, Siebenlist-Kerner, 1984). For these samples we have used a more restrictive dating criterion and considered as parameter of a reliable dating quality a *t*-values higher than 4.5 (Baillie, 1982).

The correct cross-dating between measured tree-ring series was further verified using the program COFECHA (Holmes, 1983; Grissino-Mayer 2001), which identifies segments within each ring-width series that may contain erroneous cross-dating or measurement errors.

Because of the greater number of available larch samples, and due to the better intercorrelation between their ring-width series, all the five mean site chronologies are made up only of ring-width series coming from larch samples.

Mean site chronologies were calculated using the program ARSTANwin (Cook and Holmes 1984; Cook 1985). This program operates a standardization of the time series prior to average them in a mean chronology, allowing also the selection of detrending methods and autoregressive modeling.

Standardization of raw tree-ring series is a basic operation in treating tree-ring data (Fritts, 1976). It allows to correct tree-ring width for their systematic non–climatic change due to tree age (the so called *age trend*) and to average the standardized obtained values in a mean function. Moreover it permits to adjust the series for different growth rates that are caused by individual differences in the overall rate of growth (Cook & Kairiukstis, 1990).

This process transforms ring-width values in stationary dimensionless indices that have a defined mean of 1.0 and a homogeneous variance. Dimensionless indices are computed by dividing the observed ring-width value by the one predicted by a function. The standardized indices of individual trees are averaged to compute the mean site chronology.

There are numerous ways to standardize tree-ring widths, more or less conservative, and the choice depends on the finalities of the different tree.-ring analysis that may be performed. Due to the purposes of this study, with the aim to enhance the climatic signal into the five tree-ring site chronologies, we have chosen a double detrending method (Cook, 1985).

First, a negative exponential curve or a linear regression line is fitted to the ring series, afterwards, each value of the time series where divided by the value predicted by a cubic smoothing spline function. The wave-length of the spline was fixed at 67% of the mean length of the series, with a 50% frequency cut-off, thus removing the non-climatic trends due to tree age, to tree size, and to stand dynamics effects (Cook & Peters 1981; Cook & Briffa, 1990). Individual indexed series were then computed into the mean site chronology by means of a bi-weight robust estimate of the mean, in order to reduce the effects of statistical outliers (Cook 1985; Holmes 1994).

Several statistics have been considered to evaluate the validity of the resulting five mean site chronologies.

Mean sensitivity, measures the relative differences in width from one tree-ring to the next. Douglass (1936) defined in this way this statistic: “mean percentage change from each measured yearly ring to the next”.

$$Ms_x = \frac{1}{n-1}\sum_{t=1}^{t=n-1}\left|\frac{2(x_{t+1}-x_t)}{x_{t+1}+x_t}\right| \text{ (Fritts, 1976)}$$

Where x_t is each ring width, Ms values range from 0, if all rings are the same size, to 2 if a zero value occurs next to a non-zero one in the time sequence.

The *correlation coefficient* (r) is a measure of the degree of linear relationship between two variables. In Dendroclimatolology it is also used to measure the association between time series, e.g. two chronologies or a chronology and a climate series.

$$r_{xy} = \frac{\sum_{t=1}^{t=n}(x_t - m_x)(y_t - m_y)}{(n-1)s_x s_y}$$ (Fritts, 1976)

Where m_x, m_y, s_x, s_y are the means and the standard deviations of the two set of data and n is the sample size. It can range from +1 that indicates perfect agreement to -1 that indicates inverse agreement.

Chronology *signal-to-noise ratio* (Wigley et al. 1984) has been used to evaluate the relative strength of the common variance signal in the five tree-ring chronologies

$$SNR = \frac{N\bar{r}}{(1-\bar{r})}$$ (Cook el al 1990)

Where $\bar{r}$ is the mean interseries correlation between trees and N is the number of trees.

Since our chronologies are composed by individual series of different lengths, it was important to assess the adequacy of replication in the early years of their temporal extension, for this purpose we referred to the *subsample signal strength* (SSS) (Wigley et al 1984). It allows quantifying how well a chronology based on a subset of t' trees estimate a larger t series chronology.

$$SSS = \frac{t'\left[1+(t-1)\bar{r}\right]}{t\left[1+(t'-1)\bar{r}\right]}$$ (Wigley et al, 1984)

Where t and t' are the number of tree-ring width series in the sample and in the subsample and $\bar{r}$ is the mean interseries correlation. Usually, the period used for calibrating tree-rings against climate parameters is the time when the chronology is formed by the highest number of individual series. SSS allows evaluating the possible loss of reconstruction accuracy that occurs when a chronology made up of a few series is used to reconstruct past climate, considering that the used transfer function usually derives from a chronology with a greater number of series (Wigley et al., 1984). We decided to limit our chronologies to the time period with SSS > 0,85. This threshold has been indicated by Wigley et al. (1984) to sufficiently ensure only a small loss of explained variance due to the reduced number of samples in the early part of the chronologies.

First-order autocorrelation. In time series, most of all when biological systems are involved, it is possible that one value is affected by the preconditions of the other values of the series (Fritts, 1976). The first-order autocorrelation indicates how much each value of a series is correlated with the preceding term. When the first-order autocorrelation is close to 0, each yearly value is independent of the one before, when it is close to 1, it means that each yearly value is largely influenced by the one before.

The program ARSTANwin allows to compute three different version of the mean site chronologies: a *Standard Chronology*, where standardized tree-ring index series are combined into a mean value function of all series, a *Residual Chronology* that is computed in the same way of the standard version, but using the residual series resulting from an univariate autoregressive modelling, fitting an autoregressive order to each series, and an *Arstan Chronology* computed using the autoregressive coefficient selected into a multivariate autoregressive modelling and reintroducing the pooled autoregressive model into the residual chronology (Cook & Holmes, 1984). In order to establish the proper version of the five mean site chronologies to use in the successive dendroclimatic analysis, that is whether we should use the standard or residual version of the chronologies derived from the standardization procedures, an autocorrelation analysis has been performed and the first-order autocorrelation has bee evaluated (Box & Jenkins, 1976) (see next chapter for detail on this analysis results).

In order to highlight similarity between the five mean sites chronologies, hierarchical cluster analysis was performed on their common period (1818-2004), producing clusters of the five sites (Leonelli et al, 2009). The five variables were grouping according to the average linkage method and the Euclidean distance was used as a measure of similarity.

The four residual chronologies showing the higher inter-correlation values (Avio, Presanella, Fumo, Presena) were then chosen for successive analysis.

Climate/tree-rings relationship

A fundamental phase in a dendroclimatic analysis is the recognition of the prevalent climatic features that affected tree growth in the studied area. The most commonly used statistical models in delineating climate/tree-rings width relationship are called *correlation function* and *response function* (Fritts et al., 1971; Blasing et al., 1984).

In the both methods a sequence of coefficients are computed between the tree-ring chronology and the monthly climatic variables, which are ordered in time from the previous-year growing season to the current-year one.

In the *correlation functions* the coefficients are univariate estimates of Pearson's product moment correlation (Arnold, 1990), and the function is the temporal sequence of correlation coefficients between the tree-ring chronologies and the monthly climate variables. The *response function is* a form of principal component regression and the coefficients are multivariate estimates from the principal component regression model (Fritts, 1976, Briffa and Cook, 1990a).

These two models take for granted that climate/tree growth relationship is stable in time, but in this way time-dependent changes of the climate/tree growth relationship are not considered (Biondi, 1997). Actually, response and correlation function may vary if the relationship we are trying to capture is not stable through time or if the original response function doesn't contain all the important predictor variables.

If a wealth of long climate series is available it is possible to check the stability of the relationship by calculating response and correlation functions for successive blocks of time. Therefore there are few locations, and our study area is not one of these, where a sufficient length of climate records is suitable and allows calculating successive non-overlapping response and correlation functions. For these reasons, for capturing the dynamical variability of climate signals in tree-ring chronologies the *moving correlation function* (MCF) and the *moving response function* (MRF) are now widely used. These two methods use a fixed number of years that is progressively shifted over time to calculate response and correlation coefficients (Biondi, 1997). They are based on a bootstrapping method, where the moving intervals iterate the bootstrapped correlation and response function for different time period (Fritts and Guiot 1990; Guiot, 1991).

In this study climate/growth relationships have been tested using the standard correlation function (CF) analysis to assess climate–growth relationships (Fritts, 1976) and MCF to test their stationarity and consistency over time, by applying the software package DENDROCLIM2002 (Biondi 1997; Biondi and Waikul, 2004). Each bootstrap estimate was obtained by generating 1000 samples and running numerical computation on each sample. For each interval, the median coefficients estimated from the 1000 bootstrap samples are reported in the output, and are plotted only if they are significantly different from 0 at the 0.05 probability level.

The monthly climate analysis was performed, both for mean monthly temperatures and for total monthly precipitations, choosing 18 climate variables (predictors), from July of the year before growth (t-1) to December of year (t) of growth. The analysis of residual chronologies/monthly mean temperature relationship was carried on with temperature data coming both from high elevation meteorological stations (>1400 m a.s.l.) and from low elevation stations (<1400 m a.s.l.). To provide a sufficient number of degrees of freedom, the length of the calibration period (60 years) was consistently higher than the number of predictors, which were 18 in this study. We performed this analysis with all the five mean site residual chronologies and with a composite chronology (All). The All chronology was obtained averaging the mean site residual chronologies except the Malga chronology that has revealed the lower correlation values with the other four.

To assess any intercollinearity present in the correlation function parameters, we performed response function analysis, using the same climatic variables and calibration period length. All the analysis was performed over the 1878-2004 period.

Extreme weather events have become more frequent in Europe during the last decades (Klein Tank and Können, 2003). To highlight the answer of the Adamello-Presanella larch tree-ring chronologies data set to an exceptional climate event, we have checked out how tree-ring indexes are correlated to the heat wave of summer 2003 (Pilcher & Oberhuber, 2007; Leonelli et al., 2009). Year 2003 was an extraordinary year from the climatice point of view and mean summer temperatures of central Europe exceeded the 1961–1990 mean by ca. 3,8^{o}C (Beniston, 2004; Luterbacher et al., 2004; Schär et al., 2004)

Climatic variables reconstruction

With the aim to test the efficiency of the computed larch mean site chronologies for climate reconstruction purposes, we have conducted a first tentative of climate reconstruction using the *transfer function method* (Fritts, 1976; Briffa et al. 1982; Fritts & Guiot, 1990).

In the transfer function computation the tree-ring chronologies are the predictors and the climate parameters the predictant.

The procedure that estimates the statistical tree-rings growth/climate relationship is called *calibration*. This statistical procedure involves calculating of a set of regression coefficient of a linear regression equation representing the relationship between climate parameters (temperature or precipitations) and a set of tree-ring chronologies (Briffa, 1982).

In a second time "growth records are transferred in the reconstruction of climate" (Fritts, 1976), in other words, the coefficients are applied to tree-ring data to obtain estimates or reconstructions of climate parameters (Fritts & Guiot, 1990).

A correct calibration procedure requests some important assumptions, such as the normal distribution of data (both climate and tree-ring chronologies) and the absence of autocorrelation. These are essential premises because the presence of outliers can distort the significance testing and the interdependence of observation in time can reduce the number of degrees of freedom used for statistical significance testing (Fritts & Guiot, 1990). To avoid as best as possible these potential problems we have proffered a particular care in evaluating normal distribution of tree-ring data and climate parameters, and we have chosen to use the residual chronologies as predictors because of their lower values of autocorrelation (see next chapter for details).

We used histograms to compare the frequency distributions of the climate data and the predictors.

To further asses the distribution of tree-ring data and in order to measure how well the data follow the normal distribution we performed a statistical test for normality, the *Anderson-Darling test* (Anderson & Darling, 1950).

The Anderson Darling test compares the empirical cumulative distribution function of sample data with the distribution expected if the data were normal. If the observed difference is sufficiently large, the test will reject the null hypothesis of population normality.

The hypotheses for the Anderson-Darling test are:

H_0: The data follow a specified distribution.

H_1: The data do not follow a specified distribution.

The better the distribution fits the data, the smaller this statistic will be, if the p-value for the Anderson-Darling tests is lower than the chosen significance level (0.05 in our case), then the data do not follow the specified distribution.

To clearly represent the fitting to normal distribution of our tree-ring data we have used probability plots where each value was plotted vs. the percentage of values in the sample

In any regression technique it is important to be able to test the regression equation using an independent data set. This independent testing procedure, called *verification,* allows assessing if the modelled growth/climate relationship obtained for the calibration period are valid over an independent time period. Verification is established when the reconstructed values derived from the independent predictors set is similar to the independent predictant set (Fritts, 1976). Verification on independent data is the most accurate statistical evidence that a

particular climate/tree-growth relationship is not occasional, and that the subsequent reconstruction actually represents real conditions.

In this study we have used the transfer function method with a single predictant variable. The climate parameters involved in the reconstruction are those showing better results in the MCF and MRF analysis.

In order to use as best as possible the common signal strength of the five chronologies we have discarded those chronologies (Malga chronology, see next chapter for details) presenting the lower climate/tree growth correlation and the weaker correlation with the other chronologies.

The four mean site residual chronologies chosen for the reconstruction start in different years and their different time span imply a reduced replication in the earliest period of the time series. Considering the different length of the chronologies, it is strategically important to correctly select the appropriate reconstruction technique and the more proper calibration/verification periods.

With the aim to use the full length of the tree-ring chronologies and not limiting the reconstruction to their common period, we decided to compute a series of nested principal component regression models (Meko, 1997; Cook et al., 2002, 2003). The individual calibrated models are developed using all available predictors for each time period, and are then merged together, so that a near-maximum number of predictors is used to estimate climate variables back in time. The climate variables interested by the reconstruction are those presenting the better results in response and correlation functions analysis.

We have defined three models limited by the starting year of each chronology, in fact the starting year of each chronology represents in our tree-ring data set an important point of change in the availability of the tree-ring series, and then we have used the PC calculated for each nest as the potential predictors in the nested time period. The nested multivariate regression models assure that each time period is represented by the corresponding regression model with the greatest number of available data (Meko, 1997, Briffa, 1988).

Principal component analysis

When, as in our case, the number of predictors is higher than one it is opportune to reduce them in a minor number of candidate principal component (PC) predictors (Fritts, 1976, Peters, 1981, Briffa et al. 1982; Briffa et al., 1988).

Principal Component Analysis (Peters et al 1981) is widely used to isolate a certain fraction of variance from tree-ring time series. This fraction can then be used to explain

climatic parameters *sensu lato* or more precisely summer temperatures. This method has demonstrated in many studies to be superior of simple correlation analysis (Frank & Esper, 2005b, Cook et al 2003).

With the principal component analysis the predictor variables are transformed into a new set of orthogonal and uncorrelated variables (eigenvectors or principal components) and a smaller number of transformed variables may be required to obtain the regression relationship. High-order principal components whose cumulative variance does not exceed a predefined threshold can be rejected, and, at the end, the amplitude time series for the PC predictors are regressed individually against the predictand data series (climate parameters) in the calibration process. As seen above, "to calibrate" means to develop a regression model (the *transfer function*) that we can use to convert tree ring values (or their PC) into climate variables values. In our case, in the calculation of transfer function, PC eigenvalues derived from tree-ring residual chronologies are the predictors and the climate variables are the predictand.

We decided to apply this method, even with a small number of chronologies to preserve the climatic common signal over the four chronologies used in the reconstruction.

In a first step a multiple regression technique has been performed to convert tree-ring chronologies time series (in our case residual chronologies) into their principal components, in view of the fact that we have chosen chronologies on the base of their good intercorrelations, it was probable that a lower number of eigenvalues expresses most of the variance. The PC rejection criterion follows the most common approach, to deciding the appropriate number of factors we have generated a *scree plot*. The scree plot is a two dimensional graph with factors on the x-axis and *eigenvalues* on the y-axis, in this manner it is possible to highlight which factors account for the most part of the variance. Several other plots were realized to further verify the scree plots results. The *Score plot for first 2 components* plot which plots the scores for the second principal component (y-axis) versus the scores for the first principal component (x-axis); the *Loading plot for first 2 components*: plots the loadings for the second component (y-axis) versus the loadings for the first component (x-axis). A line is drawn from each loading to the (0, 0) point; the *Biplot for first 2 components* plots an overlay of the score and loading plots for the first two components.

Even if this approach to selecting the number of factors involves a certain amount of subjective judgment, our choice was further verified using the Kaiser-Guttman rule that remove all those components for which the eigenvalues are <1.

All the statistical computations and the graph plotted in this study were realized with the computer program Minitab® 15.

Split sample procedure

As seen above, the stability of the regression, testyfied by the similarity of the regression coefficients in both the calibration and verification time period is a very important task in a tree-ring based climate reconstruction.

Into the period of instrumental-proxy overlap we have defined an adequately long calibration period (120 years) that was common to the three defined nests (1840-1959) and performed, on this period, the *calibration–verification test* using a *split sample procedure* (Meko & Graybill, 1995; Snee, 1997; Touchan et al 2003, 2005). In this technique the full length of the period is divided in two subsets, and they are alternately exchanged for calibration and verification procedures.

A regression has been run on the calibration period and tested the response diagnostics drawing several plots to test the normality of the residuals (histograms and box plots) and to verify if the variance of the residuals is stable (no trend, no autocorrelation, no Δ in variance).

The boxplots generated for each interval are the *plots of residual versus fitted values* that should show a random pattern of residual on the both sides of 0, and the *plots of residual versus order of data*. This last graph can be useful in time series analysis to verify if the residuals are uncorrelated each other. A positive correlation is indicated by a clustering of residuals with the same sign; a negative correlation is indicated by rapid changes in the signs of consecutive residuals. The presence of patterns of the same sign can be correlated with the persistence of some autocorrelation that has been further quantified with the Durbin-Watson statistic (see next paragraph).

In each nest the regression model developed for the calibration period has been used to compute predicted climate variables in the verification period from predictors' values. The same operation has been performed on the verification period to predict climate variables in the calibration period from predictors' values (Fritts, 1976, Touchan et al 2003, 2005).

If the two regression models obtained from the split sample procedure are similar in values and structure, the regression can be computed on the whole calibration-verification period. The resulted final regression model can be used to predict climate variable on the whole extension of each nest. Afterwards, the three individually calibrated models were spliced to form the total reconstructed series.

In detail, in this study, the calibration period is adequately long (120 years) and common to the three nests (1840-1959). The full length of the calibration period is divided in two subsets (1840-1899 and 1900-1959 respectively), and they are alternately exchanged for calibration and verification procedures following the split sample technique.

For each regression several plots were originated to evaluate the goodness of model fit: a *histogram of residual*, a *normal probability plot of residuals*, a *plot of residual versus fit* and a *plot of residual versus order*.

Reconstruction validation

Several statistics have been conducted to test the reliability of our split sample calibration verification procedure.

For each calibration verification period, Pearson's correlation coefficient (r), percentage of variance (R^2), reduction of error (RE), coefficient of efficiency (CE) and Durbin Watson statistics were performed.

The correlation coefficient r is a measure of the degree of linear relationship between two variables. R^2 describes the amount of variation in the observed response values that is explained by the predictors (PC1 in our case) (Arnold, 1990).

Reduction of error statistic (RE) has been performed to measure the association between the series of actual values of monthly mean temperature and their estimates (Fritts, 1976). The theoretical limits for the values of this statistic range from a maximum of +1 to minus infinity, but an RE value grater than 0 is to be considered as a positive skill (Fritts, 1976).

The *RE statistic* is calculated dividing the sum of squared differences between actual and estimated values by the sum of the squared differences between actual values and the mean of the calibrating period then subtracting the value from 1:

$$RE = 1.0 - \frac{\sum_{i=1}^{n}(y_i - \hat{y}_i)^2}{\sum_{i=1}^{n}(y_i - \bar{y}_i)^2} \quad \text{(Fritts, 1976)}$$

Where y are the measured temperatures in year i, $\hat{y}_i$ are the estimated temperatures in year i, $\bar{y}_1$ is the mean of the measured temperatures over the calibration period, and n is the number of years in the verification period.

If, as in case of presence of low-frequency variations in the predictants, the actual measured values have significantly different means in the calibration and verification periods,

RE values may remain positive even though the shift in mean is not followed by the reconstructed values (Briffa et al. 1988).

Another statistical test related to the RE that allows to measure the verification performance is the *Coefficient of Efficiency* (CE) that was originally introduced in hydrology (Nash and Sutcliffe, 1971). The CE statistic is similar to RE, but it uses the mean of the verification period at the denominator, then, if the means of calibration and verification period are similar, CE and RE values are similar too. The use of this statistic in Dendroclimatology was introduced by Briffa et al in 1988 (Briffa et al., 1988), as for RE, its theoretical limits range from +1 to minus infinity, any positive values indicating positive skill, a minus value indicates no agreement. It is a very rigorous test to pass if there are important differences between calibration and verification periods means.

Durbin-Watson statistic has been used to test the presence of autocorrelation in the residuals deriving from the regression analysis. If e_i is the residual associated with the observation at the time t, the test statistic formula is:

$$d = \sum_{t=2}^{t} \frac{(e_t - e_{t-1})^2}{\sum_{t=1}^{t} e_t^2}$$ (Durbin & Watson, 1950)

Since d is approximately equal to $2(1-r)$, where r is the sample autocorrelation of the residuals, $d=2$ indicates that appears to be no autocorrelations, its value always lies between 0 and 4. If the Durbin-Watson statistic is substantially less than 2, there is evidence of positive serial correlation, if $d > 2$ successive error terms are, on average, much different in value to one other, then negatively correlated (Durbin & Watson, 1950).

Climate Reconstruction analysis

A comparative analysis has been conducted between instrumental and reconstructed climate parameters over their common period (1760-2004). In order to highlight low and high frequency trends in the reconstructed data and their skill in describing low and high frequency climate fluctuations.

Reconstructed and instrumental temperature data are plotted over their common period (1760-2004) and the time series are smoothed with running averages of different window lengths (30, 20, 10 years), to explore the potential of the reconstructed mean temperatures in describing low frequency climate variation (Frank & Esper, 2005).

4 Results

Mean Site Tree-Ring Chronologies

Val d'Avio

The Val d'Avio mean site chronology is composed by 11 individual tree-ring series (Tab. 4-1). The total number of sampled trees was 23.The sampling campaign in Val d'Avio was conducted during the early summer 2008. The 2008 annual ring was not completed, then, in order to avoid the introduction of an erroneous low ring width value into the more recent part of the chronology time series, we decided to stop the measurement to the 2007 annual ring. One individual tree-ring series derives from a log (Avio18), its time span goes from 1711 to 1963, and the correct dating was checked cross-dating the Avio18 time series with the other Avio individual series deriving from living trees. The resulting Avio chronology length is 458 years spanning from 1550 to 2007. The mean correlation with master is consistent (r =0,684) and the mean length of the raw series 348,0 (Tab.4-2). In figures 4-1, 3-2 and 4-3 are the raw, standardized and residual individual tree-ring series. In figures 4-4 and 4-5 are plotted the raw standardize and residual Avio chronologies.

TIME PLOT OF TREE-RING SERIES: AVIO				
	Time-span	Yrs		Ident.
1	1810 2007	198	. . . . . <==========>	Avio21
2	1693 2005	313	. . . <==========>	Avio20
3	1607 2007	401	. <==========>	Avio8m
4	1567 2007	441	. <==========>	Avio19
5	1550 2007	458	<==========>	Avio15
6	1711 2007	297	. . . . <==========>	Avio16
7	1701 1963	263	. . . <==========> .	Avio18
8	1721 2007	287	. . . . <==========>	Avio12
9	1699 2007	309	. . . <==========>	Avio17
10	1552 1991	440	<==========>.	AVIO4m
11	1588 2007	420	. <==========>	AVIO8m
	1500 1550 1600 1650 1700 1750 1800 1850 1900 1950 2000			

Tab.4-1 time plot of the Avio individual tree-ring series

Series	Interval	Years	Corr. with Master
1 Avio21	1810 2007	198	0.74
2 Avio20	1693 2005	313	0.60
3 Avio8m	1607 2007	401	0.69
4 Avio19	1567 2007	441	0.70
5 Avio15	1550 2007	458	0.86
6 Avio16	1711 2007	297	0.68
7 Avio18	1701 1963	263	0.69
8 Avio12	1721 2007	287	0.73
9 Avio17	1699 2007	309	0.73
10 AVIO4m	1552 1991	440	0.60
11 AVIO8m	1588 2007	420	0.60
Total or mean:		3828	0.68

Tab. 4-2 correlation with master (the time series of maximum length) of the individual Avio time series.

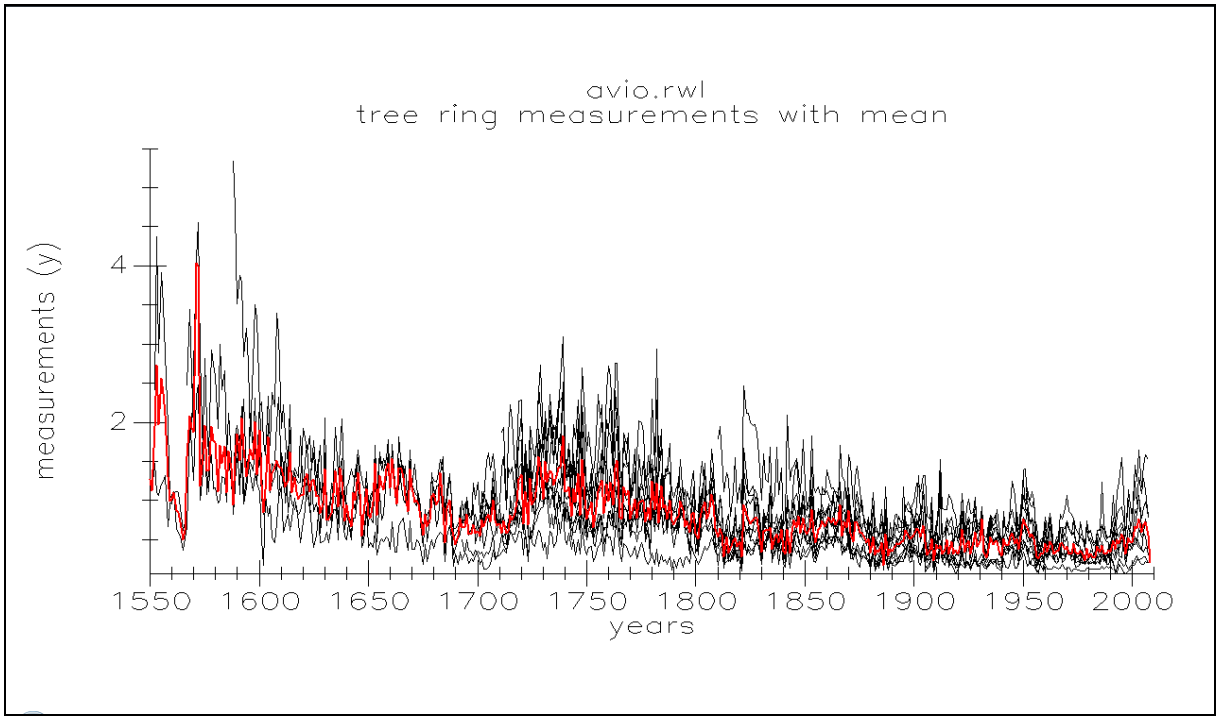

Fig. 4-1 Avio raw individual tree-ring series with mean (red line).

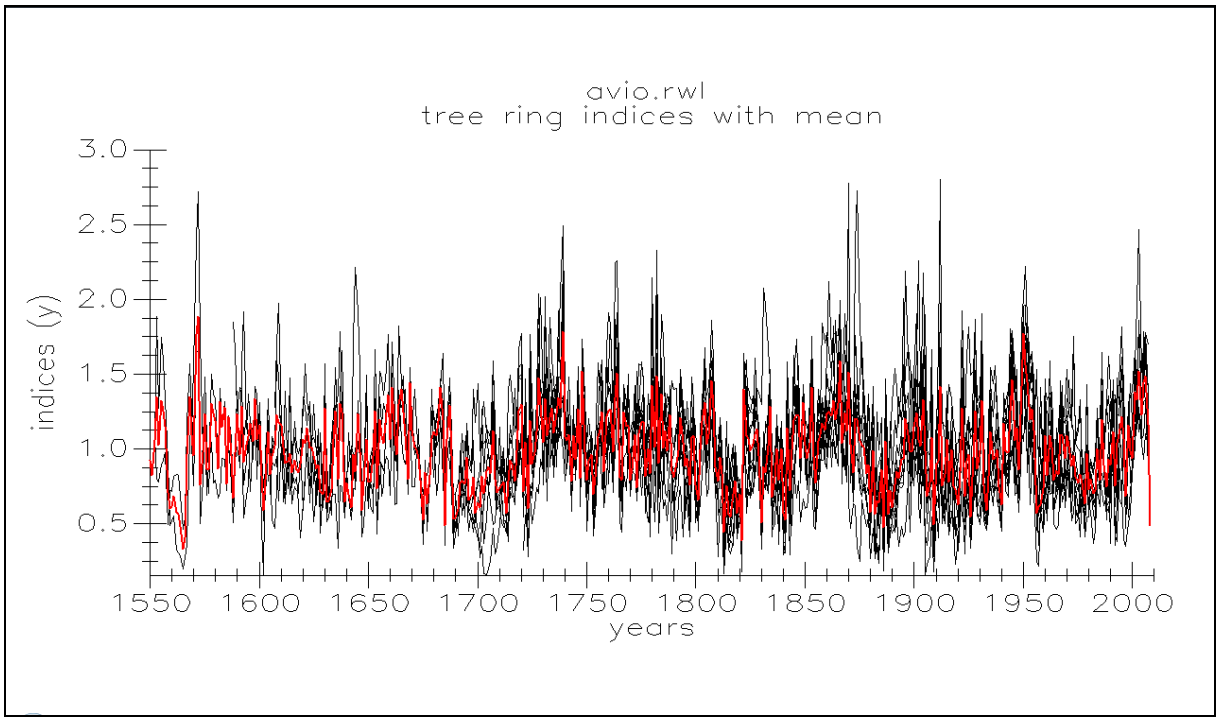

Fig. 4-2 Avio standardized individual tree-ring series with mean (red line).

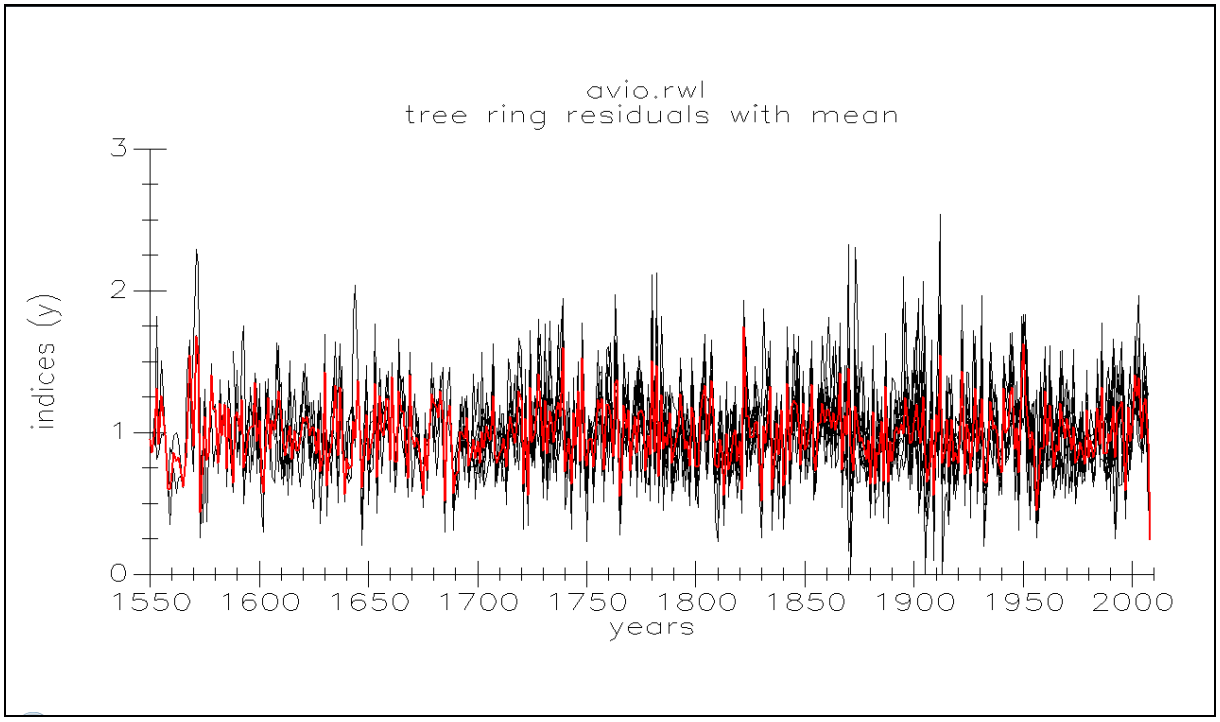

Fig. 4-3 Avio residual individual tree-ring series with mean (red line).

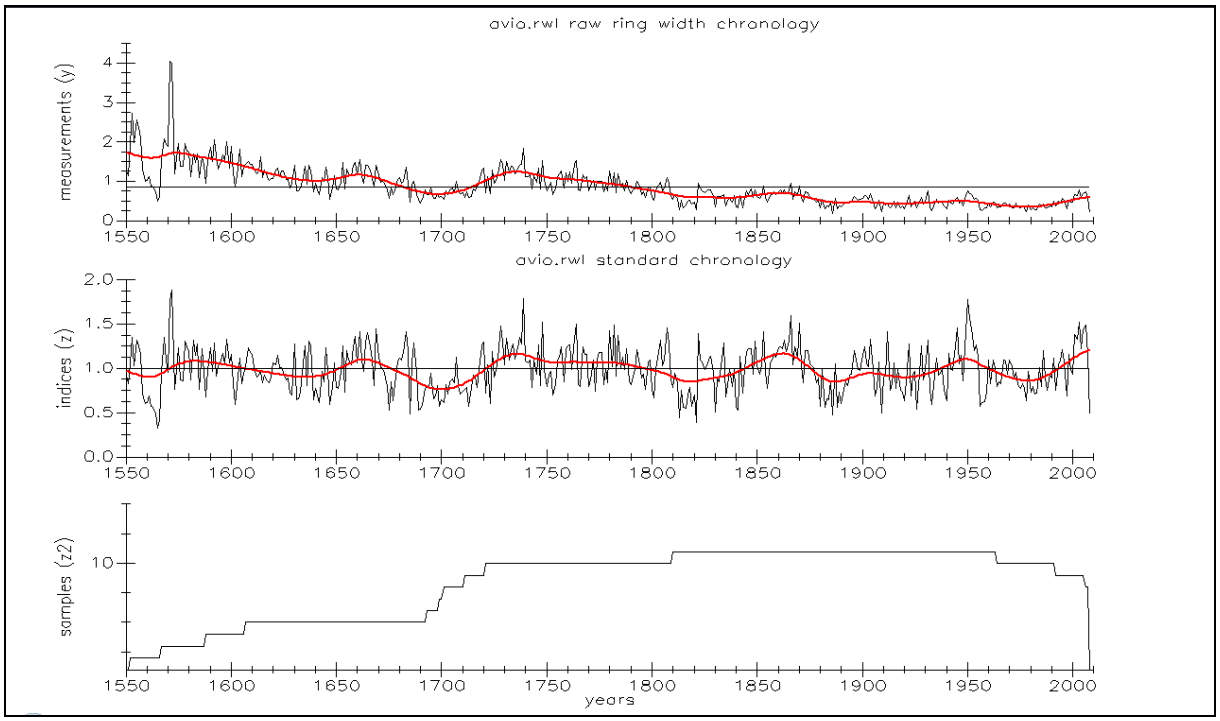

Fig. 4-4 Avio raw and standard tree-ring chronologies with mean (red line), the sample depth is visible in the figure bottom.

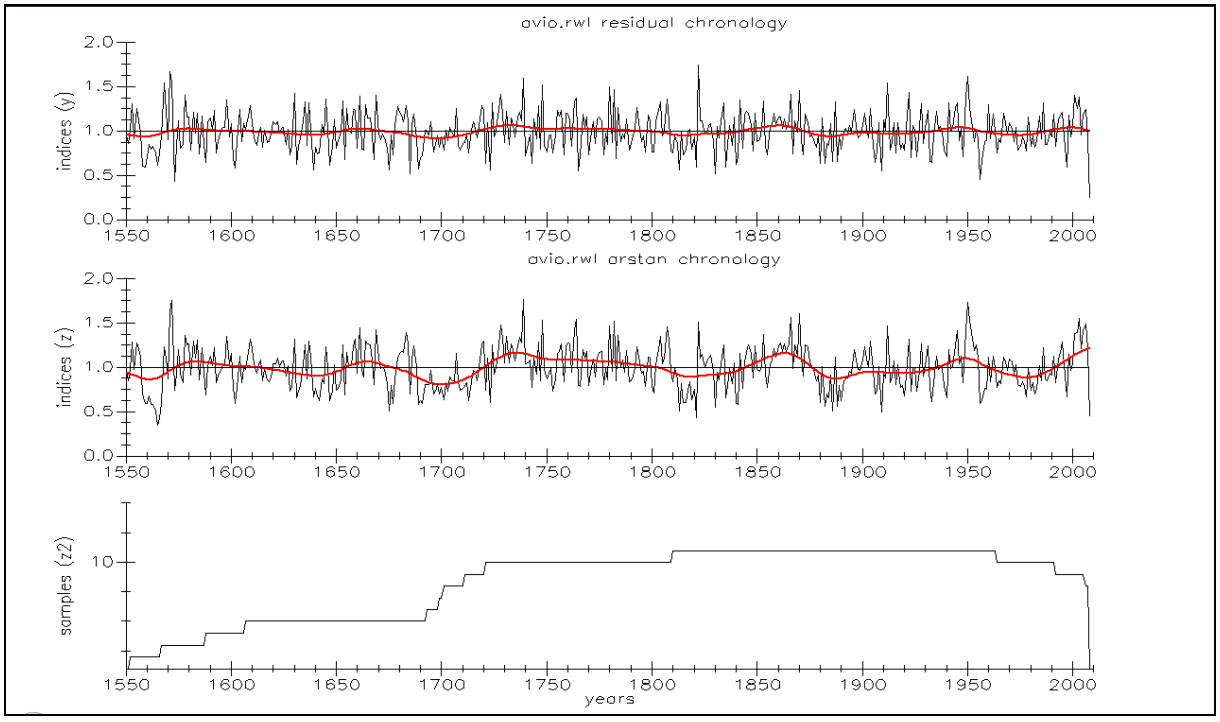

Fig. 4-5 Avio residual and Arstan tree-ring chronologies with mean (red line), the sample depth is visible in the figure bottom.

Val Presanella

The total number of sampled trees in Val Presanella was 32, larch and Norway spruce, the sampling campaigns were conducted during the early summers of 2005 and 2006.

The Presanella larch chronology consists of 14 mean individual series coming from living and historical material. It spans from 1550 to 2005 (456 years).

With the aim to improve the number of tree-ring series and the sample replication in the earlier part of the larch chronology, we have explored the possibility to use tree-ring series coming from barns' beams in the Presanella mean site chronology. We have evaluated the close provenance of timbers and the consistent correlation values of the disks' mean tree-ring series with the tree-ring individual series coming from the living trees. Finally we decided to introduce six mean tree-ring series belonging to the historical dated samples in the computation of the Presanella mean site chronology. These six samples come from four different barns. The length of these six tree-ring series is higher than 100 years. (See Appendix 1 of this chapter for details on the barns' beams dating results). The correlation with master is higher than 0,60 for all the 14 samples. In figures 4-6, 4-7 and 4-8 are plotted the raw, standardized and residual individual tree-ring series. In figures 4-9 and 4-10 are plotted the raw standardize and residual Presanella chronologies.

	Time-span	Yrs	**TIME PLOT OF TREE-RING SERIES: Presanella** larch	Ident.
1	1719 1871	153	. . . .<==========> . . .	Boai1m
2	1701 1851	151	. . . <==========> . . .	Boai2m
3	1661 1789	129	. . .<==========>	Podete
4	1761 1913	153	. . . . .<==========> . .	Mazolo
5	1634 1742	109	. . <==========>.	Mazolo
6	1550 2004	455	<==========>	PA9med
7	1632 1759	128	. . <==========>	Grìi
8	1595 2001	407	<==========>	Camp1
9	1621 2000	380	. . <==========>	Camp2
10	1601 2000	400	. <==========>	Camp3
11	1896 2004	109	. . . . <==========>	VP14me
12	1569 2004	436	.<==========>	VP23me
13	1682 2004	323	. . . <==========>	VP25me
14	1746 2005	260	. . . . <==========>	VP22me
	1500 1550 1600 1650 1700 1750 1800 1850 1900 1950 2000			

Tab. 4-3 Time plot of the Presanella individual larch tree-ring series. Samples coming from historical material are underlined.

Series	Interval	Years	Corr. with Master
1 Boai1m	1719 1871	153	0.60
2 Boai2m	1701 1851	151	0.72
3 Podete	1661 1789	129	0.61
4 Mazzolo1	1761 1913	153	0.60
5 Mazzolo2	1634 1742	109	0.62
6 PA9med	1550 2004	455	0.66
7 Grìi	1632 1759	128	0.60
8 Campl	1595 2001	407	0.63
9 Campl	1621 2000	380	0.60
10 Campl	1601 2000	400	0.61
11 VP14me	1896 2004	109	0.60
12 VP23me	1569 2004	436	0.65
13 VP25me	1682 2004	323	0.72
14 VP22me	1746 2005	260	0.62
Total or mean:		3593	0.63

Tab. 4-4 correlation with master (the time series of maximum length) of the individual Presanella larch time series. Samples coming from historical material are underlined.

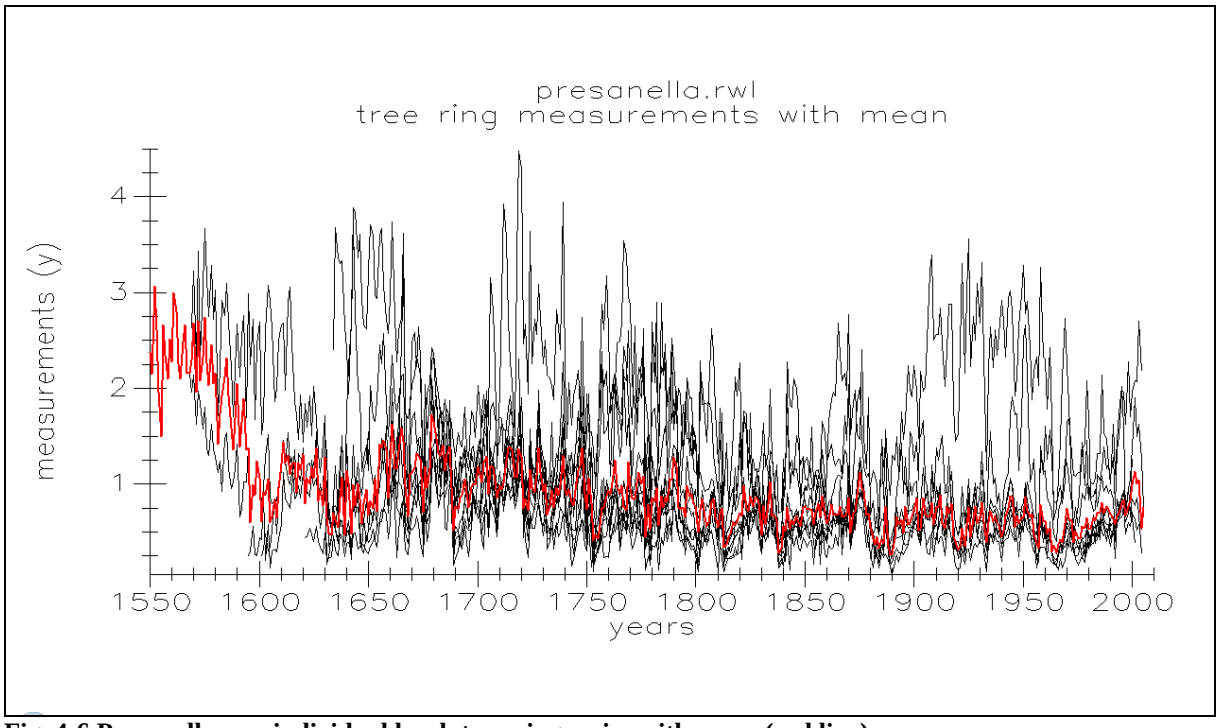

Fig. 4-6 Presanella raw individual larch tree-ring series with mean (red line).

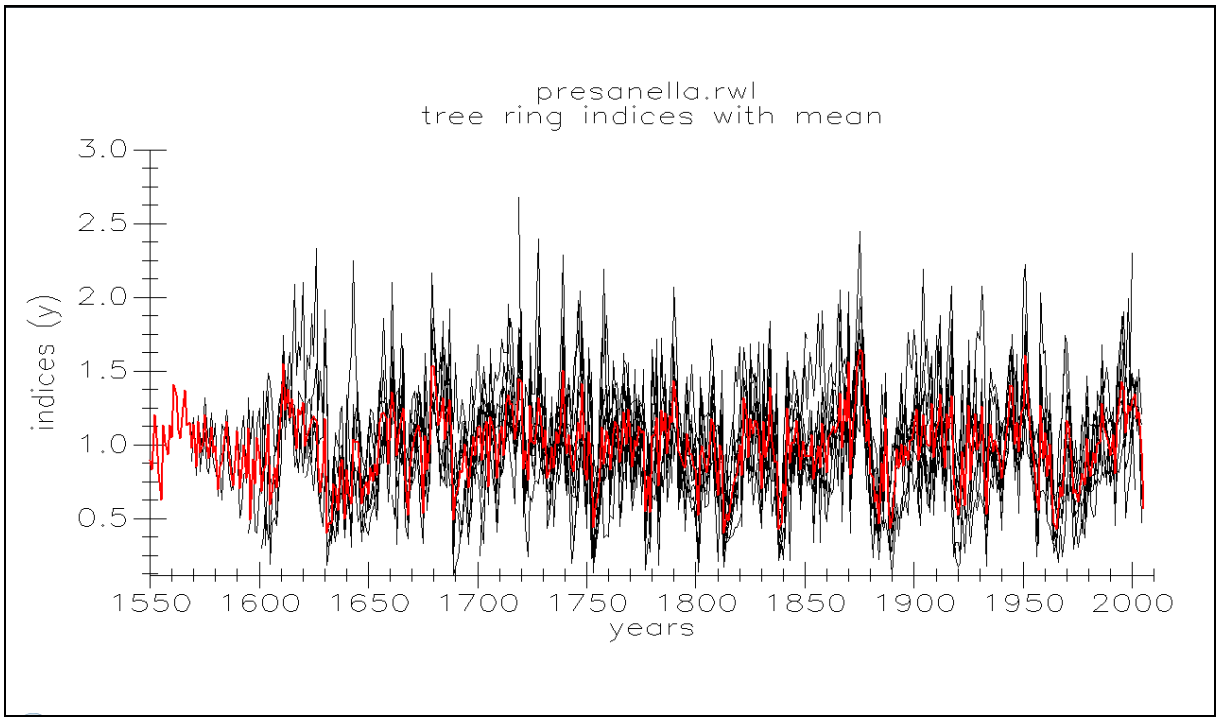

Fig. 4-7 Presanella standardized individual larch tree-ring series with mean (red line).

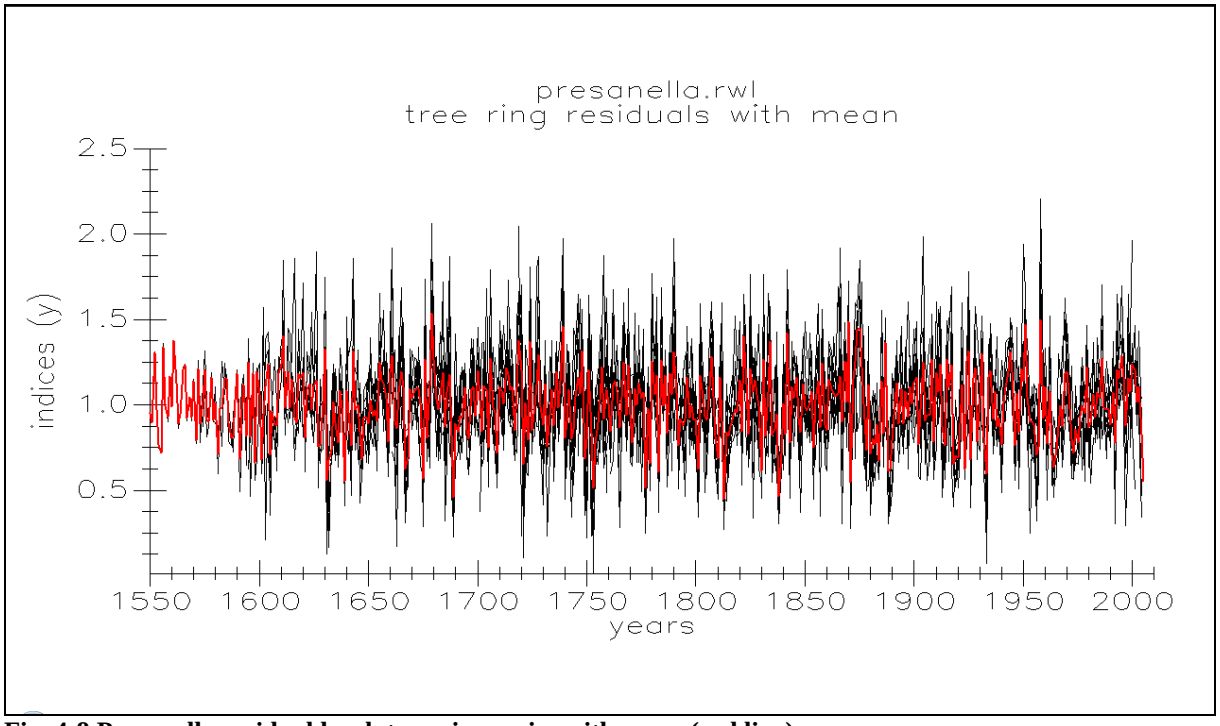

Fig. 4-8 Presanella residual larch tree-ring series with mean (red line).

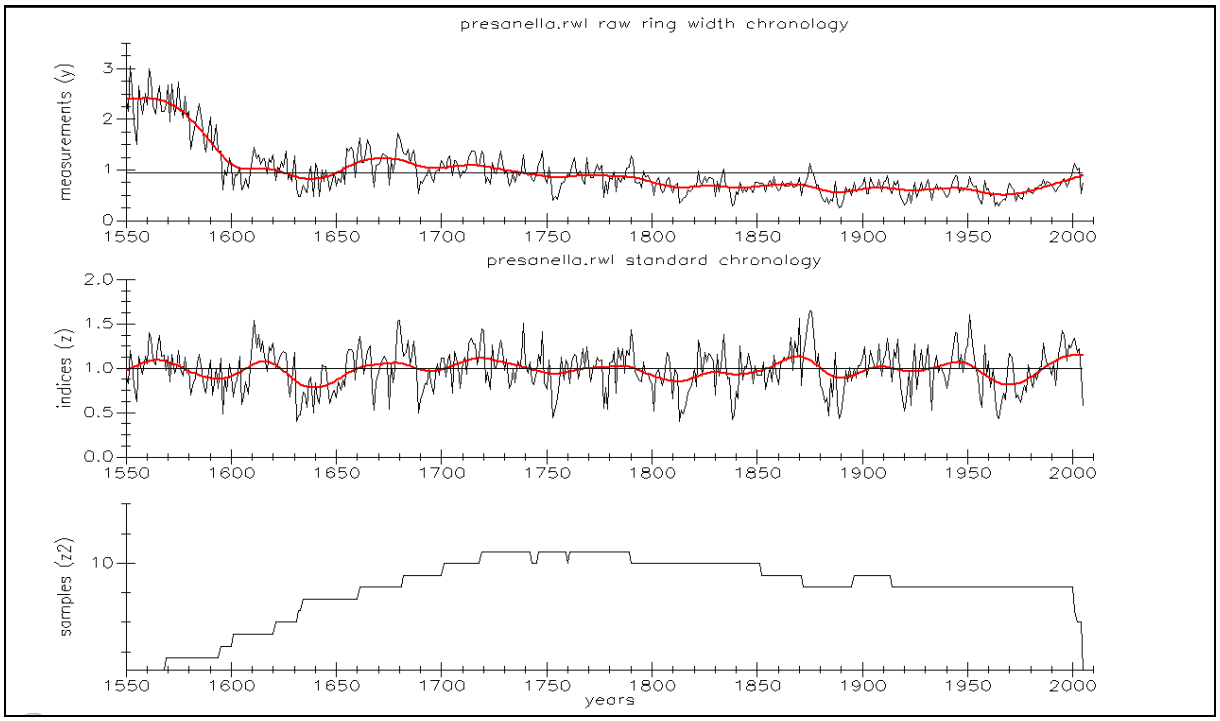

Fig.4-9 Presanella raw and standard tree-ring larch chronologies with mean (red line), the sample depth is visible in the figure bottom.

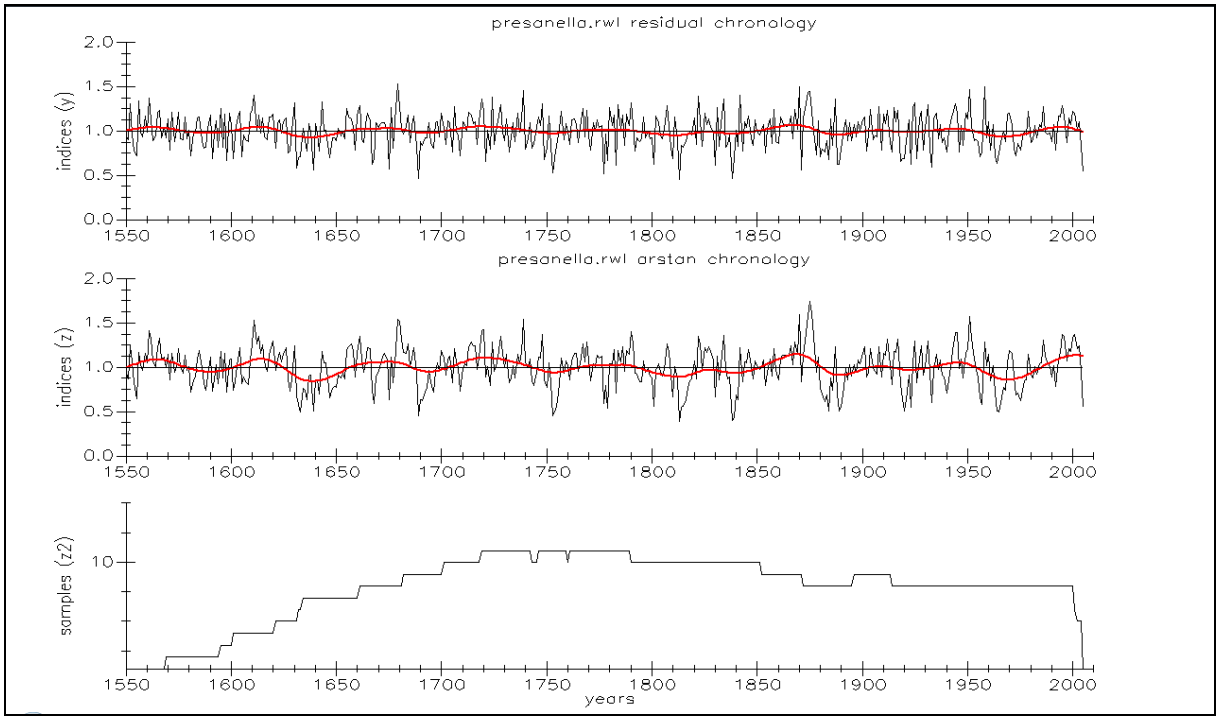

Fig. 4-10 Presanella residual and Arstan tree-ring larch chronologies with mean (red line), the sample depth is visible in the figure bottom.

The Presanella spruce raw chronology is composed by 9 individual tree-ring series. It spans from 1823 to 2005. The individual mean tree-ring series show weak intercorrelation values. Due to the shorter length of the series and the lower intercorrelation values, we decided to not use the spruce chronology in the successive climatic analysis

TIME PLOT OF TREE-RING SERIES: Presanella spruce		
Time-span Yrs		Ident
1 1899 2005 107	. . <==========>	VP4med
2 1888 2005 118	. . <==========>	VP20me
3 1885 2005 121	. . <==========>	VP19me
4 1823 2005 183	. <==========>	VP18me
5 1889 2005 117	. . <==========>	VP15me
6 1878 2005 128	. . <==========>	STAV2m
7 1883 2005 123	. . <==========>	PA8med
8 1855 2005 151	. <==========>	PA7med
9 1890 2005 116	. . <==========>	VP6med
1650 1700 1750 1800 1850 1900 1950 2000		

Tab. 4-5 time plot of the Presanella individual spruce tree-ring series.

Series	Interval	Years	Corr. with Master
1 VP4med	1899 2005	107	0.44
2 VP20me	1888 2005	118	0.46
3 VP19me	1885 2005	121	0.37
4 VP18me	1823 2005	183	0.28
5 VP15me	1889 2005	117	0.44
6 STAV2m	1878 2005	128	0.37
7 PA8med	1883 2005	123	0.59
8 PA7med	1855 2005	151	0.65
9 VP6med	1890 2005	116	0.63
Total or mean:		1315	0.49

Tab. 4-6 correlation with master (the time series of maximum length) of the individual Presanella spruce time series.

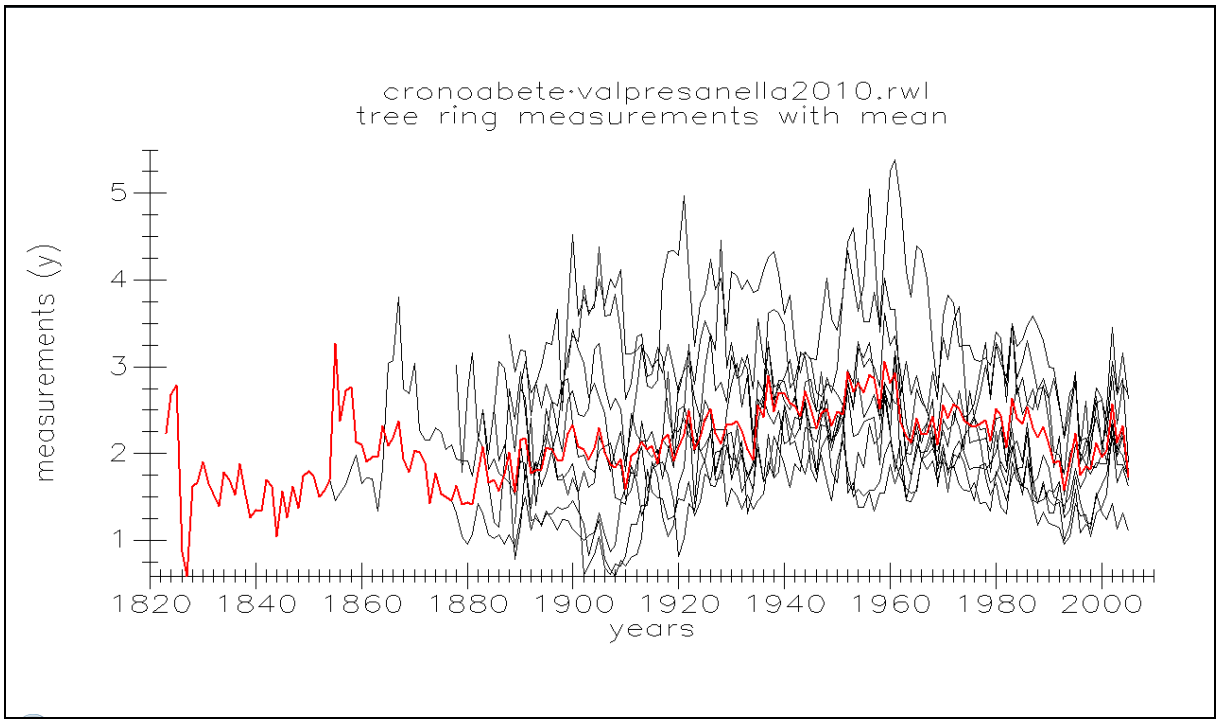

Fig. 4-11 Presanella raw individual spruce tree-ring series with mean (red line).

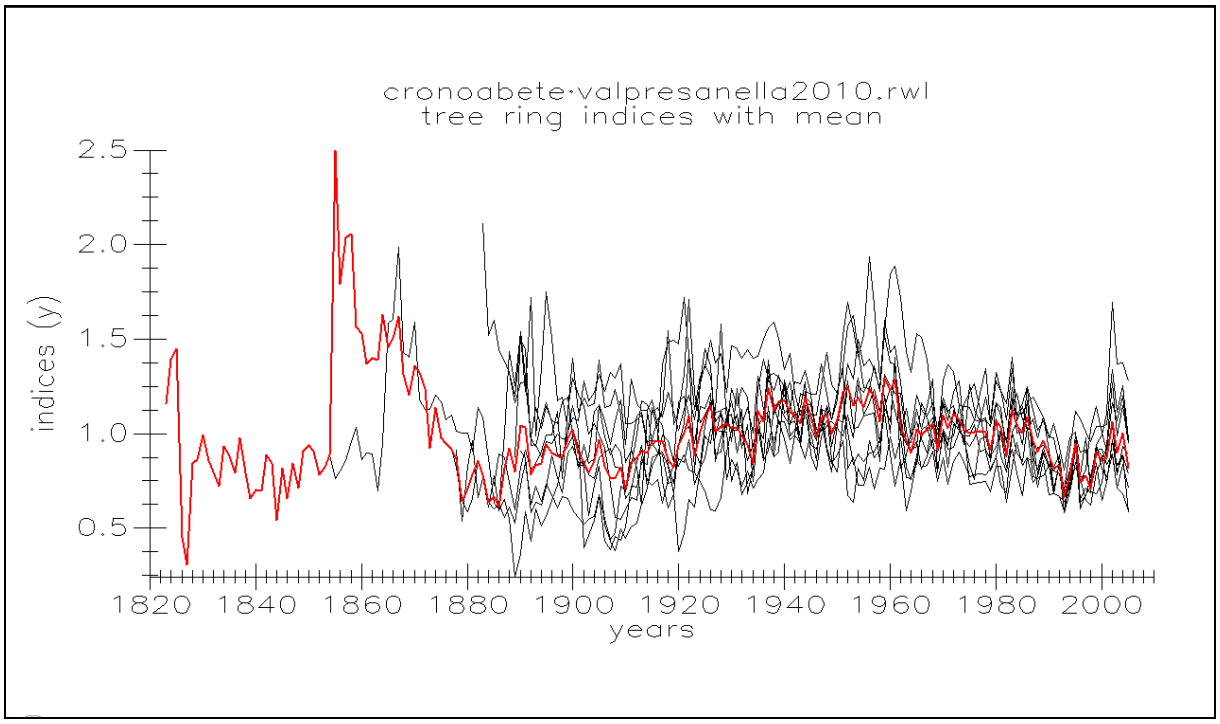

Fig. 4-12 Presanella standardized individual spruce tree-ring series with mean (red line).

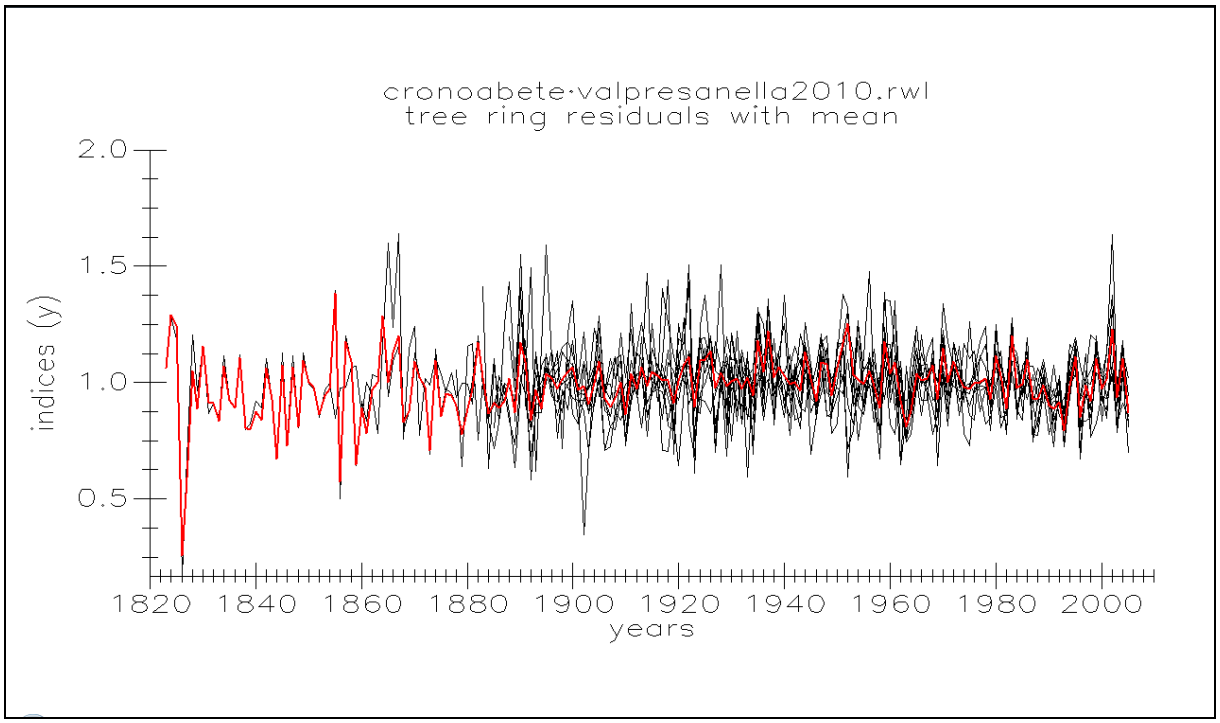

Fig. 4-13 Presanella residual spruce tree-ring series with mean (red line).

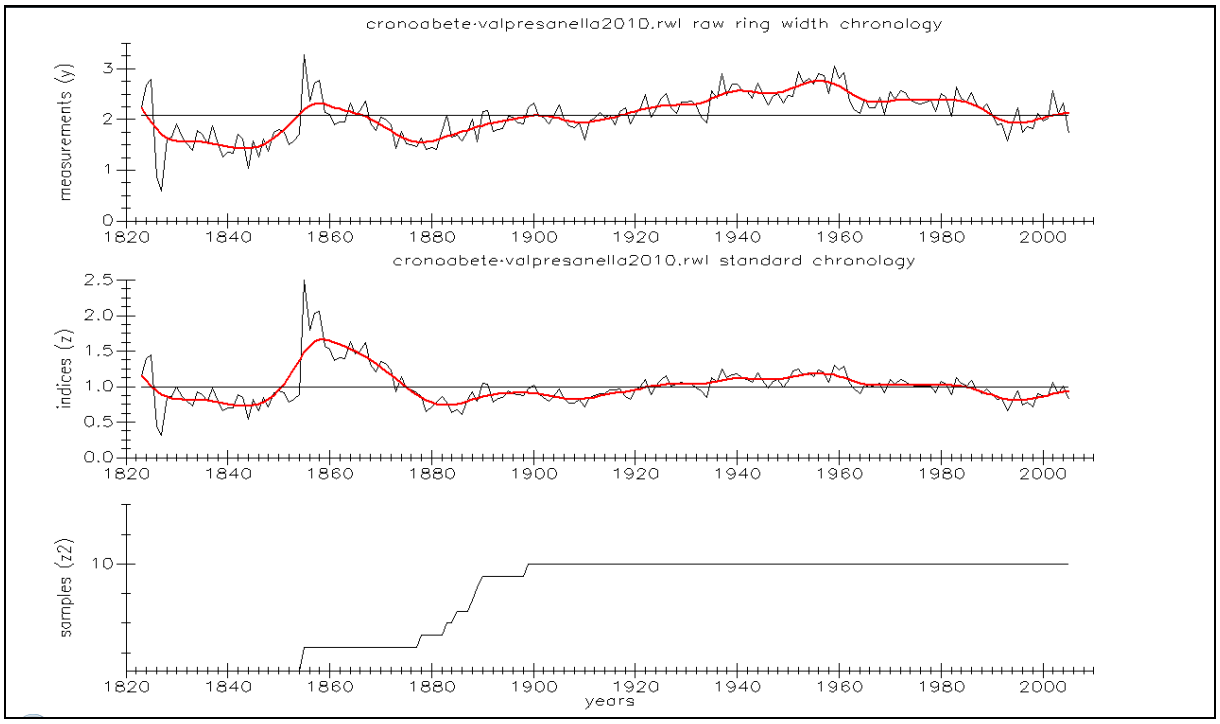

Fig. 4-14 Presanella raw and standard tree-ring spruce chronologies with mean (red line), the sample depth is visible in the figure bottom.

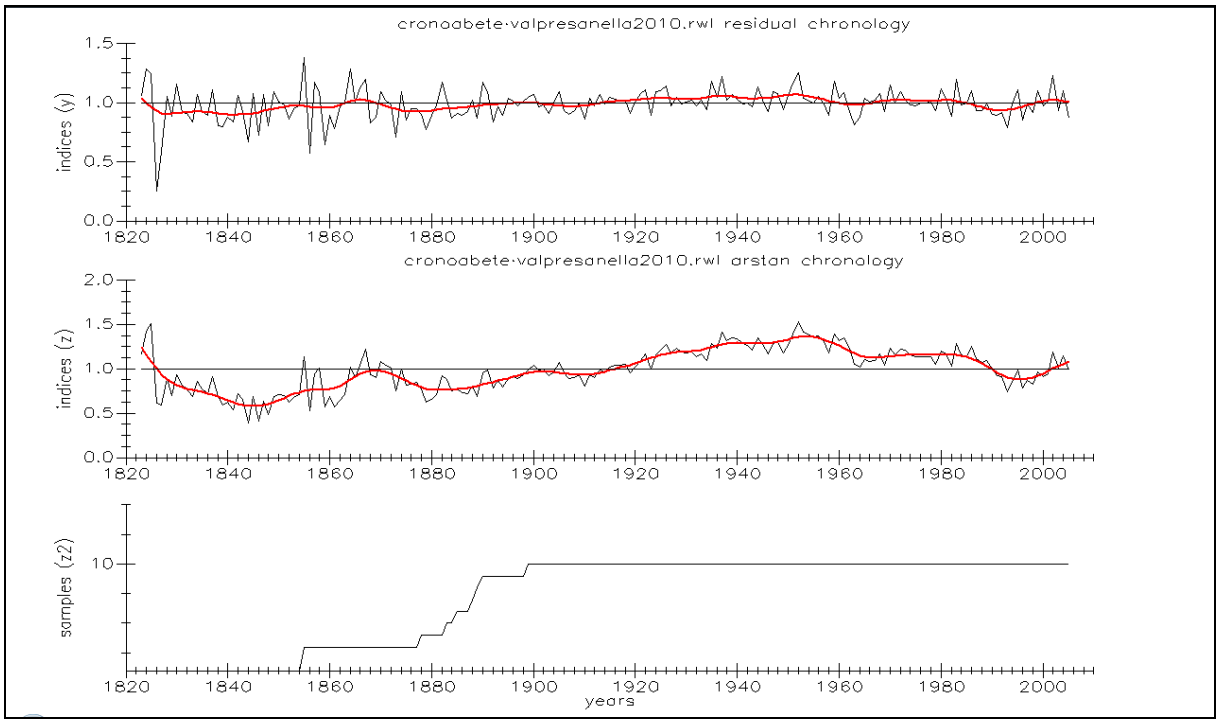

Fig. 4-15 Presanella residual and Arstan tree-ring spruce chronologies with mean (red line), the sample depth is visible in the figure bottom.

Val di Fumo

The Val di Fumo larch chronology consists of 13 mean tree-ring series, spans from 1710 to 2008 (299 years) (Tab. 4-7). The total number of sampled trees was 36, mostly larches and stone pines, the higher number of larch samples, their longer time extensions and the better intercorrelation induced us to realize the only larch chronology. The value of correlation with master 0,66) is one of the highest found in the five chronologies (Tab.4-8).

In figures 3-16, 3-17 and 3-18 are the raw, standardized and residual individual tree-ring series. In figures 3-19 and 3-20 are plotted the raw standardize and residual Presanella chronologies.

TIME PLOT OF TREE-RING SERIES: Fumo				
	Time-span Yrs			Ident.
1	1748 2008	261	. . . ←==========→	0VF10m
2	1849 2008	160	. . . . . ←==========→	0VF11m
3	1737 2008	272	. . . ←==========→	0VF12m
4	1825 2008	184	. . . . . ←==========→	0VF13m
5	1715 2008	294	. . .<==========→	0VF14m
6	1784 2008	225	. . . . ←==========→	0VF01m
7	1905 2008	104	. . . . . . ←=====→	0VF20m
8	1755 2008	254	. . . ←==========→	0VF21m
9	1889 2008	120	. . . . . . ←=======→	0VF24m
10	1727 2008	282	. . . ←==========→	0VF04m
11	1871 2008	138	. . . . . . ←========→	0VF05m
12	1710 2008	299	. . .<==========→	0VF07m
13	1810 2008	199	. . . . .<==========→	0VF09m
1600 1650 1700 1750 1800 1850 1900 1950 2000				

Tab. 4-7 time plot of the Fumo individual tree-ring series

Series	Interval	Years	Corr. With Master
1 0VF10m	1748 2008	261	0.70
2 0VF11m	1849 2008	160	0.60
3 0VF12m	1737 2008	272	0.76
4 0VF13m	1825 2008	184	0.73
5 0VF14m	1715 2008	294	0.61
6 0VF01m	1784 2008	225	0.60
7 0VF20m	1905 2008	104	0.60
8 0VF21m	1755 2008	254	0.63
9 0VF24m	1889 2008	120	0.71
10 0VF04m	1727 2008	282	0.70
11 0VF05m	1871 2008	138	0.71
12 0VF07m	1710 2008	299	0.71
13 0VF09m	1810 2008	199	0.60
Total or mean:	2792		0.66

Tab. 4-8 correlations with master (the time series of maximum length) of the individual Fumo time series.

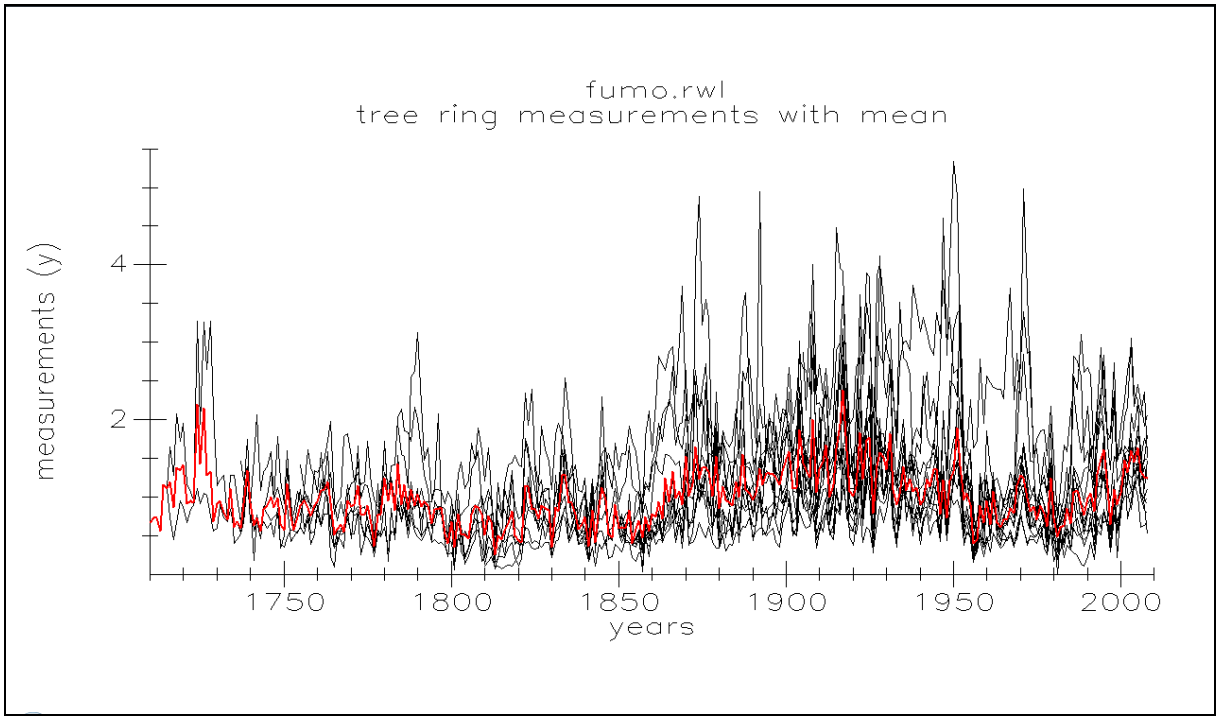

Fig. 4-16 Fumo raw tree-ring series with mean (red line).

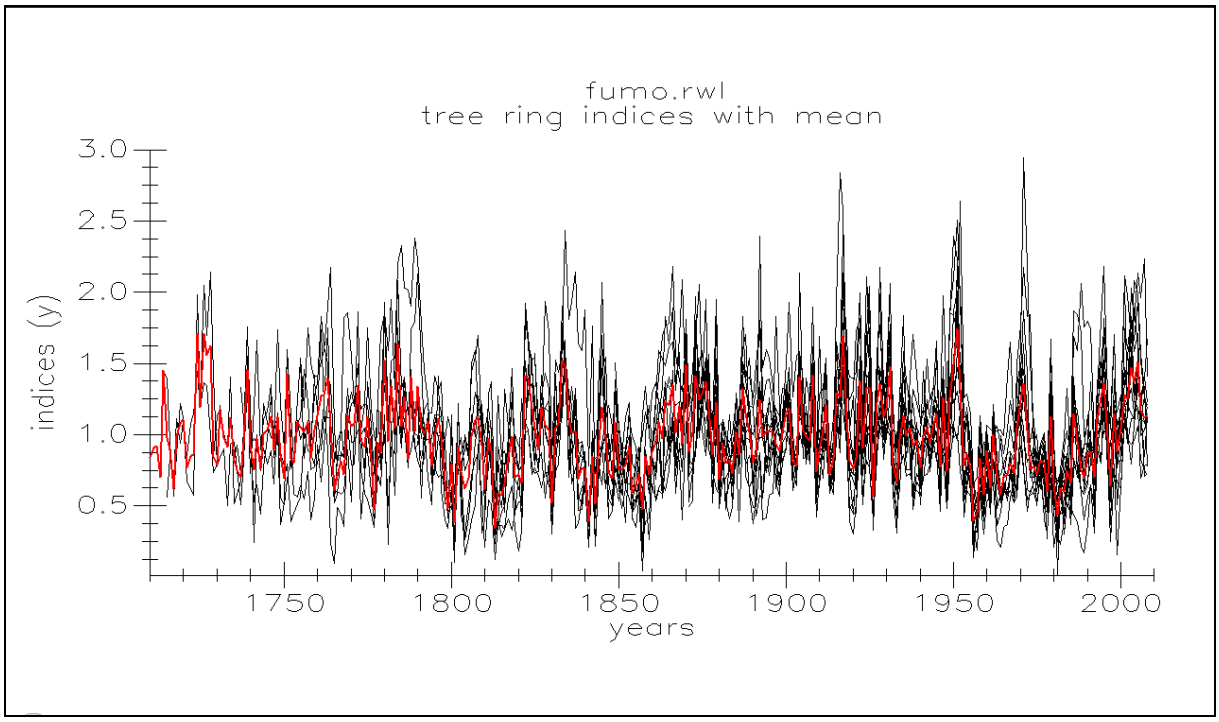

Fig. 4-17 Fumo standardized tree-ring series with mean (red line).

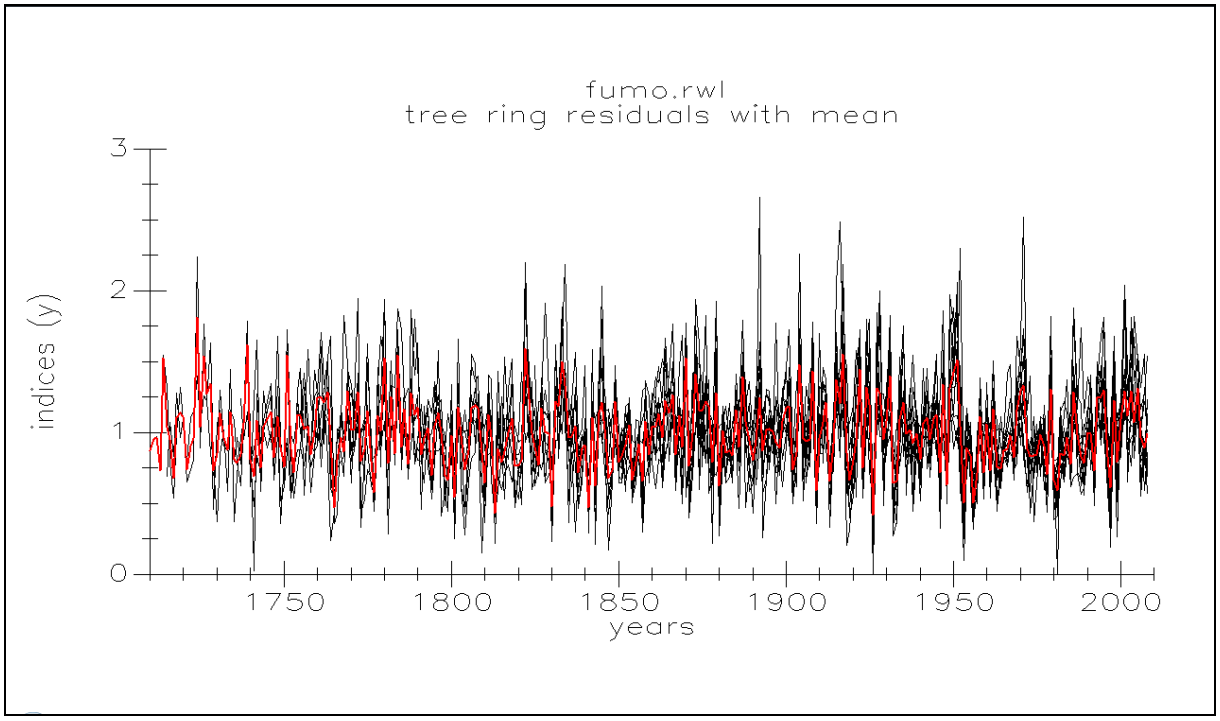

Fig. 4-18 Fumo residual tree-ring series with mean (red line).

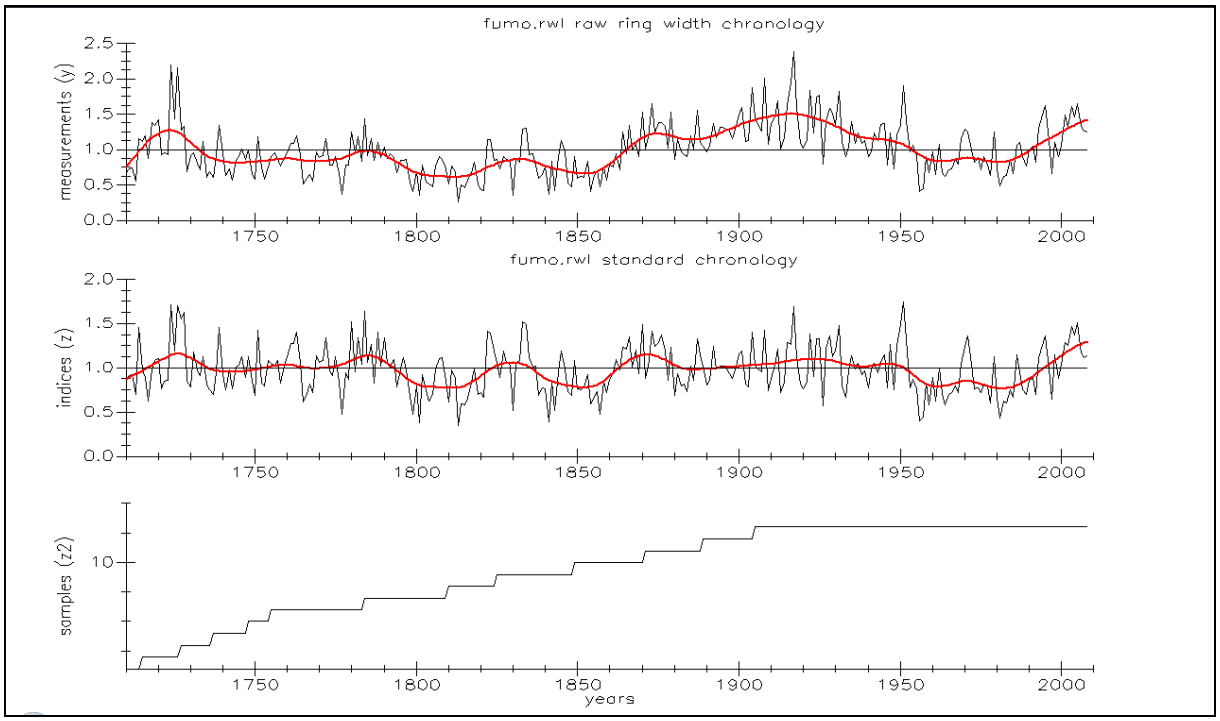

Fig. 4-19 Fumo raw and standard tree-ring chronologies with mean (red line), the sample depth is visible in the figure bottom.

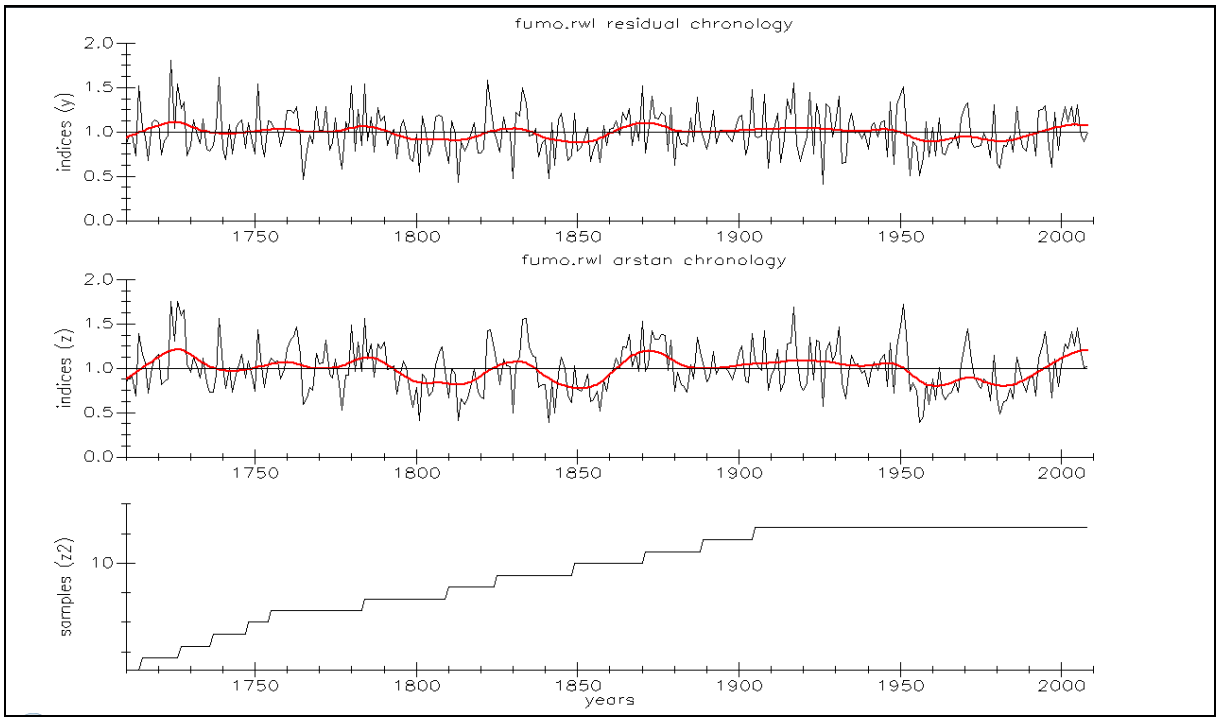

Fig. 4-20 Fumo residual and Arstan tree-ring chronologies with mean (red line), the sample depth is visible in the figure bottom.

Val Presena

The Val Presena mean site chronology is composed by 8 individual larch tree-ring series. The sampling campaign in Val Presena was conducted during June 2005. The last ring in the cores was not completed, then the tree-ring measurement was stopped at the 2004 annual ring in order two avoid an incorrect low tree-ring width value into the tree-ring series. The total sampled trees in this site were 13, but 5 of these did not get trough the minimum criterion of sample inclusion. The Presena mean site larch chronology spans from 1645 to 2004 (369 years) (Tab. 4-9 and 4-10, Figs. from 4-21 to 4-25).

	Time-span	Yrs	**TIME PLOT OF TREE-RING SERIES: Presena**	Ident
1	1899 2004	106	. . . . . <==========>	PRS11m
2	1892 2004	113	. . . . . <==========>	PRS12m
3	1889 2004	116	. . . . . <==========>	PRS13m
4	1817 2004	188	. . . .<==================>	PRS1me
5	1718 2004	287	. .<============================>	PRS5me
6	1645 2004	360	<==================================>	PRS6me
7	1880 2004	125	. . . . . <==========>	PRS7me
8	1870 2004	135	. . . . . <==========>	PRS8me
1600 1650 1700 1750 1800 1850 1900 1950 2000				

Tab. 4-9 time plot of the Presena individual tree-ring series.

Series	Interval	Years	Corr. With Master
1 PRS11m	1899 2004	106	0.67
2 PRS12m	1892 2004	113	0.74
3 PRS13m	1889 2004	116	0.62
4 PRS1me	1817 2004	188	0.60
5 PRS5me	1718 2004	287	0.60
6 PRS6me	1645 2004	360	0.60
7 PRS7me	1880 2004	125	0.62
8 PRS8me	1870 2004	135	0.70
Total or mean:	1430		0.64

Tab. 4-10 correlation with master (the time series of maximum length) of the individual Presena time series.

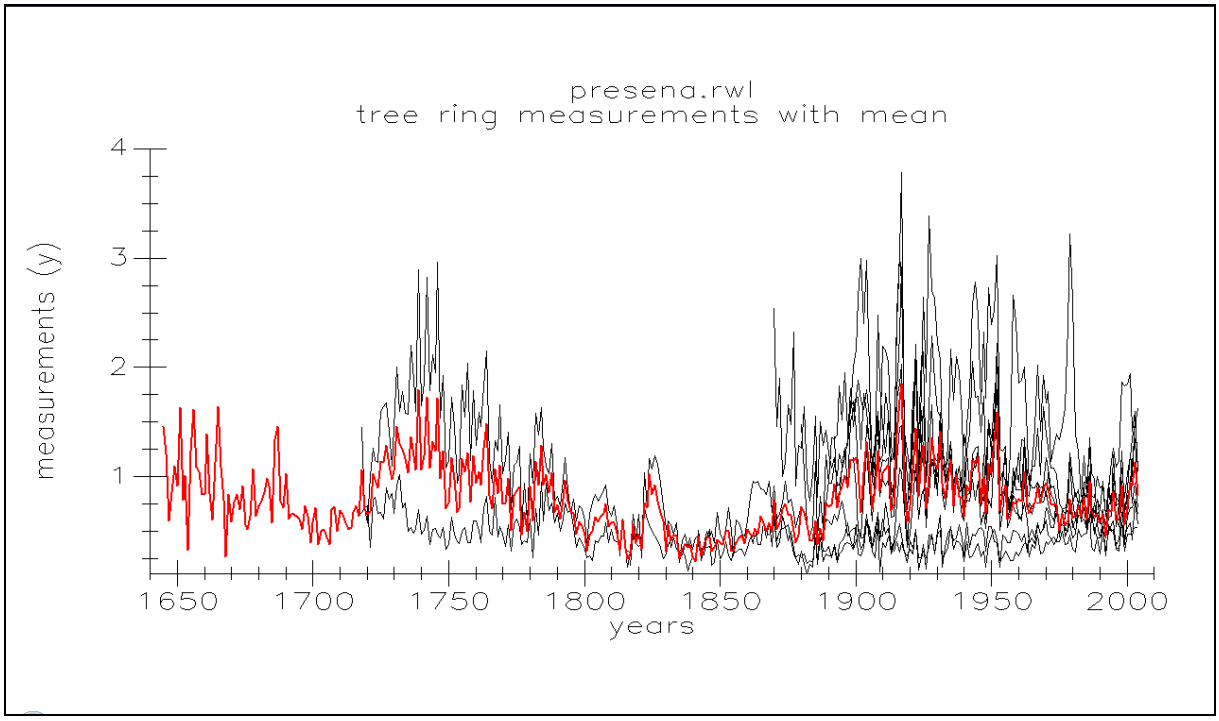

Fig. 4-21 Presena raw tree-ring series with mean (red line).

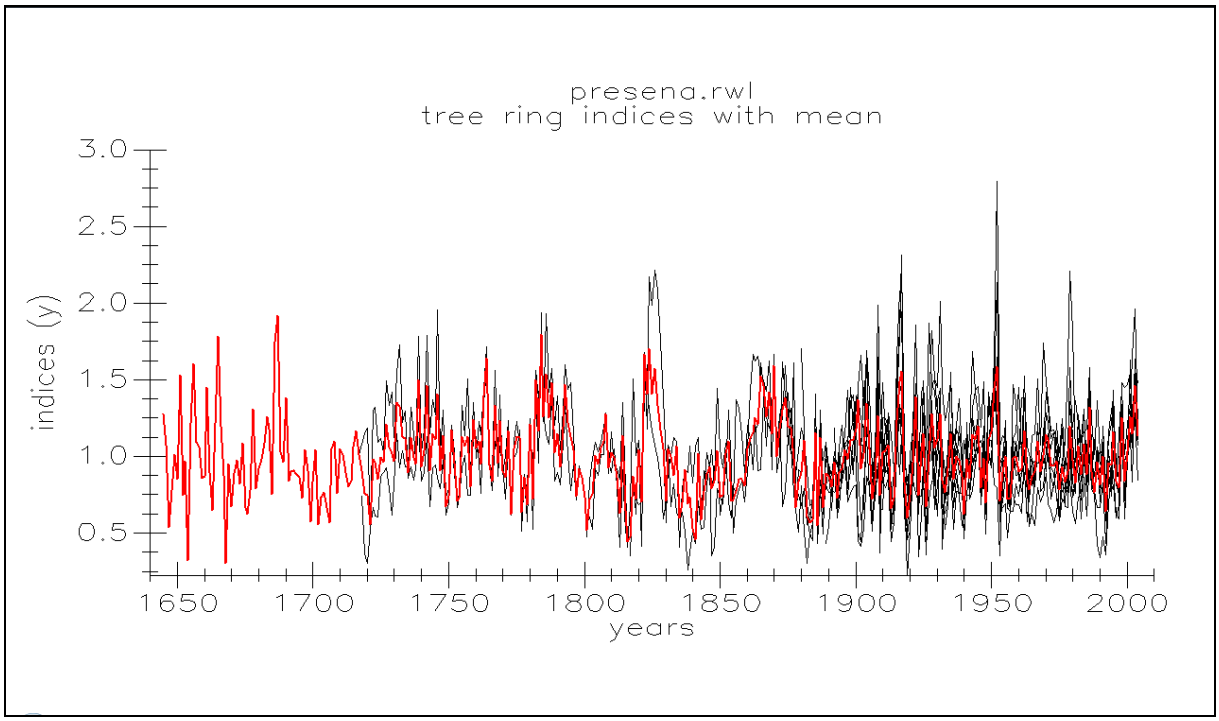

Fig. 4-22 Presena standardized tree-ring series with mean (red line).

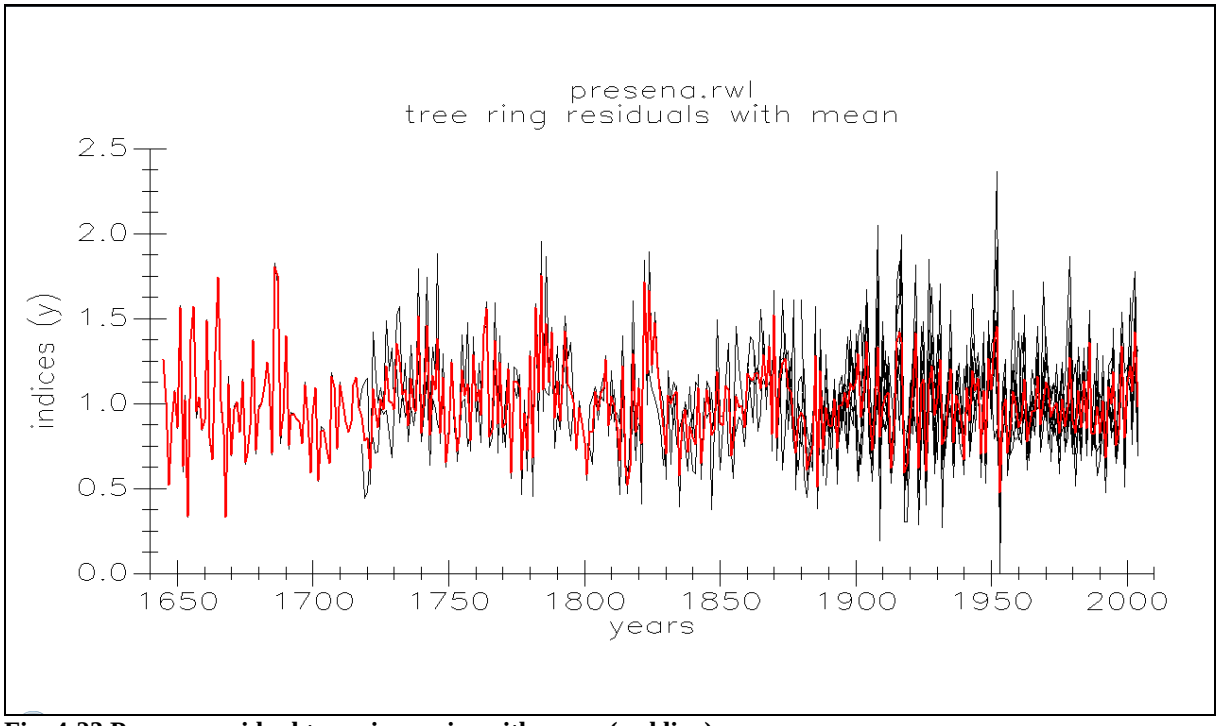

Fig. 4-23 Presena residual tree-ring series with mean (red line).

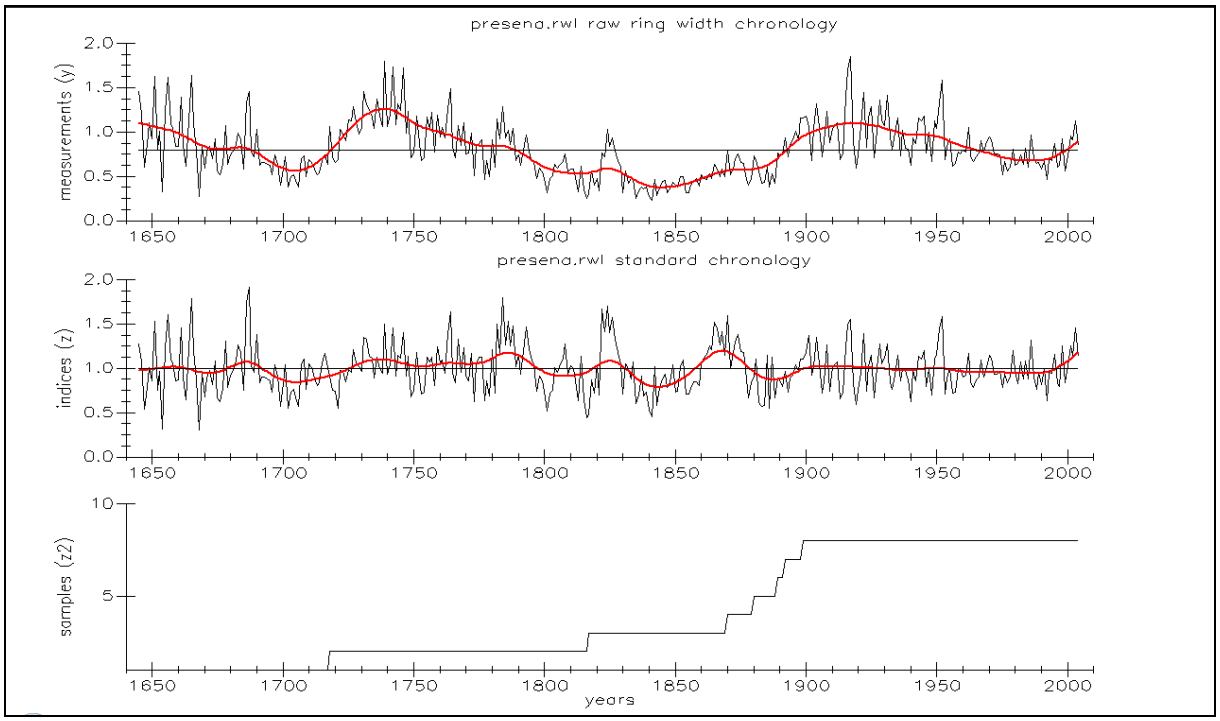

Fig.4-24 Presena raw and standard tree-ring chronologies with mean (red line), the sample depth is visible in the figure bottom.

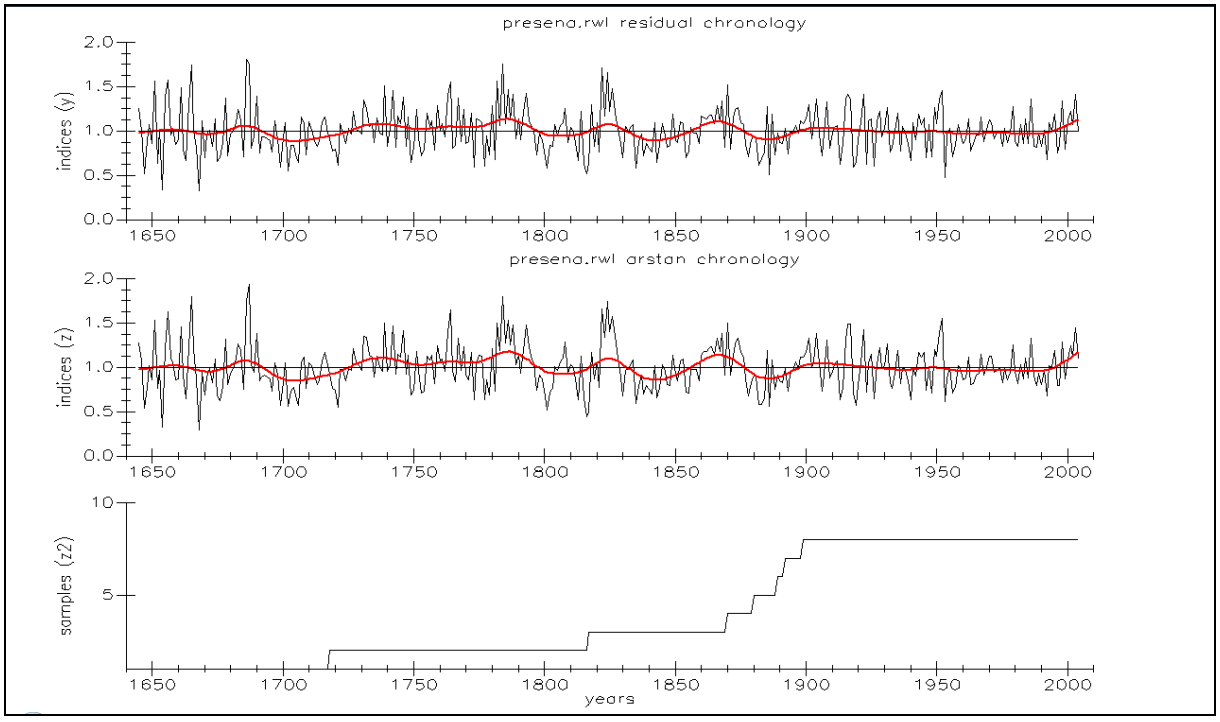

Fig. 4-25 Presena residual and Arstan tree-ring chronologies with mean (red line), the sample depth is visible in the figure bottom.

Val Malga

The Malga larch mean site chronology is composed by 11 mean individual tree-ring series. It is the shorter chronology of the entire data set, actually its length is only 202 year spanning from 1807 to 2008 (Tab. 4-11). The mean intercorrelation of the raw series is 0,66 (Tab. 4-12). In figures 4-26, 4-27 and 4-28 are the raw, standardized and residual individual tree-ring series. In figures 4-29 and 4-30 are plotted the raw standardize and residual Malga larch chronologies.

	Time-span	Yrs	**TIME PLOT OF TREE-RING SERIES: Malga**	Ident.
1	1886 2008	123	. . . <==========>	MAL70m
2	1854 2008	155	. . <==========>	MAL62m
3	1814 2008	195	. .<==========>	MAL16m
4	1807 2008	202	. <==========>	MAL17m
5	1814 2008	195	. .<==========>	MAL18m
6	1815 2008	194	. .<==========>	MAL15m
7	1902 2008	107	. . . <=========>	MAL36m
8	1891 2008	118	. . . <==========>	MAL37m
9	1893 2008	116	. . . <==========>	MAL26m
10	1883 2008	126	. . . <==========>	MAL69m
11	1872 2008	137	. . . <==========>	MAL64m
			1750 1800 1850 1900 1950 2000	

Tab. 4-11 time plot of the Malga individual tree-ring series.

Series	Interval	Years	Corr. with Master
1 MAL70m	1886 2008	123	0.67
2 MAL62m	1854 2008	155	0.56
3 MAL16m	1814 2008	195	0.75
4 MAL17m	1807 2008	202	0.70
5 MAL18m	1814 2008	195	0.62
6 MAL15m	1815 2008	194	0.78
7 MAL36m	1902 2008	107	0.70
8 MAL37m	1891 2008	118	0.63
9 MAL26m	1893 2008	116	0.57
10 MAL69m	1883 2008	126	0.64
11 MAL64m	1872 2008	137	0.62
Total or mean:		1668	0.66

Tab. 4-12 correlation with master (the time series of maximum length) of the individual Malga time series.

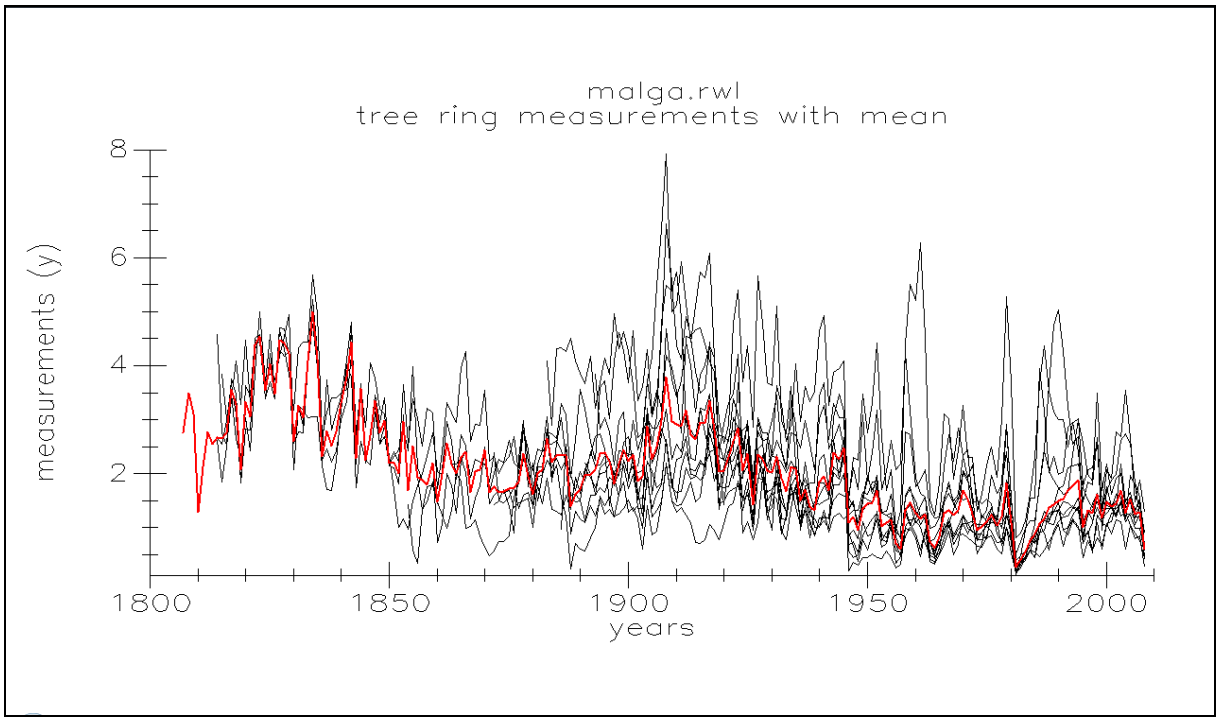

Fig. 4-26 Malga raw tree-ring series with mean (red line).

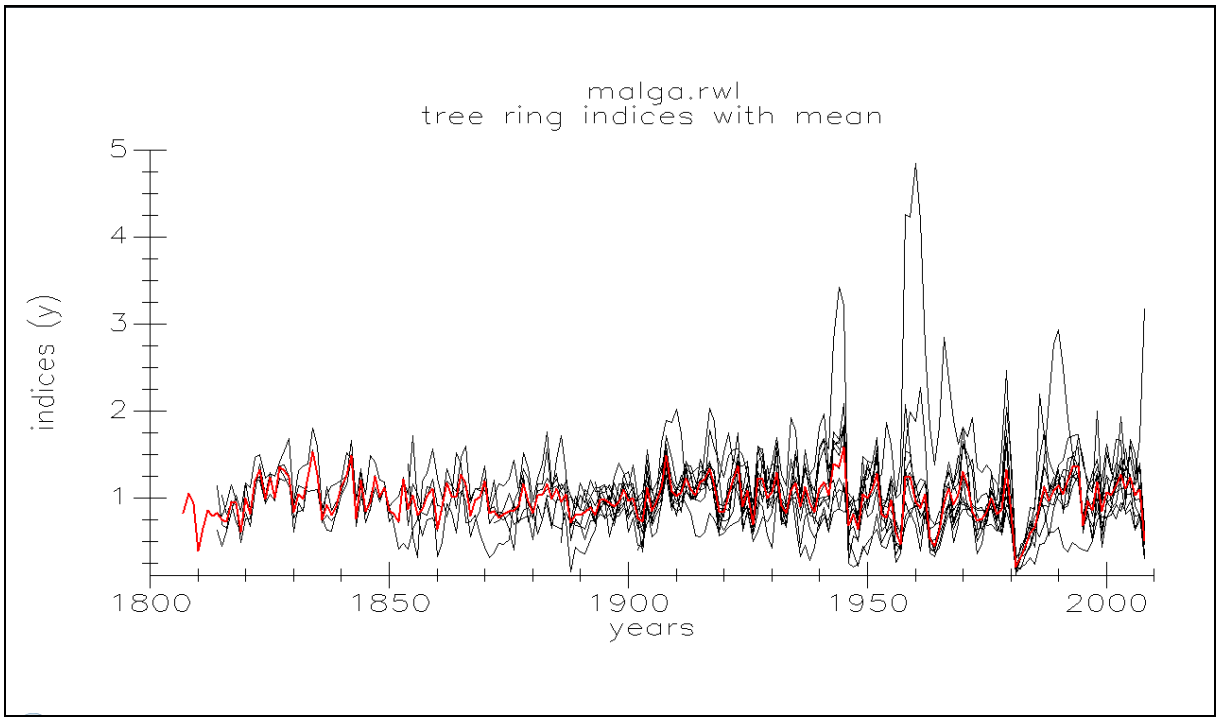

Fig. 4-27 Malga standardized tree-ring series with mean (red line).

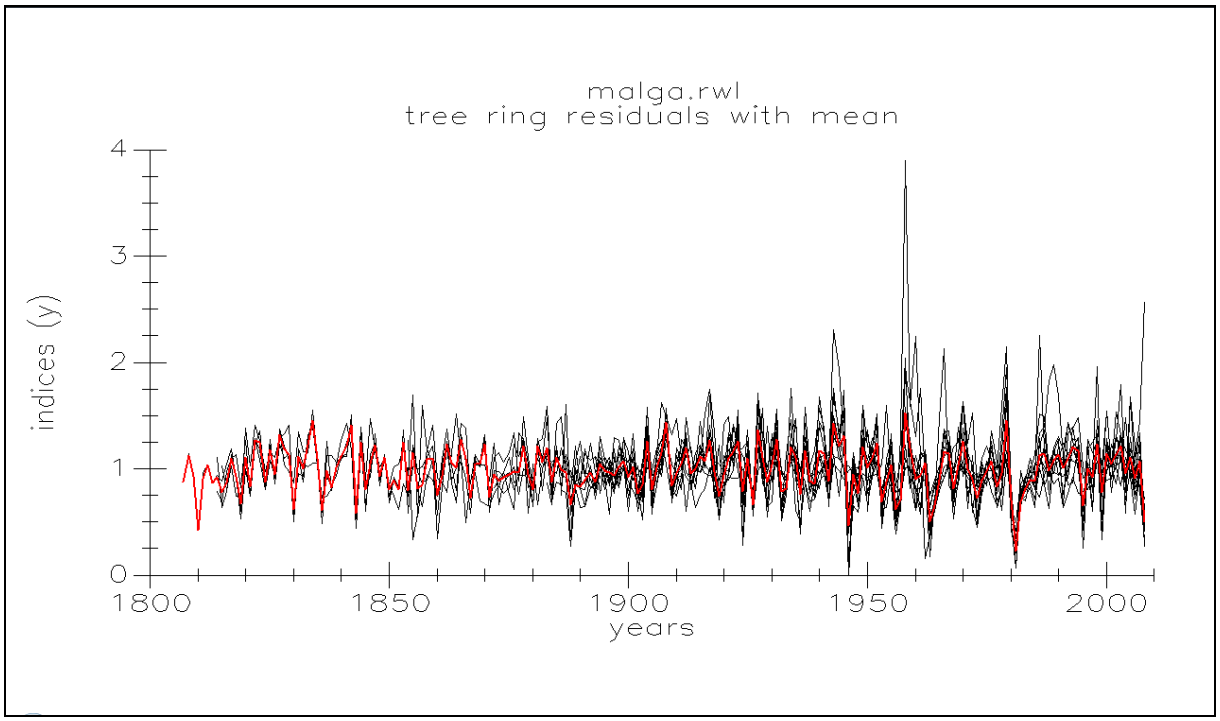

Fig. 4-28 Malga residual tree-ring series with mean (red line).

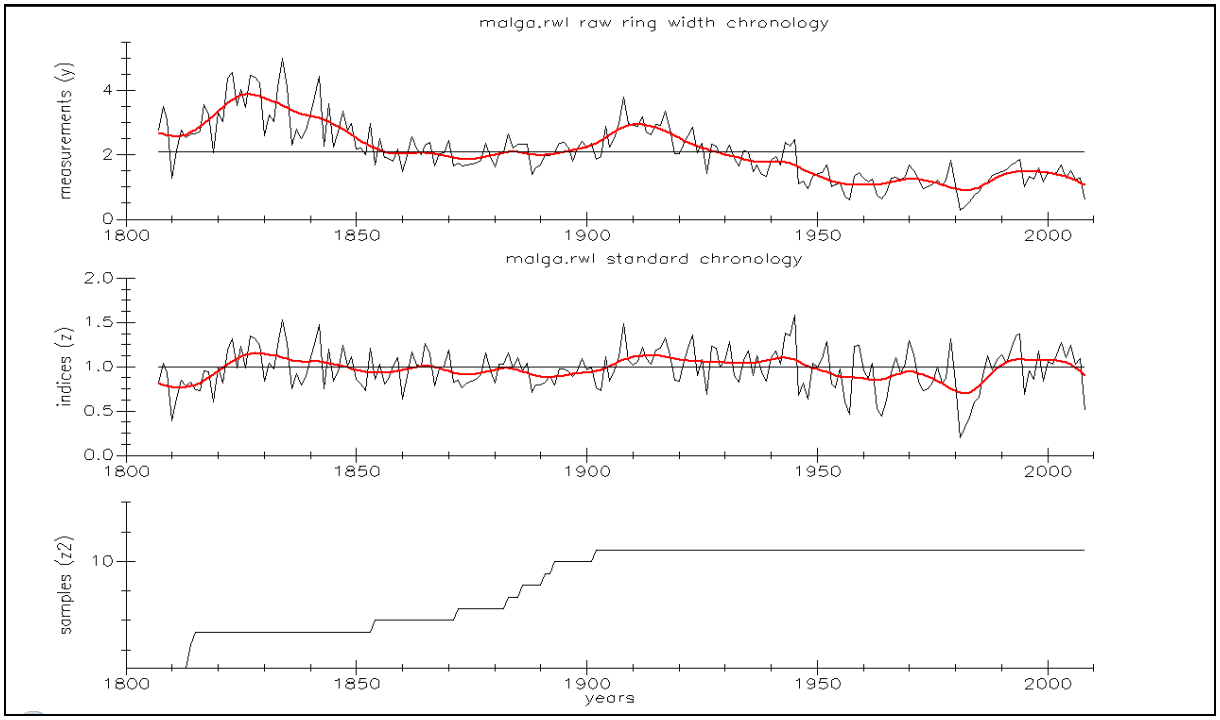

Fig. 4-29 Malga raw and standard tree-ring chronologies with mean (red line), the sample depth is visible in the figure bottom.

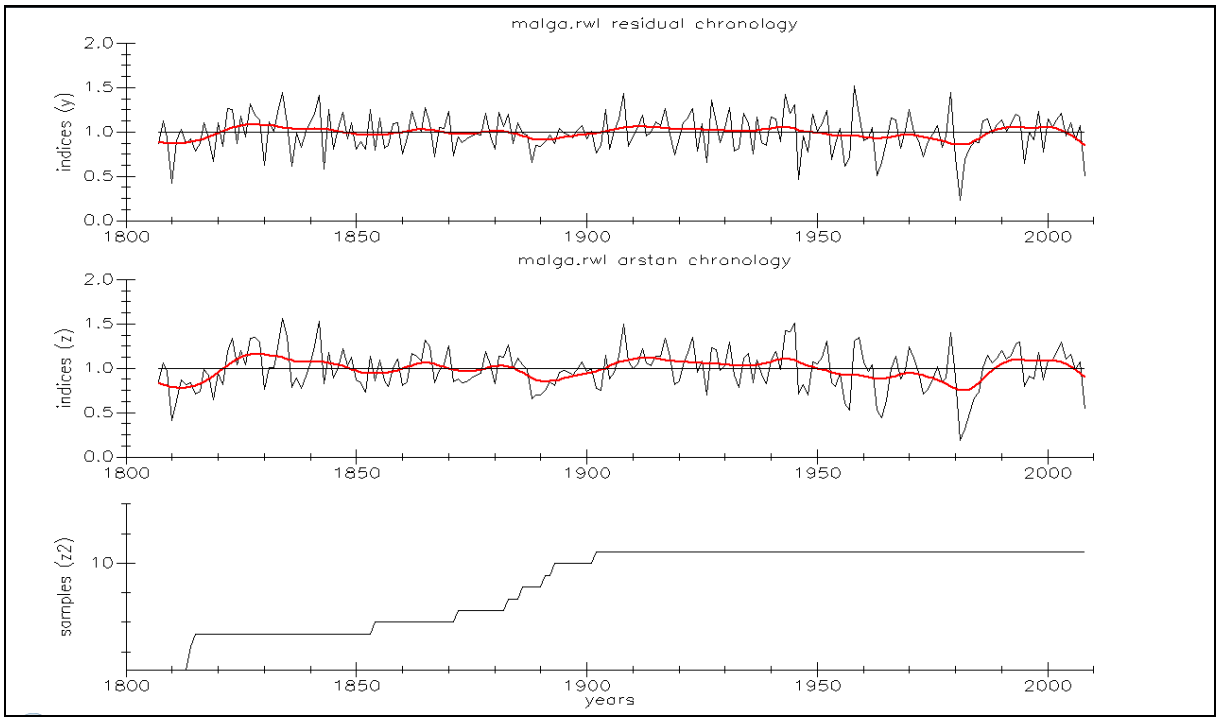

Fig.4-30 Malga residual and Arstan tree-ring chronologies with mean (red line), the sample depth is visible in the figure bottom.

Chronology descriptive statistics

The time series analysis of autocorrelation confirms the reduced value of biological persistence in the five residual chronologies compared with the standardized and raw chronologies (Fig. 4-31). For this reason we have chosen to use the residual version of the four mean site chronologies in the following climatic analysis.

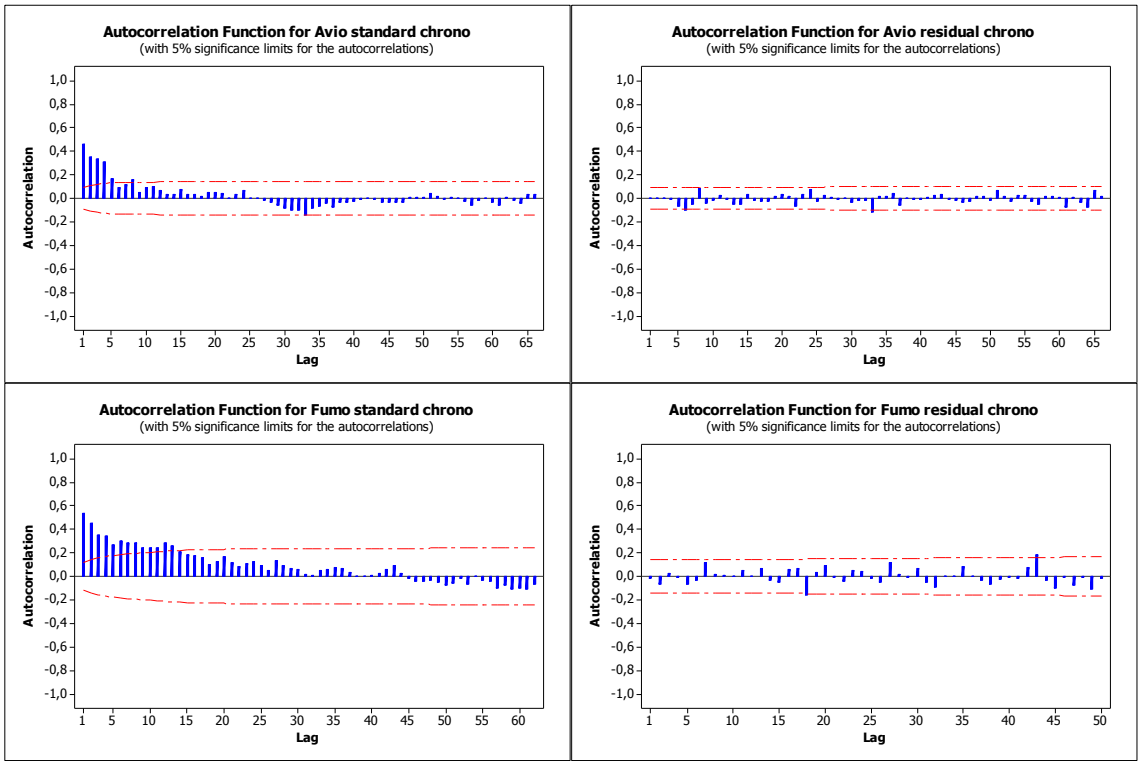

…continue from the previous page

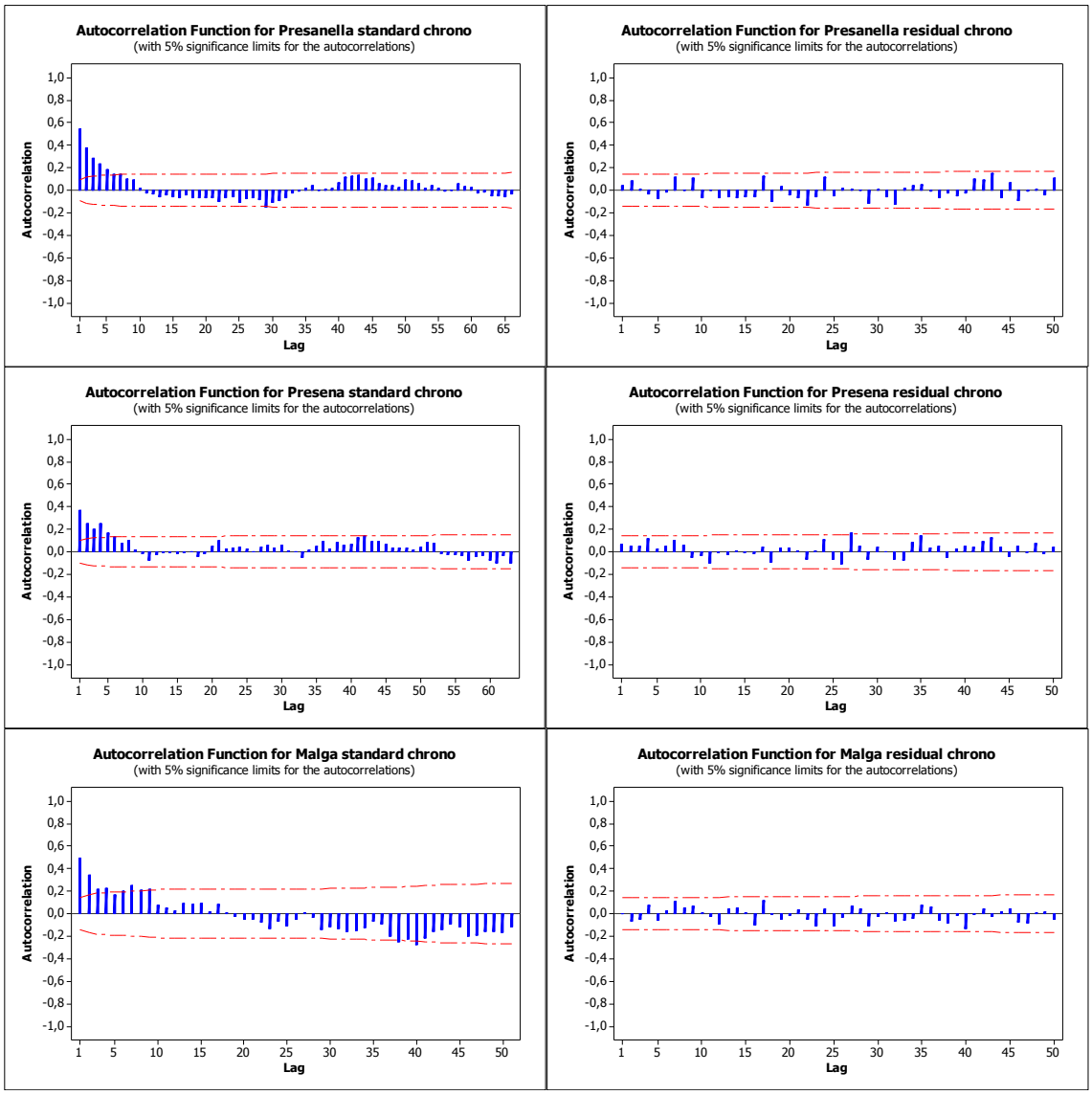

Fig. 4-31 Autocorrelation analysis results for the five mean site chronologies. On the left the autocorrelation function computed for the five standardized chronologies, on the right the autocorrelation function computed for the five residual chronologies.

The Pearson's correlation coefficient computed between the five larch residual chronologies evidences good correlation values for four of the five chronologies (Tab.4-13). A good correlation should testify a synchronous answer to environmental changing and a probable common climate signal. The Malga residual chronology reveals to be the most problematic mean site chronology, with the lowest correlation values (r ranging from 0,42 to 0,54) with all the other chronologies. The highest correlation value was found between the Presanella and the Fumo residual chronologies (r = 0,75) (Tab.4-13).

The cluster analysis performed on the common period (1818-2004), further confirm this results. It is actually evident the distance between the Malga chronology and the other

four chronologies. It appears also clear the highest similarity existing between Fumo and Presanella Chronologies (Fig. 4-32).

	Malga_res	Fumo_res	Presena_res	Presanella_res
Fumo_res	0,54			
Presena_res	0,42	0,71		
Presanella_res	0,52	0,75	0,66	
Avio_res	0,425	0,72	0,68	0,67

Tab. 4-13 matrix of correlation (r) between the five mean residual chronologies.

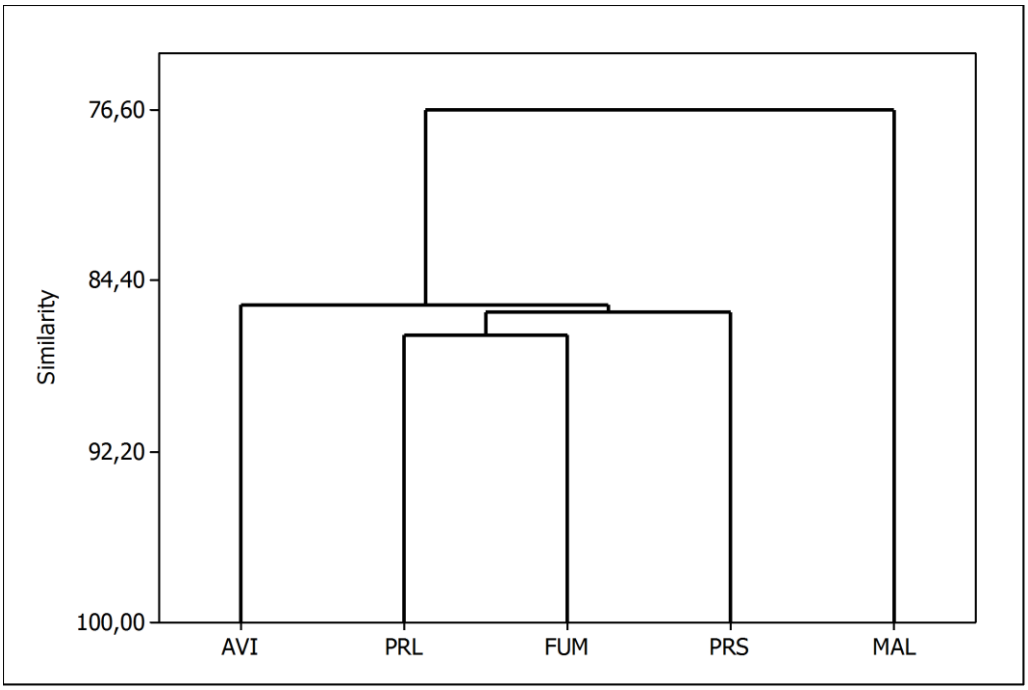

Fig. 4-32 Dendrogram resulting from the cluster analysis for the five mean residual chronologies.

In tab. 4-14 are summarized essential statistics for the five mean site residual chronologies.

It is evident the reduced values of first order autocorrelation in the residual chronologies comparing with raw and standardized chronologies. In the residual chronologies it is also evident a higher SNR value and a general reduction of standard deviation comparing with raw and standardized chronologies. The Fumo residual chronology shows the highest SNR values (16,86).

The mean sensitivity values are higher than 0,2 for all the five chronologies with the highest value (0,286) found for the Fumo residual chronology. The lowest mean sensitivity values were observed for the Presanella and Malga residual chronologies. High values of

Mean sensitivity denote an elevated proportion of high-frequency variance in our chronologies and are consistent with those reported for larch in high-altitude forest areas of the Eastern Italian Alps (Carrer & Urbinati, 2004, 2006).

Limiting our analysis to the period with an SSS of at least 0,85 imply that the five residual chronologies' length was truncated at the first year with an SSS> 0,85 (Tab.4-32, Fig. 4-33).

Statistics	Avio	Presanella	Fumo	Presena	Malga
First year of chronology	1550	1550	1710	1645	1807
Last year of chronology	2007	2005	2008	2004	2008
Chronology length (year)	459	456	299	360	202
Number of trees	11	14	13	8	11
Number of radii	22	30	26	16	22
Mean ring width (mm)	348,0	256,6	214,8	178,8	151,6
First year SSS>0,85	1589(3)	1596(3)	1738(3)	1818(3)	1816(4)
Mean sensitivity	0,256	0,231	0,286	0,283	0,263
Standard deviation	0,224	0,198	0,242	0,245	0,208
First order autocorrelation	-0,023	-0,009	-0,002	-0,061	-0,108
Common interval analysis					
First year	1818	1896	1925	1951	1936
Signal to noise ratio	10,774	4,924	16,861	8,654	12,255

Tab. 4-14 compared statistics of the five residual chronologies.

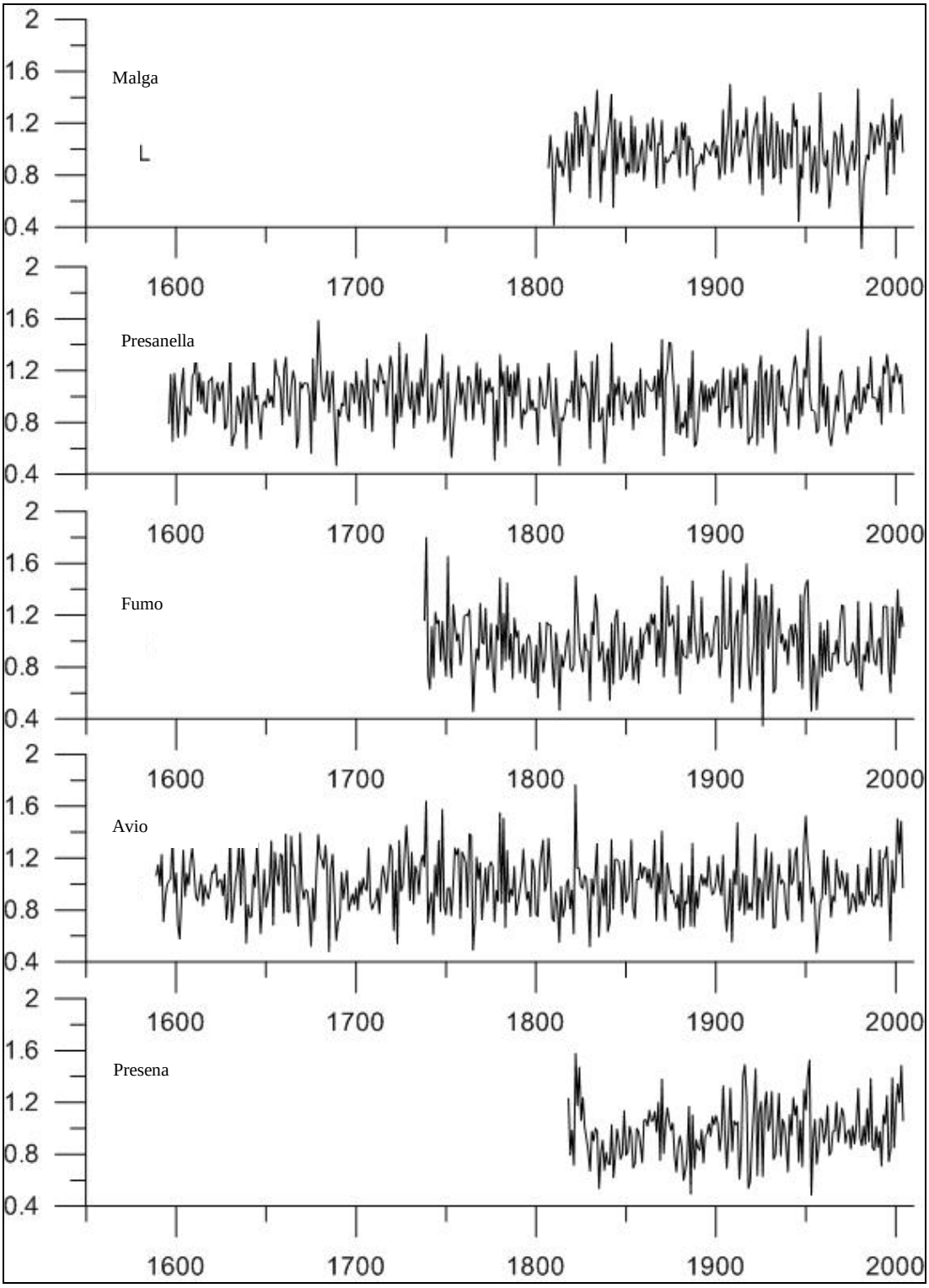

Fig. 4-33 time series plot of the five residual chronologies.

Beam sections dating results

The twelve samples coming from beams of barns in Val Vermigliana are all well-preserved. Piths are present in the whole samples, but in no one of them there is evidence of bark. The shape of cross-sections (Fig. 2-9) testifies that the larch logs have been squared and the bark removed before of their use as beams. In the most part of samples a part of sapwood is present, but it was not possible to estimate the felling date. All the dating here proposed must be considered as *non-cutting* dates (Baillie, 1982) (Tab. 4-15; Fig.4-34).

The mean growth series length spans from 57 to 153 annual rings. More in detail, five disks (Spozìni, Cavèi, Nìe, Barèe1, and Mazini) come from very young trees with tree-ring growth series shorter than 100 annual rings. For these samples we propose here only a first tentative dating (Billamboz, 2008), however they need further investigations to estimate the definitive dating. Collecting a higher number of samples from different beams belonging to the same barn could help in this purpose.

As expected, higher values of cross-correlation statistics were obtained for all samples, when cross-dating the mean tree-ring series with the two Italian reference chronologies: Eastern Alps (AOI, Bebber 1990) and Fodara Vedla (FOD, Hüsken & Schirmer, 1993).

The t-test shows significant values for 7 of the 12 analysed samples with all the four reference chronologies. These samples come from beams belonging to the barns named *Maso Cavèi*, *Maso Podéte*, *Maso Grìi*, *Malga Boai* and *Malga Mezzolo* (Tab.4-15).

Short tree-ring series (<100 annual rings) dating is often problematical, because it is actually possible that more than one dating results seem valid for the same series (Miles, 1997). Three of the analysed short series (Spozini, Nìe, and BarèeI) show several possible dating, no one of which seems to be indubitable (Baillie, 1982, Miles, 1997). The dating here proposed for these samples is that one showing the highest statistical values in the cross-dating with all the four reference chronologies (Tab.4-15).

In one case (Mazini, 89 annual rings) significant cross-dating statistics were obtained with only one of the four reference chronologies (Fodara Vedla, t = 4.32, Glk = 69.7), then the dating of this sample is not sufficiently replicated to be considered reliable (Miles, 1997).

The proposed dating for the beam collected in the *maso Nìe* (1635-1706, 72 annual rings), does not show satisfying statistics values with anyone of the four reference chronologies, and it was chosen considering that some oral evidences indicate this barn as one of the oldest in the area for its architecture.

The highest statistics values in the cross-correlation of the short tree-ring series were obtained for the sample coming from *maso Cavèi* (t value ranges from 4,24 to 6,59; Glk value ranges from 63,0 to 68,8 in the cross-dating with all the four reference chronologies). The very little number of annual rings of this sample (77), does not allow to consider this dating definitive. Therrefore, an inscription present on the barn doorstep (1788), that presumably testifies the year of construction, is absolutely consistent with our dating (1784).

A similar inscription (1781) is visible on the doorstep of *Malga Boai*, but the dating of the two samples coming from this barn (Boai1, 1719-1871; Boai2, 1701-1851), reveals two posterior dates compared to the inscribed year of building. Due to the very high statistic values of t and Glk (t > 4,5 and Glk > 60 for the both samples with the two Italian reference chronologies) and the sufficient lengths of the two tree-rig series (153-151), we suppose that *Malga Boai* came under restoration treatments with the replacement of some beams.

One of the two samples collected in *Malga Mazzolo* (Mazzolo1, 1761-1913) results more recent than the other sample coming from the same barn (Mazzolo2, 1634-1742). We suppose that the first beam could belong to a newer part of the building, made up in a second time respect to its initial component, or that the barn has received some renovating interventions with beams replacement.

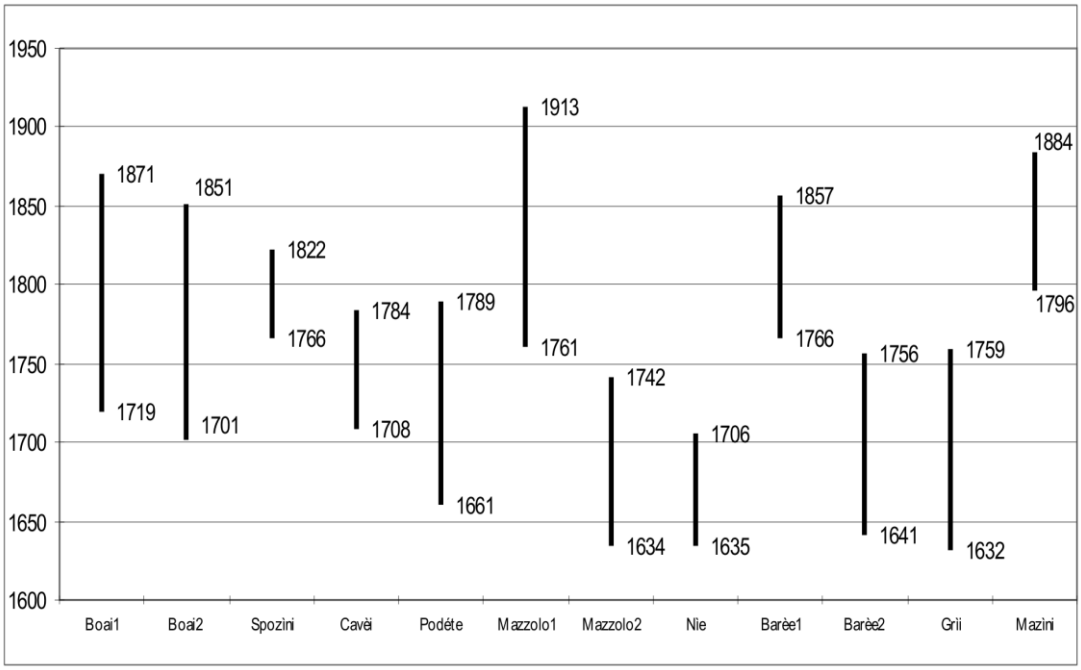

Fig. 4-34 Time plot of the twelve dated samples.

Tab. 4-15 Dating results. AOI: Alpi Orientali Italiane, Bebber 1990; FOD: Fodara Vedla, Hüsken & Schirmer, ITRDB; OBG: Obergurgl, Giertz ITRDB; OTZ: Ötzal ,Siebenlist-Kerner, 1984. The samples with the most reliable dating are underlined.

Sample	Reference chronologies	t-test	GLK	GLKsig	Rings	Dating	Inscribed date
Boai1	AOI	7.09	60.5	**	153	1719-1871	1781
	FOD	4.77	64.1	***			
	OBG	3.90	62.7	***			
	OTZ	4.02	65.7	***			
Boai2	AOI	8.99	71.5	***	151	1701-1851	
	FOD	6.12	69.2	***			
	OBG	3.63	66.6	***			
	OTZ	4.27	70.5	***			
Spozìni	AOI	3.49	59.6	-	57	1766-1822	---
	FOD	2.82	59.6	-			
	OBG	2.00	62.3	*			
	OTZ	2.27	58.8	-			
Cavèi	AOI	6.56	68.8	***	77	1708-1784	1788
	FOD	5.31	64.9	**			
	OBG	4.64	65.6	**			
	OTZ	4.24	63.0	*			
Podéte	AOI	6.23	68.6	***	129	1661-1789	---
	FOD	4.69	63.2	**			
	OBG	3.95	69.0	***			
	OTZ	4.35	67.4	***			
Mazzolo1	AOI	6.43	62.1	**	153	1761-1913	---
	FOD	5.26	63.1	***			
	OBG	5.26	62.4	**			
	OTZ	6.36	65.0	***			
Mazzolo2	AOI	7.07	71.1	***	109	1634-1742	
	FOD	7.08	66.1	***			
	OBG	2.86	58.3	*			
	OTZ	4.43	62.8	**			
Nìe	AOI	3.66	53.5	-	72	1633-1703	---
	FOD	4.65	61.1	*			
	OBG	3.29	67.4	**			
	OTZ	3.90	57.6	-			
Barèe1	AOI	3.20	67.4	***	92	1766-1857	---
	FOD	3.07	67.4	**			
	OBG	1.99	56.0	-			
	OTZ	2.42	57.6	-			
Barèe2	AOI	4.19	62.1	**	116	1641-1756	
	FOD	4.06	57.3	-			
	OBG	3.05	59.5	*			
	OTZ	2.80	54.3	-			
Grìi	AOI	6.33	71.1	***	128	1632-1759	---
	FOD	5.67	69.1	***			
	OBG	4.13	60.9	**			
	OTZ	5.23	65.2	***			
Mazini	AOI	3.22	54.5	-	89	1796-1884	---
	FOD	4.32	69.7	***			
	OBG	1.77	62.4	**			
	OTZ	2.31	60.1	*			

Climatic Analysis results

Correlations with monthly mean temperatures

The monthly climatic analysis of tree-ring growth/mean monthly temperature correlation shows a strong positive influence of Summer (JJA) temperatures on the tree growth over the whole considered time period (1818-2004). June mean temperatures present the strongest correlation coefficient values (CC). A positive influence of autumn of the previous year (SON-1) mean temperatures is also visible, even if less significant. Since the considered chronologies come from high elevation sites, we expected to obtain higher values of correlation coefficients when computed between tree-ring chronologies and temperature data coming from high-elevation stations (>1400 m, HEST). On the contrary, we found higher CC values when they were computed between chronologies and temperature data coming from low-elevation stations (<1400 m, LEST). Indeed, we found that the highest correlation coefficient values are those calculated with temperature data coming from LEST (Figs 4-35 to 4-42). This difference is higher for the CC computed with July mean temperatures (all of the five residual chronologies), and for the CC calculated with June mean temperatures (four of the five residual chronologies).

The Avio chronology shows the highest CC values in the analysis performed with June and July monthly mean temperatures (Fig. 4-36).

The only two chronologies that reveal a positive, although very weak, correlation with late spring temperatures (May) are Malga and Presena chronologies. We have obtained equal CC values if computed with HEST or LEST in the case of Malga chronology (Fig. 4-40) and higher CC values if computed with HEST than with LEST in the case of Presena chronology (Fig. 4-39, Tab. 4-16).

It is interesting to observe that the CC values computed between Presena and Presanella chronologies and August mean temperatures are not statistically significant, but show higher values if calculated with HEST than with LEST (Figs 4-38 to 4-42, Tab. 4-16). All the other chronologies show non significant correlations with August mean temperatures (Figs 4-35 to 4-37, Tab. 4-16).

The strongest CC values with autumn temperatures of the previous year are those calculated between October of the previous year mean temperature. Higher CC values were obtained if the correlation was computed with LEST than with HEST October mean temperatures. We have obtained a positive correlation of the five chronologies with

November and December LEST temperature. The correlations with November and December HEST temperature are significant only for the Fumo and Malga chronologies (November) (Figs 4-37 and 4-39, Tab. 4-16) and for Presena and Malga chronologies (December) (Figs 4-39 and 4-40 to 8, Tab 16). The master chronology (All) computed by averaging four of the five chronologies (Avio, Fumo, Presanella and Presena), summarize the correlation results obtained for the four chronologies. The climatic analysis shows the highest CC values for early Summer temperatures (June and July), a positive but not significant influence of October-1 mean temperatures, and again higher CC values with LEST than with HEST (Figs 4-35, 4-36, 4-41 and 4,42 , Tab.4-16).

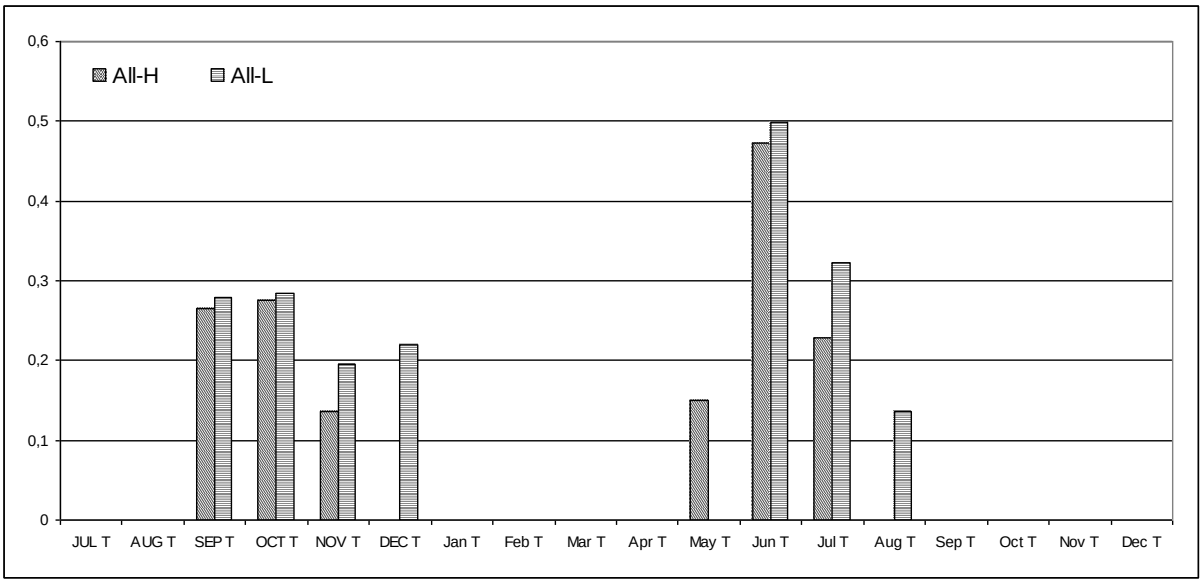

Fig. 4-35 Correlation coefficient calculated between the master chronology (All) and monthly temperatures coming from high-elevation stations (H) and low-elevation station (L). Only significant values are shown (significance assessed by means of the 95th percentile range).

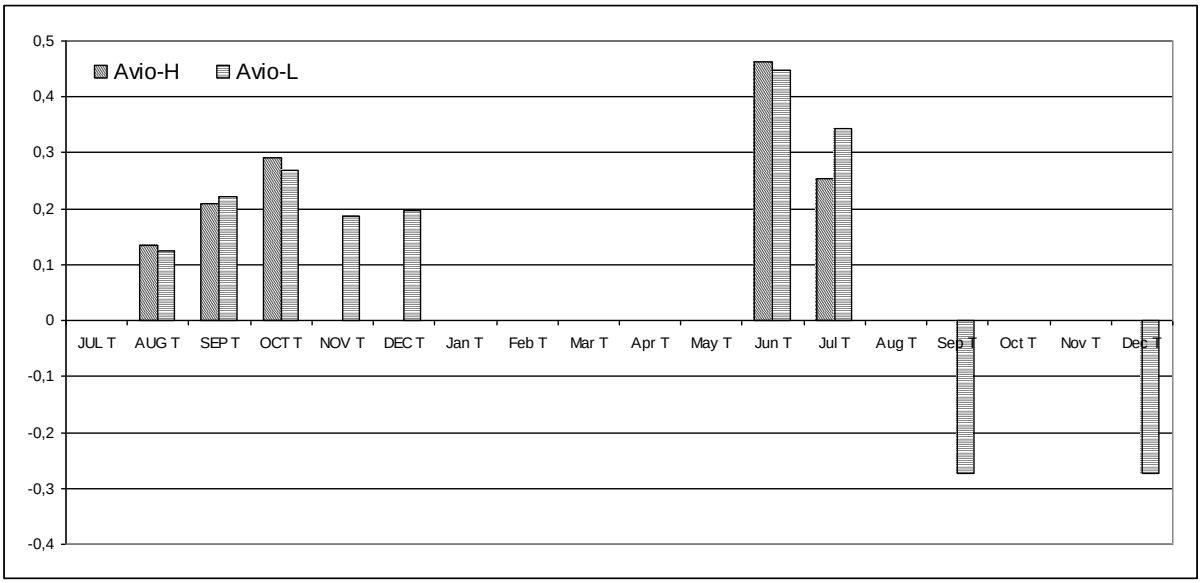

Fig. 4-36 Correlation coefficient calculated between the Avio chronology and monthly temperatures coming from high elevation stations (H) and low elevation station (L). Only significant values are shown (significance assessed by means of the 95th percentile range).

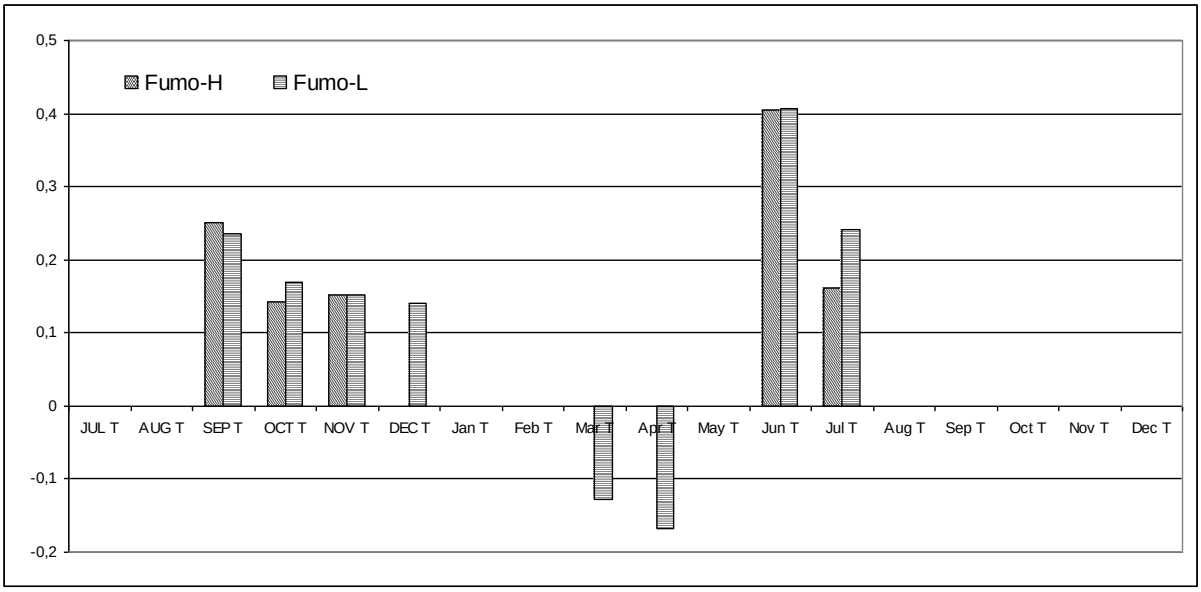

Fig. 4-37 Correlation coefficient calculated between the Fumo chronology and monthly temperatures coming from high elevation stations (H) and low elevation station (L). Only significant values are shown (significance assessed by means of the 95th percentile range).

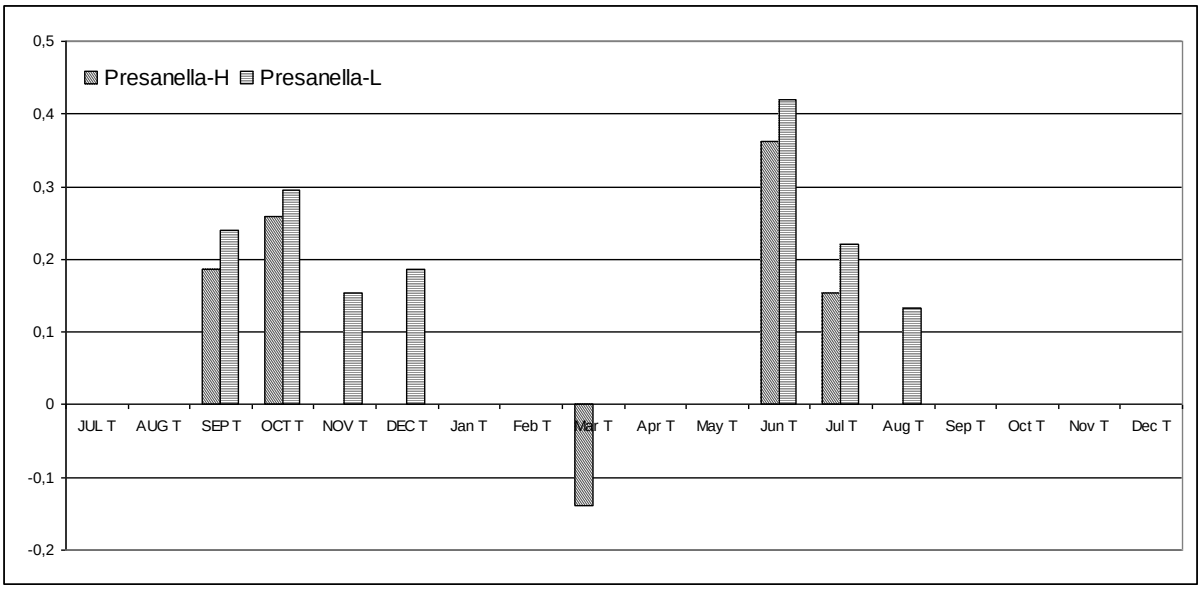

Fig. 4-38 Correlation coefficient calculated between the Presanella chronology and monthly temperatures coming from high elevation stations (H) and low elevation station (L). Only significant values are shown (significance assessed by means of the 95th percentile range).

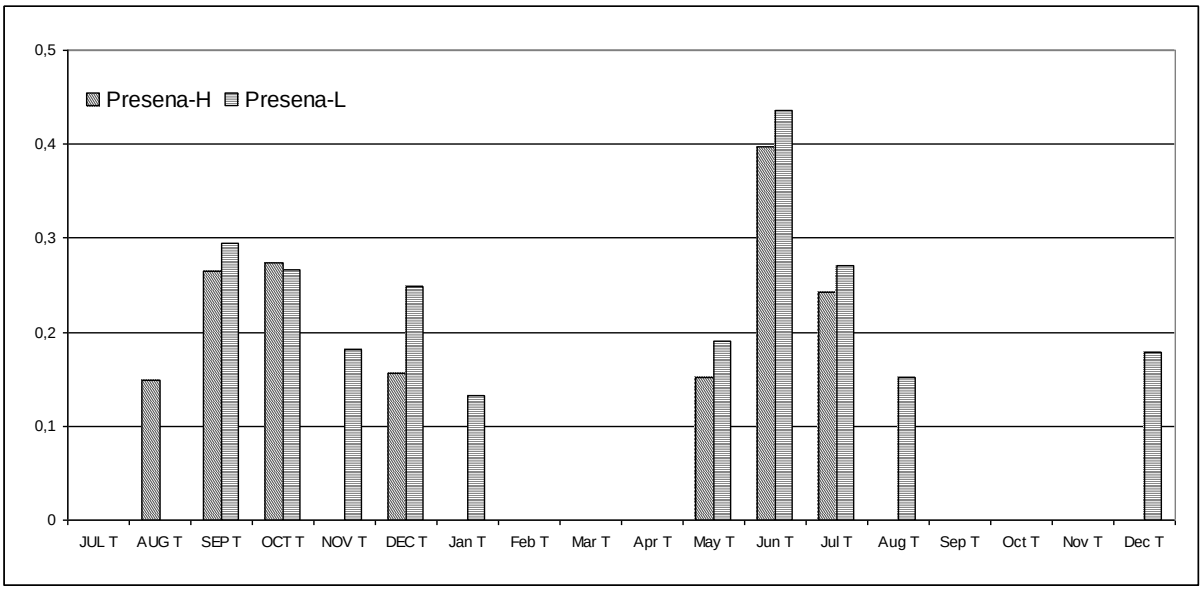

Fig. 4-39 Correlation coefficient calculated between the Presena chronology and monthly temperatures coming from high elevation stations (H) and low-elevation station (L). Only significant values are shown (significance assessed by means of the 95th percentile range).

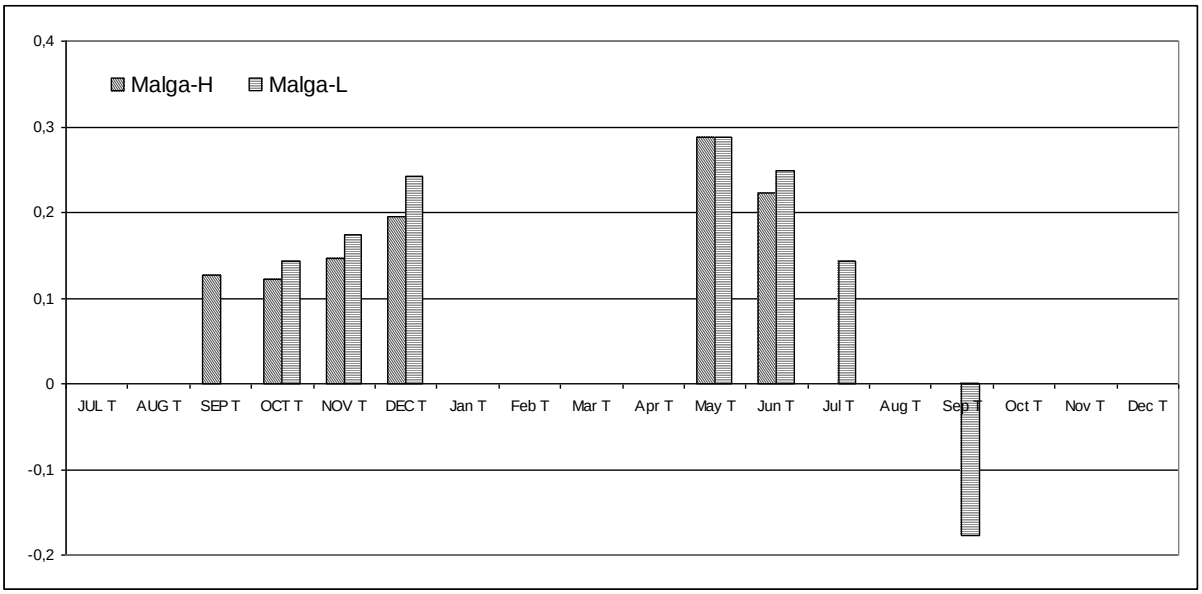

Fig. 4-40 Correlation coefficient calculated between the Malga chronology and monthly temperatures coming from high elevation stations (H) and low-elevation station (L). Only significant values are shown (significance assessed by means of the 95th percentile range).

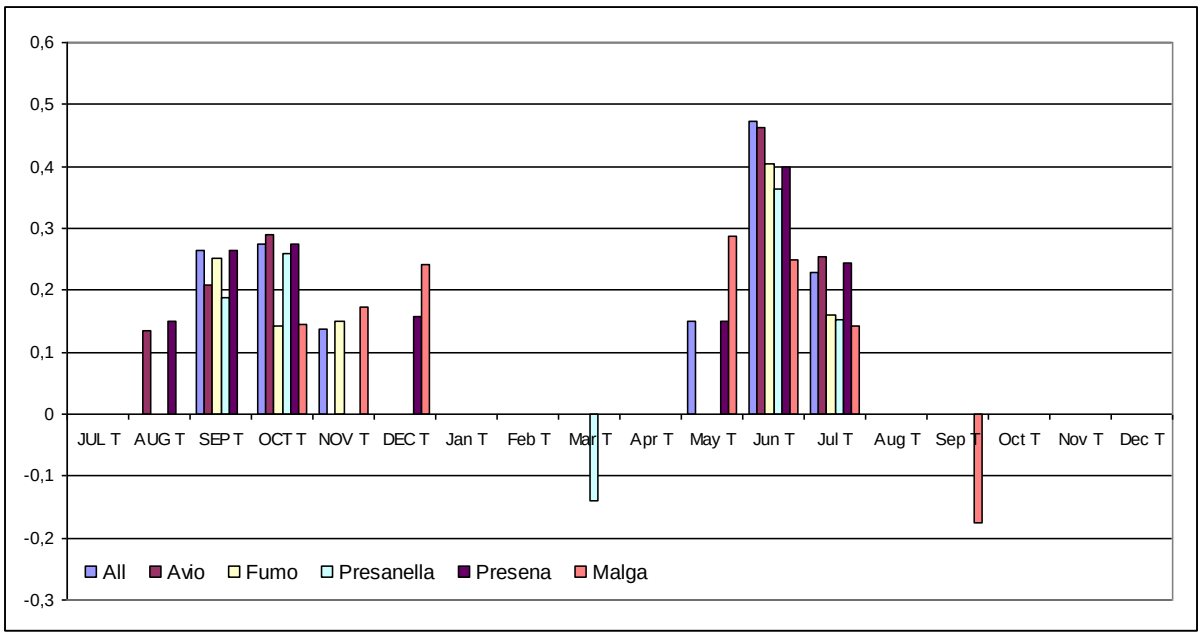

Fig. 4-41 Correlation coefficient computed between the five site chronologies, the master chronology (All) and the monthly mean temperatures coming from high-elevation stations (HEST). Only significant values are shown (significance assessed by means of the 95th percentile range).

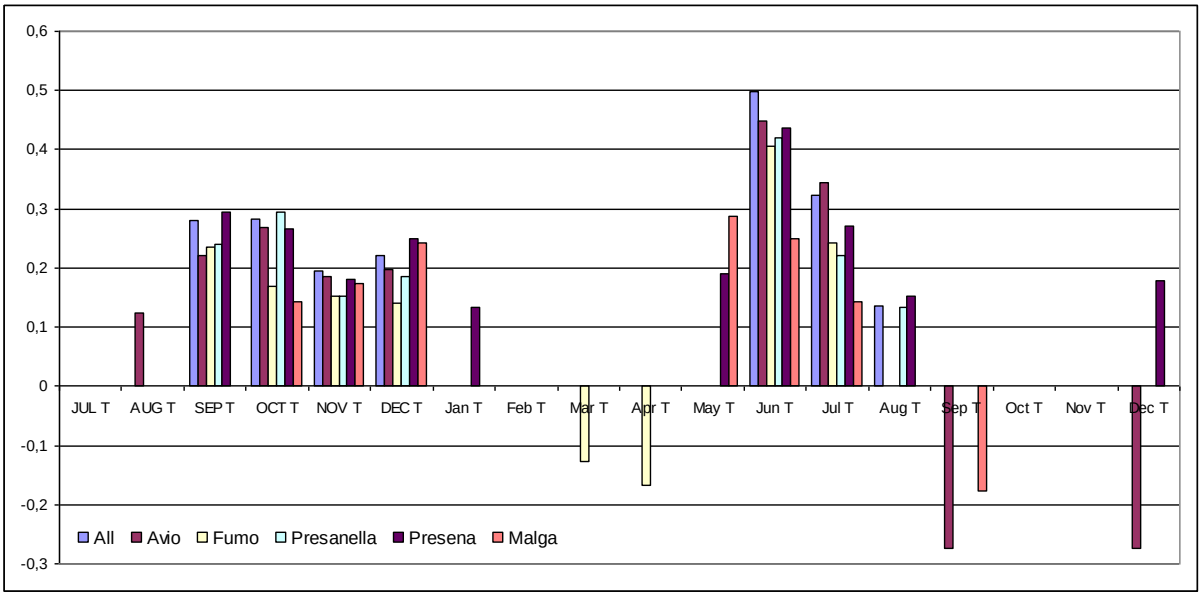

Fig. 4-42 Correlation coefficient computed between the five site chronologies, the master chronology (All) and the monthly mean temperatures coming from low-elevation stations (LEST). Only significant values are shown (significance assessed by means of the 95th percentile range).

	All-H	All-L	Avio-H	Avio-L	Fumo-H	Fumo-L	Presanella-H	Presanella-L	Presena-H	Presena-L	Malga-H	Malga-L
JUL T	0	0	0	0	0	0	0	0	0	0	0	0
AUG T	0	0	0,14	0,12	0	0	0	0	0,15	0	0	0
SEP T	0,27	0,28	0,21	0,22	0,25	0,23	0,19	0,24	0,26	0,29	0,13	0
OCT T	0,28	0,28	0,29	0,27	0,14	0,17	0,26	0,30	0,27	0,27	0,12	0,14
NOV T	0,14	0,20	0	0,19	0,15	0,15	0	0,15	0	0,18	0,15	0,17
DEC T	0	0,22	0	0,20	0	0,14	0	0,19	0,16	0,25	0,20	0,24
Jan T	0	0	0	0	0	0	0	0	0	0,13	0	0
Feb T	0	0	0	0	0	0	0	0	0	0	0	0
Mar T	0	0	0	0	0	-0,13	-0,14	0	0	0	0	0
Apr T	0	0	0	0	0	-0,17	0	0	0	0	0	0
May T	0,15	0	0	0	0	0	0	0	0,15	0,19	0,29	0,29
Jun T	0,47	0,50	0,46	0,45	0,40	0,41	0,36	0,42	0,40	0,44	0,22	0,25
Jul T	0,23	0,32	0,25	0,34	0,16	0,24	0,15	0,22	0,24	0,27	0	0,14
Aug T	0	0,14	0	0	0	0	0	0,13	0	0,15	0	0
Sep T	0	0	0	-0,27	0	0	0	0	0	0	0	-0,18
Oct T	0	0	0	0	0	0	0	0	0	0	0	0
Nov T	0	0	0	0	0	0	0	0	0	0	0	0
Dec T	0	0	0	-0,27	0	0	0	0	0	0,18	0	0

Tab. 4-16 Correlation coefficient values computed between the master (All) and site chronologies and monthly mean temperatures coming from high-elevation stations (H) and low-elevation stations (L). Correlation significance is calculated by means of the 95th percentile range and only significant correlation values are shown.

Correlations with monthly mean precipitations

A weak influence of monthly mean precipitations on tree growth was found computing correlations coefficients between the five residual tree-ring chronologies and monthly mean precipitations data. In particular, influence of precipitations of the current year on tree growth revealed to be quite irrelevant, with the sole Fumo residual chronology showing a positive correlation with March mean precipitations. Moreover, positive correlation coefficient values were found between December of the previous year precipitations and the Presena and Presanella residual chronologies (Fig.4-43, Tab. 4-17).

Furthermore, we found significant negative correlation coefficient values between all the five mean site residual chronologies and June of the current year monthly mean precipitations.

These results are consistent with those reported by Carrer & Urbinati (2006) for a *Larix decidua* chronology data set in the Eastern Italian Alps and by Leonelli et al. (2009) for an high-altitude *Pinus cembra* tree-ring network in the Ortles-Cevedale area (Italian Central Alps).

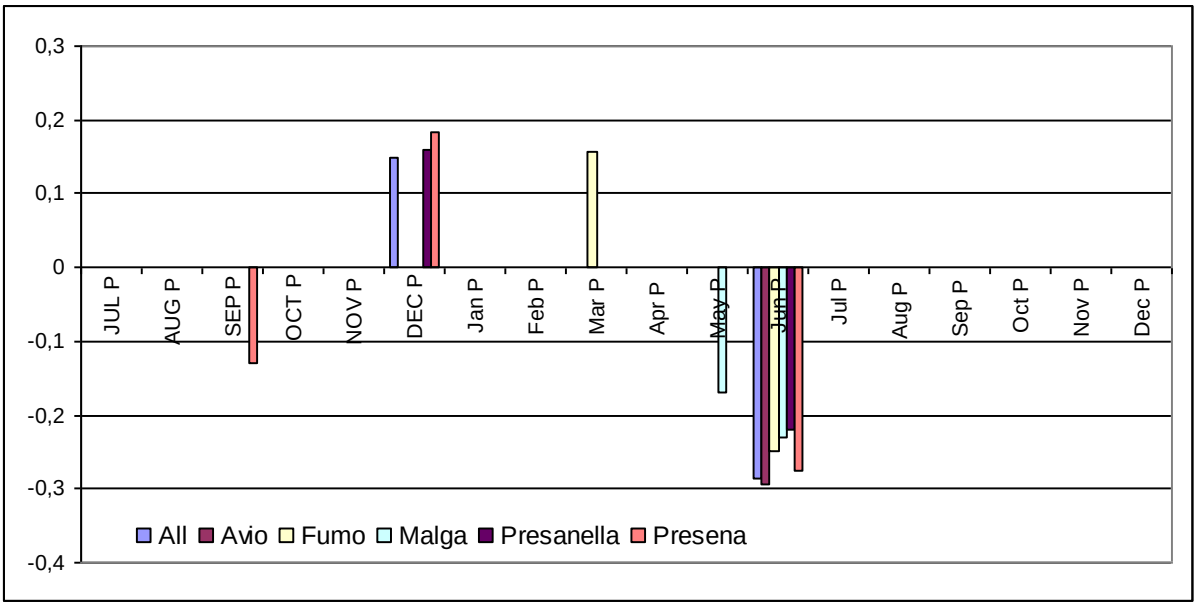

Fig. 4-43 Correlation coefficient computed between the five individual chronologies, the master chronology (All) and the monthly mean precipitations. Only significant values are shown (significance assessed by means of the 95th percentile range).

	All	Avio	Fumo	Malga	Presanella	Presena
JUL P	0	0	0	0	0	0
AUG P	0	0	0	0	0	0
SEP P	0	0	0	0	0	-0,13
OCT P	0	0	0	0	0	0
NOV P	0	0	0	0	0	0
DEC P	0,15	0	0	0	0,16	0,18
Jan P	0	0	0	0	0	0
Feb P	0	0	0	0	0	0
Mar P	0	0	0,16	0	0	0
Apr P	0	0	0	0	0	0
May P	0	0	0	-0,17	0	0
Jun P	-0,29	-0,30	-0,25	-0,23	-0,22	-0,28
Jul P	0	0	0	0	0	0
Aug P	0	0	0	0	0	0
Sep P	0	0	0	0	0	0
Oct P	0	0	0	0	0	0
Nov P	0	0	0	0	0	0
Dec P	0	0	0	0	0	0

Tab. 4-17 Correlation coefficient values computed between the master (All) and site chronologies and monthly mean precipitations. Correlation significance are calculated by means of the 95th percentile range and only significant correlation values are shown.

Moving correlation function analysis

Moving correlations with monthly mean temperatures

The monthly climatic analysis of long term changing in tree-ring growth/mean monthly temperature correlations shows that in general the temperature/tree-ring growth relationship is not stable, and that it has been changing consistently over time (Figs. 4-44 to 4-66).

All the five chronologies show a synchronous and mostly non stationary trend in CC values and correlation coefficient values are different if computed with temperature data coming from high elevation stations (HEST) or with temperature coming from low elevation stations (LEST).

To highlight the differences between early and late parts of the MCF analysis period, a t-test of differences (confidence level 0,95, α level 0,05) has been performed on CC values computed with the ALL chronology, splitting the whole time series into two parts, respectively of 63 and 64 years (1878-1940 / 1941-2004) and evaluating mean values, variability and distributions of CC values of the two time periods.

In the following graphs the chronologies' names are reported as AVI (Avio), PRL (Presanella), PRS (Presena), MAL (malga), and FUM (Fumo).

Moving correlations with May mean temperatures

CC values calculated between the five tree-ring residual chronologies and May mean temperatures are in complex weak and not significant, with slightly higher mean values for the Malga and Presena chronologies. Both correlations computed with LEST and with HEST show a little increment of CC values from the early twentieth century followed by an evident long term decrease that appears visible starting from about 1960.

Four of the five chronologies show an increasing trend in CC values in the more recent part of the time series, but anyway they don't reach significant values. A small rising of correlation coefficient values is observable in the latest years of the time series, starting from about 2000.

The differences between the first and the second period of comparison, are significant in the both the analyses, as highlighted by t and p values. T-values are considerable negative and p-values highlight the presence of significant differences between the two compared parts of the series (Tab.4-18).

The Malga chronology shows the highest and more stable values of correlation over the whole time period in both analyses, but, as all the other chronologies, a decrease of CC values is visible in the more recent part of the analysis. Only a small increment, approximately from 2000, appears in the both analysis (Figs. 4-44 and 4-45).

On comparing CC values computed only between the All chronology and the two temperature data sets, the trend looks similar with a slight increment of CC values in the second part of the time series for CC values calculated with HEST (Fig. 4-47). Overall, CC values calculated with LEST appear to have a slightly more stable signal, as evidenced by the lower values of standard deviation in the first and in the second period of analysis, compared with HEST. The difference between CC values of the two period of analysis is statistically significant both for CC calculated with HEST and for those calculated with LEST ($p<0,0001$ in the both cases, Tab. 4-18).

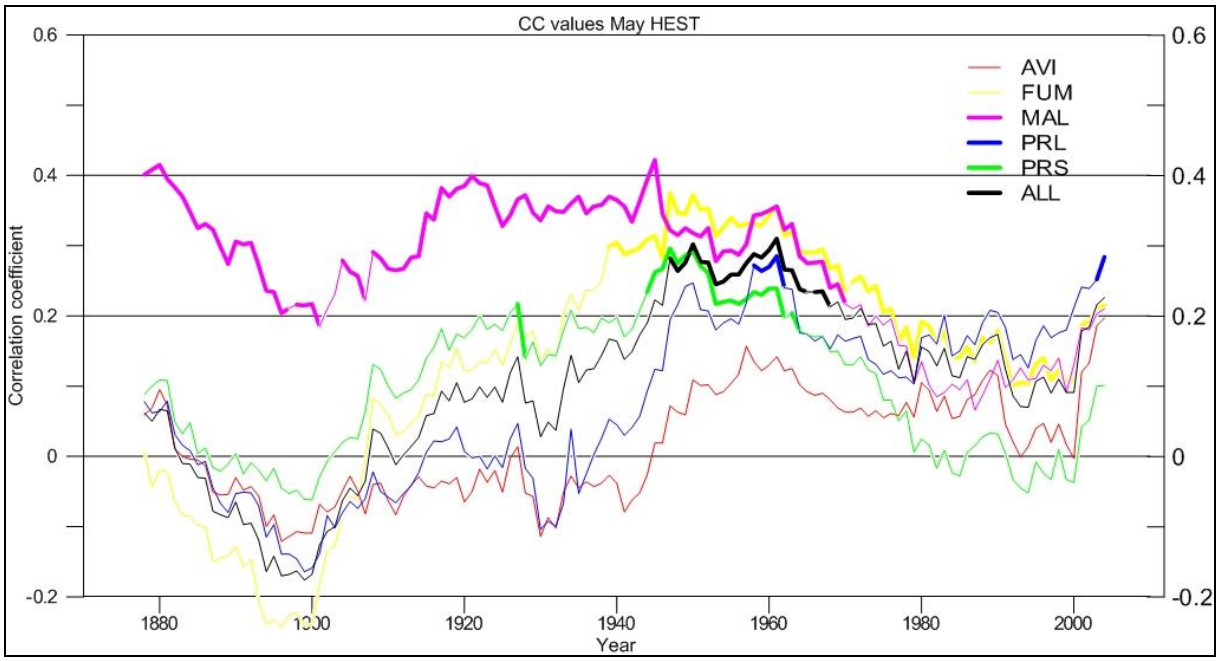

Fig. 4-44 MCF (60 yr moving window) computed between the master chronology (All), the five individual chronologies and May mean temperatures. Temperature data come from high-elevation stations (HEST >1400 m a.s.l.). The bold lines indicate significant CC values (p<0,05).

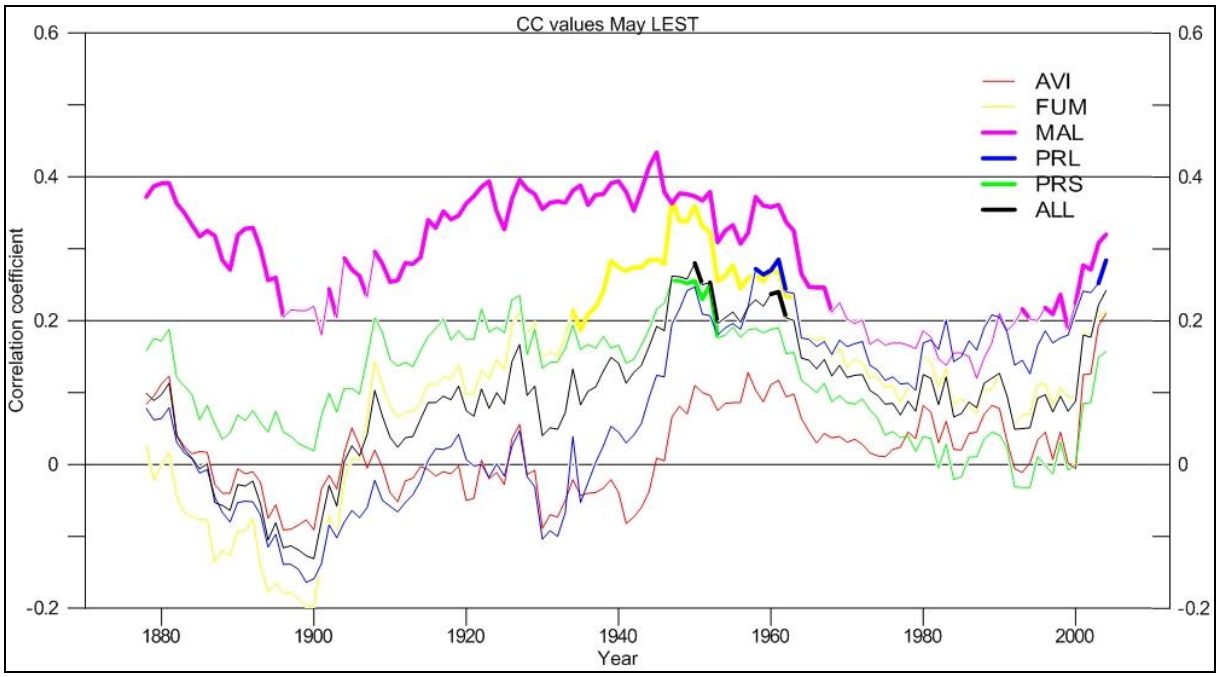

Fig. 4-45 MCF (60 yr moving window) computed between the master chronology (All), the five individual chronologies and May monthly mean temperatures. Temperature data come from low-elevation stations (LEST<1400 m a.s.l.). The bold lines indicate significant CC values (p<0,05).

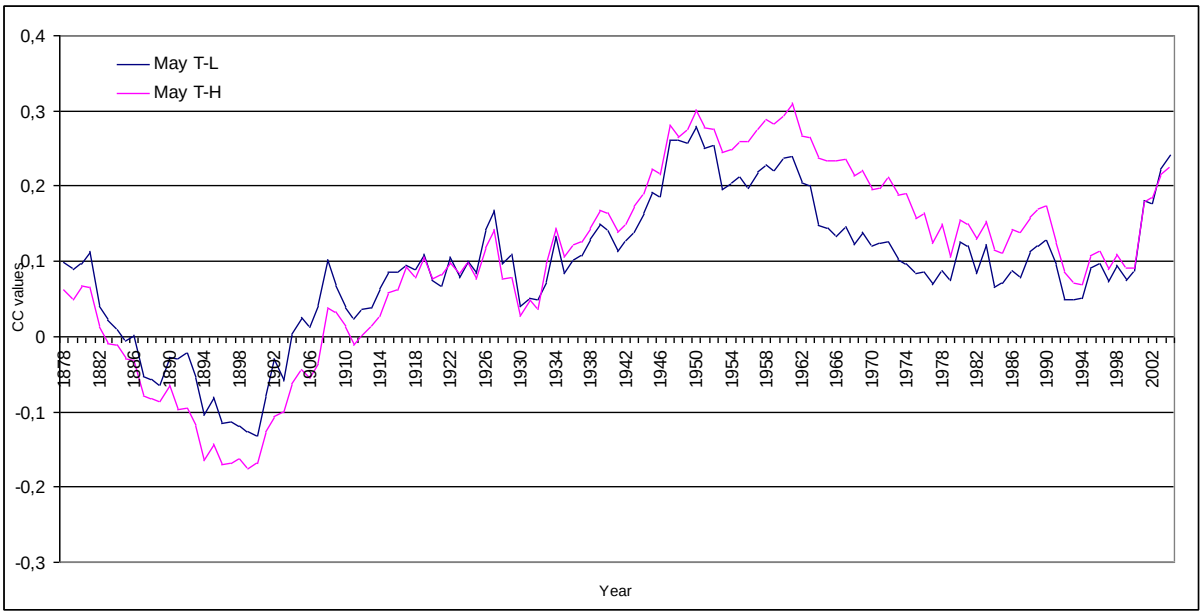

Fig. 4-46 CC values computed between the All chronology and mean May temperatures from high (H) and low (L) elevation stations.

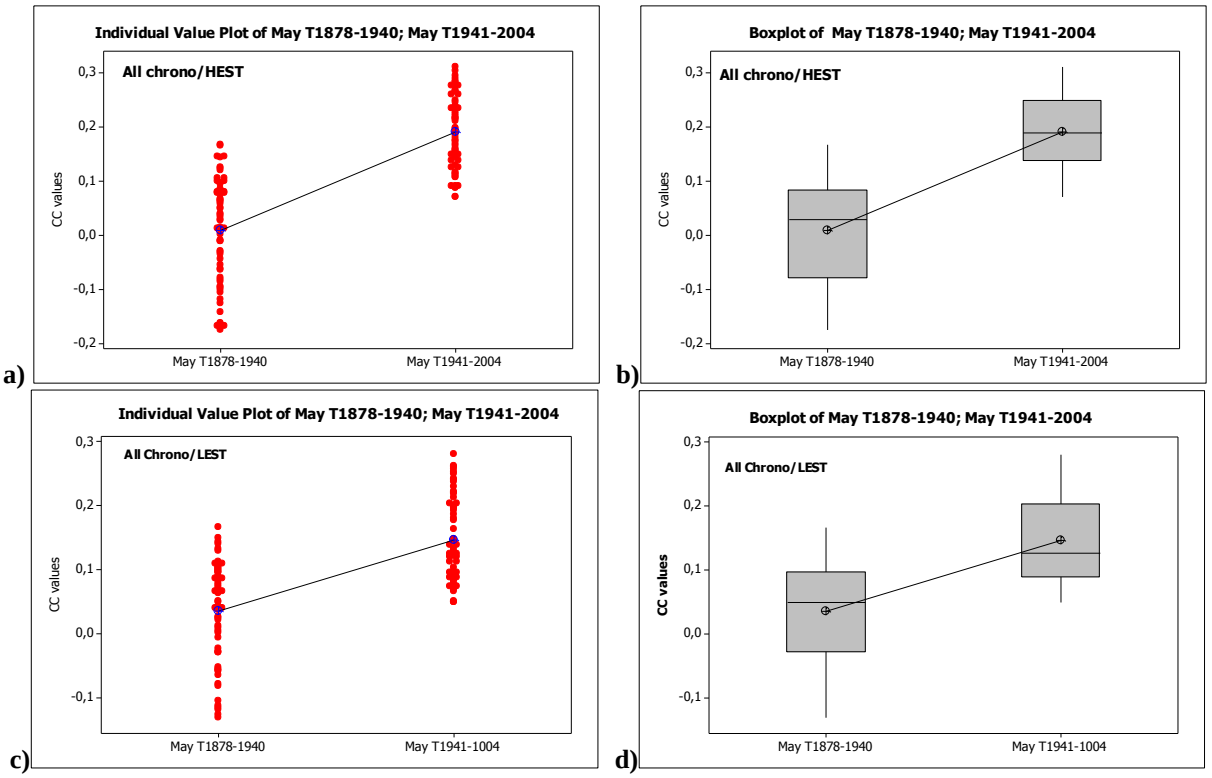

Fig. 4-47 Summaries of CC values distribution computed for the All chronology with May mean temperatures from high elevation station (HEST) and low elevation stations (LEST). 1878-1940 and 1941-2004 are the two compared period. a,c) individual CC values distributions b,d) boxplot showing shape, mean, central tendency, and variability of CC values distribution.

All chrono/HEST	N	Mean	St Dev	SE Mean
MayT_1878-1940	63	0,0078	0,0974	0,012
MayT_1941-2004	64	0,1901	0,06666	0,0083
T value	-12,29			
P-value	<0,001			
All chrono/LEST	**N**	**Mean**	**St Dev**	**SE Mean**
MayT_1878-1940	63	0,0349	0,0787	0,0099
MayT_1941-2004	64	0,1460	0,0648	0,0081
T value	-8,68			
P-value	<0,001			

Tab. 4-18 some statistics of the CC values computed with May mean temperatures for the two compared periods of the All chronology.

Moving correlations with June mean temperatures

CC calculated between residual chronologies and June mean temperatures are the highest here obtained using both high-elevation stations temperatures and low-elevation stations temperatures. The moving correlation analysis shows that CC values have a synchronous decreasing trend, which is clearly visible starting from about 1960. This decreasing trend is present in all the chronologies and in the analysis performed with the both temperatures datasets, but it appears more pronounced in the correlations computed with high elevation stations temperatures.

Actually, even though the t-test of differences between the two compared time periods, shows a mostly stable signal, the tendency goes in the direction of a reduction in the strength of relationship between tree growth and June mean temperatures (Figs 4-48 to 4-51, Tab. 4-19). A slight increase is only visible in the latest part (from about 2000) of the time series.

Correlation coefficients computed with low elevation stations temperatures have higher values and are more stable over the whole time series. They show a fewer reduction in the more recent period of comparison, and a similar mean value in the two compared periods. The more stable trend is also clearly evidenced by a very high p-value (0,954) and by minor distribution variability throughout the time (Figs 4-50and 4-51, Tab. 4-19 c,d).

The Malga residual chronology shows the lowest CC values both if it is computed with temperatures coming from high elevation stations and with temperatures coming from low elevations stations. The other four mean site residual chronologies show mostly similar correlation values.

The Presanella mean site residual chronology follows the general trend, but manifests the steepest decrement in CC values in the recent part of the curve.

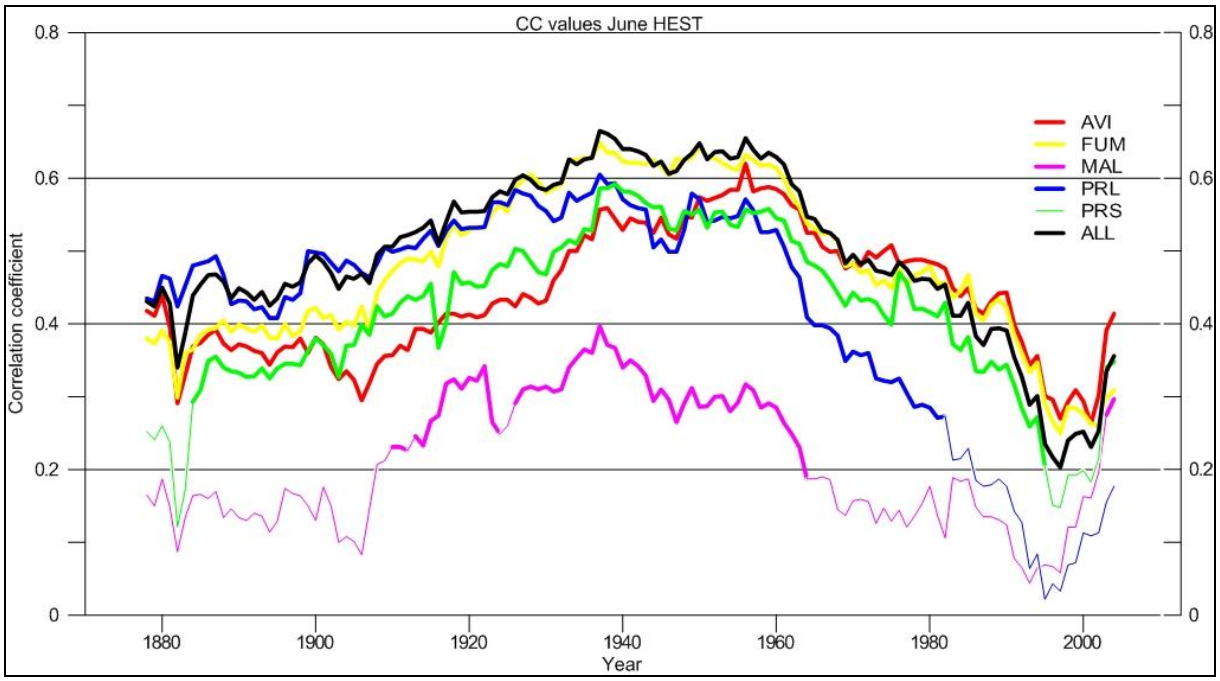

Fig. 4-48 MCF (60 yr moving window) computed between the master chronology (All), the five site chronologies and June mean temperatures. Temperature data come from high-elevation stations (>1400 m a.s.l.). The bold lines indicate significant CC values (p<0,05).

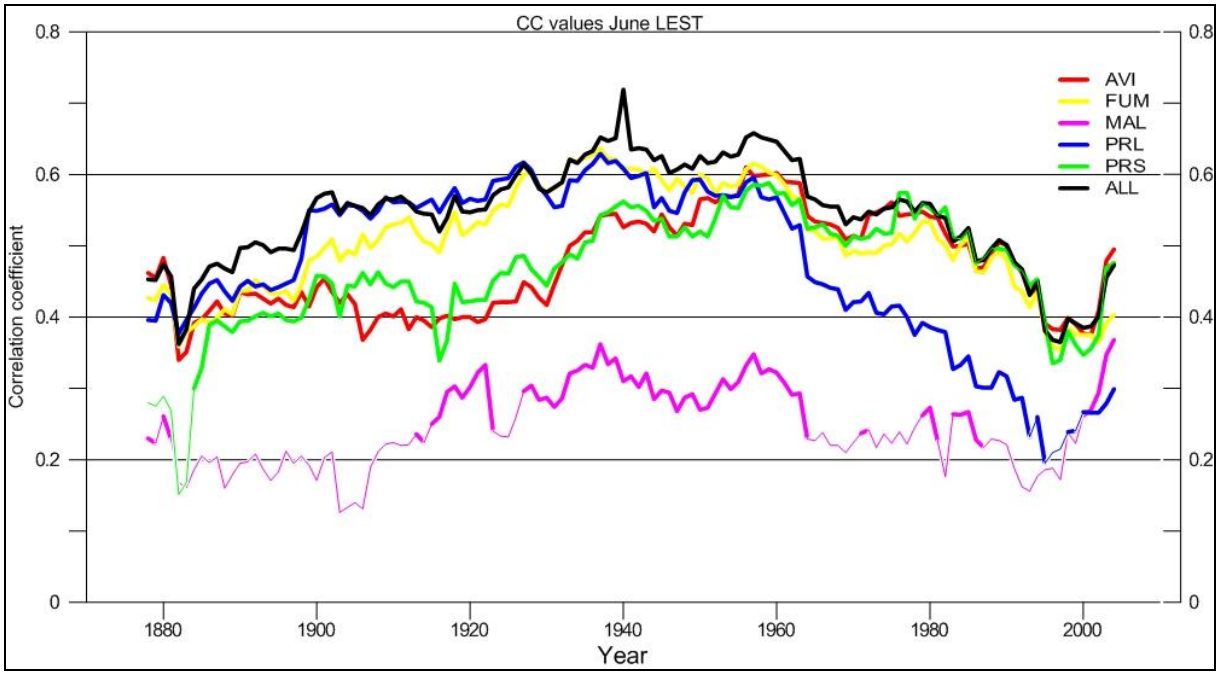

Fig. 4-49 MCF (60 yr moving window) computed between the master chronology (All), the five individual chronologies and June mean temperatures. Temperature data come from low-elevation stations (<1400 m a.s.l.). The bold lines indicate significant CC values (p<0,05).

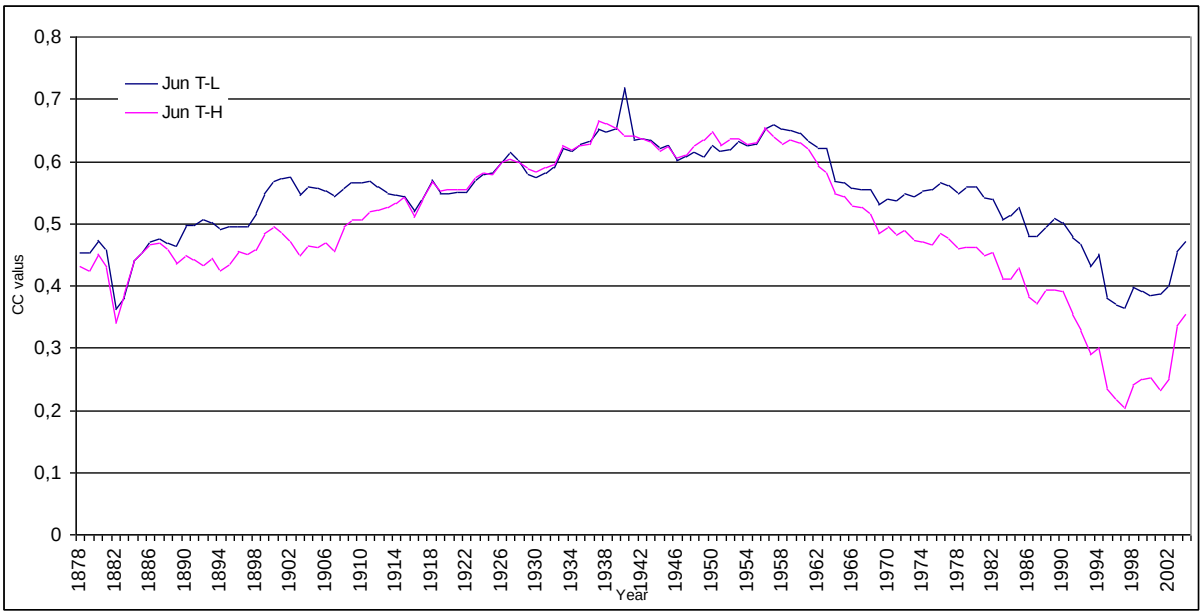

Fig. 4-50 CC values computed between the All chronology and mean June temperatures from high- (H) and low-(L) elevation stations.

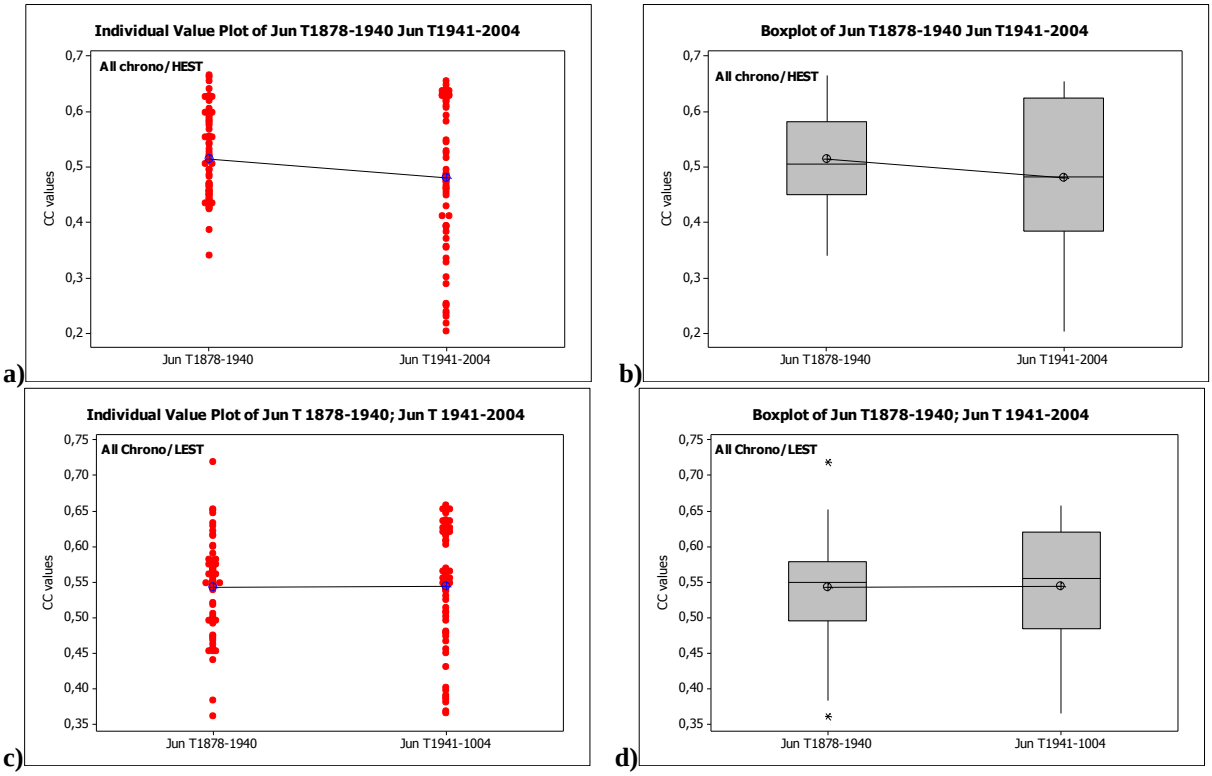

Fig. 4-51 Summaries of CC values distribution computed for the All chronology with June mean temperatures from high-elevation station (HEST) and low-elevation stations (LEST). 1878-1940 and 1941-2004 are the two compared period. a, c)individual CC values distributions b,d)boxplot showing shape, mean, central tendency, and variability of CC values distribution.

All chrono/HEST	N	Mean	St Dev	SE Mean
JuneT_1878-1940	63	0,5142	0,0760	0,0096
JuneT_1941-2004	64	0,480	0,138	0,017
T value	1,76			
P-value	0,082			
All chrono/LEST	**N**	**Mean**	**St Dev**	**SE Mean**
JuneT_1878-1940	63	0,5427	0,0654	0,0082
JuneT_1941-2004	64	0,5434	0,0835	0,010
T value	-0,06			
P-value	0,954			

Tab. 4-19 Some statistics of the CC values computed with June mean temperatures for the two compared periods of the All chronology.

Moving correlations with July mean temperatures

Correlation coefficient values computed between the five residual tree-ring width chronologies and July mean temperatures are overall positive, both in the analysis performed with low-elevation station temperatures and in the analysis performed with high-elevation stations temperatures. (Figs 4-52 and 4-53).

The trend of CC values is not stable over time and the lowest coefficient values are mostly visible in the first period of analysis (from 1878 to 1888). The CC values distribution shows that these low values are outliers (observations beyond the lower whisker in the boxplot; Fig. 4-55b,d). Successively the tendency is to a slight increment of CC values in the second time period. This increment is more evident in the CC computed with the low elevation stations temperatures (Tab.4-20).

In the moving correlations analysis carried out with July mean temperatures coming from high-elevation stations a decreasing trend is visible starting from about 1960 (as in the correlations with June mean temperatures) (Fig.4-52). On the contrary, the same trend is not visible in the correlation coefficients computed with July mean temperatures coming from low-elevation stations. In the latter case (Fig. 4-53) the trend is less stable (with significant variation in CC values; $p<0,0001$) and the correlation go towards higher values, meaning a better relationship between tree growth and July mean temperatures. These results are clearly visible in the All chronology trends graphs (Fig. 4-54) and in the distribution plots of the two compared time periods in the t-test of differences (Fig.4-55, Tab.4-20).

The moving correlation analysis for the Presanella residual chronology shows the most stable trend in CC values, even if low CC values (Figs 4-52 and 4-53).

The Malga chronology has lower CC values than the mean of the other four chronologies in the analysis with the both temperature data set.

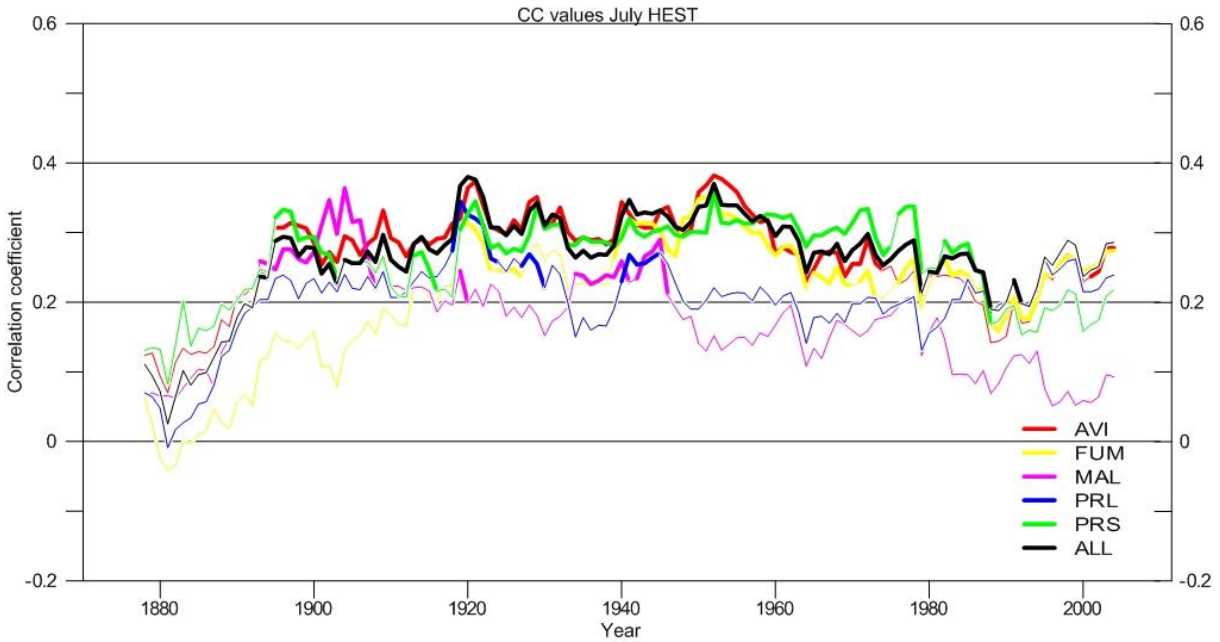

Fig. 4-52 MCF (60 yr moving window) computed between the master chronology (All), the five individual chronologies and July monthly mean temperatures. Temperature data come from high-elevation stations (>1400 m a.s.l.). The bold lines indicate significant CC values (p<0,05).

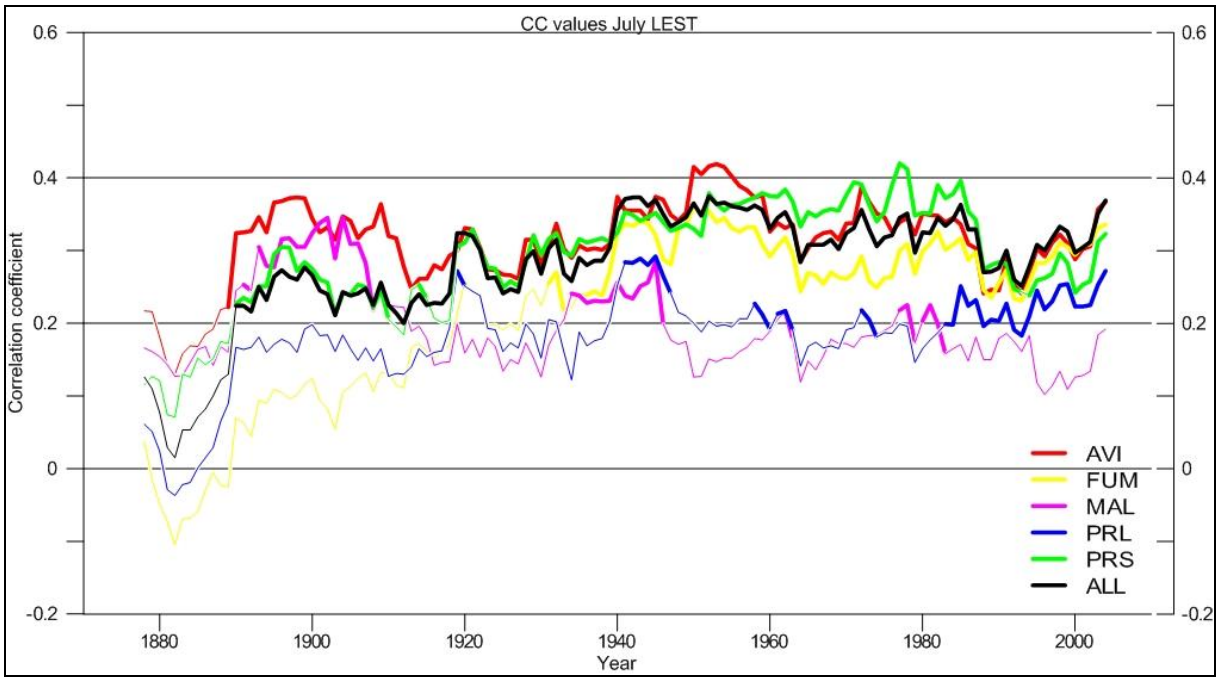

Fig. 4-53 MCF (60 yr moving window) computed between the master chronology (All), the five individual chronologies and July monthly mean temperatures. Temperature data come from low-elevation stations (<1400 m a.s.l.). The bold lines indicate significant CC values (p<0,05).

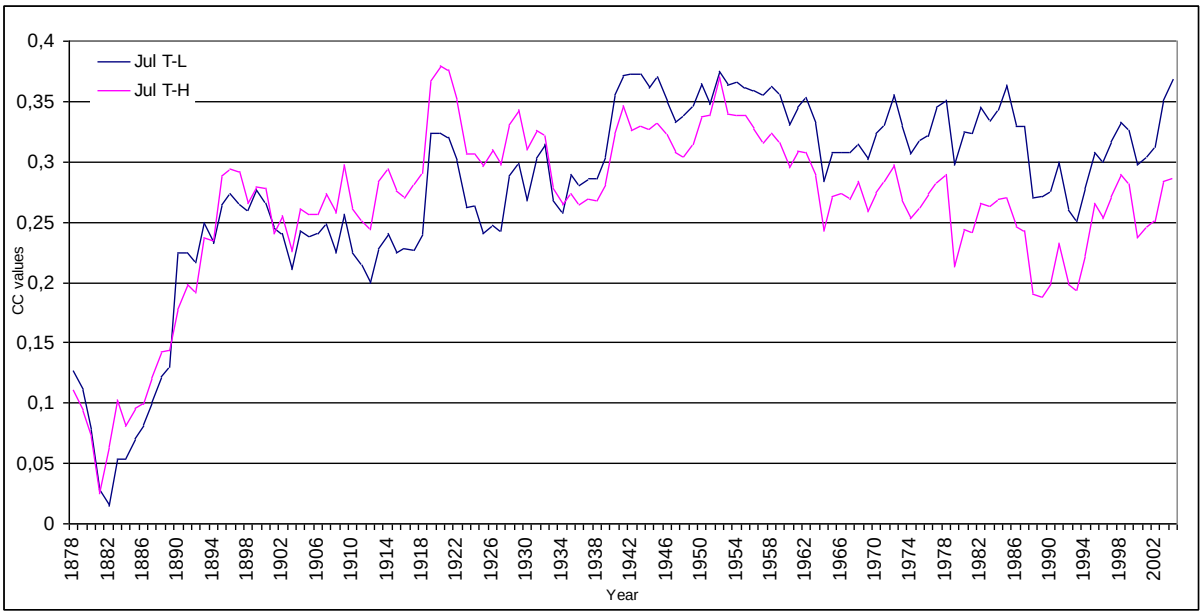

Fig. 4-54 CC values computed between the All chronology and mean July temperatures from high- (H) and low-(L) elevation stations.

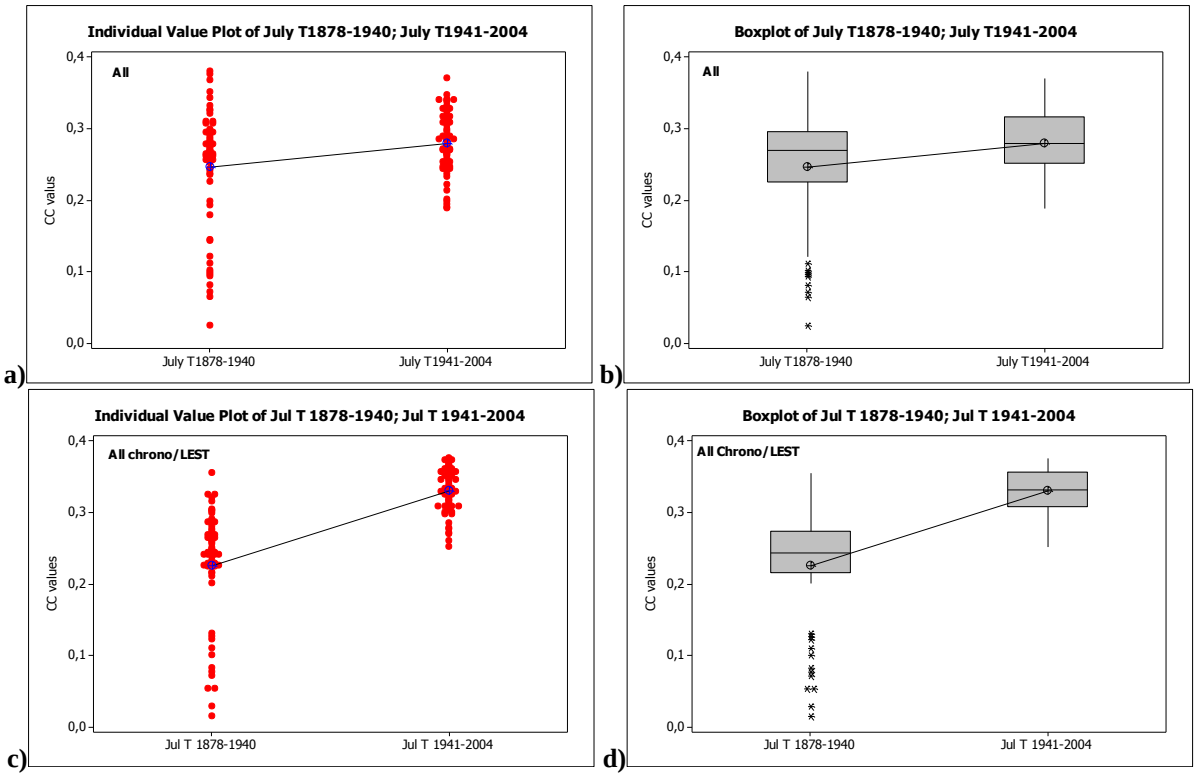

Fig. 4-55 CC values distribution for the All chronology with July mean temperature in the two compared period a)individual CC values b) boxplot showing shape, central tendency, and variability of CC values distribution.

All chrono/HEST	N	Mean	St Dev	SE Mean
JulyT_1878-1940	63	0,2462	0,0830	0,011
JulyT_1941-2004	64	0,2795	0,0426	0,0053
T-value	-2,82			
P-value	0,006			
All chrono/LEST	**N**	**Mean**	**St Dev**	**SE Mean**
JulyT_1878-1940	63	0,2257	0,0790	0,0099
JulyT_1941-2004	64	0,3298	0,0307	0,0038
T-value	-9,76			
P-value	<0,000			

Tab. 4-20 Some statistical parameters of the CC values computed with July mean temperatures for the two compared periods of the All chronology.

Moving correlations with August mean temperatures

As seen above (Figs 4-41 and 4-42), correlations of the All chronology with August mean temperatures are mostly not significant. In the moving correlation analysis, performed both with temperatures coming from low and high-elevation stations, a clear tendency to a CC values increase is noticeable. This increment starts from about 1960 (Figs 4-56, 4-57 and 4-58). In the earliest part of the time series CC values are actually constantly negative or slightly above zero and their distribution are uniform and restricted around the mean, with very low St Dev values (Tab.4-21). In the more recent part of the time series, CC values are more widely distributed and extended from the minimum to the maximum values of the series (Fig. 4-59). The significant differences between the two compared periods are clearly highlighted in the All chronology by a low p-value (<0,001) and a negative value of t (Tab. 4-21).

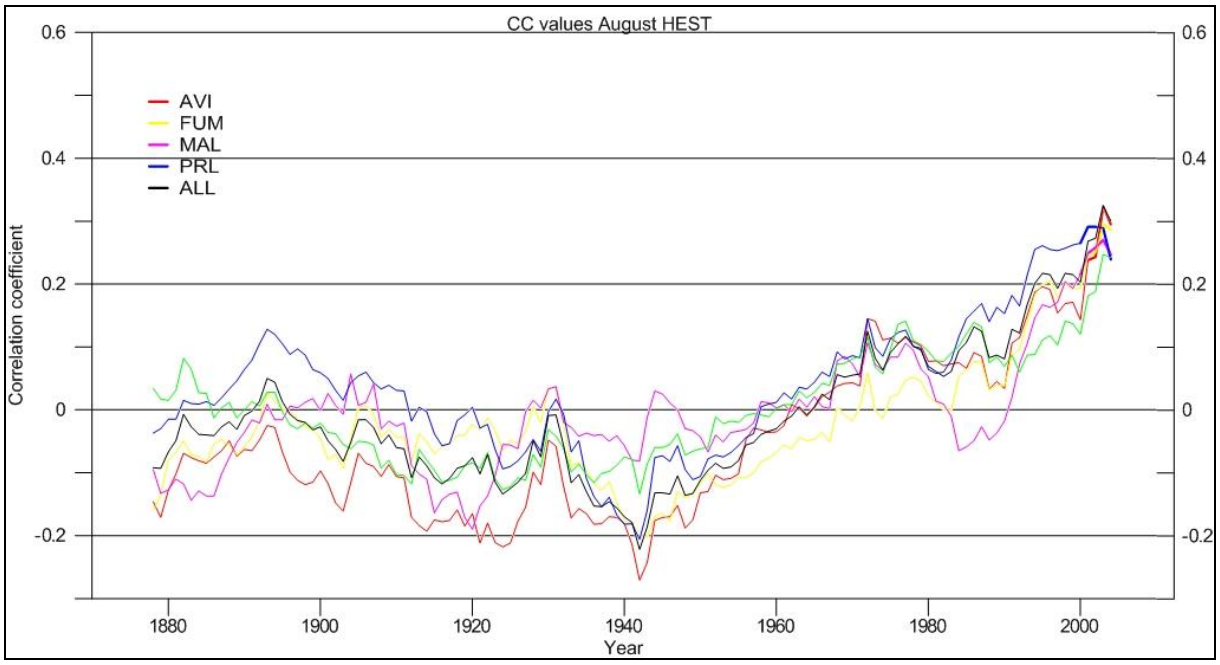

Fig. 4-56 MCF (60 yr moving window) computed between the master chronology (All), the five individual chronologies and August monthly mean temperatures. Temperature data come from high-elevation stations (>1400 m a.s.l.).

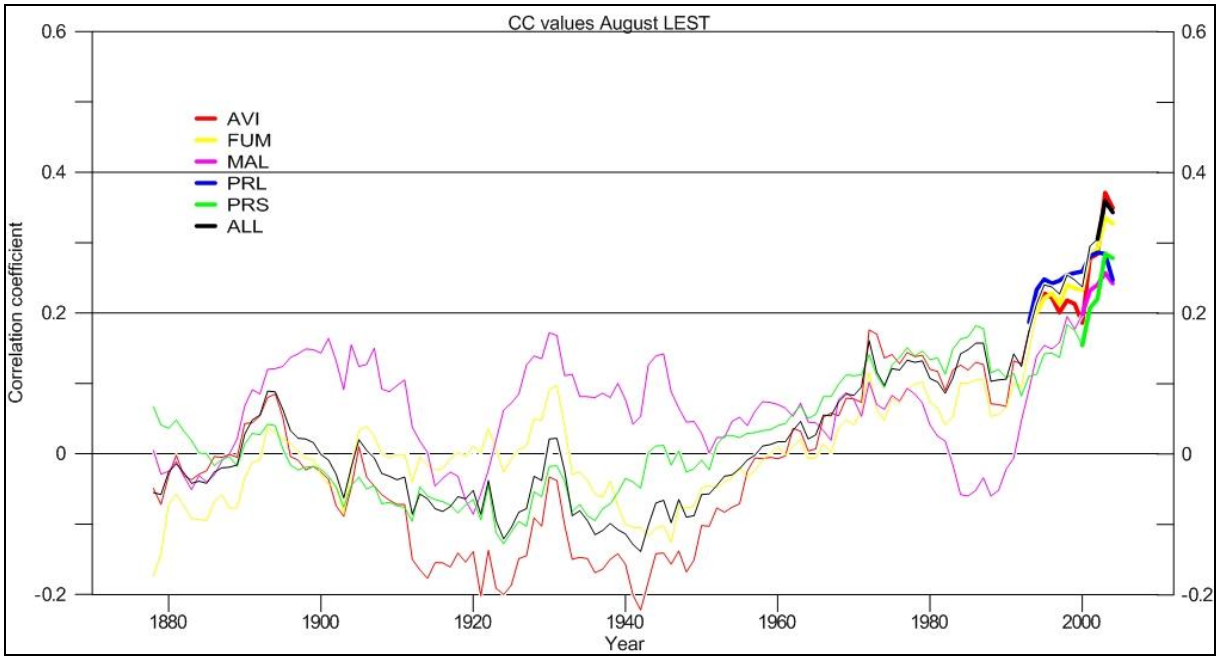

Fig. 4-57 MCF (60 yr moving window) computed between the master chronology (All), the five individual chronologies and August monthly mean temperatures. Temperature data come from low-elevation stations (<1400 m a.s.l.). The bold lines indicate significant CC values (p<0,05).

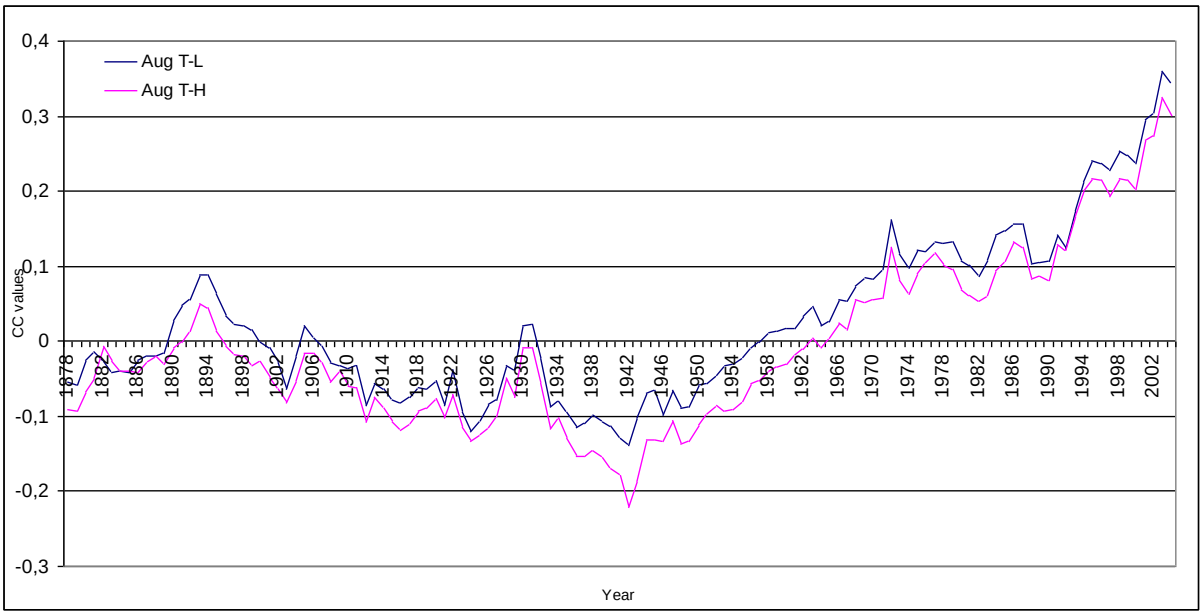

Fig. 4-58 CC values computed between the All chronology and mean August temperatures from high (H) and low(L) elevation stations.

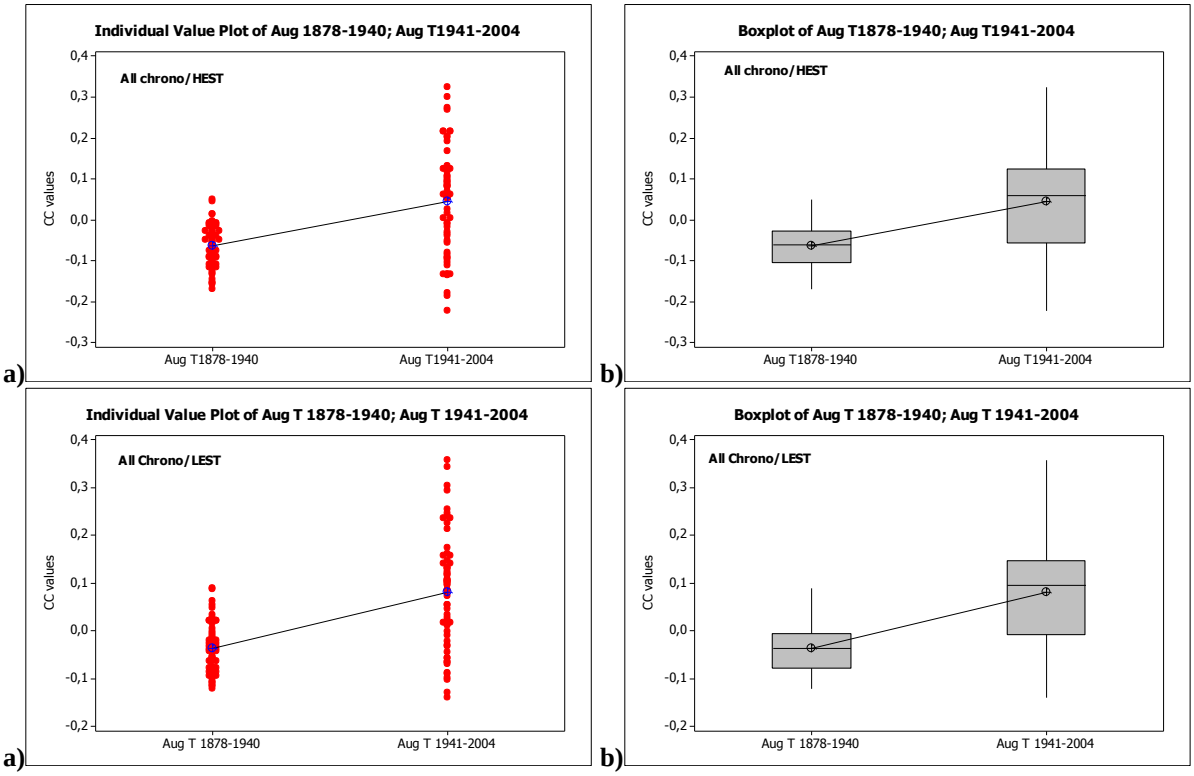

Fig. 4-59 Summaries of CC values distribution for the All chronology with August mean temperature of two compared period a)individual CC values b) boxplot showing shape, central tendency, and variability of CC values distribution.

All chrono/HEST	N	Mean	St Dev	SE Mean
AugT_1878-1940	63	-0,0635	0,0506	0,0064
AugT_1941-2004	64	0,045	0,128	0,016
T value	-6,29			
P-value	<0,001			
All chrono/LEST	**N**	**Mean**	**St Dev**	**SE Mean**
AugT_1878-1940	63	-0,0355	0,0508	0,0064
AugT_1941-2004	64	0,082	0,118	0,015
T value	-7,29			
P-value	<0,001			

Tab. 4-21 Some CC values statistical parameters computed with August mean temperatures for the two compared periods of the All chronology.

Moving correlations with Oct-1 mean temperatures

Our chronologies have shown a quite good correlation with October mean temperatures of the previous year (Figs 4-41 and 4-42). This good correlation means a positive influence of Oct-1 temperatures on tree-rings growth. The moving correlation analysis shows that the relationship between Oct-1 temperatures and tree growth is on the whole stable, with a slight decrease in the earliest and in the latest parts of the time series. CC values are similar in the analysis performed with both temperatures data sets, and only slightly higher when correlation coefficients are computed with temperatures coming from low elevation stations (Figs. 4-60, 4-61 and 4-62).

Minimum values are restricted in the first years of the analysis (1881 is the only outlier resulting from the t-test of differences in the CC values for the All chronology; Fig. 4-63b, d). The t-test of differences on the two compared periods of the All chronology produced similar mean values and a very high value of p (Tab. 4-22). A better correlation with LES temperatures is visible in the last twenty years of analysis.

The lowest CC values with Oct-1 temperatures were found for the Malga residual chronology when computed both with HEST and with LEST.

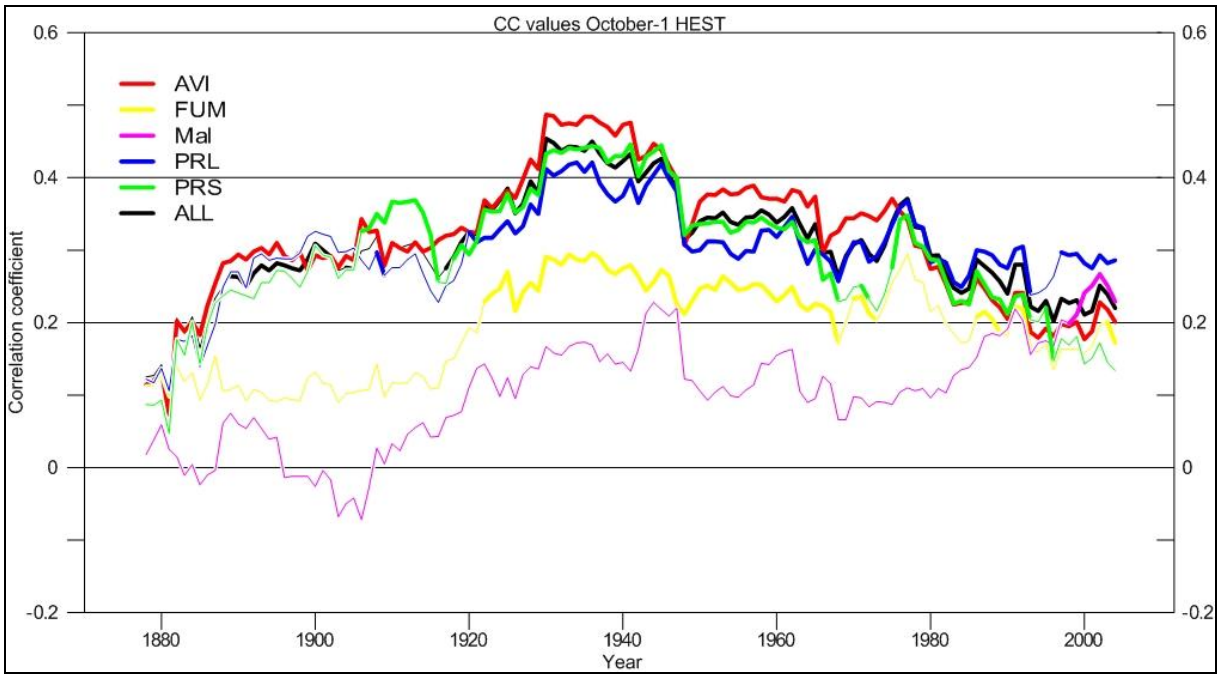

Fig. 4-60 MCF (60 yr moving window) computed between the master chronology (All), the five individual chronologies and October of the previous year (Oct-1) monthly mean temperatures. Temperature data come from high-elevation stations (>1400 m a.s.l.). The bold lines indicate significant CC values (p<0,05).

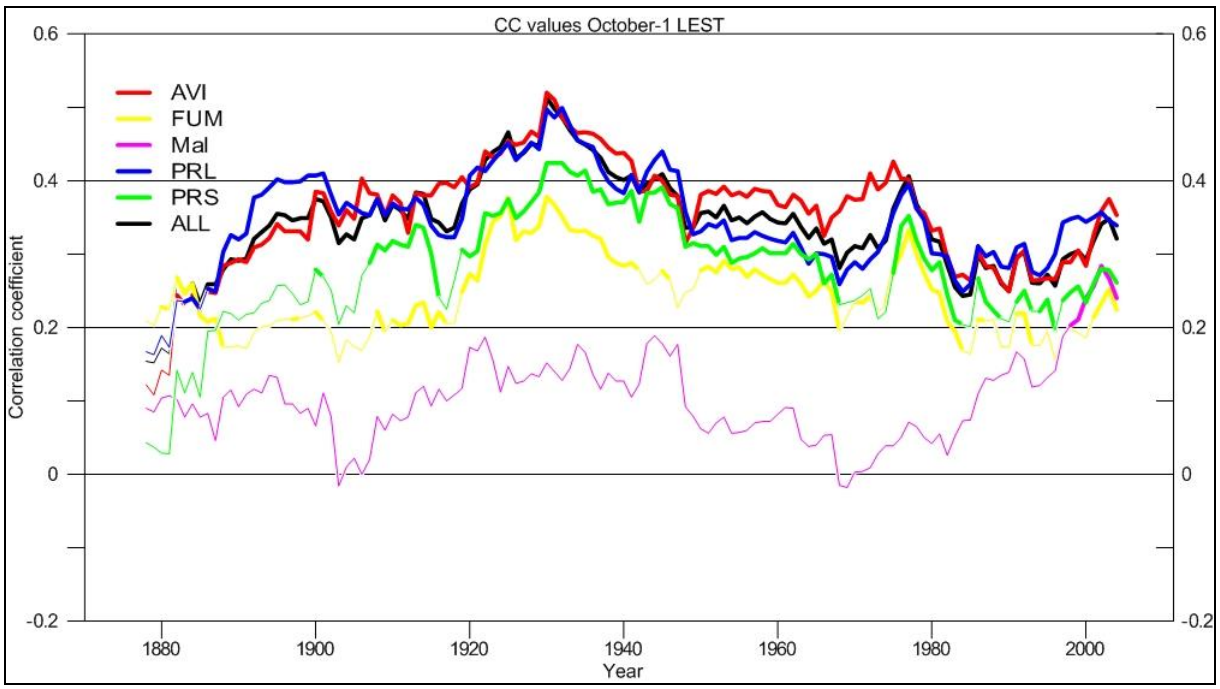

Fig. 4-61 MCF (60 yr moving window) computed between the master chronology (All), the five individual chronologies and October of the previous year (Oct-1) monthly mean temperatures. Temperature data come from high-elevation stations (>1400 m a.s.l.). The bold lines indicate significant CC values (p<0,05).

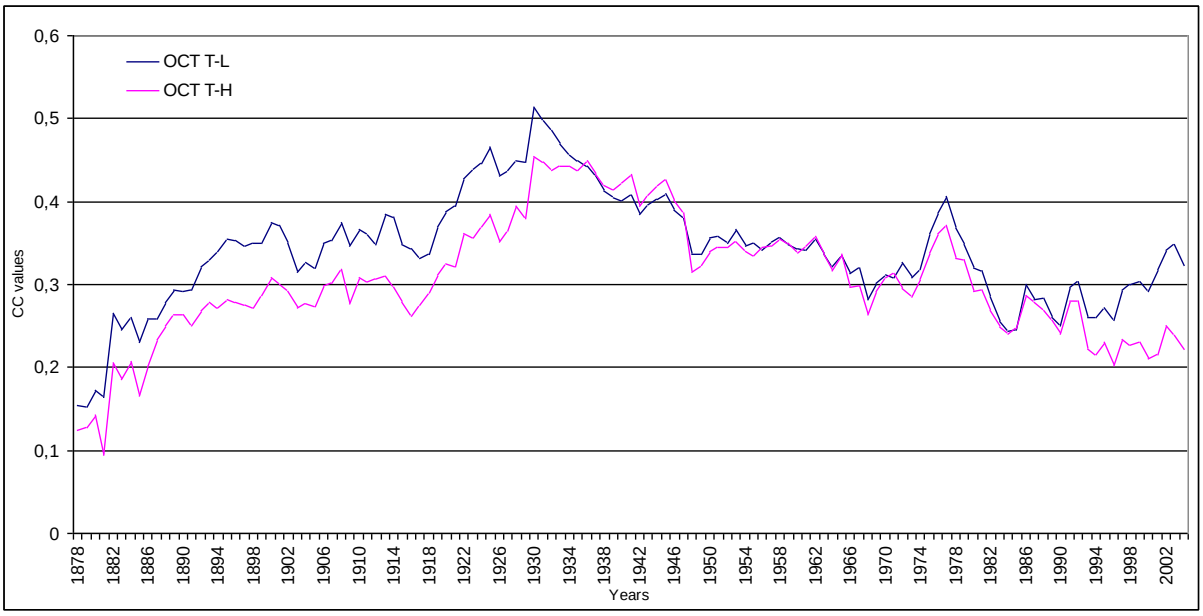

Fig. 4-62 CC values computed between the All chronology and mean October-1 temperatures from high (H) and low(L) elevation stations.

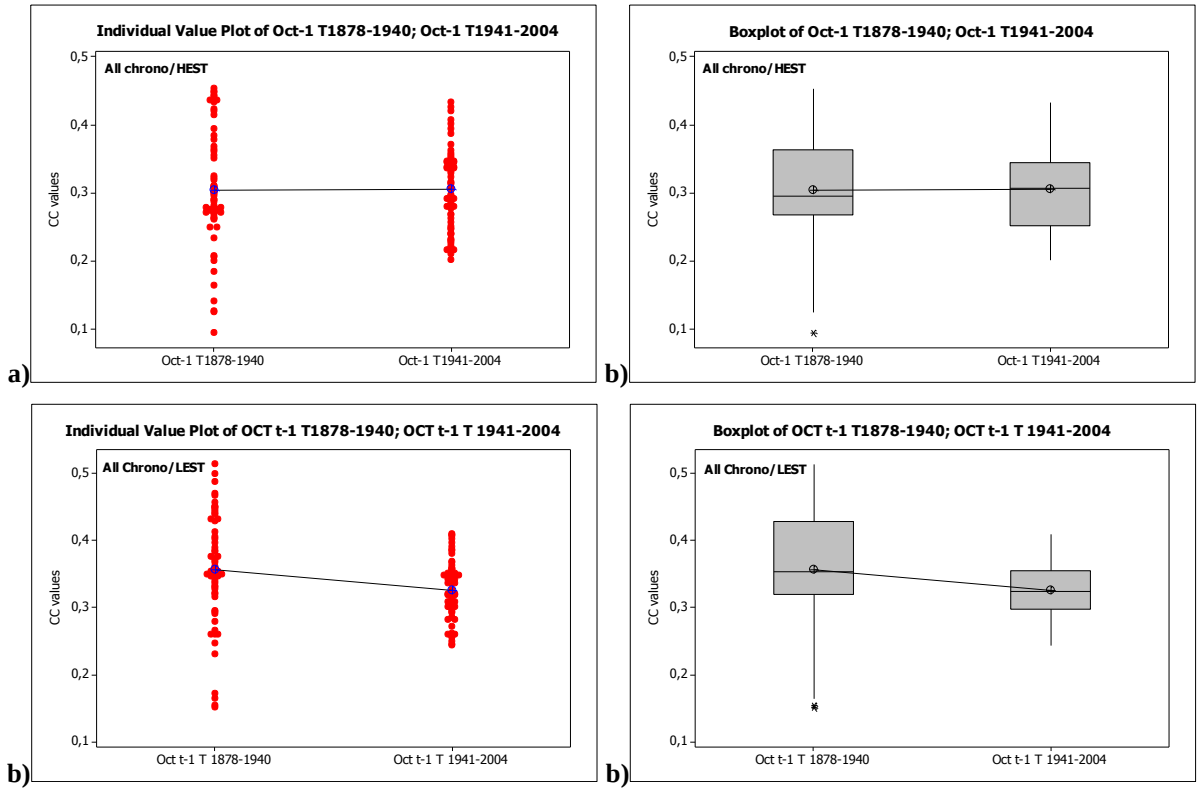

Fig. 4-63 Summaries of CC values distribution for the All chronology with October of the previous year (Oct-1) mean temperature of two compared period a)individual CC values b) boxplot showing shape, central tendency, and variability of CC values distribution.

All chono/HEST	N	Mean	St Dev	SE Mean
AugT_1878-1940	63	0,3047	0,0857	0,011
AugT_1941-2004	64	0,3056	0,0587	0,0073
T value	-0,07			
P-value	0,947			
All chrono/LEST	**N**	**Mean**	**St Dev**	**SE Mean**
AugT_1878-1940	63	0,3556	0,0827	0,010
AugT_1941-2004	64	0,3260	0,0432	0,0054
T value	2,52			
P-value	0,013			

Tab. 4-22 Some statistical parameters of the CC values computed with Oct-1 mean temperatures for the two compared periods for the All chronology.

Moving correlations with Monthly mean precipitations

Moving correlations analysis of long-term changes in mean monthly precipitation/tree-ring growth reveals, as for temperatures, that climate/tree-rings growth relationship is not stable and has considerably changed over time.

Again, as with the temperatures, all the five residual chronologies show a synchronous and mostly non-stationary CC values trend. Overall positive significant correlation coefficient values are found only if calculated with mean precipitations of December of the previous year (Fig.4-64). CC values are relevant only for a short period, after which they gradually decrease until the minimum values of the series, in the most recent part of the curve. The non-stationary trend is further confirmed and highlighted by the t-test of differences performed on the CC for the All chronology (Fig. 4-65, Tab. 4-23).

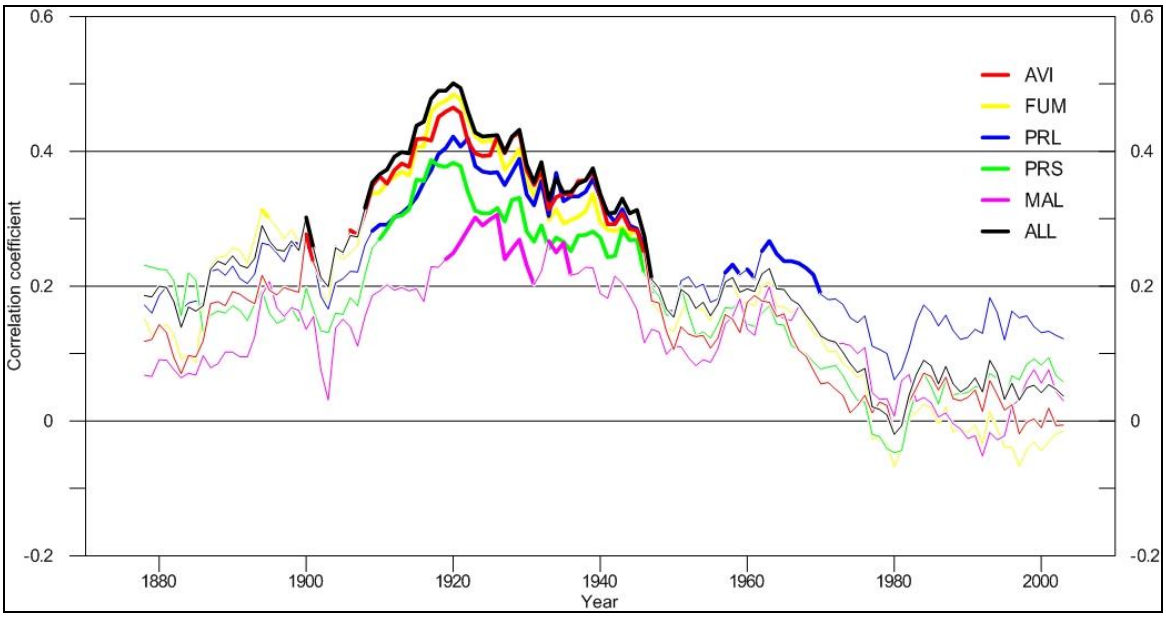

Fig. 4-64 MCF (60 yr moving window) computed between the master chronology (All), the five individual chronologies and December of the previous year (Dec-1) monthly mean precipitations. The bold lines indicate significant CC values (p<0,05).

a) 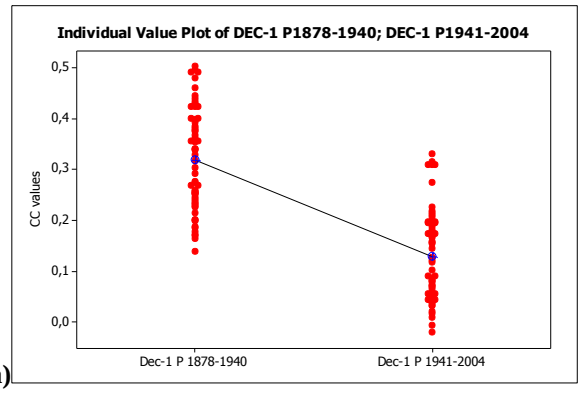

b) 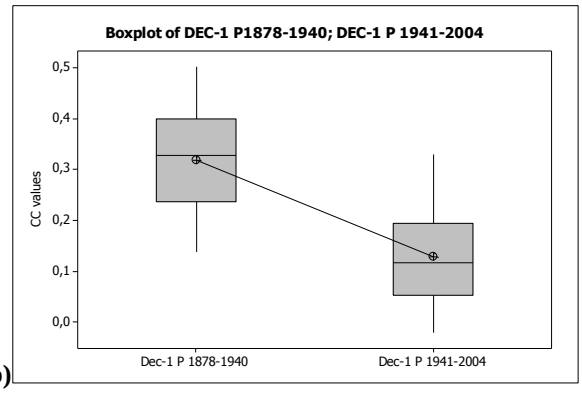

Fig. 4-65 Summaries of CC values distribution for the All chronology with December of the previous year (Dec-1) mean precipitations of two compared period a)individual CC values b) boxplot showing shape, central tendency, and variability of CC values distribution.

All chrono	N	Mean	St Dev	SE Mean
AugT_1878-1940	63	0,3187	0,0993	0,013
AugT_1941-2003	63	0,1280	0,0887	0,011
T value	11,37			
P-value	<0,0001			

Tab. 4-23 Some statistical parameters of the CC values computed with December of the previous year (Dec-1) mean precipitations for the two compared periods of the All chronology.

Significantly negative CC values were found computing moving correlation analysis with June mean precipitations. Again, in the second period of analysis a decrease in CC values is visible (Fig. 4-66 and 4-67, Tab. 4-24). The Presanella residual chronology shows the same decreasing trend but higher CC values over the whole period of analysis.

Results obtained for the moving correlation function analysis with December and June mean precipitations are consistent with those reported by Leonelli et al. (2009) for *Pinus cembra* L. in the Ortles Cevedale Group.

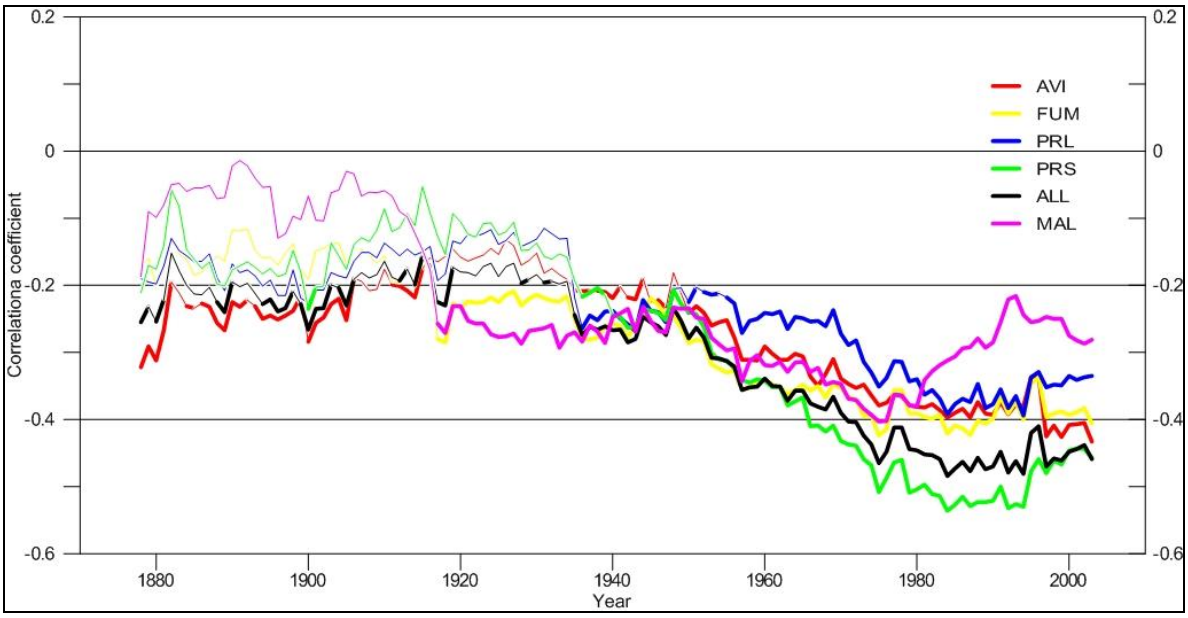

Fig. 4-66 MCF (60 yr moving window) computed between the master chronology (All), the five individual chronologies and June monthly mean precipitations. The bold lines indicate significant CC values (p<0,05).

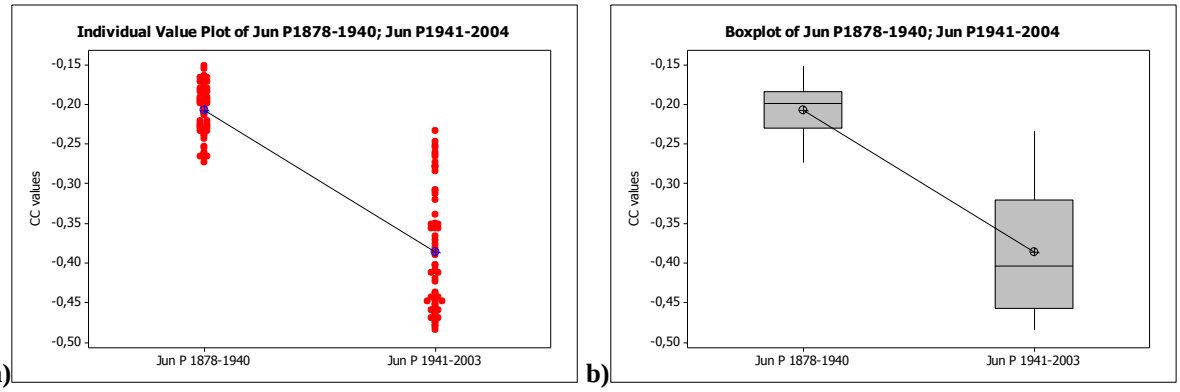

Fig. 4-67 Summaries of CC values distribution for the All chronology with June mean precipitations of two compared period a)individual CC values b) boxplot showing shape, central tendency, and variability of CC values distribution.

All chrono	N	Mean	St Dev	SE Mean
AugT_1878-1940	63	-0,3076	0,0309	0,0039
AugT_1941-2003	63	-0,3864	0,0764	0,0096
T value	17,22			
P-value	<0,0001			

Tab. 4-24 Some statistical parameters of the CC values computed with June mean precipitations for the two compared periods of the All chronology.

Moving response function analysis

The moving response function analysis reveals results similar to moving correlation analysis. These results are illustrated in figures 4-68 to 4-77.

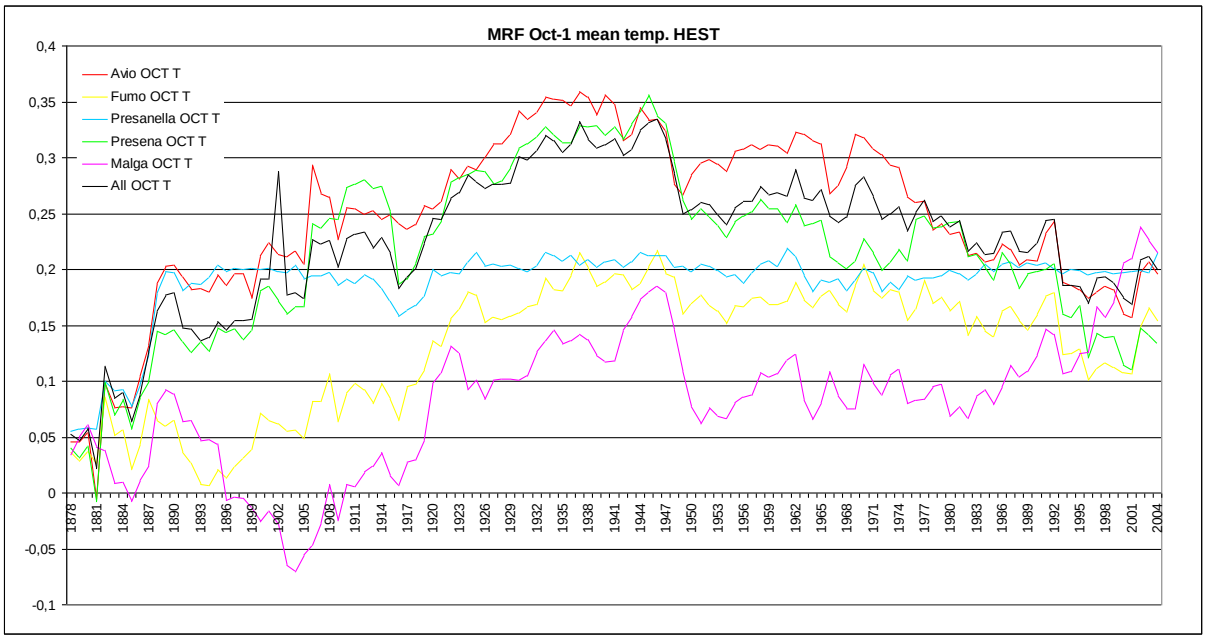

Fig. 4-68 MRF (60 yr moving window) computed between the master chronology (All), the five individual chronologies and October of the previous year (Oct-1) monthly mean temperatures. Temperature data come from high-elevation stations (>1400 m a.s.l.).

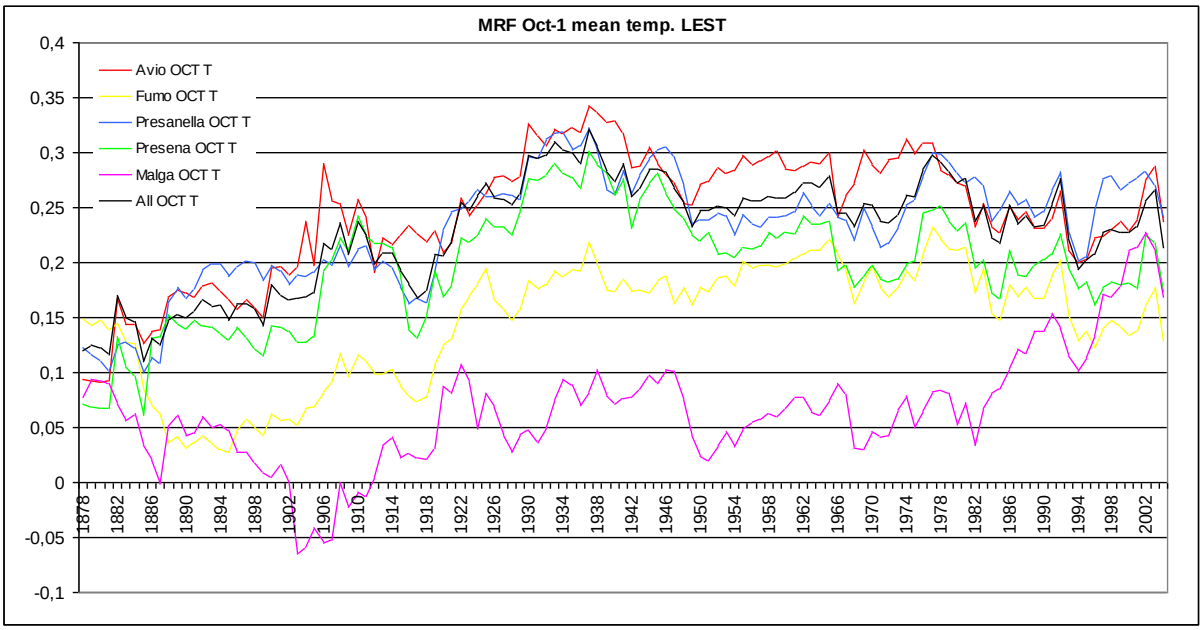

Fig. 4-69 MRF (60 yr moving window) computed between the master chronology (All), the five individual chronologies and October of the previous year (Oct-1) monthly mean temperatures. Temperature data come from low-elevation stations (<1400 m a.s.l.).

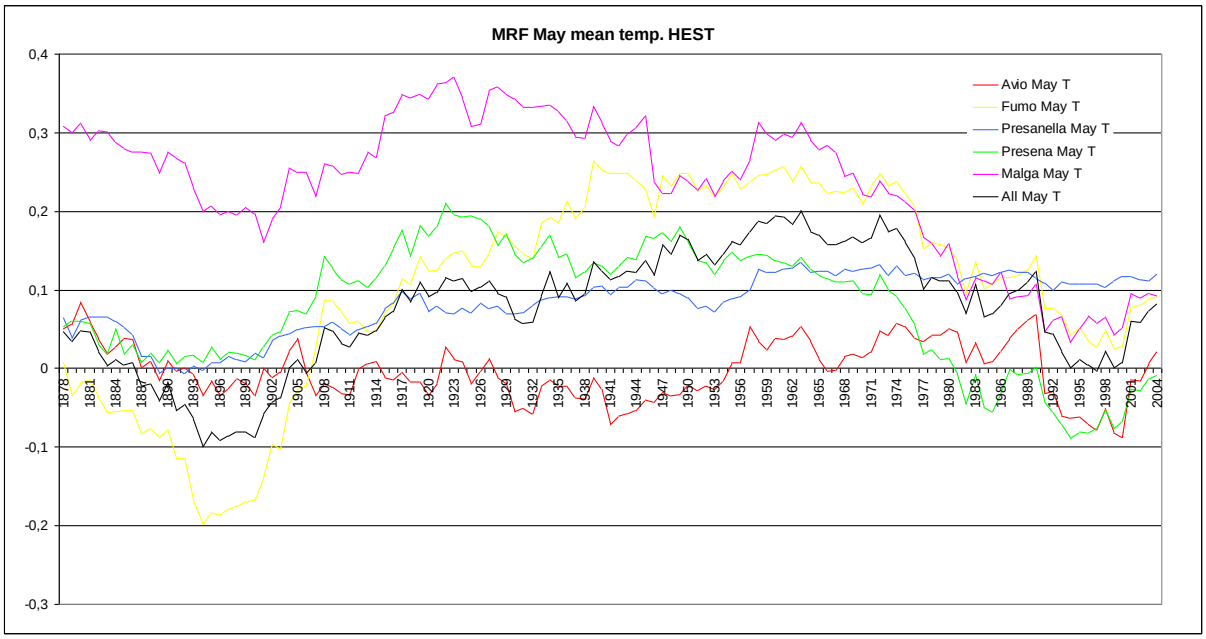

Fig. 4-70 MRF (60 yr moving window) computed between the master chronology (All), the five individual chronologies and May monthly mean temperatures. Temperature data come from high-elevation stations (>1400 m a.s.l.).

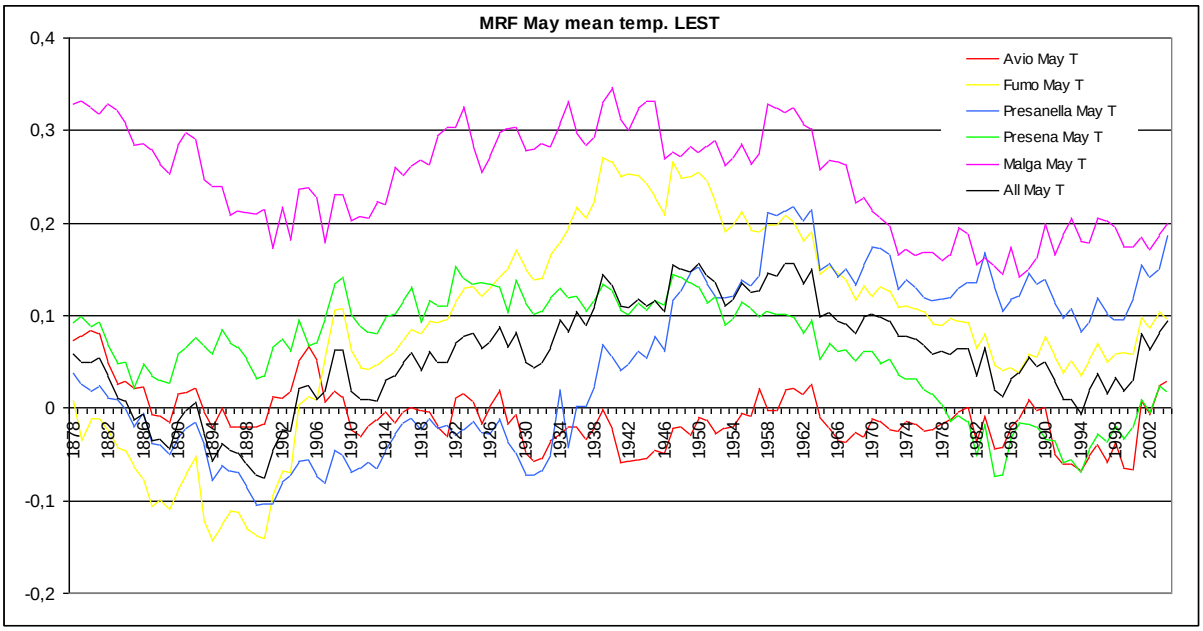

Fig. 4-71 MRF (60 yr moving window) computed between the master chronology (All), the five individual chronologies and May monthly mean temperatures. Temperature data come from low-elevation stations (<1400 m a.s.l.).

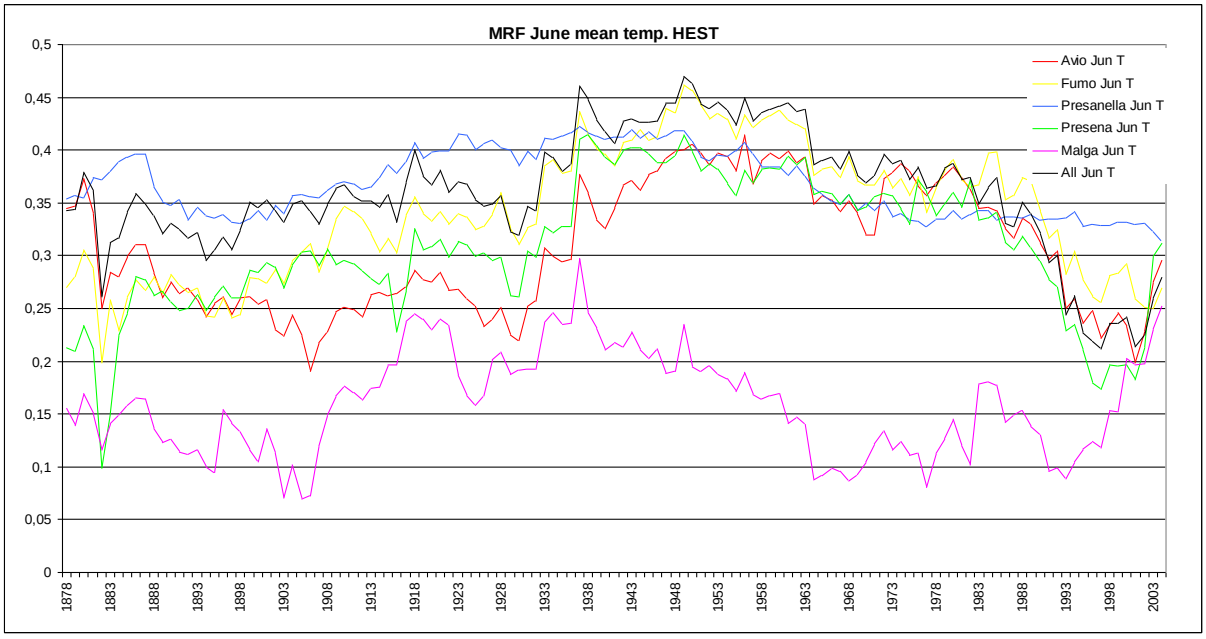

Fig. 4-72 MRF (60 yr moving window) computed between the master chronology (All), the five individual chronologies and June monthly mean temperatures. Temperature data come from high-elevation stations (>1400 m a.s.l.).

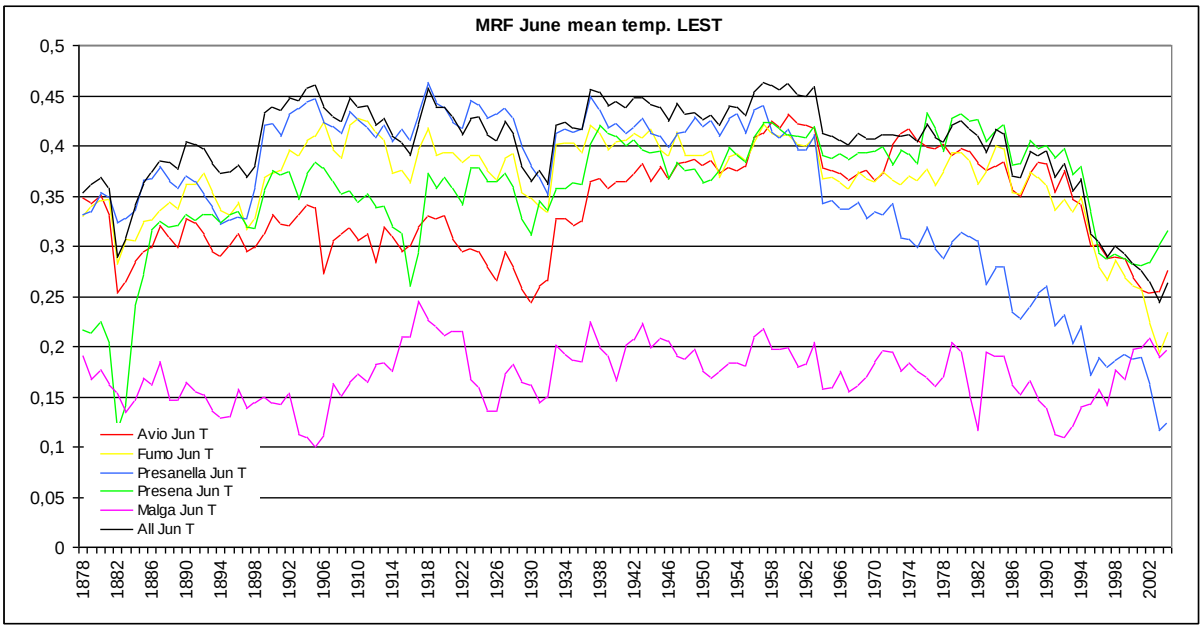

Fig. 4-73 MRF (60 yr moving window) computed between the master chronology (All), the five individual chronologies and June monthly mean temperatures. Temperature data come from low-elevation stations (<1400 m a.s.l.).

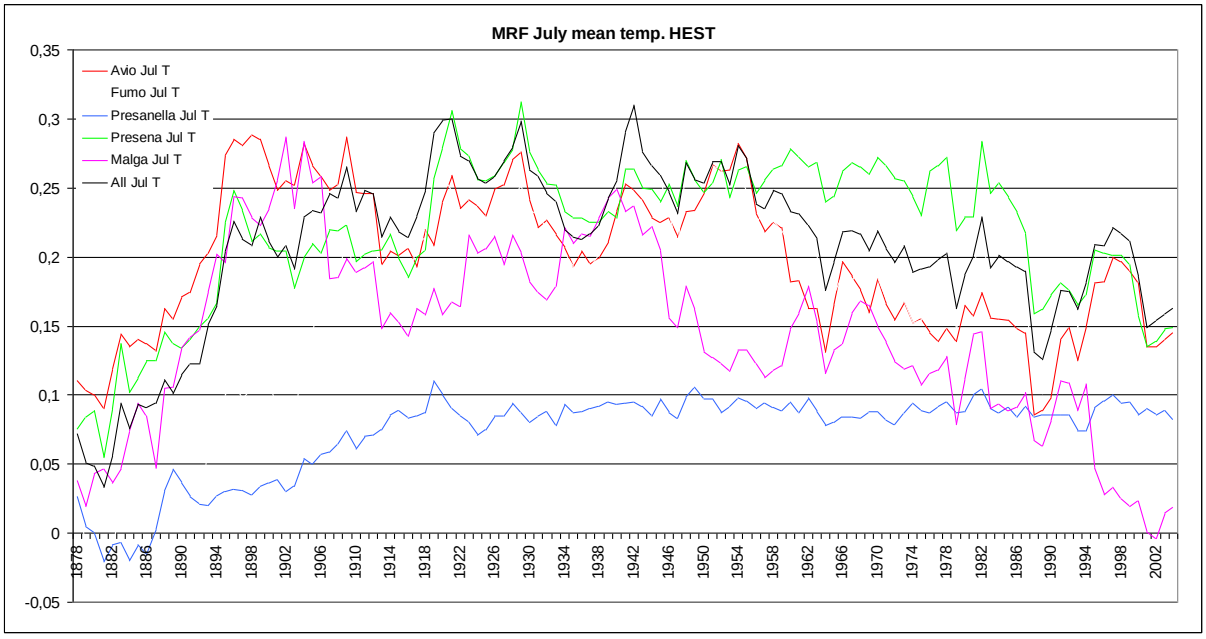

Fig. 4-74 MRF (60 yr moving window) computed between the master chronology (All), the five individual chronologies and July monthly mean temperatures. Temperature data come from high-elevation stations (>1400 m a.s.l.).

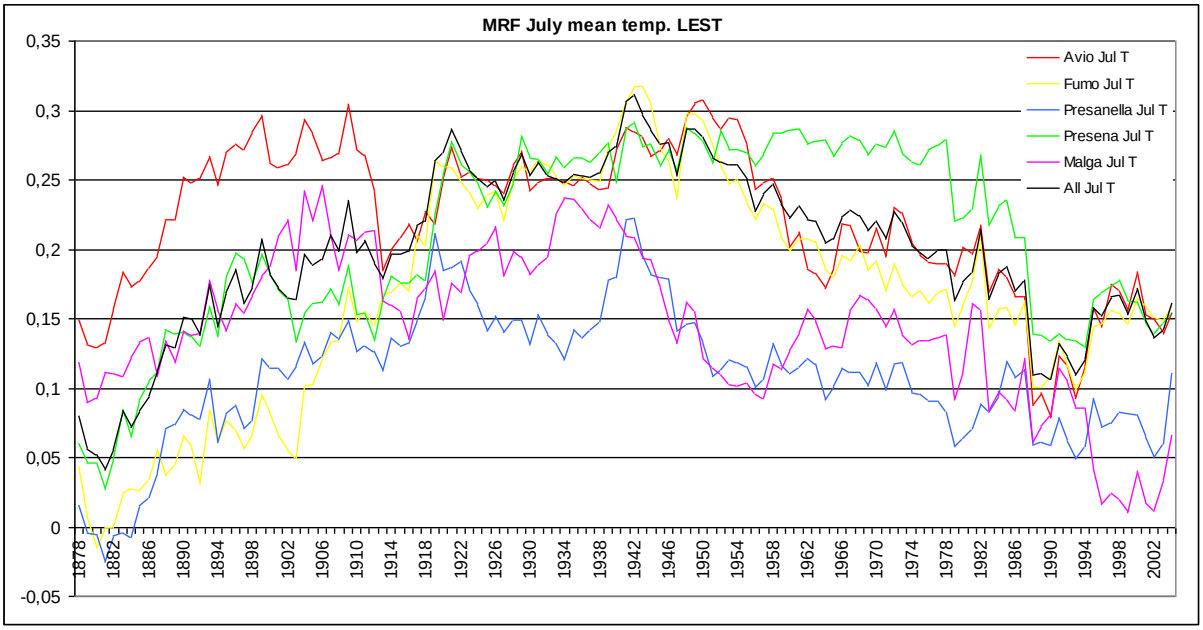

Fig. 4-75 MRF (60 yr moving window) computed between the master chronology (All), the five individual chronologies and July monthly mean temperatures. Temperature data come from low-elevation stations (<1400 m a.s.l.).

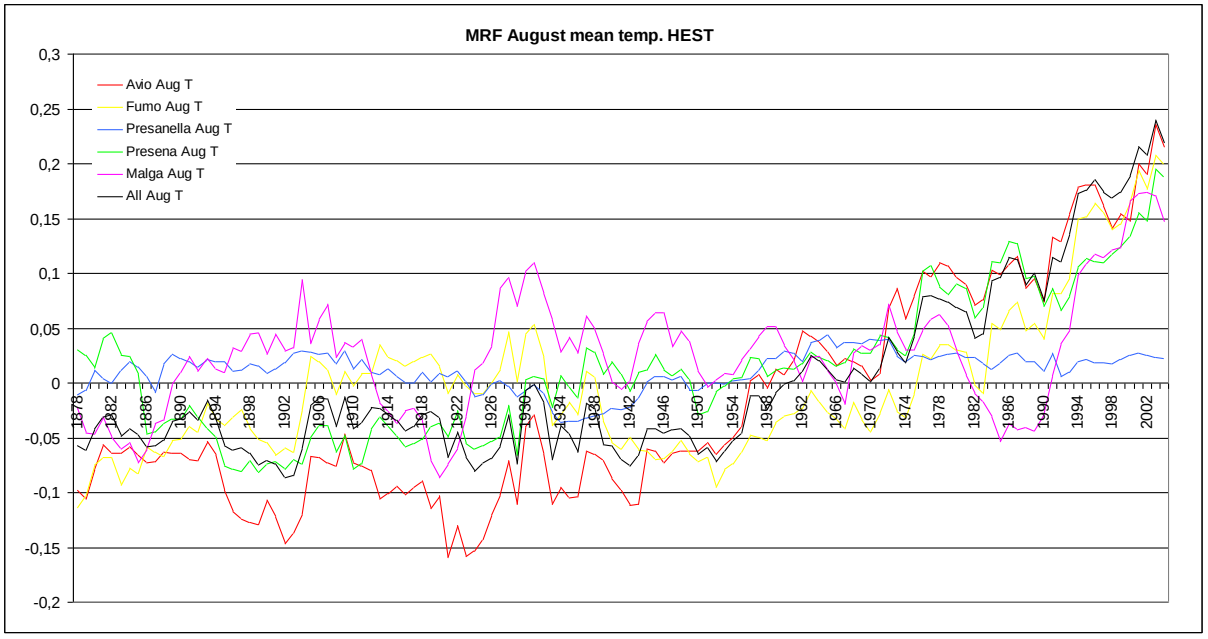

Fig. 4-76 MRF (60 yr moving window) computed between the master chronology (All), the five individual chronologies and August monthly mean temperatures. Temperature data come from high-elevation stations (>1400 m a.s.l.).

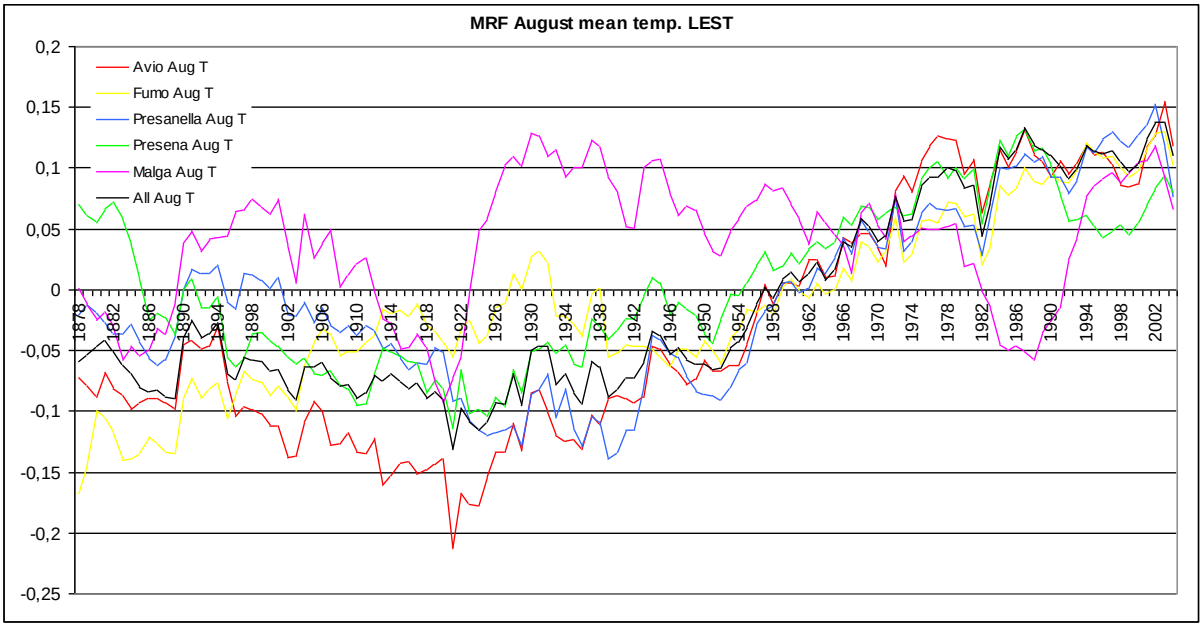

Fig. 4-77 MRF (60 yr moving window) computed between the master chronology (All), the five individual chronologies and August monthly mean temperatures. Temperature data come from low-elevation stations (<1400 m a.s.l).

Checking how the five residual tree-ring chronologies responded to the heat wave of summer 2003, we found a not consistent growth release (Fig.4-78). Ring width index remain within the mean of index values.

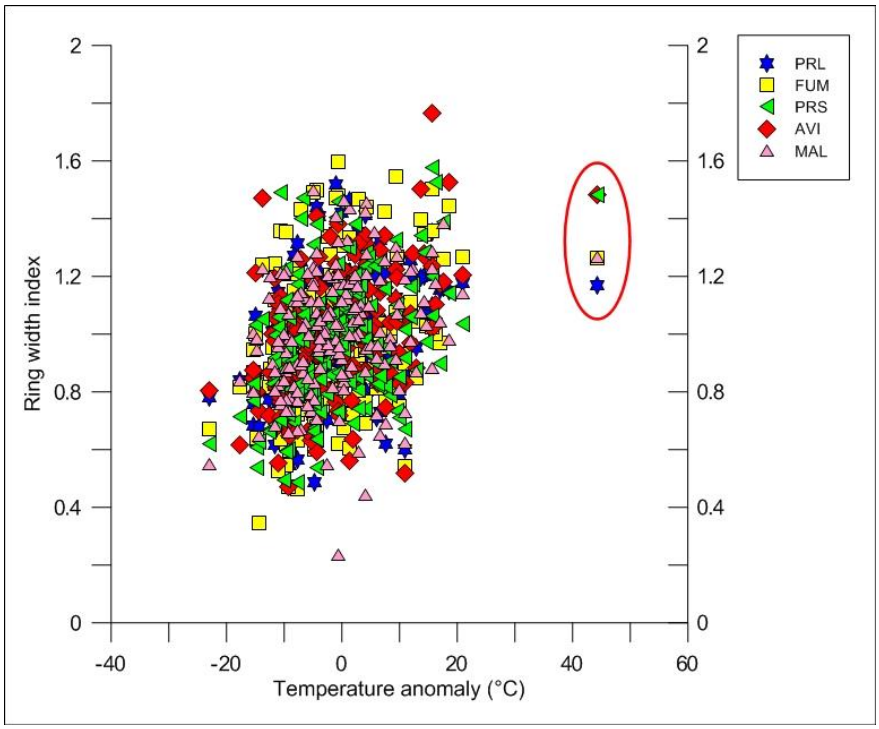

Fig. 4-78 scatter plot of he five residual larch chronologies versus JJA mean temperaure over the period 1878-2004. The red circle indicates the 2003 index values.

June July mean temperature reconstruction

The correlation analysis of climate/tree rings growth relationships revealed a quite good correlation between four of the five tree-ring width chronologies (Avio, Fumo Presena and Presanella) and June/July mean temperatures. Afterwards, we decided to use these four chronologies in the early summer (June-July) mean temperatures reconstruction, discarding the Malga chronology.

In the regression model (transfer function) we used to convert tree-ring values into climate variables values, PC eigenvalues are the predictors and the climate variables (June-July mean temperature) are the predictand.

We have defined three principal component nested models limited, by the starting year of each chronology (1818-2004, 1738-2004 and 1596-2004). The starting year of each chronology represents in our tree-ring data set an important point of change in the availability of the tree-ring series. We used PC calculated for each nest as the potential predictors in the nested time period, so that it is represented by the corresponding regression model with the greatest number of available data (Meko, 1997, Briffa, 1988). Indeed, it is well known that better reconstruction skills are usually obtained when a greater number of tree-ring chronologies are available (Young, 1994; Meko, 1996),

Considering that, in the MC Analysis, June-July mean temperature/tree-ring growth correlations decrease starting from 1960, we decided to exclude the time period successive to this date from the calibration/verification models (Jacoby et al. 2000, Briffa et al 2001).

Principal component analysis results

In tables 4-25, 4-26 and 4-27, are reported results obtained from the principal component analysis for each nest. As evidenced by the scree plots, in all the three models the first principal component (PC1) accounts for a very large percentage of the variance (77%, 79% and 81% respectively) (Figs, 4-79, 4-80 and 4-81). Such an elevated explained variance expressed by the first PC is highly indicative of common signals, demonstrating that PC eigenvalues can capture common climatic information across our chronologies' network. These results allow retaining only the first principal component as predictor for each nest.

All the other three types of plots, computed for each model to better evaluate the relative importance of the principal components and for examining the scores of the first two principal components (*Score plot for first 2 components Loading plot for first 2 components*,

Biplot for first 2 components), confirm the goodness of the choice of the only first principal component (Figs, 4-79, 4-80 and 4-81).

Moreover, this choice is consistent with the Kaiser-Gutman rule. In all the three models, the eigenvalues of an order higher than one are <1, then they can be discarded without loosing an important fraction of variance.

Eigenanalysis of the Correlation Matrix first nest 1818-2004				
Eigenvalue	3,0840	0,3513	0,3194	0,2453
Proportion	0,771	0,088	0,080	0,061
Cumulative	0,771	0,859	0,939	1,000
Variable	PC1	PC2	PC3	PC4
Avio	0,493	0,589	-0,608	0,200
Presanella	0,496	-0,721	-0,146	0,461
Fumo	0,514	-0,176	-0,030	-0,839
Presena	0,496	0,318	0,780	0,210

Tab. 4-25 results obtained from the principal component analysis for the first nest.

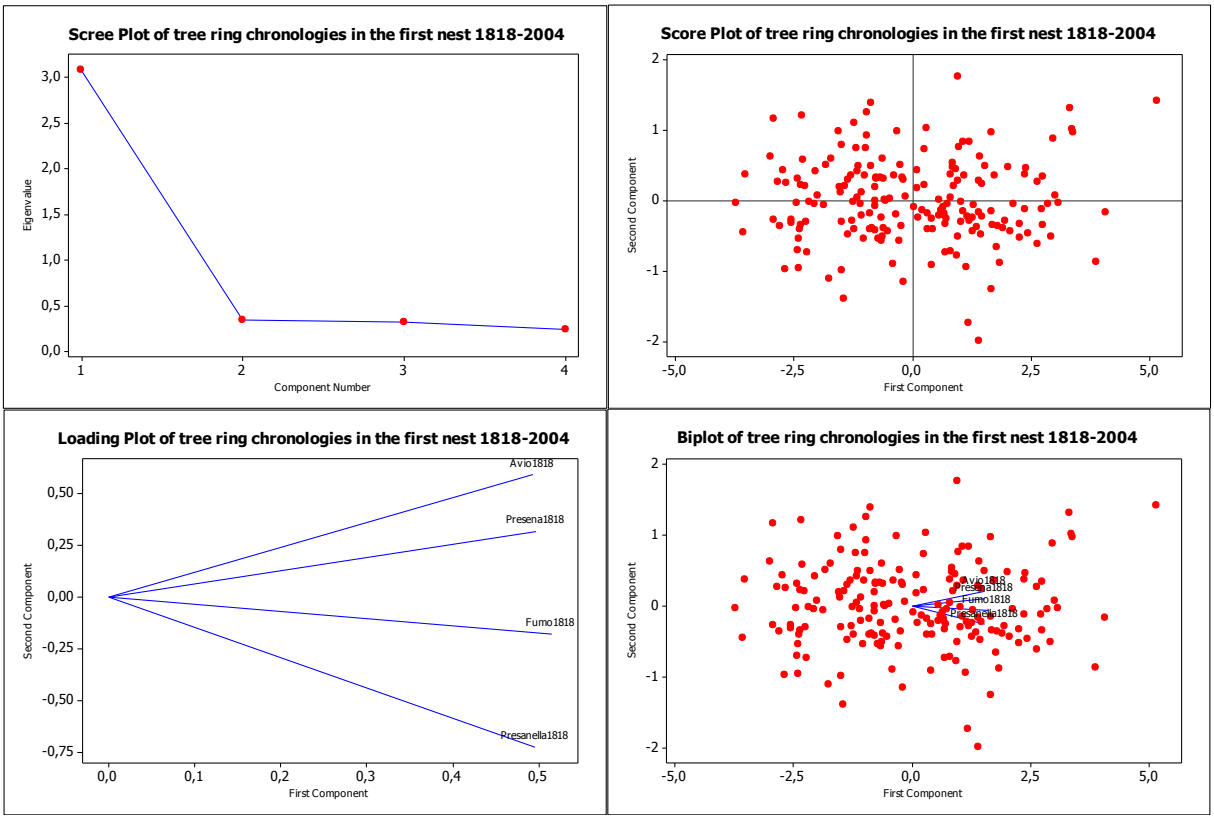

Fig 4-79 plots used for evaluating the importance of the different principal component, and for examining the scores of the first two principal component in the first nest.

Eigenanalysis of the Correlation Matrix 2°nd nest 1736-2004			
Eigenvalue	2,3581	0,3587	0,2831
Proportion	0,786	0,120	0,094
Cumulative	0,786	0,906	1,000
Variable	PC1	PC2	PC3
Avio	0,567	-0,810	-0,150
Presanella	0,579	0,521	-0,626
Fumo	0,586	0,268	0,765

Tab. 4-26 results obtained from the principal component analysis for the second nest.

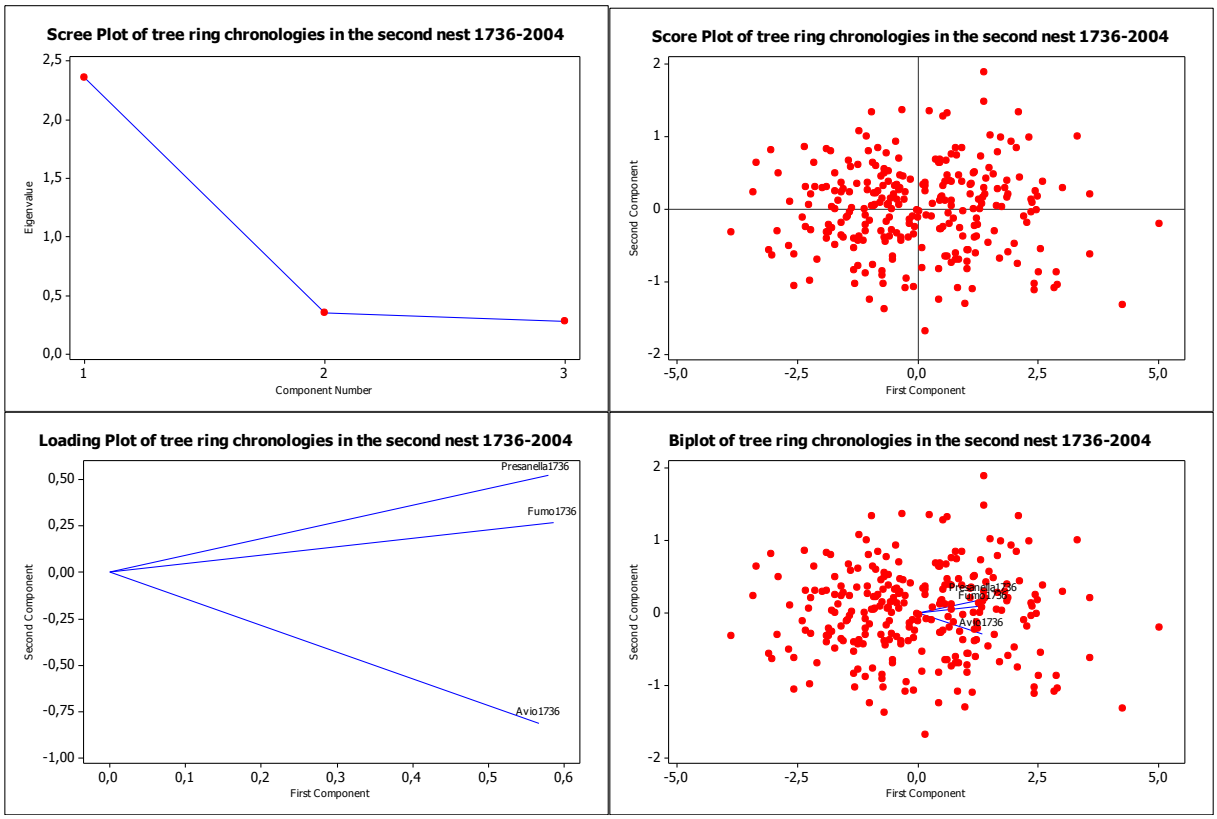

Fig. 4-80 plots used for evaluating the importance of the different principal component, and for examining the scores of the first two principal component in the second nest.

Eigenanalysis of the Correlation Matrix 3°rd nest 1596-2004		
Eigenvalue	1,6137	0,3863
Proportion	0,807	0,193
Cumulative	0,807	1,000
Variable	PC1	PC2
Avio	0,707	-0,707
Presanella	0,707	0,707

Tab. 4-27 results obtained from the principal component analysis for the third nest.

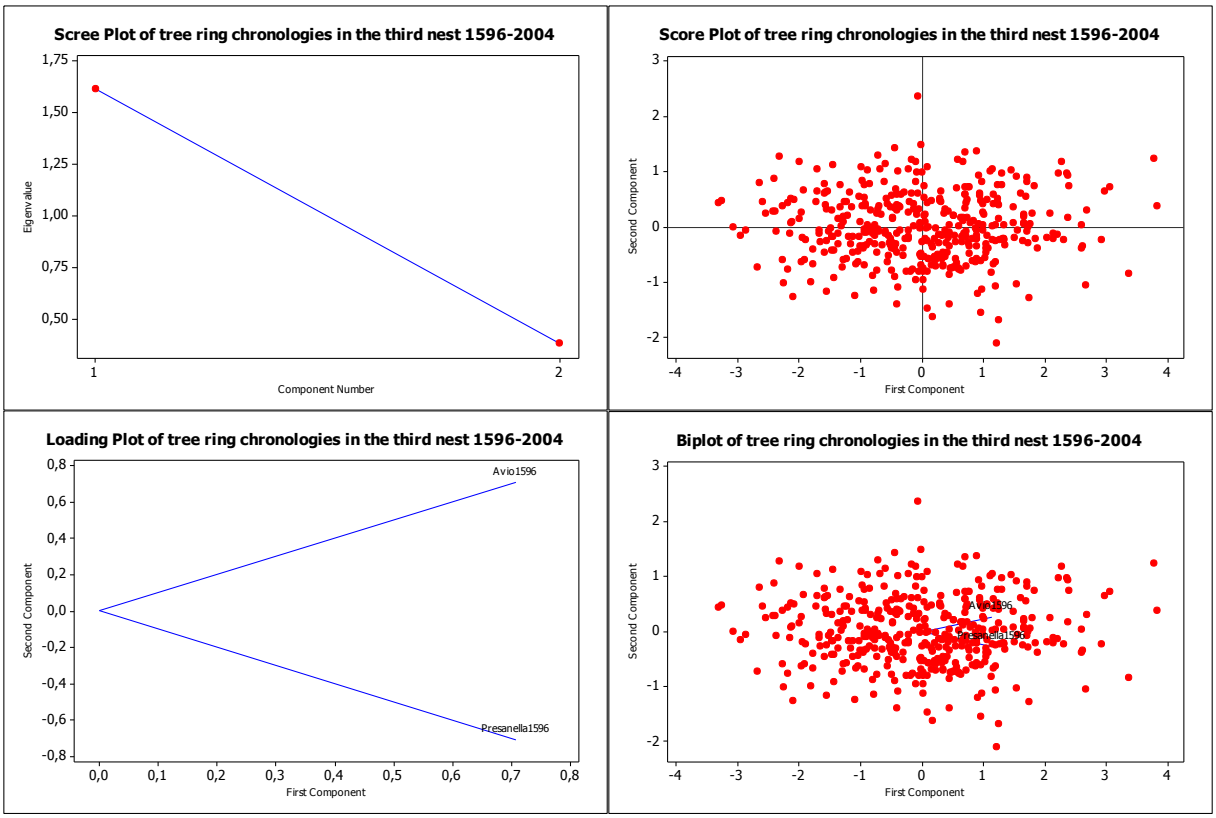

Fig. 4-81 plots used for evaluating the importance of the different principal component, and for examining the scores of the first two principal component in the third nest.

Histograms used to compare the frequency distributions of the climate data (June-July mean temperatures) and of the tree-ring series (PC1) (Fig.4-82), show that the distribution of PC1 of the first nest is mostly normal, but slightly positively skewed. The distribution of PC1 of the second and third nest is almost normal.

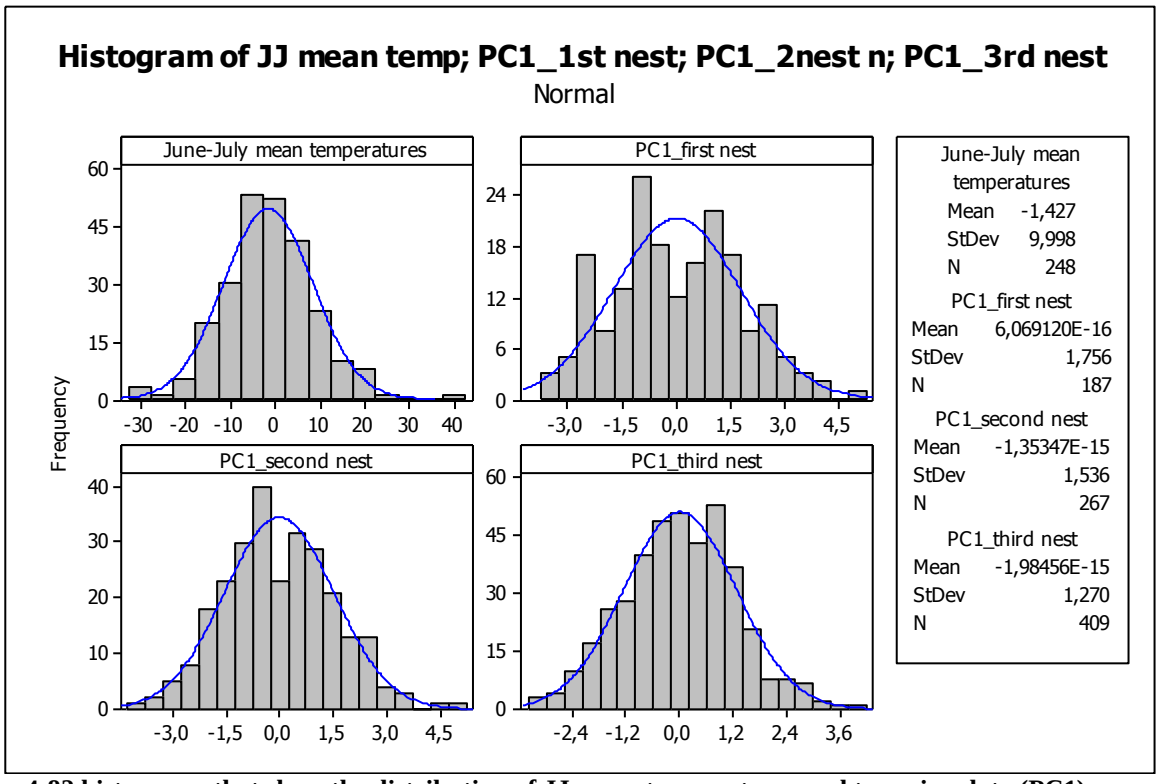

Fig. 4-82 histograms that show the distribution of JJ mean temperatures and tree-ring data (PC1).

The fitting to normal distribution of our tree-ring data is highlighted in the probability plots. We have plotted each value vs. the percentage of values in the sample that are less than or equal to it, along a fitted distribution line (middle blue line). It results in three probability graphs, one for each PC1 (Fig 4-83). The approximate 95% confidence intervals (curved blue lines) for the percentiles and a table with distribution parameter estimates along with the Anderson-Darling statistic and P-value are displayed.

We can see that all our data fit the normal distribution, actually the plotted points form a quite precise straight line and fall rather closely to the distribution line, the Anderson-Darling statistic are small (<1) and the p values are larger then the chosen α level (0,05).

The PC1 of the first nest shows lower results in the test for normality, the p value is hardly above the α level (0,06) and the Darling-Anderson statistic has the highest value (0,714), but, in any case, the condition for normality are respected and we don't need to operate any data transformation.

The distribution with the smallest Anderson-Darling statistic, which means with the closest fit to normality, is the PC1 of the third nest that shows a very high p value (0,741) and the lower AD value (0,215).

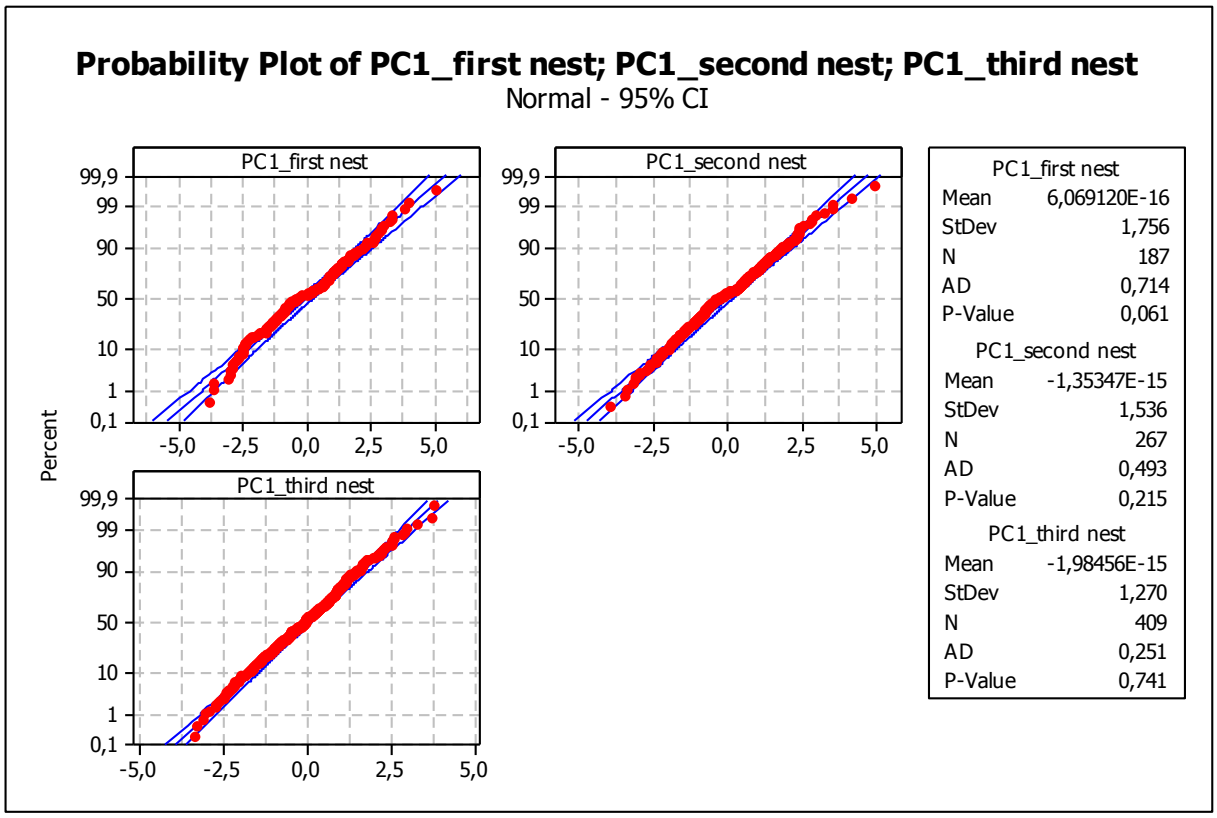

Fig. 4-83probability plots of the three PC1.

To further explore the relationship between climate data and predictors a scatterplot has been drawn between the first nest PC1 and the same period of the available June July mean temperature series. As highlighted in Fig. 6, we found that climate data are positively and directly correlated (Fig. 4-84).

We then used PC1 values as predictors into the successive regression computations.

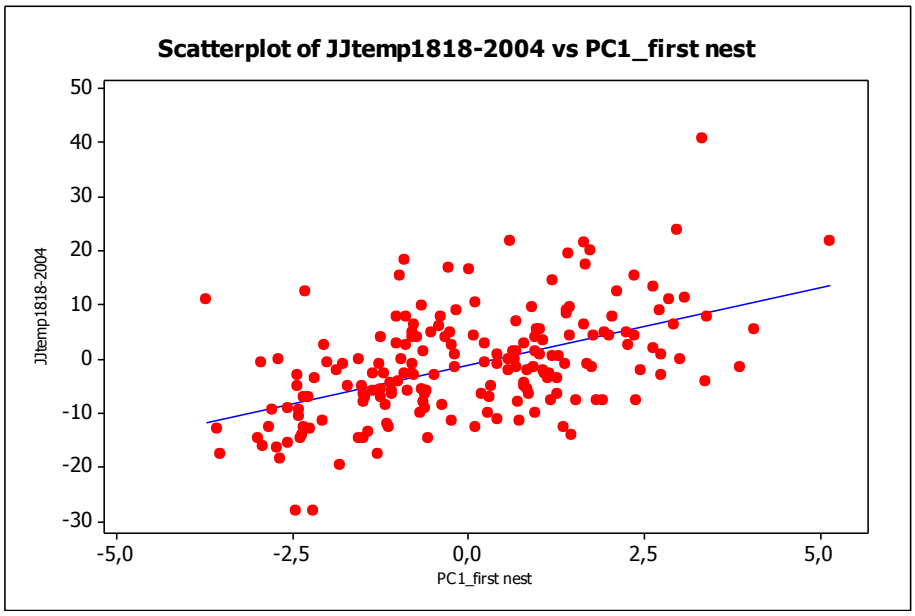

Fig. 4-84 Scatterplot of PC1 of the first nest versus climate data.

Calibration verification procedure results

The entire calibration period (120 years) is common to the three nests (1840-1959). The full length of the calibration period is divided in two subsets (1840-1899 and 1900-1959 respectively), and they are alternately exchanged for calibration and verification procedures following the split sample technique.

Since the two regression models deriving from the split sample procedure were similar in values and structure, we ran the regression on the whole period (1840-1959) and used the resulted final regression model to predict climate variable on the whole extension of each nest. Afterwards, the three individually calibrated models were spliced to form the 1596-2004 June July mean temperature reconstructed series (Fig. 4-85 up to 4-96).

The histograms of residuals in the calibration periods of the three nests show a positive skew, but only in the second nest the test for normality (*sensu* Anderson-Darling) has lower values than the minimum threshold (p=0,038, α level 0,05), and the normal probability plot of residuals describes a quite precise straight line.

The *plots of residual versus fitted values* should show a random pattern of residual on the both sides of 0, and this assumption is quite respected in both calibration and verification periods in the three nests.

The *plots of residual versus order of data* allows to verify if the residuals are uncorrelated each other, a positive correlation is indicated by a clustering of residuals with the same sign, a negative correlation is indicated by rapid changes in the signs of consecutive residuals. In the calibration-period plots the presence of patters of residuals of the same sign is visible. This result let us suppose the persistence of some autocorrelation that has been quantified with the Durbin-Watson statistic (see next paragraph).

Reconstruction validation results

Pearson's correlation values computed between actual and reconstructed climate data for each calibration and verification period, range from 0,58 to 0,62 (Tab.4-28, and 4-29).

Split sample calibration/verification shows that the nested reconstructions are skilful as function of time and tree-ring data, and account for a quite good fraction of the expressed variance (R^2 ranges from 34,1% to 38,3%).

In particular, in the calibration period the explained variance of the regression ranges from 38,3% to 33,7%, with smaller values occurring when the predictor (PC1) derives from a

fewer number of chronologies. Explained variance in the verification periods ranges from 34,1 to 37,2% (Tab.4-28).

In the whole models values of RE and CE statistics are greater than zero, indicating that models have predictive skill in comparison both to the mean of the calibration period, and to the mean of verification period. In particular, the positive values of the Coefficient of Efficiency indicate good reconstruction skills of our model in the low frequency components too.

RE and CE statistics have very similar values that means similar mean values both in calibration and verification periods in all the three models (Tabs 4-28 an 4-29).

The Durbin Watson statistic values are very close to 2 in all the regressions (Tab 4-28) testifying a quite complete absence of autocorrelation. DW values obtained in the three models in the calibration periods are higher then DW values obtained in the verification periods, it means that there is evidence of some positive serial correlation, even if not significant, confirming what seen in the plots of residual versus order of data.

FIRST NEST

Calibration period

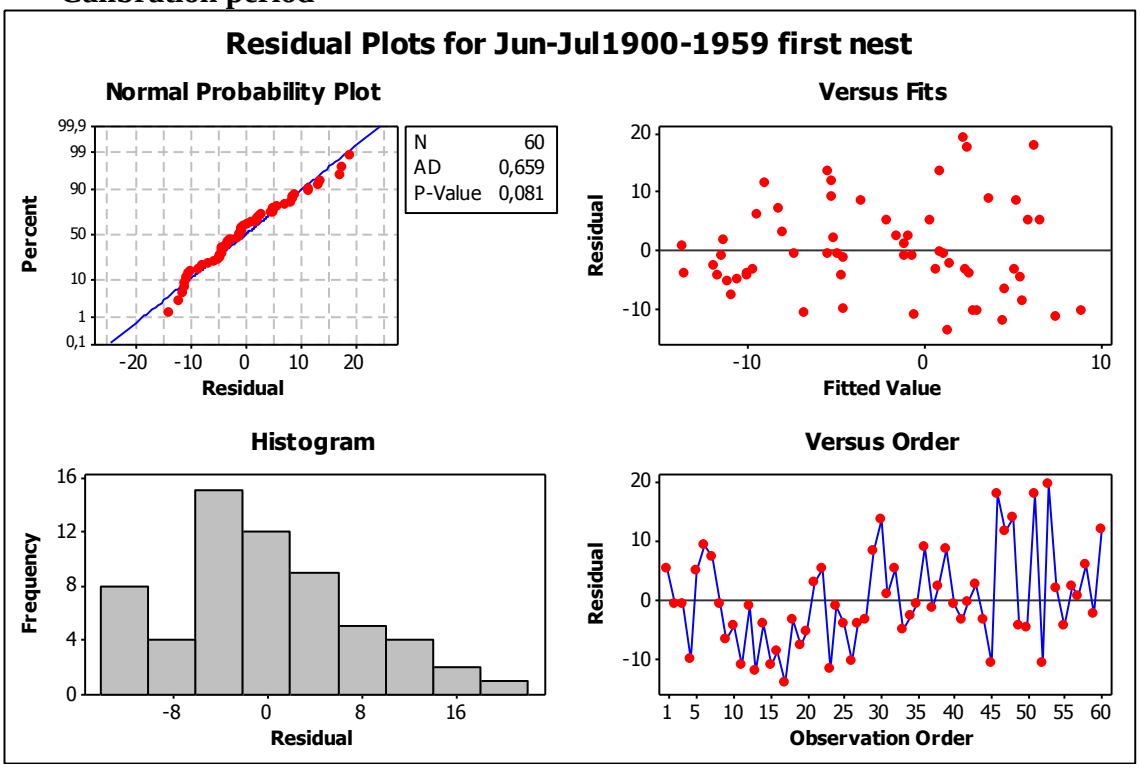

Fig. 4-85 Residual plots for the calibration period (1900-1959) in the first nest

The regression equation is: Jun-Jul1900-1959 = - 2,83 + 3,04 PC11900-1959

Verification period

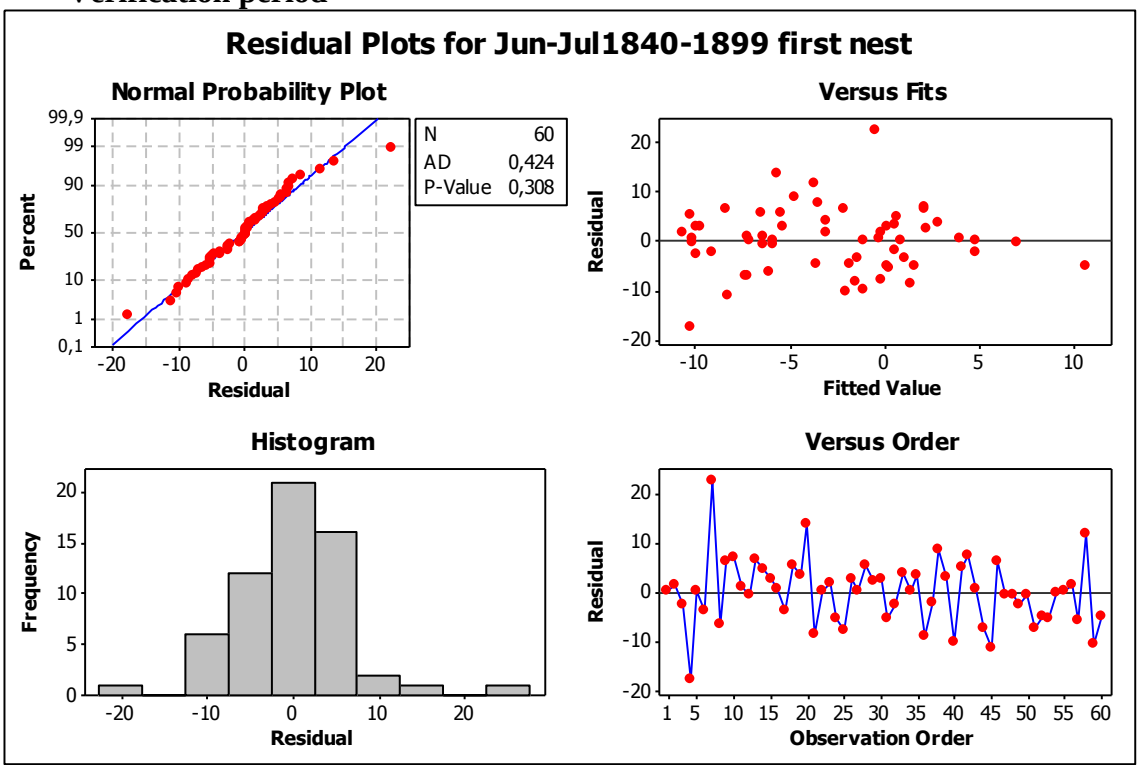

Fig. 4-86 Residual plots for the verification period (1840-1899) in the first nest

The regression equation is: Jun-Jul1840-1899 = - 2,44 + 3,21 PC11840-1899

Calibration period

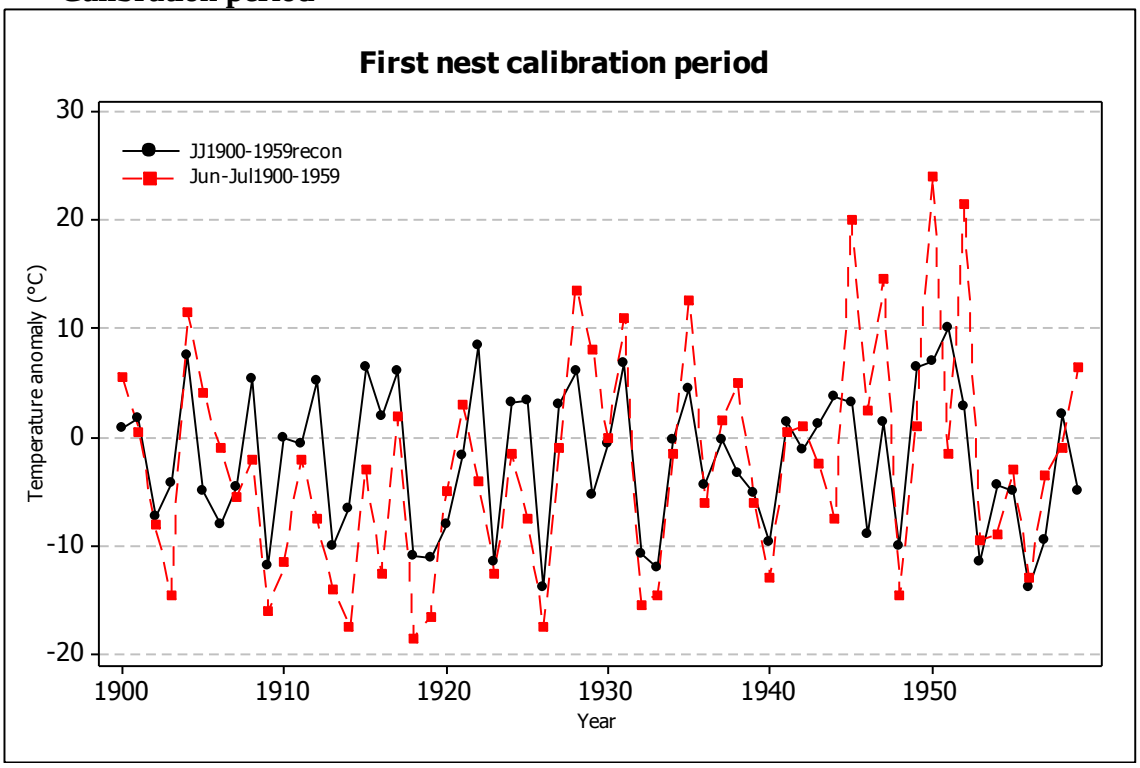

Fig. 4-87 Time series plot of actual and reconstructed JJ mean temp. for the calibration period.

Pearson correlation of JJ1900-1959recon and Jun-Jul1900-1959 instr.=0,619

Verification period

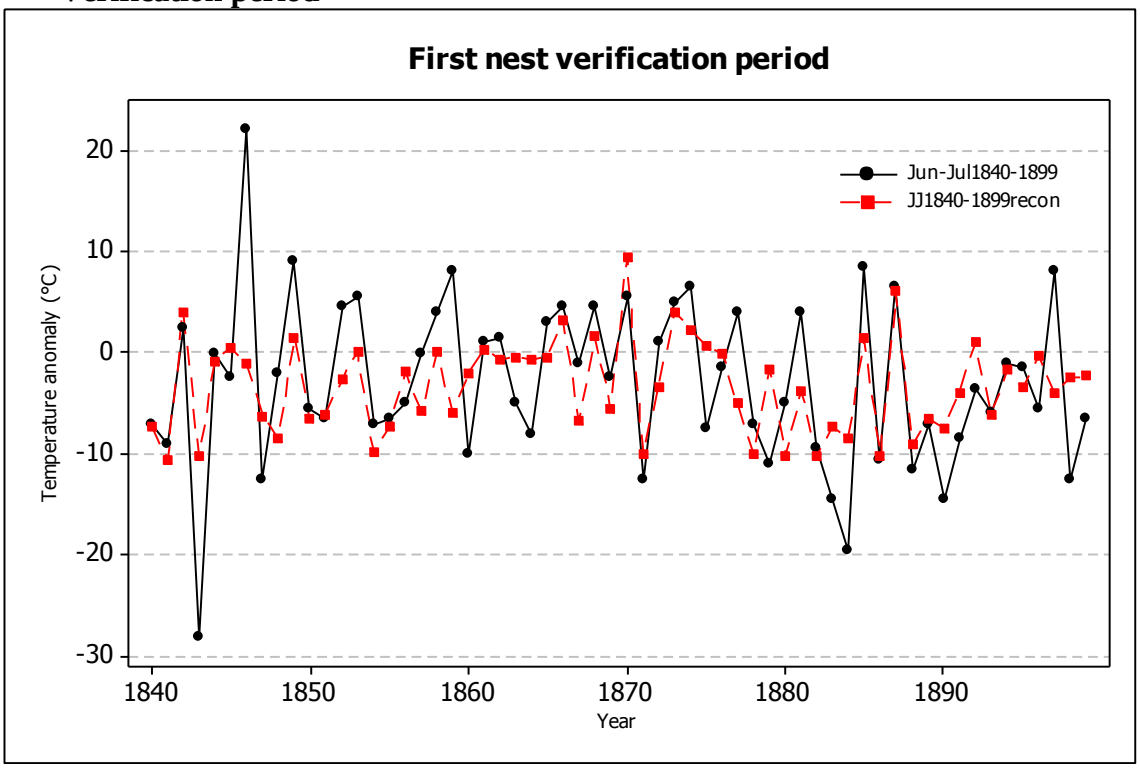

Fig. 4-88 Time series plot of actual and reconstructed JJ mean temp. for the verification period.

Pearson correlation of JJ1840-1899recon and Jun-Jul1840-1899 instr. = 0,597

SECOND NEST

Calibration period

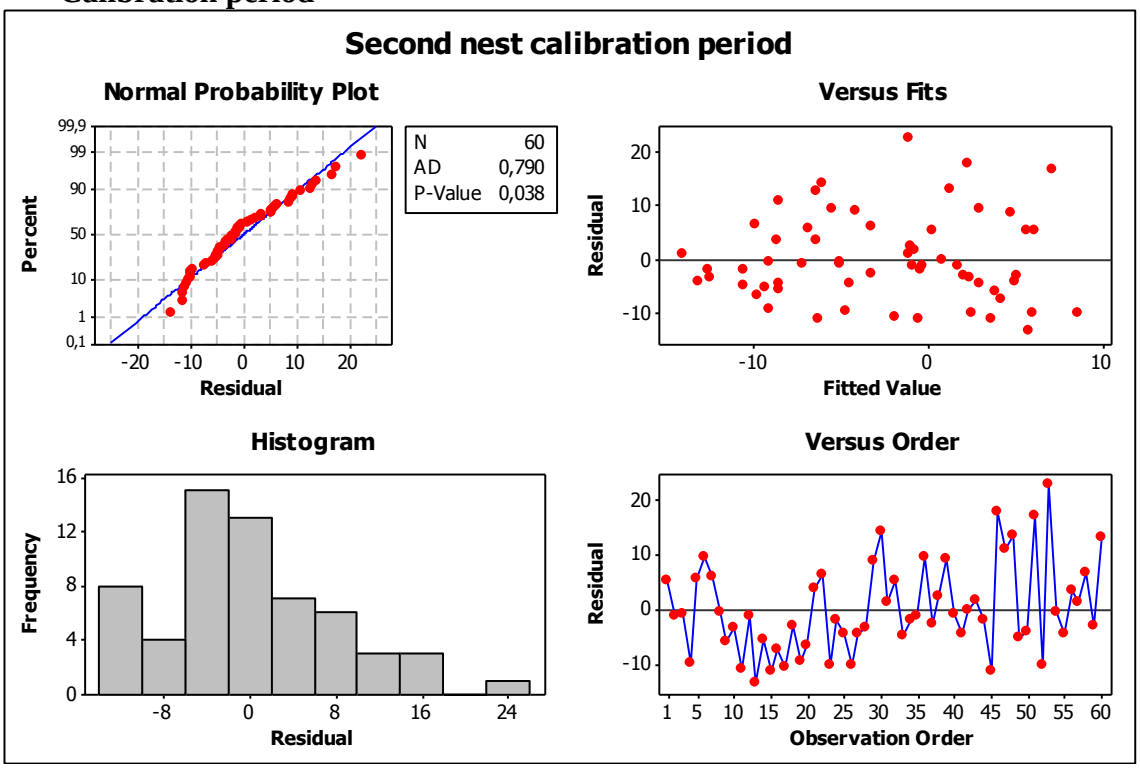

Fig. 4-89 Residual plots for the calibration period (1900-1959) in the second nest.

The regression equation is: Jun-Jul1900-1959 = - 2,68 + 3,40 PC11900-1959

Verification period

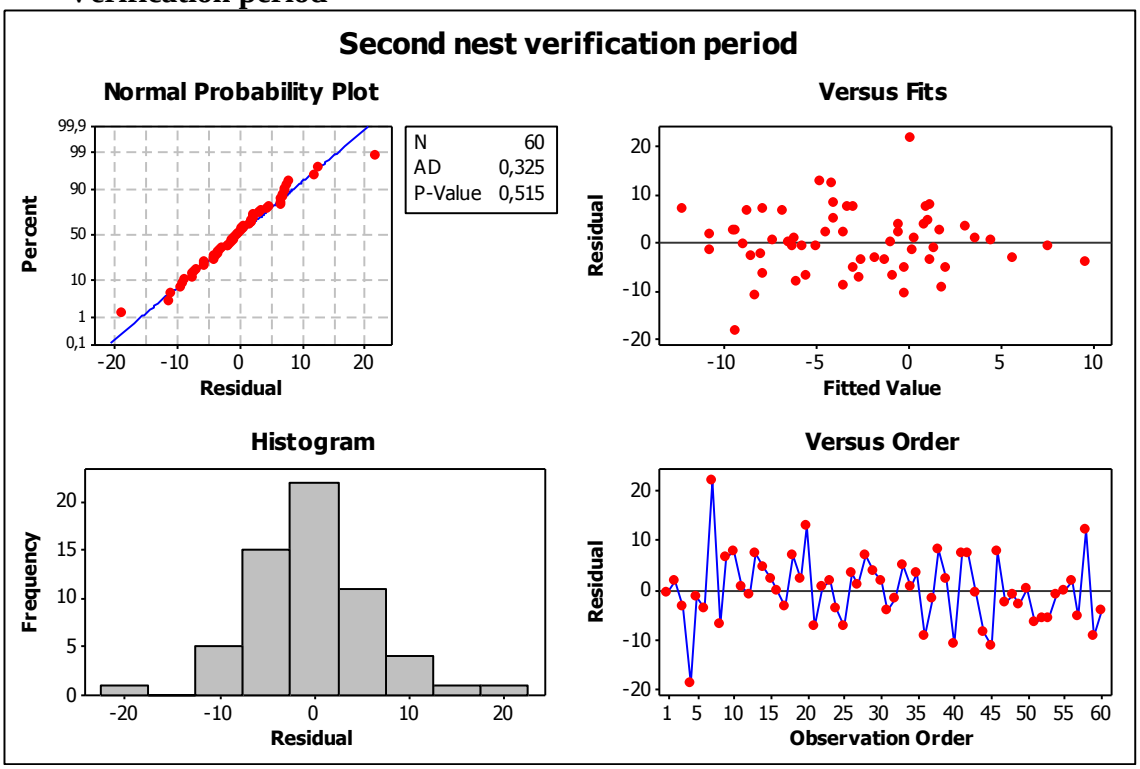

Fig. 4-90 Residual plots for the verification period (1840-1899) in the second nest.

The regression equation is: Jun-Jul1840-1899 = - 2,94 + 3,49 PC11840-1899

Calibration period

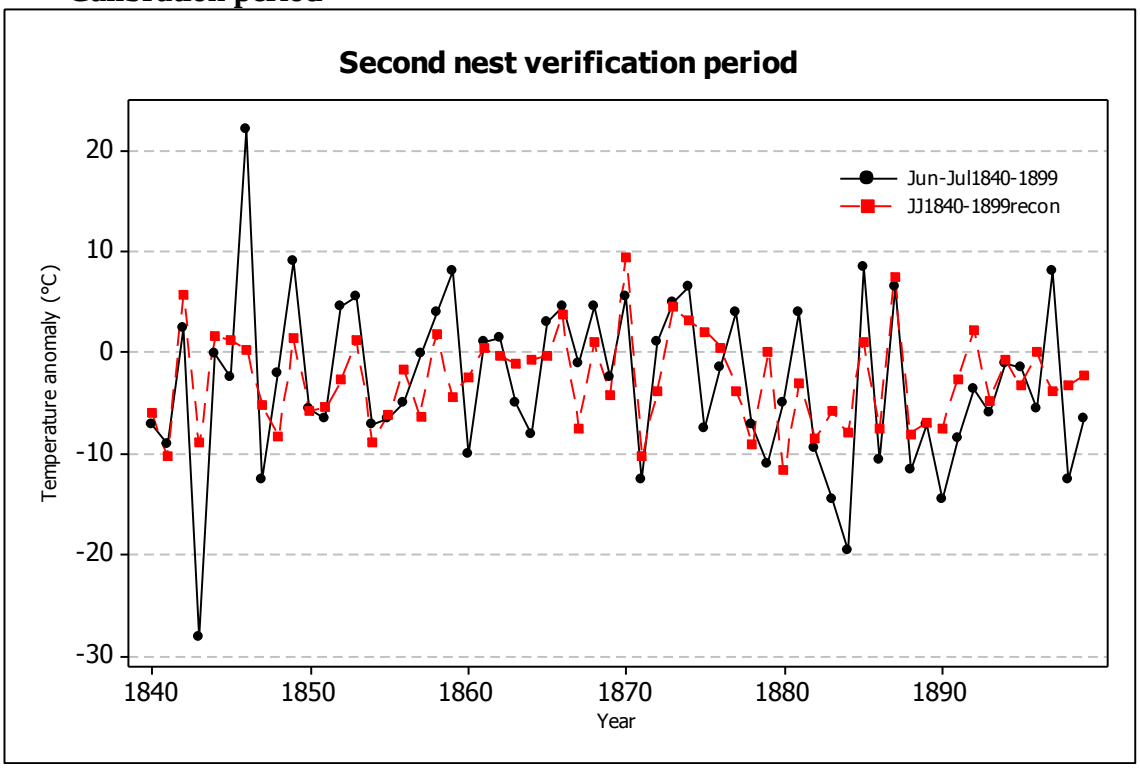

Fig. 4-91 Time series plot of actual and reconstructed JJ mean temp. for the calibration period.

Pearson correlation of JJ1900-1959recon and Jun-Jul1900-1959 instr. = 0,596

Verification period

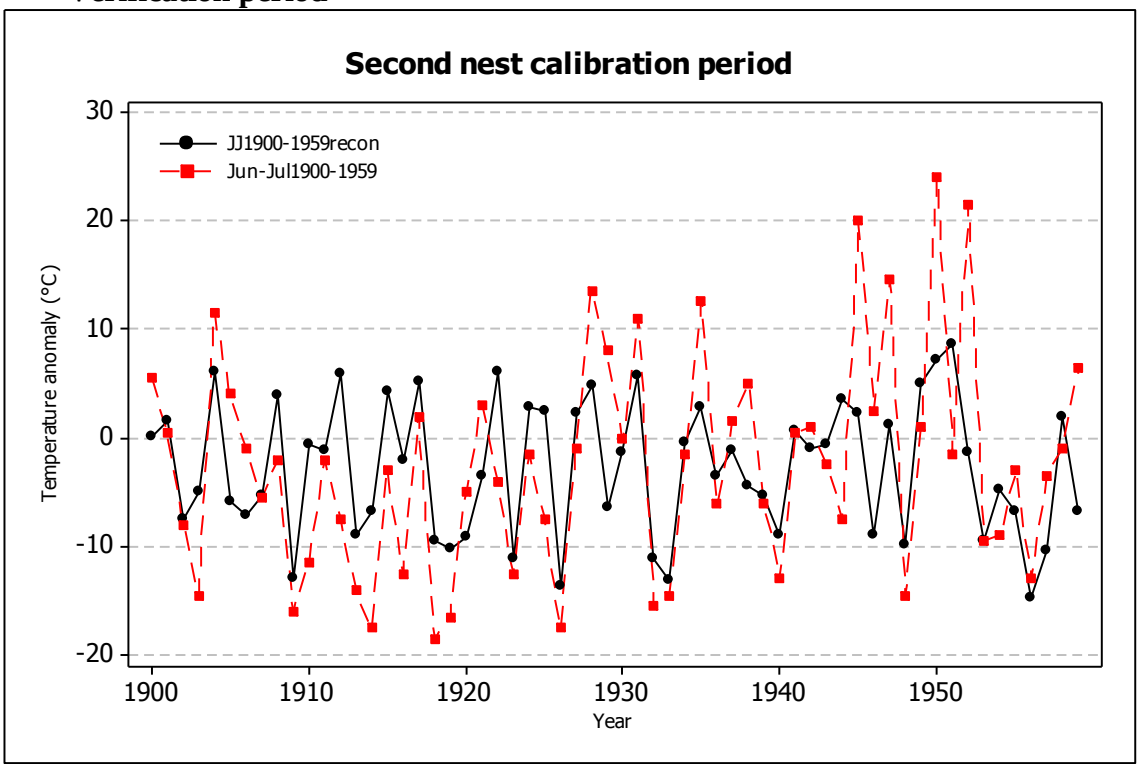

Fig. 4-92 Time series plot of actual and reconstructed JJ mean temp. for the verification period.

Pearson correlation of JJ1840-1899recon and Jun-Jul1840-1899 instr. = 0,584

THIRD NEST

Calibration period

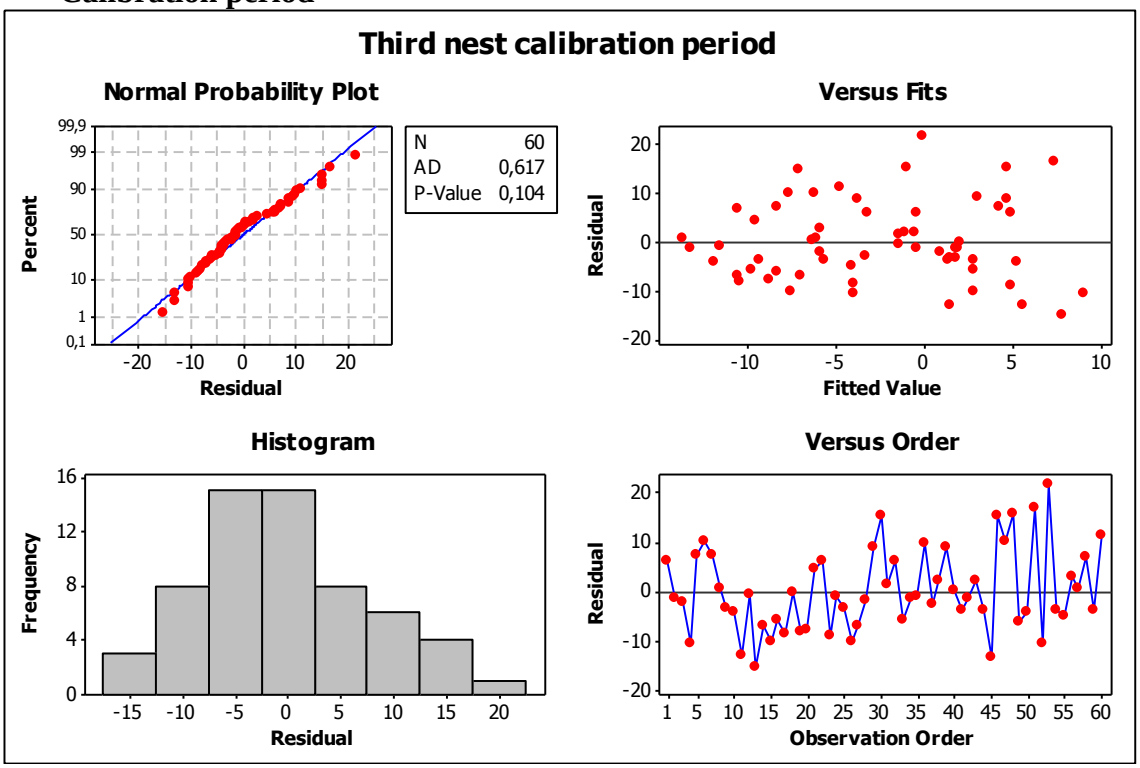

Fig. 4-93 Residual plots for the calibration period (1900-1959) in the third nest.

The regression equation is: Jun-Jul1900-1959 = - 2,31 + 4,21 PC11900-1959

Verification period

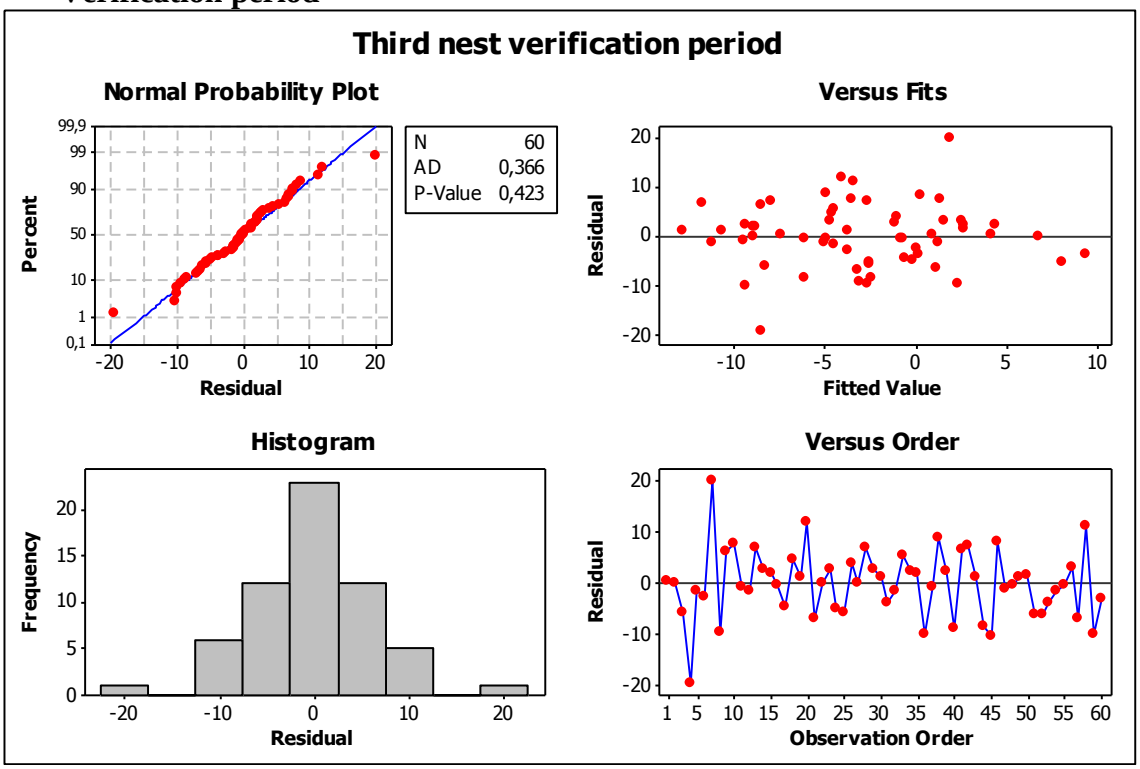

Fig. 4-94 Residual plots for the verification period (1840-1899) in the third nest.

The regression equation is: Jun-Jul1840-1899 = - 2,82 + 4,15 PC11840-1899

Calibration period

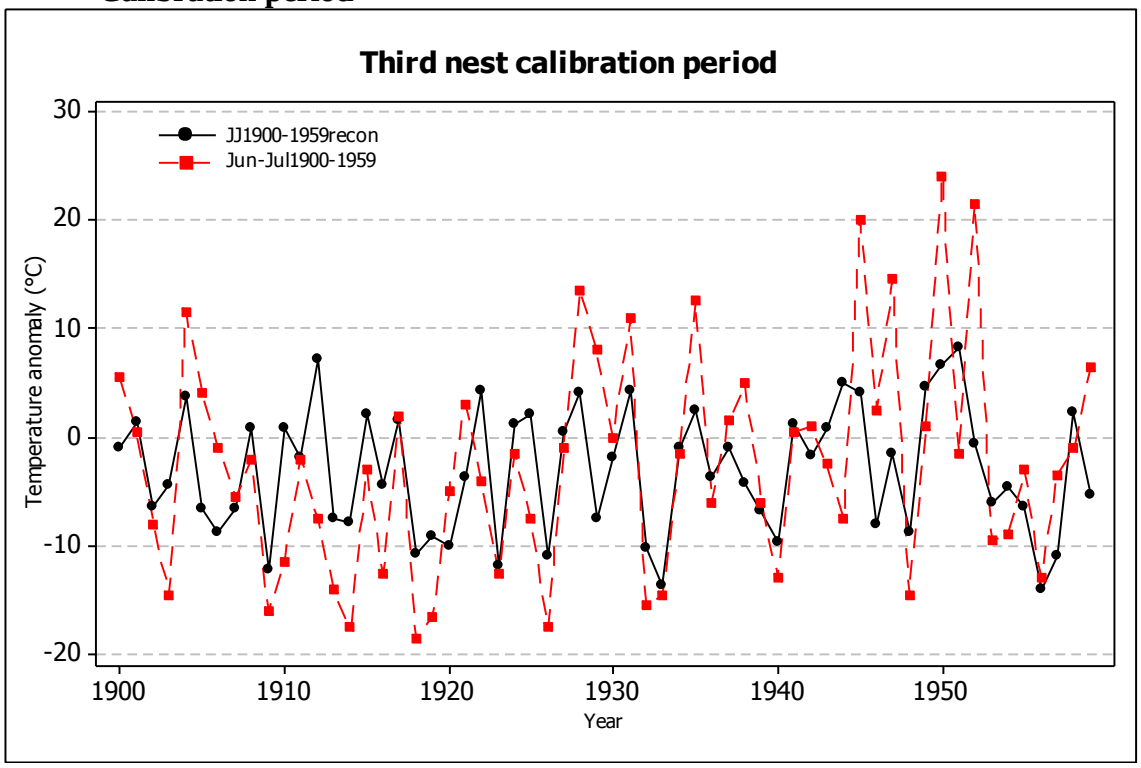

Fig. 4-95 Time series plot of actual and reconstructed JJ mean temp. for the calibration period.

Pearson correlation of JJ1900-1959recon and Jun-Jul1900-1959 instr. = 0,581

Verification period

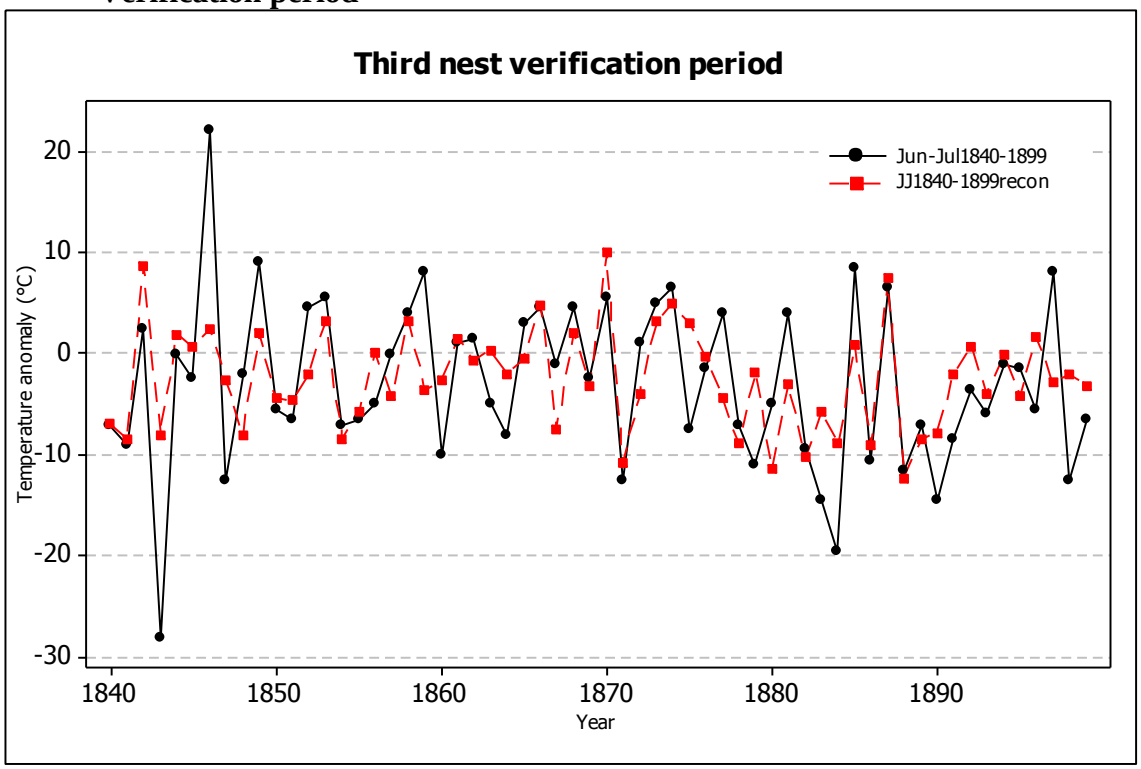

Fig. 4-96 Time series plot of actual and reconstructed JJ mean temp. for the verification period.

Pearson correlation of JJ1840-1899recon and Jun-Jul1840-1899 instr. = 0,610

Model	Period	r(calib.)	RE	CE	R^2(calib.)	DW
1	1818-2004	0,619	0,381	0,380	38,3%	1,75
2	1738-2004	0,596	0,355	0,354	35,5%	1,81
3	1596-2004	0,581	0,370	0,369	33,7%	1,88

Tab. 4-28 Calibration statistics for the nested temperature models.

Model	Period	r(verif.)	RE	CE	R^2(verif.)	DW
1	1818-2004	0,597	0,353	0,355	35,7%	2,24
2	1738-2004	0,584	0,342	0,340	34,1%	2,22
3	1596-2004	0,610	0,340	0.334	37,2%	2,25

Tab.4-29 Verification statistics for the nested temperature models.

Correlations: 1stnest1818-2004; 2ndnest1818-2004; 3tdnest1818-2004		
	1stnest1818-2004	2ndnest1818-2004
2ndnest1818-2004	0,983	
3tdnest1818-2004	0,955	0,973

Tab. 4-30 Pearson's correlation values between the common periods of the three models.

The three individual subset models show similar patterns in both extreme values, and in decadal and in multi decadal fluctuations, as it derives from the high Pearson's correlation coefficient values calculated over the common period to the three models (1818-2004) (Tab. 4-30). The lowest correlation, even if still highly significant ($r = 0,955$ $p<0,001$), is the one obtained between the first and the third nest.

Overall, results of the statistics tests, performed for the split sample calibration/verification procedure, indicate stability of the relationships between instrumental data and predictors over halves of the instrumental period chosen for calibration. Moreover, the coefficients of the regression functions, computed for each period in all the nests, are quite similar. It was then possible to calculate the regression over the entire calibration period (1840-1959). This procedure allowed obtaining the coefficients of a transfer function (Fritts, 1976) that have been used for reconstructing June-July mean temperatures over the total extension of the three models (Tabs). The resulted time series were spliced together to form the final June July mean temperatures reconstruction spanning from 1596 to 2004.

The merged composite reconstruction is formed by the complete length of the first model plus the time series 1738-1817 derived from the second model and the time series 1596-1737 of the third model. So that the first model is used over its full time span and the further models sequentially attached (Fig. 4-97).

The complete June-July mean temperature reconstruction is illustrated in figures 4-98 and 4-99.

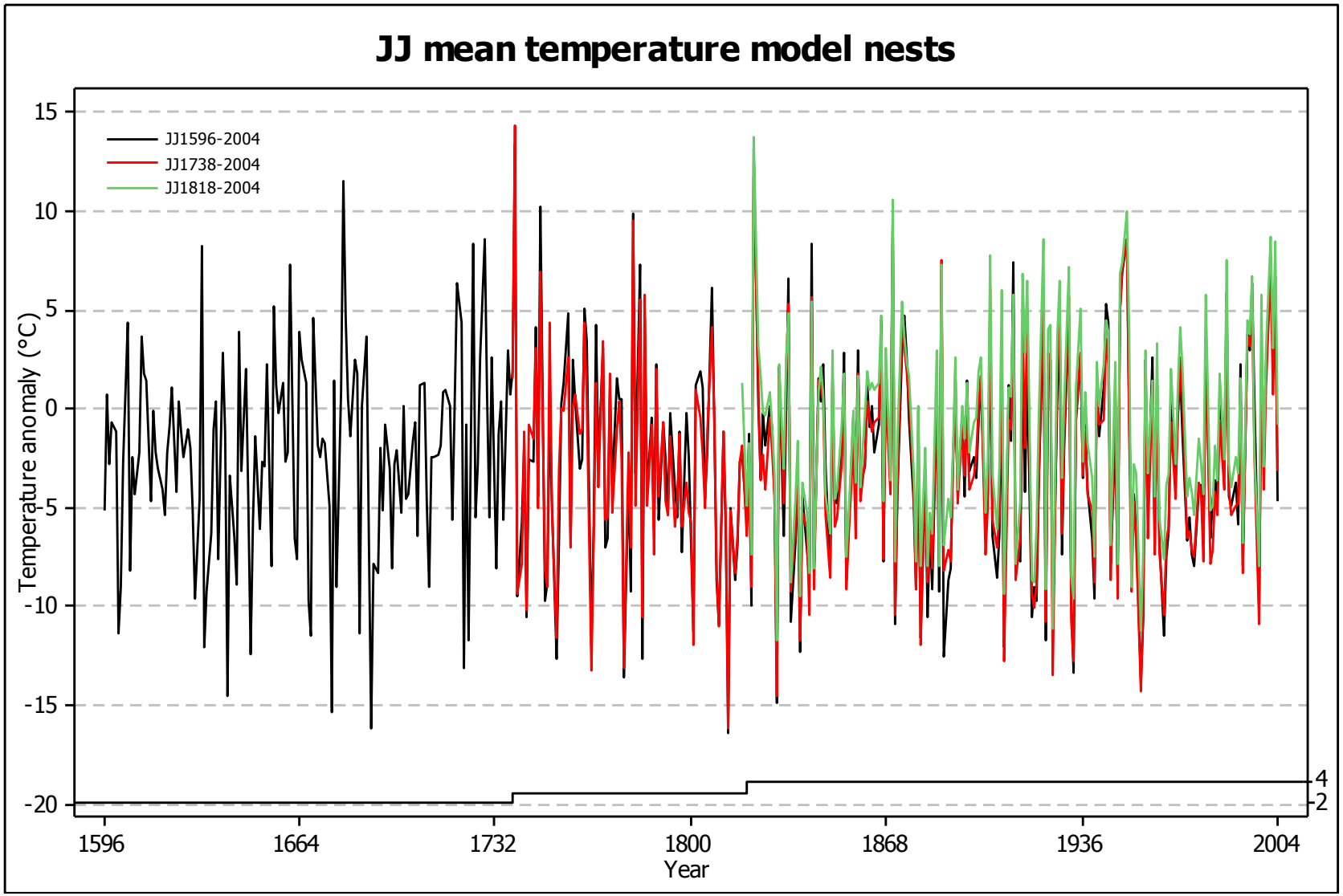

Fig. 4-97 JJ temperature models derived from the full 1840-1959 calibration period. Temperatures are anomalies with respect to the XX century average. The tree ring width nests and the available number of chronologies in each time period for PC regression are visible.

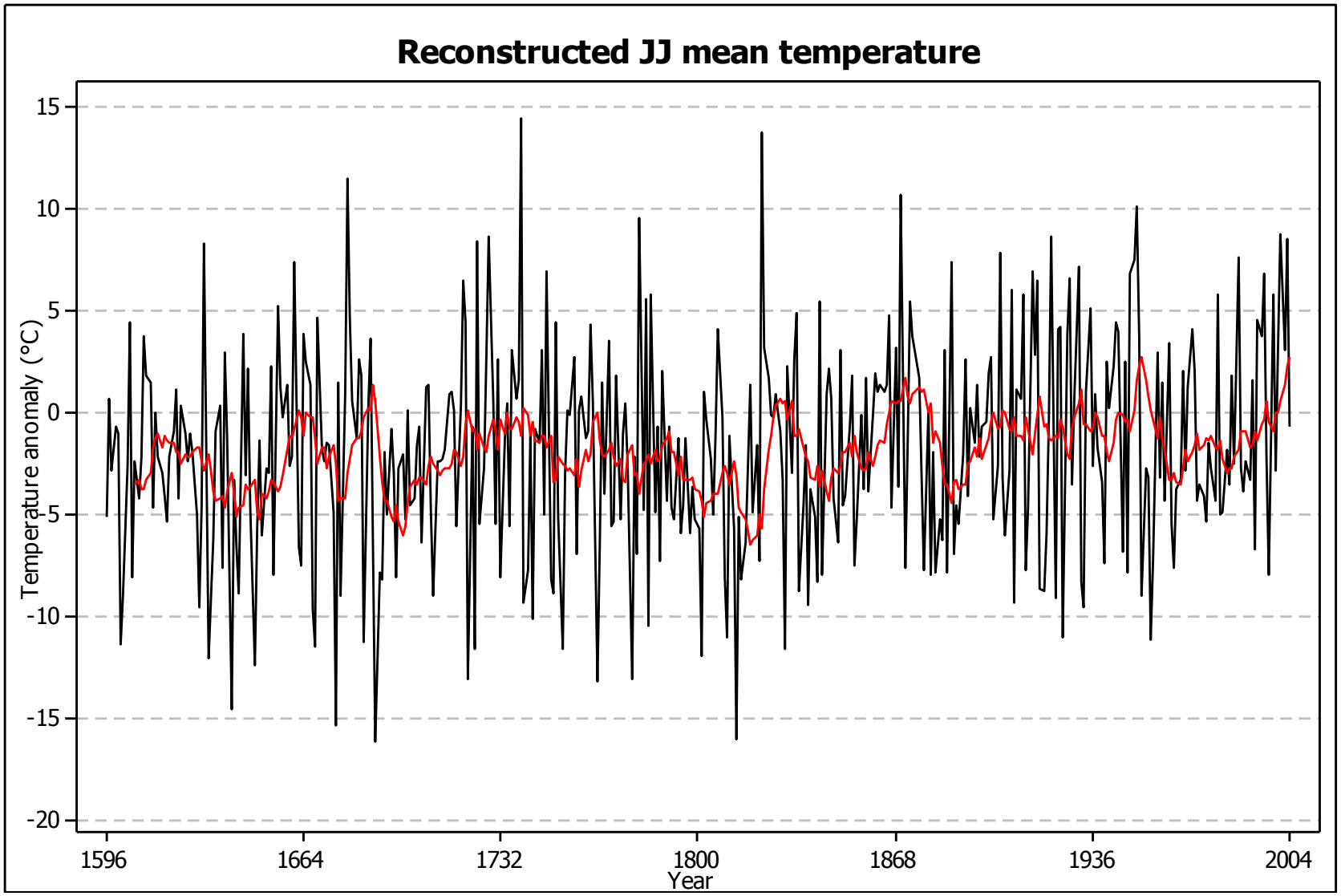

Fig. 4-98 June-July mean temperature reconstruction, the red line is a 10 yr moving average.

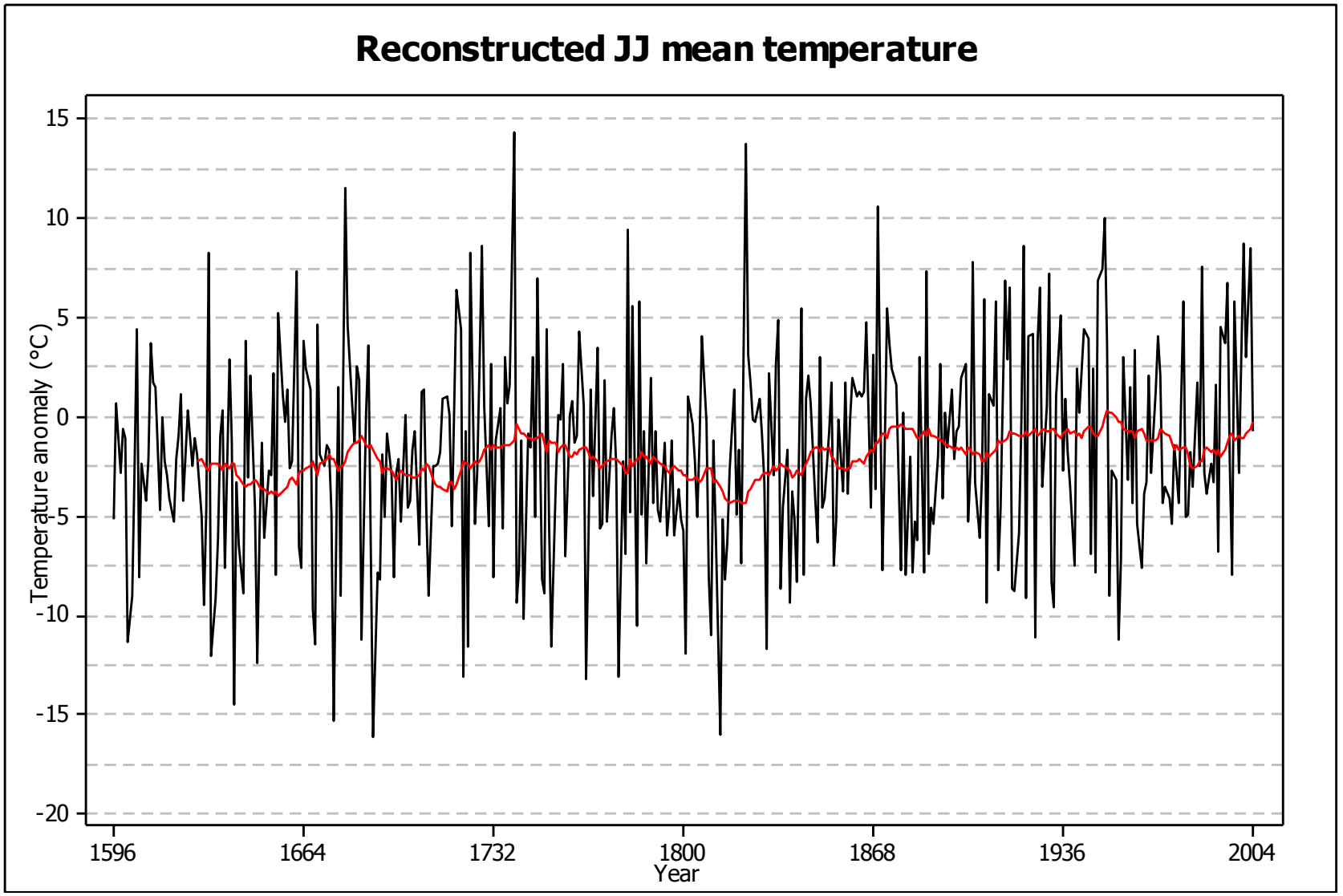

Fig. 4-99 June-July mean temperature reconstruction, the red line is a 30 years moving average.

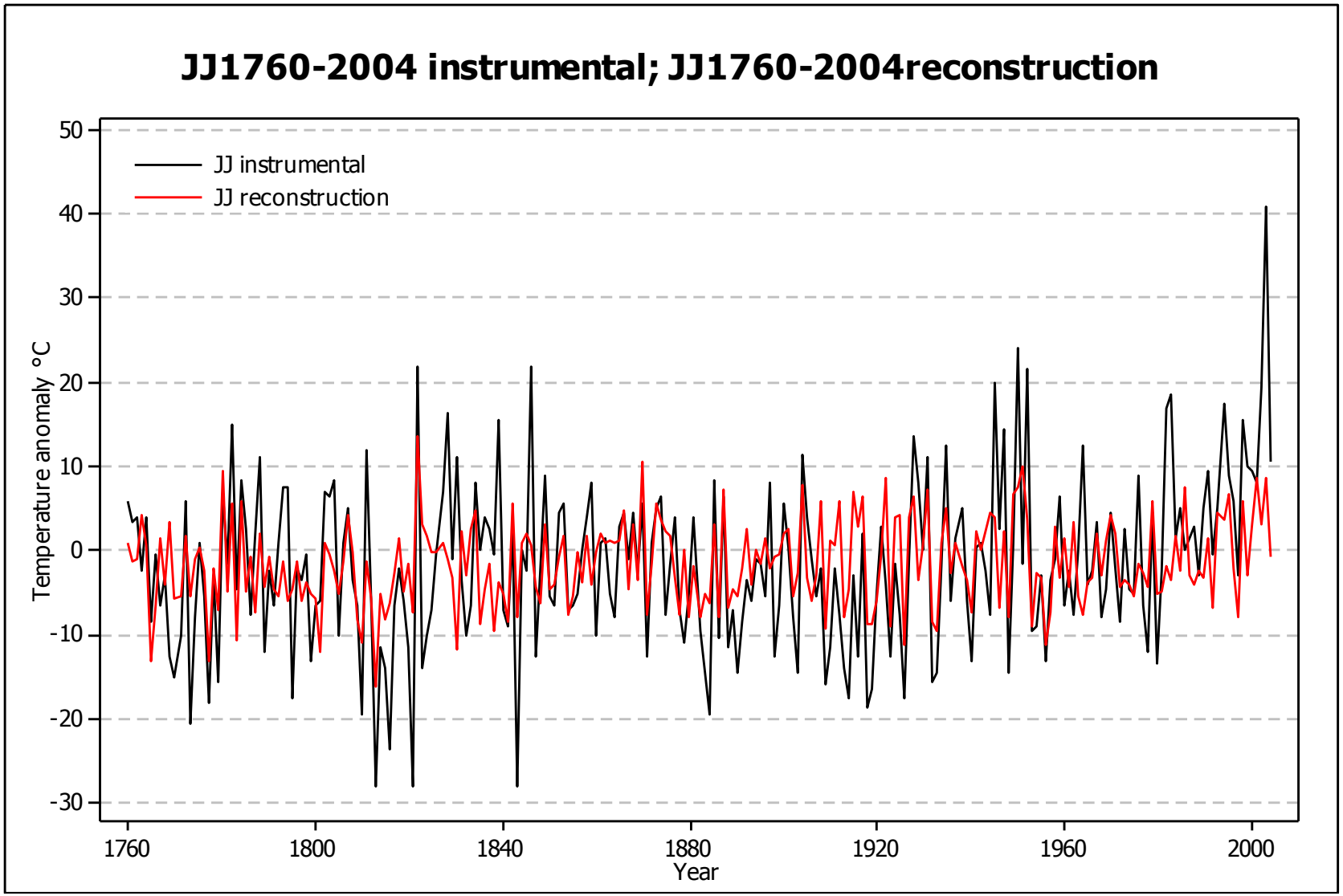

Fig. 4-100 JJ mean temperature reconstruction and instrumental data over their common period. The Pearson's correlation coefficient between the two time series is 0,545.

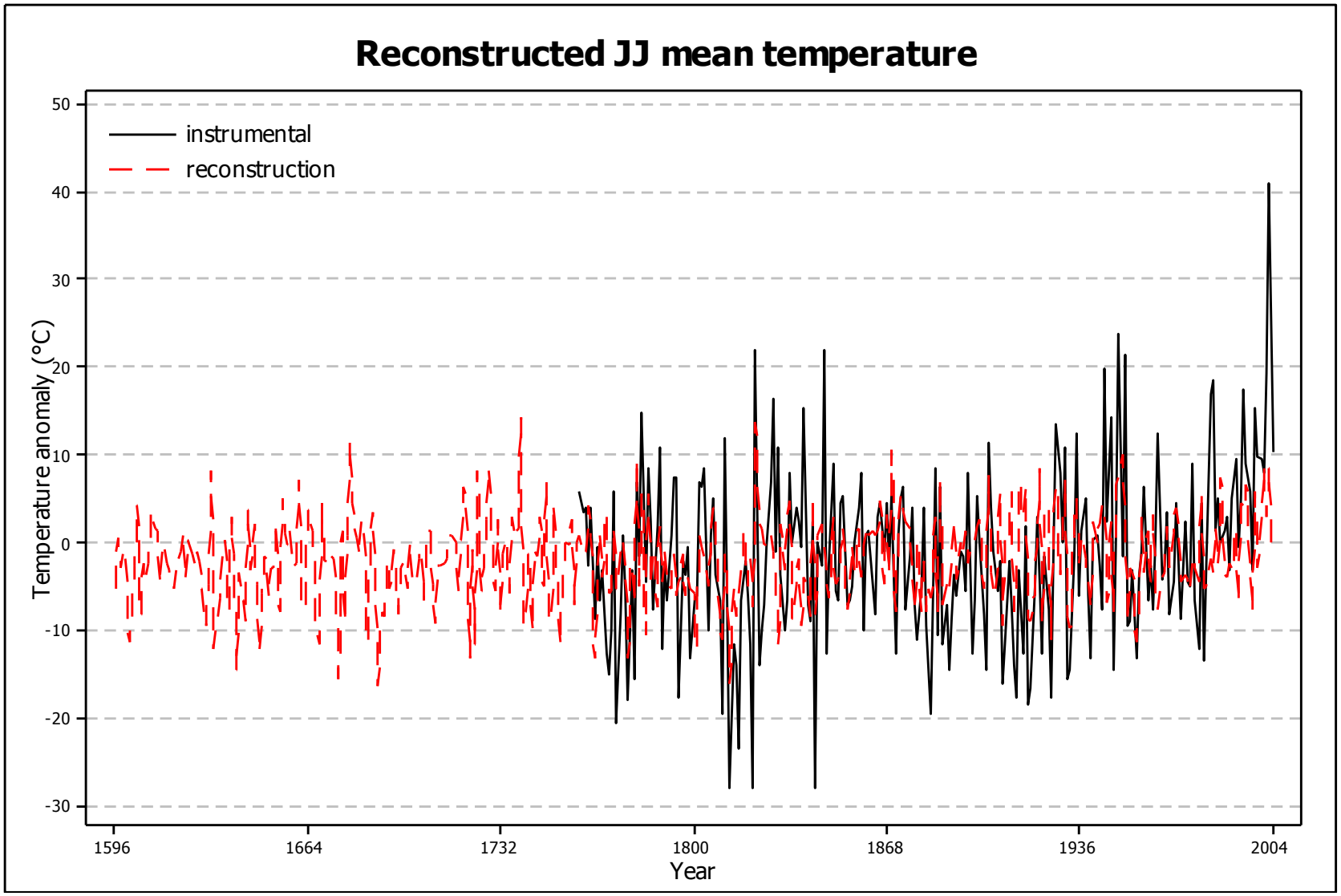

Fig. 4-101 complete extension of JJ mean temperature reconstruction and instrumental data.

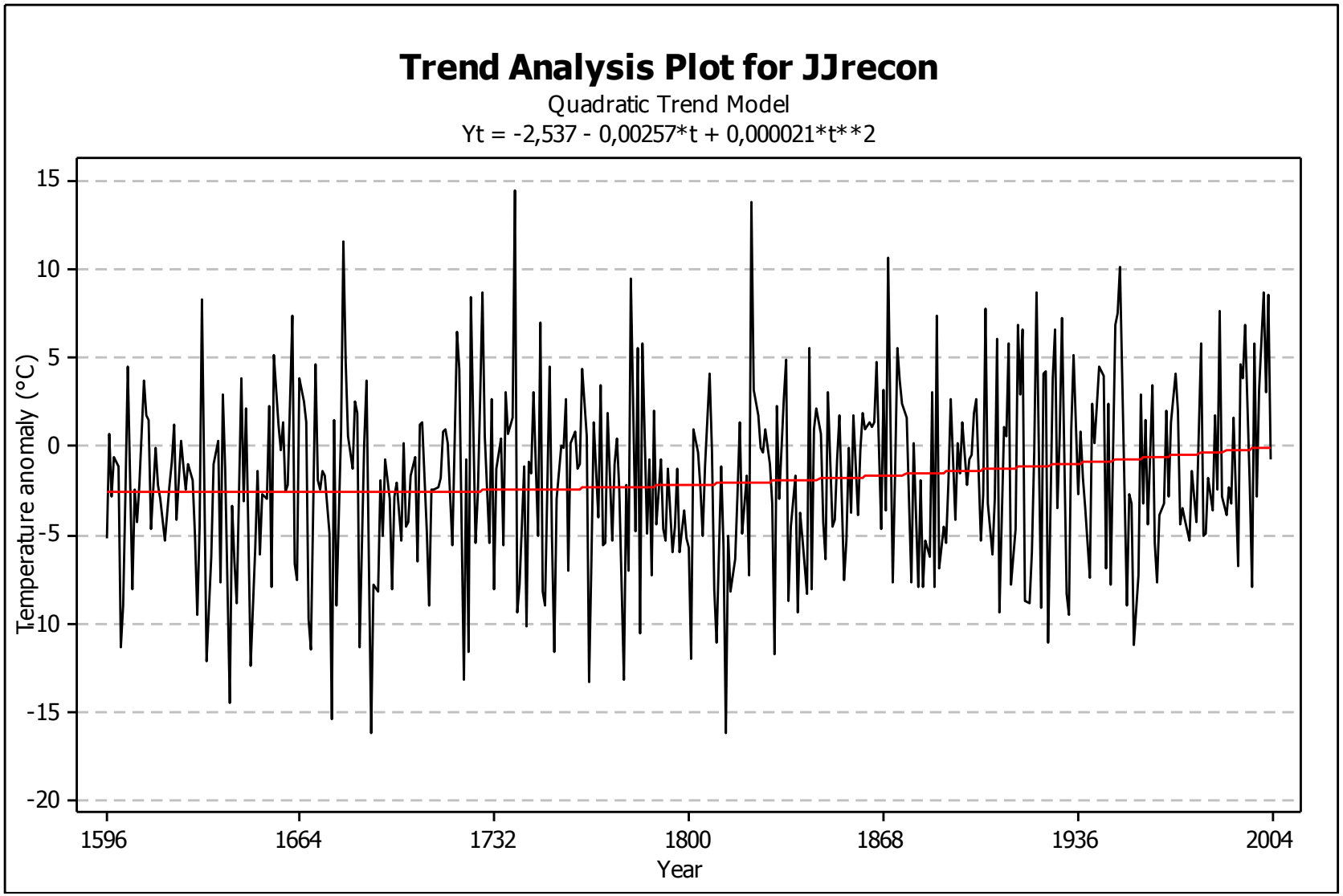

Fig. 4-102 trend analysis of the reconstructed JJ mean temperature the red line shows the *quadratic trend model* that accounts for simple curvature in the data, its general formula is: $Y_t = b0 + b_1 * t + (b_2 * t^2) + e_t$

5 Discussion

Climate/tree-growth correlations

As expected, the correlation analysis of climate parameters (mean monthly Temperatures and mean monthly Precipitation) versus residual larch chronologies, confirms that temperatures rather than precipitations exert the main control on radial growth at the upper tree-line (Jacoby & D'Arrigo 1989, Esper 2000, Briffa et al.2002, Esper et al. 2002a, b, 2003). Due to the high elevation provenance of the tree-ring samples, we expected to obtain meanly higher correlation values between the residual chronologies and temperatures recorded by high elevation stations. On the contrary, correlation values with temperature data coming from low elevation stations are clearly higher.

Moving correlation analysis reveals that the four chronologies show almost synchronous variations in CC values to monthly mean temperatures over the studied time period (1878-2004) with a strong positive influence of early Summer (JJ) temperatures on tree growth.

The record-breaking heat-wave in summer 2003 was expected to have a strong impact on tree growth, especially where, like in our study, trees grow at their ecological limits. The correlation analysis performed between the all five residual chronologies and the 2003 summer monthly mean temperatures shows that larch trees in our study area did not respond to the heat wave exceptional climate conditions by producing a wider tree ring. The results of our study are consistent with those reported by Leonelli et al. (2009) for stone pine in the Ortles-Cevedale Group. Another study performed on *Pinus sylvestris* L. and *Picea abies* (L.) Karst. in Tyrol, Austria (Pilcher & Oberhuber 2007) shows moderate growth responses. Carrer et al (1998) have demonstrated that the linear temperature response of *Picea abies L*. in subalpine environments may change above a temperature threshold, and how this conifer species seem unable to take full advantage from warm and sunny days at temperatures above ~ 13°C. Larch trees, because of their intrinsic physiologic characteristics, are likely to have a better skill to survive in increased, temperature-induced, drought condition. Due to their deciduous habit, larch trees are generally able to preserve a high photosynthetic capacity during the short growing season despite any variation in water availability. Moreover, they have a deep root system that allows trees to reach deep and wet soil layers (Tranquillini 1964; Farjon, 1990; Valentini et al. 1994). Nevertheless, in our our findings based on larch tree-ring network, it is present the same loss of thermal sensitivity that was found in Alpine pine and

spruce trees. These results are consistent with those reported in Carrer et al (1998) and in Carrer & Urbinati (2006) for a subalpine larch chronology network in the Eastern Alps.

Reconstructed June-July mean temperatures

Temperature reconstruction characteristics

Figures 4-94 and 4-97 show the June July mean temperature reconstruction for the Adamello-Presanella Group for the 1596-2004 period.

The mean temperature computed over the whole period (1596-2004) is 1,05 °C colder than the 1901–2000 instrumental reference period, and, as it clearly emerges from the trend analysis of the entire series (Fig 26), the whole period trend goes clearly towards an increase of early summer mean temperatures.

Looking more in detail to the reconstruction, relatively cool conditions appear during much of the seventeenth and early eighteenth centuries, with some decadal and multi decadal fluctuations. A slight increase in JJ mean temperature is visible starting from about 1650 to 1780 and from early 1720s until about 1740, when it starts a progressive decrease that continue until 1821.

The lowest temperatures of the entire series are found in the 1813-1821 period, actually this decade is known as one of the colder phases during the entire Little Ice Age period (Bradley & Jones, 1993; Fliri, 1991; Grove, 1988), characterized by the maximum holocenic extension of Alpine glaciers (Holzhauser 2002; Nicolussi & Patzelt 2000). This period corresponds with the Dalton minimum in solar activity (Wagner 2005; Wilson 1998) and follows extensive volcanic activity, including the 1815 eruption of Tambora, on the Indonesian Sumbawa Island (Briffa et al. 1998b, D'Arrigo & Jacoby 1999, Sadler & Grattam 1999; Crowley 2000; Oppenhaimer 2003), resulting in a manifest recrudescence of summer temperatures over the Northern Hemisphere (Briffa et al. 1998b; Cole-Daiet al. 1997; Grove 1988). The lowest reconstructed value in this cold period corresponds to the year 1813 that also represents the lowest value of our entire reconstruction. The 1816 year, known as the "year without a summer" on global climate for the consequences of the Tambora eruption (Skeen 1981), does not show an expected low value of early summer temperature in our reconstruction.

The successive period is characterized by a relatively constant increase in temperature following the events of the recent atmosphere warming trend, with some minor fluctuations.

This constant increase of reconstructed JJ mean temperatures is partially interrupted at the end of 1830s and in 1850s when a slight recrudescence is visible, followed by a sharp rising that ends in early 1880s. Another slight decrease follows, ceasing around 1910, when the start up of a first recent warming episode is clearly visible. This increase of temperatures goes forward until 1950s, when a new fluctuation brings the reconstructed JJ mean temperatures to relative lower values with minimum in the early 1980s, then a constant rise starts and goes on up to the end of the time series.

Overall the reconstruction of JJ mean temperature here performed for the Adamello-Presanella Group is substantially consistent with other annually-resolved summer-temperatures reconstructions for the European Alps (Büntgen et al. 2005, 2006, Frank et al 2005, Frank & Esper 2005b) and with European multiproxy findings (Luterbacher et al. 2004) currently present in literature.

Low and high frequency patterns of the JJ mean temperature reconstruction

The difficulty to retain long-term temperature variations is well known in Dendroclimatology (Esper et al 2004, 2007). Low- and high-frequency discrepancies between the tree-ring width based reconstruction of JJ mean temperatures for the Adamello-Presanella Group and instrumental data are highlighted in figs. 5-1, 5-2, and 5-3.

With the aim to emphasize low and high-frequency trends, reconstructed and instrumental data are plotted over their common period (1760-2004) and the time series are smoothed with running averages of different lengths (30, 20, 10 years).

Anomalies calculated between the reconstructed and the instrumental data smoothed with a 30-year running average, show the higher discrepancies. Reconstructed values largely underestimate JJ mean temperatures during the most part of the overlap period, and the higher differences are visible in the 1880-1950 interval. Colder reconstructed JJ mean temperatures are visible in the 1800-1818, 1847-1869, 1952-2004 intervals and the Pearson's correlation value computed between reconstructed and instrumental complete series is 0,29 ($p<0,0001$).

A better synchronicity between instrumental and reconstructed series is visible in the trends of anomalies calculated between the two series after smoothing with a 20 and 10-year running average.

In the 10-years moving average the Pearson's correlation value between instrumental and reconstructed series raises to 0,51 ($p<0,0001$), time intervals in which the reconstructed series show colder temperatures than the instrumental series are 1784-1813, 1830-1849, 1835-1839, 1964-1973, 1982-2004. Synchronous short-term fluctuations that were removed by the

high-pass average are now clearly visible within the 1880-1950 period, that nevertheless remains one of the intervals with the more consistent divergences between reconstructed and instrumental time series.

JJ reconstructed values lower than the instrumental series centered on the 1850s are evident in the 20-year moving average too. Furthermore, lower reconstructed values are evident during the late 1700s in all the three comparison. These results are consistent with those reported by Büntgen *et al*. (2005).

As a general result, in all the three moving average smoothed series, clearly emerges a rather decreased potential of the tree-ring series in reconstructing exceptionally cold or warm JJ temperatures. This inadequacy appears clearly evident in the early nineteenth century, when exceptionally cold temperatures are recorded, and in the more recent part of the time series. In fact, the recent increasing trend in summer temperatures is not evidenced by an increasing of the same magnitude in the reconstructed series.

Pearson' s correlation and p values computed between reconstructed and instrumental moving averages (30, 20 and 10 years length) for successive time intervals are reported in tables 5-1, 5-2 and 5-3. Pearson's correlation values computed over consecutive sub-periods (50 years length), allows to highlight that correlation values change rather significantly throughout the time series length.

As we have seen above, the Pearson's correlation value between the complete reconstructed and instrumental 10yMA (MA=moving average) series (1769-2004) is 0,51 ($p<0,0001$) and 0,29 ($p<0,0001$) if computed between the 30yMA series (1789-2004). The correlation between the instrumental and reconstructed 20yMA series calculated over their complete length (1779-2004) is 0,377 ($p <0,0001$).

The reconstructed and instrumental 10yMA series shows better partial correlation values. These values reach a very high significance level in the most recent part of the series. In particular, in the last fifty years of overlap (1955-2004) the Pearson correlation value is 0,86 ($p<0,0001$). This undoubtedly good result become weaker going back in time towards the ancient part of the time series, showing lower and lower r values, that in the 1769-1818 period are even not significant ($r = 0,271$, $p = 0,11$).

The reconstructed and instrumental 30yMA series has lower correlation values in all the analysed sub-period, but with rather good values in the more recent part of the series ($r = 0,63$, $p<0,0001$). The lowest correlation value ($r = 0,019$, 1855-1904 period) coincides with one of the periods of maximum divergence between the instrumental and the reconstructed series. The minimum in correlation values also correspond to one of the time periods,

following the end of the Little Ice Age, that are characterized by a steep increment of summer temperature. In this time interval short-term JJ mean temperature fluctuations are significant (Bradley, 1993) and they are clearly better accounted by the 10yMA time series.

During the last part of the Little Ice Age the advance of glaciers in the Alps conflicts with the summer temperature signal (Intergovernmental Panel on Climate Change, 2001). The end of this cooling phase coincides with the glacier retreat (mid-nineteenth century) (Groove, 2001). The onset of glacier retreat is discordant both with mean annual temperatures based on instrumental data (Jones et al., 2001) and with other pale-temperature reconstructions (Mann et al., 1999). The same conflict results from our mean temperatures reconstruction where a clear increasing in temperatures starts after the second half of the nineteenth century,

Vincent et al (2005) have demonstrated that this conflict is likely to be related to a reduced amount of winter precipitations than to an increasing of summer temperatures.

The reconstructed and instrumental 20yMA series show correlation values similar to the 10yMA, with higher values in the recent sub-periods and an evident decrease going back in time. The more ancient period, instead, shows the lowest, even if still significant (p = 0,014), r values (0,280).

	1769-1818	**1819-1854**	**1855-1904**	**1905-1954**	**1955-2004**
r	0,271	0,444	0,746	0,610	0,856
p	0,110	0,001	<0,0001	<0,0001	<0,0001

Tab. 5-1 r and p values (α level = 0,05) computed between instrumental and reconstructed 10 years MA

	1779-1854	**1855-1904**	**1905-1954**	**1955-2004**
r	0,280	0,668	0,566	0,807
p	0,014	<0,0001	<0,0001	<0,0001

Tab. 5-2 r and p values (α level = 0,05) computed between instrumental and reconstructed 20 years MA

	1796-1854	**1855-1904**	**1905-1954**	**1955-2004**
r	0,458	0,019	0,500	0,630
p	<0,0001	0,897	<0,0001	<0,0001

Tab. 5-3 r and p values (α level = 0,05) computed between instrumental and reconstructed 30 years MA

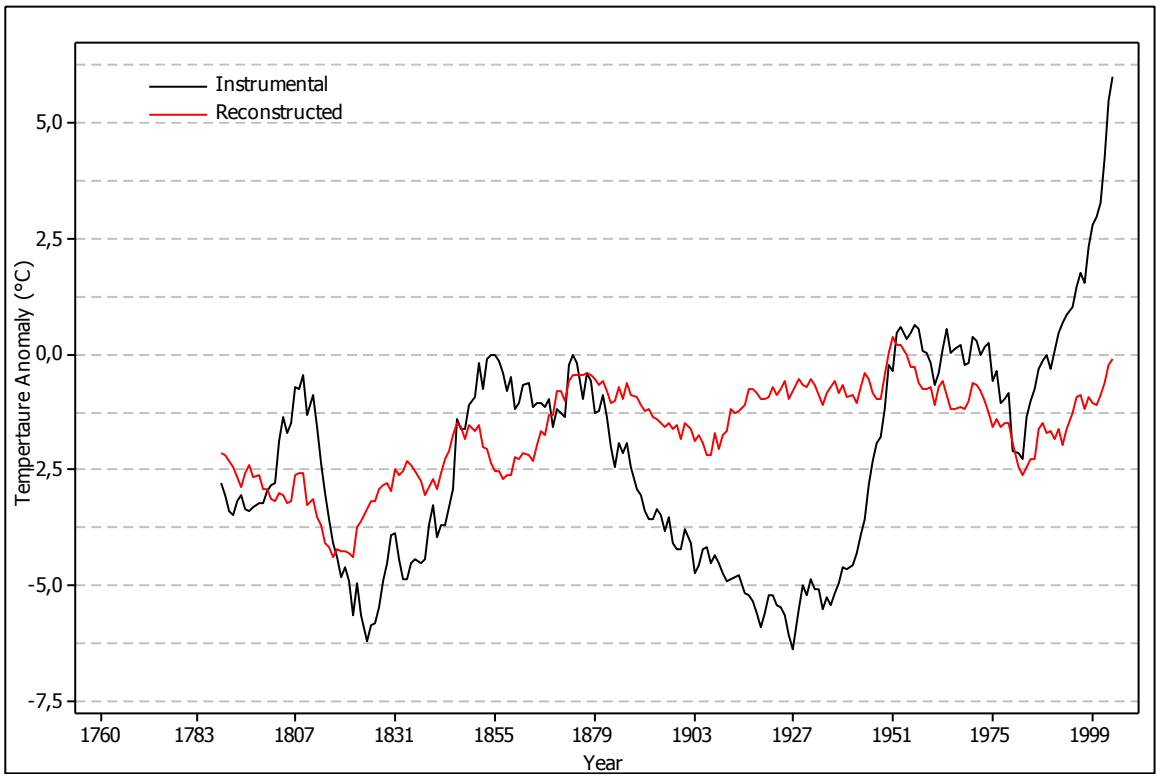

Fig.5-1 Moving averages (30-year length) of instrumental and reconstructed time series over the common period 1760-2004.

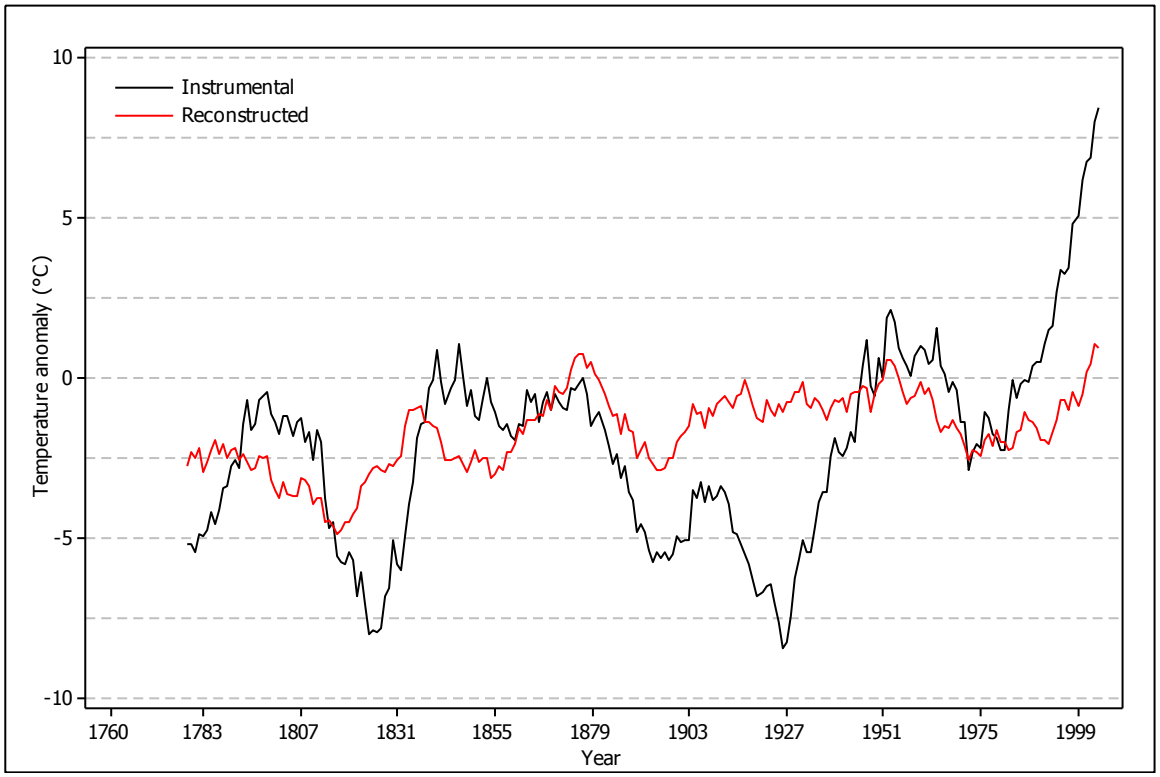

Fig. 5-2 Moving averages (20-year length) of instrumental and reconstructed time series over the common period 1760-2004.

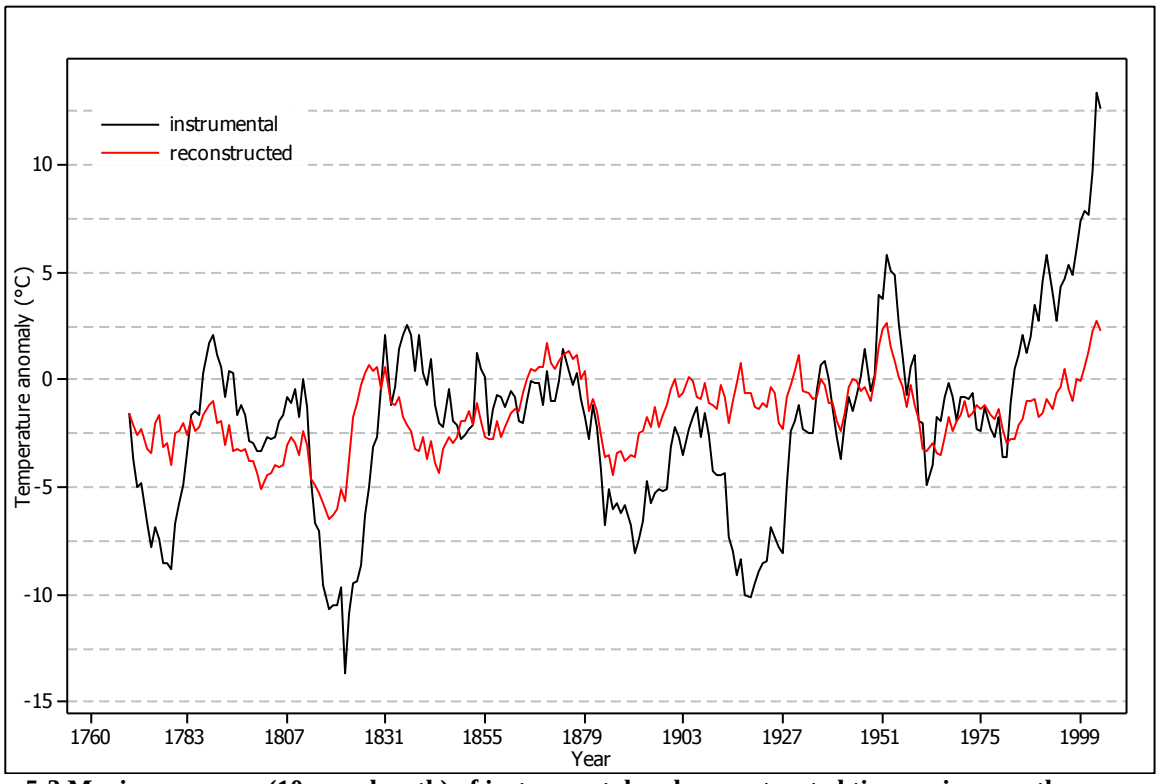

Fig. 5-3 Moving averages (10-year length) of instrumental and reconstructed time series over the common period 1760-2004.

In general, it is visible a better skill of the reconstruction in describing high-frequency variability of early summer mean temperatures.

It is also possible to recognize a quite good response of the tree rings (evidenced in the reconstructed JJ mean temperatures) to the mid-20th century (1940–1950s) summer warmth, even if with underestimations. These results are consistent with those reported in Büntgen *et al.*, 2008.

A high correspondence between instrumental and reconstructed series is also visible in the 1980s early summer temperatures cooling, but the distance between reconstructed and instrumental series increases even if the correlation score remains significant.

With the aim to underline this important divergence in the recent parts of the time series, we realized three different boxplots of the moving average values for the 1980-2004 period (Fig 4, 5 and 6).

The boxplot is a graphical summary of the distribution of a sample that shows its shape, central tendency, and variability. We have plotted the JJ mean temperatures moving average values (30, 20 and 10 window lengths) for the 1980-2004 intervals of measured and reconstructed time series.

Differences between instrumental and reconstructed moving average values are clearly evidenced in the three box-plots. Reconstructed values are manifestly smaller than

instrumental values and mean and median values are sensibly different in all the three compared moving averages time series.

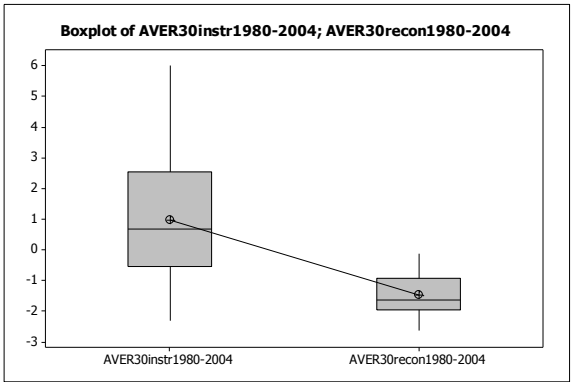

Fig. 5-4 Boxplot of instrumental and reconstructed 30yMA values.

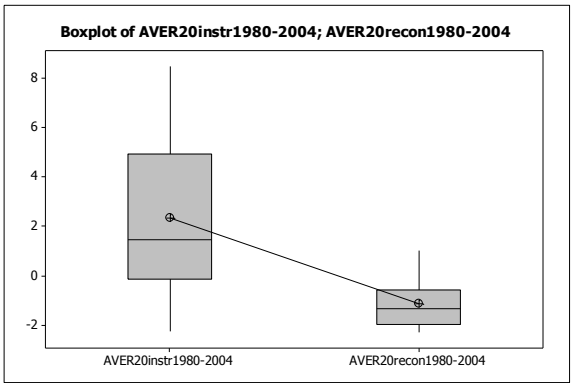

Fig. 5-5 Boxplot of instrumental and reconstructed 20yMA values.

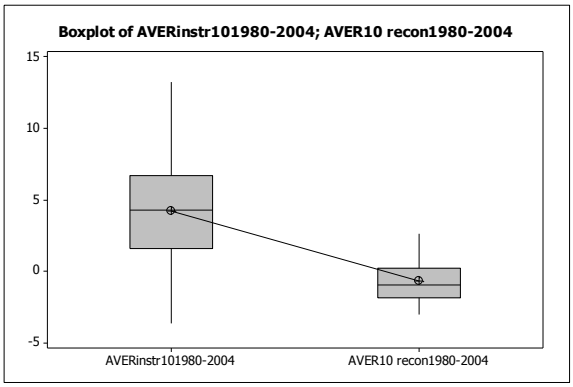

Fig. 5-6 Boxplot of instrumental and reconstructed 10yMA values.

In the JJ mean temperature reconstruction for the Adamello-Presanella Group it is therefore possible to recognize evidences of the well known "divergence problem" (Briffa et al 1998a, Carrer & Urbinati 2006, D'Arrigo *et al*. 2008; Leonelli et al 2009), that will be more widely discuss in the next paragraph.

The "Divergence Problem"

A reduction in tree-ring indices and temperature sensitivity has been observed recently from many northern latitude sites. D'Arrigo et al. (2008) defined the DP as "the tendency for tree growth at some previously temperature-limited northern sites to demonstrate a weakening in mean temperature response in recent decades, with the divergence being expressed as a loss in climate sensitivity and/or an offset in trend". The causes of this reduced sensitivity to variation in summer temperatures are still unknown, but some explanations at local to regional scale have been suggested. Several authors (e.g. Jacoby & D'Arrigo 1995, Barber et al. 2000, Lloyd & Fastie 2002, Frank & Esper 2005b,c; Büntgen et al. 2006) proposed a correlation with late-summer drought stress induced by increasing temperature that characterized the recent warming trend. Vaganov et al.(1999) noted a relationship between decreasing temperature sensitivity and an increasing trend in winter precipitation since the 1960s. This positive trend resulted in delayed melting of snowpack and a delayed growing season producing lower growth rates and reduced temperature/tree-growth correlation. Moreover, several studies suggest that it is likely that tree growth may be more conditioned by annual then by seasonal temperature variability, due to biological and physical processes such as needle growth and retention in most conifers, photosynthesis occurring outside the growing season, soil temperatures and their effect on root activities (D'Arrigo et al., 1992). The use of an imprecise instrumental target for calibration, e.g., when trends in maximum and minimum temperatures are markedly different, maximum temperatures may be more appropriate in studies with temperature sensitive tree-ring data, than the more widely used mean temperatures (Wilson & Luckman 2002, 2003, Büntgen et al. 2008c, Youngblut & Luckman 2008), and effects of airborne pollution (Yonenobu & Eckstein 2006) are other proposed explanations of the phenomenon. From all these studies derives that the divergence between tree-ring based climate reconstruction and instrumental data can potentially be explained considering the wider aspect of biological and ecological response of trees to climate. In addition to these issues there are methodological-induced uncertainties to consider. These methodological concerns include the diverse tree-ring detrending methods applied during the standardization processes of three-ring chronologies, and 'end-effect' issues emerging from different techniques of chronology development (Cook & Peters 1997). All together these biological and methodological controversial aspects drive to differences in large-scale reconstructions that use only temperature sensitive tree-ring data or combine tree-ring and other proxy data (Mann et al. 1998, 1999; Lutherbacher et al., 2004).

In the JJ temperature reconstruction here proposed for the Adamello-Presanella Group, in the more recent part of the time series, starting from about 1980, the underestimation of early summer temperatures is evident. We may simply ascribe this trend to the "Divergence Problem", but some methodological considerations related to the reconstruction techniques are needed, and in particular to the type of regression applied to the series. It is important to notice that when, as in the reconstruction here performed, linear regression is used for calibration procedures, the variance of the proxy record shows the tendency to remains below the variance of the instrumental data, as reported in Frank & Esper (2005a) "leaving the visual impression that the recent dynamics are substantially larger than the historic ones when splicing such records together". Analyzing the common signal after the smoothing procedures, it results more similar amplitude between reconstructed and instrumental record. This improvement of reconstructed variance amplitude is however less efficient in the more recent part (1980-2004) of the time series that remains consistently below the instrumental record.

We think that a convergence of factors may have produced this result. On the one hand the methodological procedures here used for tree-ring data treatment and the linear regression used during calibration, may have produced a slight underestimation of JJ mean temperatures. As well, we must take account of the moving correlation analysis results that clearly show a loss in thermal response of tree-ring width chronologies in our data-set since about 1960. A superimposed effect of these two elements it is likely to be the cause of the reduction in JJ temperature reconstruction values in the more recent part of the time series.

As seen above, the recent changing in thermal response has been related by several authors to a change in climate sensitivity of high latitude and high altitude tree-ring datasets due to an increased influence of precipitation rates on tree-ring growth. The moving correlation analysis performed between the five mean site residual chronologies and monthly mean precipitation showed a synchronous decreasing trend, indicating that, as well as for temperatures, precipitation/tree-rings growth relationship has been not stable over time and has considerably changed over time. In particular, the moving correlation analysis calculated between June mean precipitations and the tree-ring dataset show an increasing negative correlation that is consistent with the results of Carrer & Urbinati (2006), in a geographically close high-altitude larch tree-ring network. The same result is reported in Leonelli et al. (2009) for stone pine (*Pinus cembra* L.) at upper timberline in the Ortles-Cevedale Group. A similar decrease of correlation coefficient values was found with Dec-1 precipitation.

The decreasing trend in CC values with early summer temperatures may let us suppose the presence of some "moisture-related" effect on tree growth in our sampling sites, but the possibility that a drought stress occurred to our tree-ring data set is not supported by the increased CC values between tree-ring and monthly mean early summer (JJ) precipitation as reported for spruce in Büntgen et al. 2006. The loss of climate sensitivity seems to involve precipitation as same as temperatures in our larch tree-ring dataset. It is possible that, as reported in D'Arrigo et al. (2004), effects related to the overcoming of an optimum temperature threshold combined to the consequent soil-moisture stress may explain the evident loss in climate/tree-growth correlation. The possibility that a shorter growing season due to an increasing trend of winter precipitation associated with delayed snow melt (Vaganov et al., 1999; Kirdyanov et al., 2003) may exert an influence on divergence, needs further analysis. On the contrary, numerous studies have reported an enlargement of growing season in Europe due to recent temperature increasing (Menzel and Fabian 1999; Sparks et al. 2002; Walther et al. 2002; Menzel et al. 2006). The found synchronous increasing trend in CC values computed between the five tree-ring chronologies and the August mean temperatures, even if in the range of not statistically significant values, let us suppose a possible influence of the lengthening of growing season in our sampling sites.

6 Conclusions

Tree-ring chronologies of high climate-sensitive species at their ecological limit confirm in this study to be powerful tools in studying local and global climate patterns and to represent valuable proxy data for paleoclimatic reconstructions. A careful sampling and a rigorous statistical approach to the calibration and independent verification of climate growth models, permit an exceptional possibility to explore past climate variability.

Even if the suitability of larch for climatic purposes has been questioned because of the periodic outbreaks of larch budmoth, this species confirms in this study to be highly climate-sensitive.

The analysis of climate/tree ring growth relationships performed on five larch tree-ring chronologies produced results that are consistent with the more recent dendroclimatic studies in the Alpine Region, confirming the presence of a common climatic signal for conifers living at the timberline ecotone.

In the Adamello-Presanella Group, as in other alpine sectors and in high-latitudes areas, early summer (JJ) temperatures resulted to exert the main control on larch radial growth at the upper tree-line.

Although the limitation of larch growth at timberlines in our sampling sites by prevailing summer temperature was verified, correlation and response function analysis show a clearly visible loss of thermal response of radial tree growth during last decades. Overall our results reveal a temporal instability in growth/climate response similar to what reported in several recent studies for other European conifer sites.

The noticed correlation decrease suggest that the causes of growth variations are complex, and that some other factors that have not be taking into account in our models (e.g. CO_2 air concentrations increase, N-deposition or human impact), may be involved. Moreover, it is actually probable that tree-ring chronologies contain substantial climatic signals outside those related to the warm season. Looking more in detail to the climate/tree growth analysis, the decreasing trend in correlation values computed with monthly mean temperatures and monthly mean precipitations since about 1960s let us suppose the presence of some "moisture-related" effect on tree growth in our sampling sites. We infer that a likely cause of divergence can be addressed to a change in snow melting time, in a different winter precipitation rates and/or in an increasing drought stress on cambial activity. Moreover, a lengthening of tree growing season can be hypothesized.

Our study confirms the supposition that it is likely that linear regression models are not sufficient to describe conifer cambial processes in response to external environmental conditions. The use of multivariate rather than linear regression model is a plausible evolution of future dendroclimatic studies.

Nevertheless, the reconstruction here proposed for 1595-2004 JJ mean temperatures based on four larch mean site residual chronologies built at the upper tree-line, is statistically valuable, but it shows an higher skill in describing high frequency than low frequency early mean summer temperatures changes.

Further dendroclimatic reconstructions in the Adamello-Presanella Group need the development of a larger number of tree-rings chronologies from ecologically analogous sampling sites. In order to highlight long term trends in climate parameters, producing robust estimates of low-frequency climate, it could be useful using composite detrending methods, like as Regional Curve Standardization (RCS, Briffa et a. 1992) and Age Banding (Briffa et al 2001). These detrending methods need extensive tree-ring data-sets, then it may be important, in addition to the development of an higher number of tree-ring chronologies, to extent the study area to the neighbouring mountain Groups.

7 Bibliography

Anderson T., W., Darling D., A., 1954: A test of goodness of fit. Journal of the American Statistical Association, 49(268) 764-769.

Anfodillo, T., Urbinati, C., 2001. Foreste di alta quota in ambiente alpino: fisionomia, ecologia e possibili dinamismi. Monti e Boschi, 3-4: 31-39.

ARSTANwin, http://www.ldeo.columbia.edu/res/fac/trl/public/publicSoftware.html

Arnold, S.,F., 1990. Mathematical Statistics. Prentice-Hall. Englewood Cliffs, N.J.

Auer, I, Böhm R, and Schöner W, 2001. Final report of EU-project ALPCLIM. Chapter 3: Instrumental Climate.

Auer, I, Böhm R, Maugeri M, 2001. A new long-term gridded precipitation dataset for the Alps and its application for MAP and ALPCLIM. Physics and Chemistry of the Earth (B) 26: 421-424.

Auer, I., Böhm, R., Jurkovic, A., Lipa, W., Orlik, A., Potzmann, R.,Schöner, W., Ungersböck, M., Matulla, C., Briffa, K., Jones, P., Efthymiadis, D., Brunetti, M., Nanni, T., Maugeri, M.,Mercalli, L., Mestre, O., Moisselin, J.-M., Begert, M., Müller-Westermeier, G., Kveton, V., Bochnicek, O., Stastny, P., Lapin,M., Szalai, S., Szentimrey, T., Cegnar, T., Dolinar, M.,Gajic-Capka, M., Zaninovic, K., Majstorovic, Z., Nieplova,E., 2007: HISTALP – historical instrumental climatological surface time series of the Greater Alpine Region. International Journal of Climatology, 27: 17–46.

Baillie, M.G.L., 1982. Tree ring dating and Archaeology. The University of Chicago Press, Chicago, 265 pp.

Baillie, M.G.L. & Pilcher, J.R. (1973) A simple crossdating program for tree-ring research. Tree-Ring Bull. **33**, 7–14.

Baltensweiler, W., 1985: On the extent and the mechanisms of the outbreaks of the larch bud moth (Zeiraphera diniana Gn., Lepidoptera, Tortricidae) and its impact on the subalpine larchcembran pine ecosystem. In: Turner H, Tranquillini W.(eds) Establishment and tending of subalpine forest: research and management, vol. 270. Eidg Anst Forstl Versuchswes, Riederalp, pp 215–219.

Baltensweiler, W., Fischlin, A., 1988. The larch bud moth in the Alps. In: Berryman, A.A. (Ed.), Dynamics of Forest Insect Populations: Patterns, Causes, Implications. Plenum Publishing Corporation, New York a.o, pp. 331–351.

Baltensweiler, W., Benz, G., Bovey, P., Delucchi, V. 1977: Dynamics of larch bud moth populations. Annu. Rev. Entomol. 22, 79–100. (doi:10.1146/annurev.en.22.010177.000455)

Barber, V., Juday, G., Finney, B. 2000: Reduced growth of Alaska white spruce in the twentieth century from temperature-induced drought stress. Nature 405: 668-672.

Betti Parenti, G., 2001: Geomorfologia del versante settentrionale del Gruppo della Presanella (Alpi Centrali) e variazioni delle linee d'equilibrio delle vedrette Presanella, Busazza e Presena dalla Piccola Età Glaciale ad oggi. Tesi di laurea in Scienze Geologiche, A.A. 2001-2001, Università di Pisa.

Barber VA, Juday GP, Finney BP 2000. Reduced growth of Alaskan white spruce in the twentieth century from temperature-induced drought stress. Nature 405:668–672.

Baroni, C.; Carton, A., 1990. Variazioni glaciali oloceniche nel Gruppo del M. Adamello. Memorie della Società Geologica Italiana, 45: 877-882.

Baroni, C.; Carton, A., Martinelli N., Pignatelli, O. 1992. Dendrocronologia e variazioni glaciali oloceniche in Val di Genova (M. Adamello, Alpi Centrali). Nota preliminare. Geografia fisica e dinamica quaternaria, 15: 39-40.

Baroni, C.; Carton, A., 1996. Geomorfologia dell'alta Val Di Genova (Gruppo dell'Adamello, Alpi Centrali). Geografia fisica e dinamica quaternaria, 19: 3-17.

Baroni, C.; Carton A.; Seppi, R., 2004: Distribution and Behaviour of Rock Glaciers in the Adamello–Presanella Massif (Italian Alps). Permafrost and Periglac. Process. 15: 243–259.

Bebber, A., 1990. Una cronologia del larice (Larix decidua Mill.) delle Alpi orientali italiane. Dendrochronologia 8, 119-140.

Beniston, M., 2004. The 2003 heat wave in Europe: a shape of things to come? An analysis based on Swiss climatological data and model simulations. Geophys. Res. Lett. 31, 2022–2026.

Bianchi, A., Dal Piaz, G.B., 1940. Il settore nord-occidentale del massiccio dell'Adamello.Relazione preliminare sul rilevamento e sugli studi geologico-petrografici compiuti durante l'anno 1939 nell'alta VaI Camonica. Boll. R. Uff. Geol. It., 65: 1-18. Roma.

Bianchi, A., Dal Piaz, G.B., 1948. Differenziazioni petrografiche e metamorfismi selettivi di contatto nel massiccio dell'Adamello. Rend. Soc. Miner. lt., 5: 79 -102. Pavia.

Bianchi, A., Callegari, E., Jobstraibizer P., G., 1970. I tipi petrografici fondamentali del plutone dell'Adamello. Tonaliti-quarzodioriti-granodioriti e loro varietà leucocratiche. Mem. Ist. Geol, e Mi Univ. Padova, 27: 1-148 (con schizzi geologico 1:200.000).

Billamboz, A., 2005. Classes of dating quality. Proceedings of the EuroDendro 2005. September 29–October 1, 2005. Viterbo, Italy, 12 pp.

Billamboz, A., 2008. Dealing with heteroconnections and short tree-ring series at different levels of dating in the dendrochronology of the Southwest German. Dendrochronologia doi:10.1016/j.dendro.2008.07.001

Bjørnstad, O. N., Peltonen, M., Liebhold, A. M., Baltensweiler,W., 2002. Waves of larch budmoth outbreaks in the European Alps. Science 298, 1020–1023. (doi:10. 126/science.1075182)

Biondi, F., 1997: Evolutionary and moving response functions in dendroclimatology. Dendrochronologia 15:139–150.

Biondi, F., Waikul, K., 2004. Dendroclim 2002: a C+ program for calibration of climate signals in tree-ring chronologies. Computer in Geosciences 30, 303-311.

Blasing, T.J., Solomon, A.M., Duvick, D.N., 1984. Response functions revisited. Tree-Ring Bulletin 44, 1–15.

Böhm R., Auer I, Brunetti M, Maugeri M, Nanni T, Schöner W. 2001. Regional temperature variability in the European Alps 1760-1998 from homogenized instrumental time series. Int. J. Climatol. **21**: 1779-1801.

Böhm R., Auer I., Schöner W., Ganekind M., Gruber C., Jurkovic A., Orlik A., Ungersböck M., 2009. Eine neue Webseite mit instrumentellen Qualitäts-Klimadaten für den Grossraum Alpen zurück bis 1760. Wiener Mitteilungen Band 216: Hochwässer: Bemessung, Risikoanalyse und Vorhersage.

Box, G. E. P., and Jenkins, G. 1976. Time Series Analysis: Forecasting and Control, Holden-Day.

Bradley, R.S. and Jones, P.D., 1992: Climatic variations over the last 500 years. In: Bradley, R.S. and Jones, P.D. (eds): Climate Since AD 1500. Routledge. London. 649–665.

Bradley, R. S.; Jones, P. D., 1993: "Little Ice Age" summer temperature variations: their nature and relevance to recent global warming trends. The Holocene 3,4: 367-376.

Bradley, R.S., Briffa, K.R., Cole, J., Hughes, M.K. and Osborn,T.J., 2003: The climate of the last millennium. In: Alverson, K.D., Bradley, R.S. and Pedersen, T.F. (eds): Paleoclimate, Global Change and the Future. Springer. Berlin. 105–141.

Braun-Blanquet, J. (1964). Pflanzensoziologie—Grundzüge der Vegetationskunde. Wien, New York: Springer.

Briffa KR, Jones PD, Schweingruber FH 1988a Summer temperature patterns over Europe: A reconstruction from 1750 A.D. based on maximum latewood density indices of conifers. Quat. Res 30:36–52.

Briffa K., R., Jones P., D., Pilcher J., R., Hughes M., K., 1988b: Reconstructing Summer Temperatures in Northern Fennoscandinavia Back to A.D. 1700 Using Tree-Ring Data from Scots Pine. Arctic and Alpine Research, **20** (4) 385-394.

Briffa, K.R., Cook, E., 1990a: Methods of response function analysis. In Cook, E.R. and Kairiukstis, L.A., editors, Methods of dendrochronology: applications in the environmental sciences, Dordrecht: Kluwer, 240-247.

Briffa, K.R., Cook, E., 1990b: Basic chronology statistics and assessment. In Cook, E.R. and Kairiukstis, L.A., editors, Methods of dendrochronology: applications in the environmental sciences, Dordrecht: Kluwer, 137–152.

Briffa, K. R., Jones, P. D., Bartholin, T. S., Eckstein, D., Schweingruber, F. H., Karlen, W., Zetterberg, P. & Eronen, M., 1992: Fennoscandian summers from AD 500: temperature changes on short and long timescales. Climate Dynamics 7: 111–11.

Briffa, K.,R., Schweingruber F., H., Jones P., D., Osborn T. J., Harris I., C., Shiyatov S., G., Vaganov E., A., Grudd H. 1998a: Trees tell of past climates: but are they speaking less clearly today?, Phil.Trans. R. Soc. Lond. B 353, 65-73.

Briffa, K., R., Jones, P., D., Schweingruber F., H., Osborn T., J.,1998b: Influence of volcanic eruptions on Northern Hemisphere summer temperature over the past 600 year. Nature **393**, 450-455.

Briffa, K R. et al.1998c Reduced sensitivity of recent tree-growth to temperature at high northern latitudes. Nature 391, 678-682.

Briffa, K., R., Osborn T., J., Schweingruber F., H., Jones, P., D., Shiyatov SG, Vaganov EA 2001: Low-frequency temperature variations from a northern tree ring density network. Journal of Geophysical Research 106: 2929-2941.

Briffa K., R, Osborn TJ, Schweingruber FH, Jones PD, Shiyatov SG, Vaganov EA. 2002. Tree-ring width and density data around the Northern Hemisphere: part 1, local and regional climate signals. The Holocene **12**: 737–757.

Briffa, K.R., Shishov, V.V., Melvin, T.M., Vaganov, E.A., Grudd, H., Hantemirov, R.M., Eronen, M., Naurzbaev, M. M., 2008: Trends in recent temperature and radial tree growth spanning 2000 years across northwest Eurasia. Philos Trans R Soc B 363:2271–2284. doi:10.1098/rstb.2007.2199

Buffoni, L., Brunetti, M., Mangianti, F., Maugeri, M., Monti, F., Nanni, T. Atti workshop "CLIMAGRI - Cambiamenti Climatici e Agricoltura" Cagliari, 16-17 gennaio 2003 Ricostruzione del cliam italiano negli ultimi 130 anni e scenari per il XXI secolo.

Büntgen, U., J. Esper, D. C. Frank, K. Nicolussi, and M. Schmidhalter, 2005: A 1052-year tree-ring proxy of Alpine summer temperatures. Climate Dyn., **25**: 141–153.

Büntgen, U., Frank, D.C., Schmidhalter, M., Neuwirth, B., Seifert, M., Esper, J., 2006a: Growth/climate response shift in a long subalpine spruce chronology. Trees. doi: 10.1007/ s00468-005-0017-3.

Büntgen, U., Frank, D.C., Nievergelt D., Esper, J., 2006b: Summer Temperature Variations in the European Alps, A.D. 755–2004. Journal of Climate 19: 5606-5623.

Büntgen, U., Frank, D.C., Wilson, R., Carrer, M., Urbinati, C., Esper, J. 2008a: Testing for tree-ring divergence in the European Alps. Global Change Biology 14: 2443-2453.

Büntgen, U., Wilson, R., Wilmking, M., Niedzwiedz, T.4 Bräuning A. 2008b: The 'Divergence Problem' in tree-ring research in Kaczka R, Malik I, Owczarek P, Gärtner H, Helle G, Heinrich I (eds.) (2009): TRACE - Tree Rings in Archaeology, Climatology and Ecology, Vol. 7. GFZ Potsdam, Scientific Technical Report STR 09/03, Potsdam, pp. 226.

Büntgen, U., Frank, D.C., Grudd, H., Esper, J. (2008a): Long-term summer temperature variationsin the Pyrenees. Climate Dynamics 31: 615-631.

Callegari, E., 1983. Note introduttive alla geologia del massiccio dell'Adamello. In: «Il magmatismo tardo-alpino nelle Alpi. Escursione Adamello-Bregaglia». Soc. Geol. It. - Soc. It. Miner. Petr.: 14-18. Luglio 1983. Padova.

Callegari, E. 1985. Geological and petrological aspects of the magmatic activity at Adamello (northern Italy). Mem. Soc. Geol. It., 26 (1983): 83-103. Roma.

Callegari E., e Dal Piaz G.B., 1973. Field reiationships between the main igneous masses of the Adainello intrusiv massif (Northern Italy). Mem. Ist. Geol. e Miner. Univ. Padova, 29: 3-39.

Carrer M, Anfodillo T, Urbinati C, Carraro V (1998) High altitude forest sensitivity to global warming: results from long-term and short-term analyses in the Eastern Italien Alps. In: Beniston M, Innes JL (eds) The impacts of climate variability on forests, Lecture notes in earth sciences, 74. Springer, Berlin Heidelberg New York, pp 171–189.

Carrer, M. and Urbinati, C., 2004: Age-dependent tree-ring growth responses to climate in Larix decidua and Pinus cembra. Ecology, 85(3), 2004, pp. 730–740.

Carrer, M. and Urbinati, C., 2006: Long-term change in the sensitivity of tree-ring growth to climate forcing in Larix decidua. New Phytologist, 1 70: 861–872.

Castiglioni, G. B.,2001: Geomorfologia. UTET-Torino.

Castiglioni, G. B., 1961: I depositi morenici del gruppo Adamello-Presanella con particolare riguardo agli stadi glaciali postwürmiani. 121 pp.

Ceriani, M.; Carelli, M., 2000: Carta delle Precipitazioni Medie, Massime e Minime Annue del Territorio Alpino della Regione Lombardia. Direzione Generale Territorio e Urbanistica Regione Lombardia.

Cole-Dai J., Mosley-Thompson E., Thompson L.G., 1997. Annually resolved southern hemisphere volcanic history from two Antarctic ice cores. J Geophys Res 102:16761–16771.

Cook, E.,R., 1985 A time series analysis approach to tree-ring standardization. PhD thesis, University of Arizona, Arizona.

Cook ER (1987) The decomposition of tree-ring series for environmental studies. Tree-Ring Bull 47:37–59.

Cook, E. R., Briffa K. R., Shiyatov, S., Mazepa, V., 1990. Tree-ring standardization and Growth trend estimation, in Methods of Dendrochronology, edited by E. R. Cook and L. A. Kairiukstis, pp. 104– 123, Kluwer, Dordrecht.

Cook, E. R., and K. R. Briffa 1990. A comparison of some tree-ring standardization methods, in Methods of Dendrochronology, edited by E. R. Cook and L. A. Kairiukstis, pp. 104– 123, Kluwer, Dordrecht.

Cook, E.R., Holmes, R.,L., 1984: Program ARSTAN user manual: laboratory of tree ring research. University of Arizona, Tucson.

Cook, E.R., Kairiukstis, L.A., 1990. Methods of Dendrochronology: Applications in the Environmental Sciences. International Institute for Applied Systems Analysis, Kluwer Academic Publishers, Boston, MA.

Cook, E.R., Peters, K., 1981. The smoothing spline: a new approach to standardizing forest interior tree-ring width series for dendroclimatic studies. Tree-Ring Bulletin 41, 45–53.

Cook, E., Peters, K. 1997: Calculating unbiased tree-ring indices for the study of climatic andenvironmental change. The Holocene 7: 361-370.

Cook, E. R., Buckley, B. M., D'Arrigo R. D., Peterson M. J., 2000: Warm-season temperatures since 1600 BC reconstructed from Tasmanian tree rings and their relationship to large-scale sea surface temperature. Climate Dynamics 16:79-91.

Cook ER, D'Arrigo RD, Mann ME. 2002. A well-verified, multiproxy reconstruction of the winter North Atlantic Oscillation index since A.D. 1400. Journal of Climate **15**: 1754–1764.

Cook ER, Krusic PJ, Jones PD. 2003. Dendroclimatic signals in long tree-ring chronologies from the Himalayas of Nepal. International Journal of Climatology **23**: 707–732.

Crowley T., J., 2000: Causes of climate change over the past 1000 years. Science **289**: 270–277.

Dalla Fior, G., 1963: La nostra flora: guida alla conoscenza della flora della regione Trentino Alto Adige. Casa Editrice G. B. Monauni, Trento.

Dal Piaz, G. V., 1973: Guida alla lettura della Carta geologica del Gruppo Adamello-Presanella. Università degli Studi, Padova.

D'Arrigo RD, Jacoby GC, Free R. 1992. Tree ring-width and maximum latewood density at the North American tree line: parameters of climatic change. Canadian Journal of Forest Research **22**: 1290–1296.

D'Arrigo, R. D. and Jacoby, G. C.: 1999. Northern North American tree-ring evidence for regional temperature changes after major volcanic events Clim. Change **41**, 1-15.

D'Arrigo, R., Kaufmann, R., Davi, N., Jacoby, G., Laskowski, C., Myneni, R., Cherubini, P. (2004): Thresholds for warming-induced growth decline at elevational treeline in the Yukon Territory.Global Biogeochemical Cycles 18: doi:10.1029/2004GBO02249.

D'Arrigo, R., Wilson, R., Liepert, B and Cherubini, P. (2008): On the 'Divergence Problem' in Northern Forests: A Review of the Tree-Ring Evidence and Possible Causes. Global and Planetary Change 60: 289-305.

Del Moro, A., Pardini, G.C., Quercioli, C., Villa, I., Callegari E., 1985. Rb/Sr and K/Ar chronology of Adamello granitoids, southern Alps. Mcm. Soc. Geol. It., Roma. 26 (1983): 285-299.

Didier, L., 2001. Invasion patterns of European larch and Swiss stone pine in subalpine pastures in the French Alps. Forest Ecol. Manage. 145, 67–77.

Durbin J., Watson G.S., (1950): Testing for serial correlation in least squares regression I. Biometrika 37:409–428.

Easterling, D. R., G. A. Meehl, C. Parmesan, S. A. Changnon, T. R. Karl, and L. O. Mearns, 2000: Climate extremes: Observations, modeling, and impacts. Science, 289: 2068–2074.

Eckstein, D., 1982. Europe. In Hughes MK Kelly PM Pilcher JR La Marche VC (eds), Climate from tree-rings, Cambridge University Press, Cambridge: 142-148.

Eddy, J. A., 1976: The Maunder Minimum. Science, **192,** 1189–1202.

Esper, J., Cook, E.,R., Schweingruber, F., H., 2002. Reconstructing Past Temperature Variability Low-Frequency Signals in Long Tree-Ring Chronologies. Science 295: 2250.

Esper, J., Cook, E.,R., Schweingruber, F., H., Winiger M., 2002. 1300 years of climatic historyfor Western Central Asia inferrd from tree-rings. The Holocene12, 267-277.

Esper, J., Cook, E.,R., Shiyatov S.,G., Mazepa, V., S., Wilson, R., J., S., Graybill, D., A., Funkhouser, G., 2003. Temperature-sensitive Tien Shan tree ring chronlogies show multi-centennial growth trends. Climate Dynamics 8, 699-706.

Esper, J., Frank, D., C., Wilson, R., J., S., 2004: Temperature reconstructions-low frequency ambition and high frequency ratification. EOS 85:114, 120.

Esper, J., Frank, D., Luterbacher, J., 2007: On select issues and challenges in Dendroclimatology. In F. Kienast, O. Wildi & S. Ghosh (eds), A changing world. Challenges for landscape research. 113-132.

Evans et al., 2006 M. Evans, B. Reichert, A. Kaplan, K. Anchukaitis, E. Vaganov, M. Hughes and M. Cane, A forward modeling approach to paleoclimatic interpretation of tree-ring data, J. Geophys. Res. Vol. 111, G03008, doi:10.1029/2006JG000166, 2006111.

Farjon, A.. 1990. Pinaceae: drawings and descriptions of the genera Abies, Cedrus, Pseudolarix, Keteleeria, Nothotsuga, Tsuga, Cathaya, Pseudotsuga, Larix and Picea. Königstein: Koeltz Scientific Books.

Ferguson, C., W., 1970: Concept and techniques of Dendrochronology in Scientific Methods in medieval Archaeology. Rainer Berger, Editor. University of California Press.

Fernaroli, L., 1936: Il larice nelle Alpi Centrali Italiane. Il Larice nella montagna lombarda. Pubblicazioni della R. Stazione Sperimentale di selvicoltura. Firenze.

Filion L, Payette S, Gauthier L, Boutin Y 1986: Light rings in subarctic conifers as a dendrochronological tool. Quat Res 26:272–279.

Fliri, F., 1975: Das Klima der Alpen in Raume von Tirol. Monographien zur Landeskunde Tirols, Folge 1, Universitaets-Verlag Wagner.

Fliri, F., 1991:Cambiamenti del clima delle Alpi Orientali negli ultimi 200 anni con particolare considerazione degli ultimi decenni. Atti del Convegno della Soc. Geografica Italiana (Roma 5-6 Aprile 1990), in Memorie S. G. I. vol. XLVI, 273-281.

Frank, D., Esper, J., 2005a: Effect of scaling and regression on reconstructed temperature amplitude for the past millennium. Geoph. Res. Letters. 32, L07711, doi:10.1029/2004GL021236

Frank, D., Esper, J., 2005b: Temperature reconstructions and comparison with instrumental data from a tree-ring network for the European Alps. Int. J. Climatol. 25: 1437–1454 .

Frank, D., Esper, J., 2005c: Characterization and climate response patterns of a high-elevation, multi-species tree-ring network in the European Alps. Dendrochronologia 22: 107-121.

Frank, D., Wilson, R. & Esper, J. 2005: Synchronous variability changes in Alpine temperature and tree-ring data over the past two centuries. Boreas, 34: 498–505. Oslo. ISSN 0300-9483.

Frattini, S., 1988: I fiori del Parco dell'Adamello. Società Ed. Vannini Brescia. 222 pp.

Fritts, H. C., Vaganov, E. A., Sviderskaya, I. V. & Shashkin, A. V. 1991. Climatic variation and tree-ring structure in conifers: a statistical simulative model of tree-ring width, number of cells, cell wallthickness and wood density. Clim. Res. 1, 37-54.

Fritts, H. C., 1976: Tree Rings and Climate, 567 pp. Academic Press, New York.

Fritts, H.,C., Swetnam T.,W.,1986. Dendroecology: a tool for evaluating variations in past and present forest environments. Univ. of Arizona, Tucson.

Fritts, H.C., Guiot, J., 1990: Methods of calibration, verification and reconstruction. In Cook, E.R. and Kairiukstis, L.A., editors, Methods of dendrochronology: applications in the environmental sciences, Dordrecht: Kluwer, 163-217.

Gafta, D.; Pedrotti, F., 1998: Fitoclima del Trentino Alto Adige. Studi Trentini di Scienze Naturali-Acta Biologica 73 (1996): 55-111.

Guiot, J., 1991: The bootstrapped response function. Tree Ring Bull. 51, 39-41.

Grabherr G., 1980: Variability and Ecology of the Alpine Dwarf Shrub Community Loiseleurio-Cetrarietum Vegetatio, 41 (2): 111-120.

Grabherr, G., Gottfried, M., Pauli, H., 2010. Climate Change Impacts in Alpine Environments. Geography Compass 4, 8: 1133–1153.

Grace, J., Berninger, F., Laszlo, N., 2002. Impacts of Climate Change on the Tree Line. Annals of Botany 90: 537-544.

Grissino-Mayer, H.D. 2001: Evaluating crossdating accuracy: a manual and tutorial fpr the computer program COFECHA. Tree-Ring Res 57:205–221.

Holmes, R.L., 1983. Computer-assisted quality control in tree-ring dating and measurement. Tree–Ring Bulletin 43, 69–78.

Holzhauser HP (2002) Dendrochronologische Auswertung fossiler Hölzer zur Rekonstruktion der nacheiszeitlichen Gletschergeschichte. Schweiz Z Forstwes 153:17–28.

Hughes, M.K., Kelly, P.M., Pilcher, J.R., LaMarche Jr., V.C. (Eds.), 1982. Climate From Tree Rings. Cambridge University Press, Cambridge.

Hüscher, W., Schirmer W. 1993. Drei Jarrigchronologien aus den Pragser Dolomiten/Südtirol. Dendrochronologia 11, 123-137.

Houghton JT, Ding Y, Griggs DJ, Noguer M, van der Linden PJ, D. Xiaosu, (Eds), 2001. Climate Change 2001: The Scientific Basis ± Contribution of Working Group I to the IPCC Third Assessment Report. Cambridge University Press: Cambridge, 944 pp.

Houghton JT, Jenkins GJ, Ephraums JJ, (Eds), 1990. Climate Change: The IPCC Scientific Assessment ± Report of IPCC Working Group I. Cambridge University Press: Cambridge, 365 pp.

ITRDB, World Data Center for Paleoclimatology, NOAA/NGDC Paleoclimatology Program, Boulder CO USA http://www.ngdc.noaa.gov/paleo/ftp-treering.html

Kirdyanov A, Hughes H, Vaganov E, Schweingruber F, Silkin P 2003. The importance of early summer temperature and date of snow melt for tree growth in Siberian Subarctic. Trees 17:61–69.

Klein Tank, A.M.G., Können, G.P., 2003. Trends in indices of daily temperature and precipitation extremes in Europe, 1946–99. J. Clim. 16, 3665–3680.

Körner, C., Larcher., W., 1988: Plant Life in Cold Climates. In Plants and Temperature (Long SF, Woodward FI eds). The Company of Biol. Ltd., Cambridge, UK, pp. 25-57.

Körner, C., 1998. A re-assessment of high elevation treeline positions and their explanation. Oecologia 115:445-459.

Jacoby, G. C., Lovelius, N. V., Shumilov, O. I., Raspopov, O. M., Karbainov, J. M. & Frank, D. C. 2000. Long-term temperature trends and tree growth in the Taimyr region of northern Siberia. Quatern. Res. 53, 312–318. (doi:10.1006/qres.2000.2130)

Jacoby, G. C., D'Arrigo R., 1989. Reconstructed northern hemisphere annual temperature since 1671 based on high- latitude tree-ring data from north America. Climatic Change 14: 39-59.

Jones, P. D., T. J. Osborn, and K. R. Briffa 2001, The evolution of climate over the last millennium, Science, 292: 662– 667.

Leonelli, G., Pelfini, M., Battipaglia, G., Cherubini, P., 2009: Site-aspect influence on climate sensitivity over time of a high-altitude Pinus cembra tree-ring network. Climatic Change **96**:185–201. DOI 10.1007/s10584-009-9574-6

Lloyd, A., Fastie, C. 2002: Spatial and temporal variability in the growth and climate response of treeline trees in Alaska. Climatic Change 58: 481-509.

Liang C., Filion L., Cournoyer L., 1997. Wood structure of biotically and climatically induced light rings in eastern larch (Larix laricina). Can J For Res 27:1538–1547.

Luckman, B. H., Wilson, R. J. S. 2005: Summer temperatures in the Canadian Rockies during the last millennium:a revised record. Climate Dynamics 24: 131–144.doi: 0.1007/s00382-004-0511-0

Luterbacher, J., Dietrich, D., Xoplaki, E., Grosjean, M., Wanner, H., 2004. European seasonal and annual temperature variability, trends, and extremes since 1500. Science 303, 1499–1503.

Mann, M. E., Hughes M. K. 2002. Tree-ring chronologies and climate variability, Science296, 848.

Mann, M. E., R. S. Bradley, Hughes M. K., 1998. Global Scale Temperature Patterns and Climate Forcing over the Past Six Centuries. Nature, 392, 779-787.

Mann, M. E., R. S. Bradley, Hughes M. K., 1999. Northern hemisphere temperatures during the past millennium: Inferences, uncertainties, and limitations. Geophys. Res. Lett.,26, 759–762.

MCPFE (2007). State of Europe's Forests 2007. The MCPFE Report on Sustainable Forest Management in Europe. Warsaw, Ministerial Conference on the Protection of Forests in Europe**:** 247.

Meehl, G. A., and Coauthors, 2000: An introduction to trends in extreme weather and climate events: Observations, socioeconomic impacts, terrestrial ecological impacts, and model projections. Bull. Amer. Meteor. Soc., 81**,** 413–416.

Meko DM. 1997. Dendroclimatic reconstruction with time varying predictor subsets of tree indices. Journal of Climate 10: 687–696.

Menzel A, Fabian P (1999) Growing season extended in Europe. Nature 397:659.

Menzel A, Sparks TH, Estrella N, Koch E, Aasa A, Ahas R, Alm-Ku¨bler K, Bissolli P, Braslavska O, Briede A, Chmielewski FM,Crepinsek Z, Curnel Y, Dahl A ° , Defila C, Donnelly A, Filella Y,Jatczak K, Mage F, Mestre A, Nordli Ø, Penuelas J, Pirinen P,Remisova V, Scheifinger H, Striz M, Susnik A, Van Vliet AJH,Wielgolaski F-E, Zach S, Zust A (2006) European phenologicalresponse to climate change matches the warming pattern. GlobalChange Biol 12(10):1969–1976.

Meteotrentino http://www.meteotrentino.it/

Nash, J., E., Sutcliffe, J., V., 1971: Riverflow forecasting through conceptual models. 1 A discussion of principles. Journal of Hydrology, **10**: 282-290.

Nicolussi K, Patzelt G (2000) Discovery of Early Holocene wood and peat on the forefield of the Pasterze Glacier, Eastern Alps, Austria. The Holocene 10:191–199.

Oppenheimer C., 2003: Climatic, environmental and human consequences of the largest known historic eruption: Tambora volcano (Indonesia) 1815. Progress in Physical Geography **27** (2): 230–259.

Ozenda P. 1985. La végétation de la chaıˆne alpine dans l'espace montagnard européen. Paris: Masson.

Pallmann, H., Haffter, P., 1933: Pflanzensoziologische und bodenkundliche Untersuchungen im Oberengadin mit beson derer Berücksichtigung der Zwergstrauchgesellschaften der Ordnung Rhodoreto- Vaccinietalia. Ber. Schweiz. Bot. Ges. 42:357-466.

Pauli, H., Gottfried, M., and Grabherr, G. (2003). Effects of climate change on the alpine and nival vegetation of the Alps. J. M. E. Journal of Mountain Ecology 7: 9-12.

Peters, K., Jacoby, G., C., Cook, E., R., 1981: Principal component analysis of tree- ring sites. Tree-ring bulletin 41: 1-19.

Pignatelli, O.; Bleuler, M., 1988: Anni caratteristici come indicatori di attacchi della tortice grigia del larice (Zeiraphera diniana Gn.). Dendrochronologia 6: 163-170.

Pignatti E.., Pignatti S., Tartaglini N., 1988: Uomo e vegetazione al limite superiore delle foreste nelle Alpi Orientali Meridionali. Homenaje a Pedro Montserrat, JACA y HUESCA 695-703.

Pignatti, S., 1995: Ecologia vegetale. UTET-Torino. 531 pp.

Pilcher, J.,R., 1990 Sample preparation, cross-dating and measurement. In: Cook ER, Kairiukstis L (eds) Methods of dendrochronology: applications in the environmental sciences. Kluwer, Dordrecht, pp 40–51

Pilchler, P., Oberhuber W., 2007. Radial growth response of coniferous forest trees in an inner Alpine environment to heat-wave in 2003. Forest Ecology and Management 242: 688–699

Rinn, F., 1996. TSAP (Time series Analysis and Presentation), Version 3.0. Heidelberg, Germany.

Ranzi R., Grossi G., Gitti A., Taschner S., 2010. Energy and mass balance of the Mandrone Glacier (Adamello, Central Alps). Geografia Fisica e Dinamica Quaternaria, 33, 45-60.

Rolland, C., Petitcolas, V., Michalet, R., 1998: Changes in radial tree growth for Picea abies, Larix decidua, Pinus cembra and Pinus uncinata near the alpine timberline since 1750. Trees 13:40–53.

Rolland C, Baltensweiler W, Petitcolas V (2001) The potential for using Larix decidua ring widths in reconstructions of larch budmoth (Zeiraphera diniana) outbreak history: dendrochronological estimates compared with insect surveys. Trees 15:414–424

Ronchi, Q., 1927. La Guerra dell'Adamello. S. Daniele, Ed. Tobacro, 203 pp.

Rübel, E. 1930. Pflanzengesellschaften der Erde. Bern-Berlin.

Sadler, J. P., Grattan, J. P., 1999: Volcanoes as agents of past environmental change. Global and Planetary Change 21, 181–196.

Salzer, W., Kipfmueller, K. F., 2005: Reconstructed Temperature and precipitation on a millennial timescale from tree-rings in the southern Colorado Plateau, U.S.A. Climatic Change 70, 465-487.

Sartori, G.; Mancabelli, A.; Wolf U.; Corradini F., 2005: Atlante dei suoli del Parco Naturale Adamello-Brenta. Suoli e paesaggi. Museo Tridentino di Scienze Naturali.

Schär, C., Vidale, P.L., Lu¨thi, D., Frei, C., Ha¨berli, C., Liniger, M.A., Appenzeller, C., 2004. The role of increasing temperature variability in European summer heatwaves. Nature 427, 332–336.

Schweingruber, F.H., 1988. Tree Rings. Basics and Applications of Dendrochronology. Kluwer, Dordrecht, 276 pp.

Schweingruber, F. H., 1993: Trees and wood in dendrochronology. Morphological Anatomical and tree-ring analytical aspects. Springer-Verlag, 402 pp.

Schweingruber, F. H., 1996: Tree rings and environment. Dendroecology. 609 pp.

Siebenlist-Kerner V., 1984. Der Aufbau von Jahrringchronologien für Zirbelkiefer, Lärche und Fichte eines alpinen Hochgebirgsstandortes. Dendrochronologia 2: 9-29.

Skeen C., E., 1981: The Year without a Summer: A Historical View Journal of the Early Republic, **1** (1) 51-67.

Snee, R., D., 1997: Validation of regression models: methods and examples. Technometrics 19 (4), 415-428.

Sparks TH, Menzel A 2002. Observed changes in the seasons: an overview. International Journal on Climatology, 22, 1715–1725.

Stokes, M.A., Smiley T.L., 1968. An Introduction to Tree-Ring Dating. University of Chicago Press, Chicago, IL, 73 pp.

Swetnam, T.W., Lynch, A.M. 1993. Multicentury, regional-scale patterns of western spruce budworm outbreaks. Ecological Monographs 63(4): 399-424.

Swetnam, T.W., Thompson, M.A., Sutherland, E.K 1985. Using dendrochronology to measure radial growth of defoliated trees. USDA Forest Service Agricultural Handbook No. 639. 39 pp.

Tappeiner U., G. Tappeiner, A. Hilbert and E. Mattanovich, 2003 The EU Agricultural Policy and the Environment. Evaluation of the Alpine Region, Blackwell, Berlin, Germany.

Tessier, L., 1986: Chronologie des Mélèzes des Alpes et petit âge glaciaire. Dendrochronologia 4: 97–113.

Theurillat JP, Guisan A. 2001. Potential impact of climate change on vegetation in the European Alps: A review. Climatic Change 50:77 109.

Touchan, R., Meko, Aloui A. 2008, Precipitations reconstructions for Nortthwestern Tunisia from tree-ring width. Journal of Arid Environments. 72, 1887-1896

Touchan, R., Garfin, G. M., Meko, D. M., Funkhouser, G., Erkan, N., Hughes, M. K., and Wallin, B. S.: 2003, Preliminary reconstructions of spring precipitation in southwestern Turkey from tree-ring width. Int. J. Clim. 23, 157–171.

Touchan, R., Funkhouser, G., Hughes, M. K., and Erkan, N.: 2005, Standardized precipitation indices reconstructed from Turkish tree-ring width. Climatic change. 72(3), 339–353.

Tranquillini W (1964) The physiology of plants at high altitudes. Annu Rev Plant Physiol 15:345–362.

Vaganov, E. A., M. K. Hughes, and A. V. Shashkin 2006. Growth Dynamics of Tree Rings: Images of Past and Future Environments, Springer, New York.

Vaganov, E. A., M. K. Hughes, A. V. Kirdyanov, F. H. Schweingruber, and P. P. Silkin (1999), Influence of snowfall and melt timing on tree growth in subarctic Eurasia, Nature, 400, 149–151.

Valentini R, Anfodillo T, Ehlringer J (1994)Water sources utilization and carbon isotope composition (δ13C) of co-occurring species along an altitudinal gradient in the Italian Alps. Can J For Res 24:1575–1578.

Viazzi, L. 1981: I diavoli dell'Adamello: la guerra a quota tremila, 1915-1918. Milano: Mursia, 510 pp.

Viazzi, L., Cavacicchi, A., 1996. L'impresa dell'Adamello. Ed. Nordpress, 92 pp.

Vincent, C., Le Meur, E., Six, D., Funk M., 2005: Solving the paradox of the end of the Little Ice Age in the Alps Geophys. Res. Lett., 32, L09706, doi:10.1029/2005GL022552.

Walther GR, Post E, Convey P, Menzel A, Parmesan C, Beebee TJC, Fromentin O, Hoegh-Guldberg J-M, Bairlein F (2002) Ecological responses to recent climate change. Nature 416:389–395.

Wagner S., Zorita E., 2005: The influence of volcanic, solar and CO2 forcing on the temperatures in the Dalton Minimum (1790–1830): a model study. Climate Dynamics 25: 205–218.

Walther, P. (1986). Land Abandonment in the Swiss Alps: a new understanding of a land use problem. Mountain Research and Development 6, 305–314.

Weber, U.,M,, 1997. Dendroecological reconstruction and interpretation of larch budmoth (Zeiraphera diniana) outbreaks in two central alpine valleys of Switzerland from 1470 to 1990. Trees 11:277–290.

Wigley, T. M. L., Briffa, K. R., and Jones, P. D.:1984, On the average value of correlated time series, with applications in dendroclimatology and hydrometeorology, J. Clim. Appl. Meteorol. **23**, 201–213.

Wilson, R., M. 1998: Volcanism, Cold Temperature, and Paucity of Sunspot Observing Days (1818-1858): A Connection?, The Smithsonian/NASA Astrophysics Data System NASA/TP—1998–208592.

Wilson, R.J.S., Luckman, B.H., 2003: Dendroclimatic reconstruction of maximum summer temperatures from upper treeline sites in interior British Columbia, Canada. Holocene 13:851–861.

Wilson, R.J.S., Luckman, B. H., 2002: Tree-ring reconstruction of maximum and minimum temperatures and the diurnal temperature range in British Columbia, Canada. Dendrochronologia 20:257–268.

Wilson R.J.S., Topham, J., 2004. Violins and climate. Theor. Appl. Climatol. 77, 9–24 DOI 10.1007/s00704-003-0025-4

Wilson R.J.S., Esper J., Luckman B.H., 2004. Utilising historical tree-ring data for dendroclimatic calibration: a case study from the Bavarian Forest, Germany. Dendrochronologia 21/2: 53-68.

Young, K. C., 1994: Reconstructing streamflow time series in central Arizona using monthly precipitation and tree ring record. J. Climate, **7**, 361-374.

Yonenobu, H., Eckstein, D. (2006): Reconstruction of early spring temperature for central Japan from the tree-ring widths of Hinoki cypress and its verification by other proxy records. Geophysical Research Letters 33: doi:10.1029/2006GL026170, 2006.

Youngblut, D., Luckman, B. (2008): Maximum June-July temperatures in the southwest Yukon over the last 300 years reconstructed from tree rings. Dendrochronologia 25/3: 153-166.

I. Appendix 1. Dendrogeomorphological dating of a rockfall by means of traumatic resin ducts. A case study in Val Malga (Adamello-Presanella Group, Central Italian Alps)

Introduction

Rapid mass movements as debris flows, rock falls or rock avalanches are common geomorphic events in mountain environments and represent a major threat in many parts of the Alpine arch. Their occurrence is one of the most important natural hazards both for human activities and for infrastructures. The study and temporal reconstruction of past geomorphic events represent important tools into the planning of future preventive measures.

When trees are present, geomorphic processes may directly influence tree growth (Alestalo, 1971; Shroder, 1978, 1980; Schweingruber, 2001). Dendrochronological techniques have been widely used in defining the occurrence and magnitude of geomorphological events (Strunk 1997; Stoffel et al 2005a, 2005b), and recently applied in studied focused on hazard assessment and risk analysis (Stoffel, 2006). Frequency and magnitude of mass movements can be influenced by recent global warming (O'Connor, 1993; Harris, 2001), then the possibility of dating and identify past geomorphic processes by means of tree-ring records provides a base on which compare future developments of geomorphic systems.

During the sampling campaign conducted in summer 2008 in Val Malga, we have localized a rock fall detached from the north facing slope of the valley. The event had involved an open forest mainly dominated by of Norway spruce (P*icea abies* (L.) Karst.) and European larch (*Larix decidua* Mill.)(Fig. 1 and 2).

Considered the absence of official reports on this event, we decided to perform the dendrochronological dating of the rock fall.

Study area

The valley is located into the intrusive Adamello massif, which forms the largest pluton of Alpine age of the Alpine arch (Callegari, 1983, 1985). The outcropping magmatic intrusive rock is named "Tonalite". Tonalite has a felsic composition, with phaneritic texture. Feldspar is present as plagioclase (typically oligoclase or andesine) with 10% or less alkali feldspar. Quartz is present as more than 20% of the rock. Amphiboles and pyroxenes are common accessory minerals (Bianchi et Al., 1970; Callegari & Dal Piaz, 1973).

The treeline run at about 1850 m a.s.l, this very low altitude seems to be influenced by recurrent geomorphic processes (Leonelli et al 2010). The detachment niche was located at about 1900 m a.s.l., the lower part of the deposit reached about 1750 m a.s.l., with singular boulders found at 1670 m a.s.l.

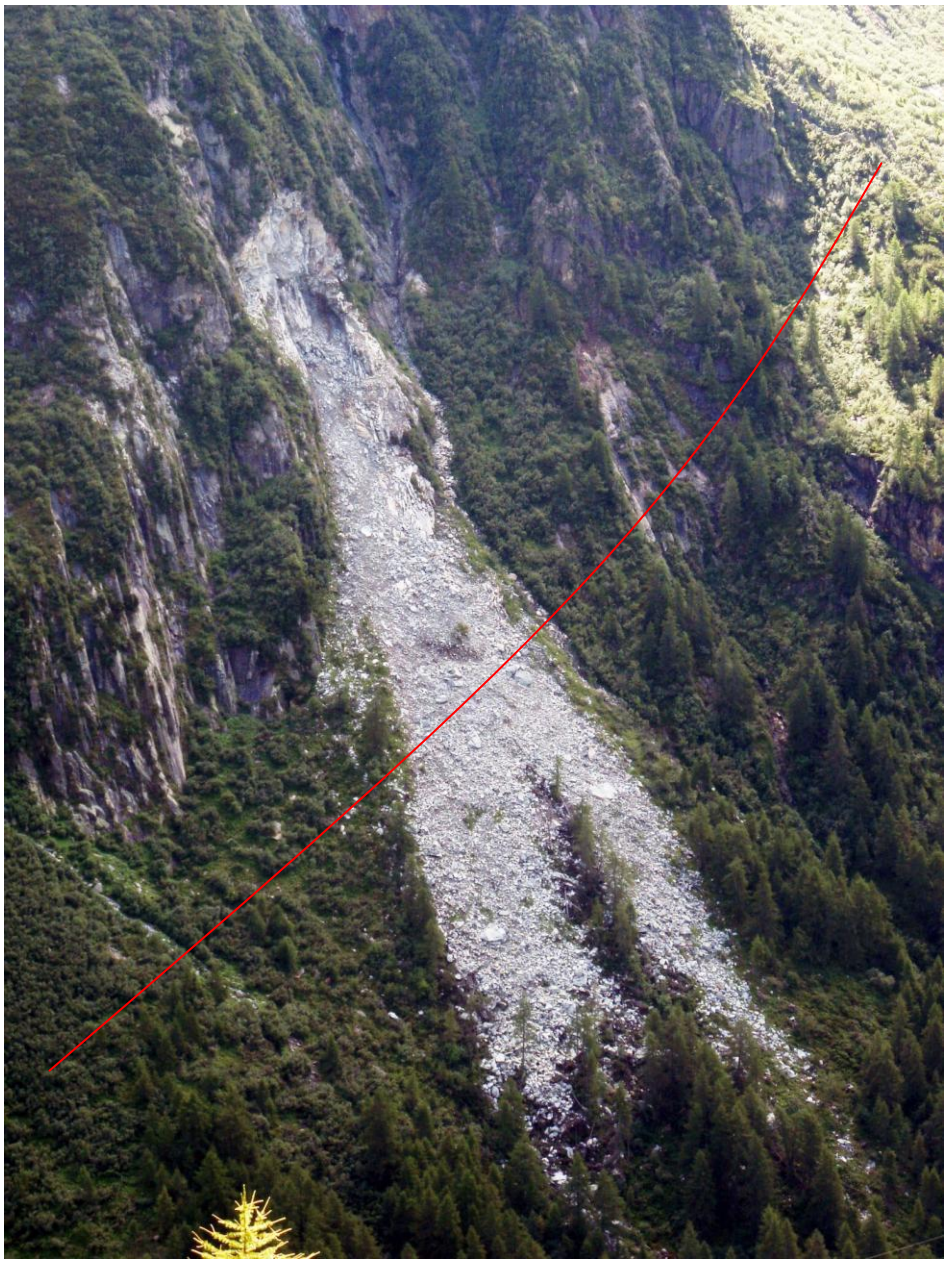

Fig. I-1 The detachment niche is located at about 1900 m a.s.l from the north-facing slope of the valley and hit a larch wood below (Fig. 1, 2). The tree line (marked with a red line) runs at about 1850 m a.s.l.

Materials and methods

We sampled several affected trees from the both sides and in the middle of the rockfall path, where a limited number of trees survived to the impacts with boulders (Fig. 1 and 3). Trees with evident signs of damages caused by the impact with the rocks (injured or

decapitated trees), and uprooted trees found on the deposit (Fig. 1 and 3) were chosen for sampling.

Rockfalls tipically produce a free or rebounding fall of material from cliff faces down steep slopes (Selby, 1993; Luckman, 2004) and the impact of rocks and boulders on trees can produce scars to the stem surface or even decapitate trees.

Conifer trees affected by impacts with rocks react forming callus tissue, tangential rows of traumatic resin ducts (Stoffel et al., 2005b,c; Perret et al., 2006), reaction wood (Braam et al., 1987; Fantucci and Sorriso-Valvo, 1999; Stefanini, 2004; Stoffel et al., 2005a) or react with an abrupt growth suppression or release (Strunk, 1997).

Two cores per tree were extracted at 90^{o} degrees with increment borers, one on the impact side, another one on the opposite side of the trunk. On the impact side the cores were extracted in proximity of the wounds, in order to highlight growth disturbances (Stoffel & Perret, 2006). We collected samples from undisturbed trees in order to build a reference chronology (Fig. 4). In all, we analysed samples coming from 70 trees (*Larix decidua* Mill.).

Fig. I-2 View of Val Malga. The rock fall and the location of sample sites (red circles) are visible on the right.

Fig. I-3 Uprooted and severely damaged trees

Samples were prepared in the laboratory following standard dendrochronological procedures (Ferguson, 1970; Pilcher, 1990). Ring widths of disturbed and reference increment cores were measured using a digital LINTAB positioning table connected to a Leica microscope and TSAP 3·0 software (Time Series Analysis and Presentation; Rinntech, 2006).

The reference chronology was built choosing tree-ring series longer than 100 years with higher statistics results (T test>2 and Gleichläufigkeit>60) in the cross-dating procedures (Baillie & Pilcher, 1973; Schweingruber, 1988).

Dating of the growth tree ring series derived from uprooted trees was performed cross-dating the undated floating series with the reference chronology.

Results

The Val Malga reference chronology spans from 1807 to 2008 and it is composed by 20 tree-ring series.

The last ring produced by the uprooted trees was the 2006 annual ring, as it results by the cross-dating with the reference chronology (Fig. 5). This last ring appears to be complete, therefore the uprooted trees surely died after the end of the growing season 2006.

In the most part of samples coming from severely damaged, but survived, trees, the 2007 annual ring starts with an evident row of traumatic resin ducts (Fig. 4-a,b,c). The rows are clearly tangentially oriented with a compact and continuous arrangement of ducts.

In the remaining samples coming from injured trees, the tree-ring series show an evident abrupt growth reduction that starts on the 2007 ring (Fig. 4-d).

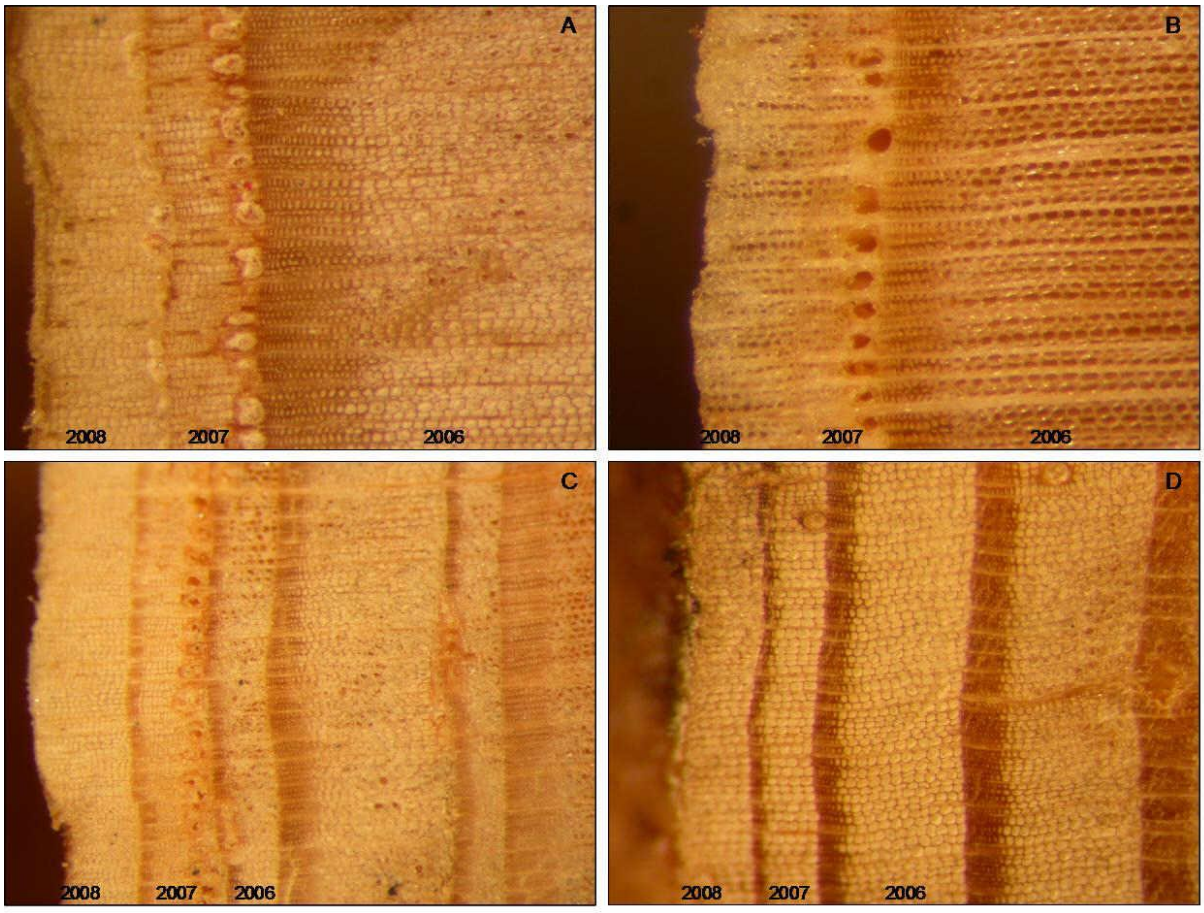

Fig. I-4 Detailed view of the tree ring sequences in severely damaged trees.

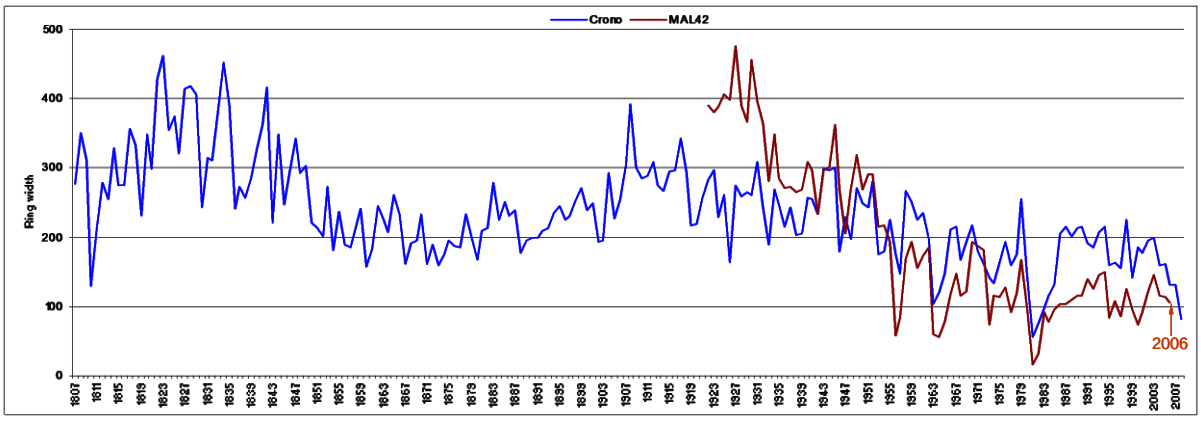

Fig. I-5 Dating of an uprooted tree (Mal 42).

Discussion and conclusion

Growth anomalies have been widely used in Dendrogeomorphology to reconstruct frequencies and extensions of geomorphic processes. Examples of successful employ of growth disturbance analysis in dendrogeomorphological studies are reported in current literature for different types of ecosystems and tree species (Denneler & Schweingruber 1993; Gärtner *et al.* 2003; Bodoque *et al.* 2005).

Traumatic resin ducts are growth anomalies typically present in conifer trees. Resin is produced by most conifer species in the xylem and in the phloem as an effective protection from various kinds of pathogens or mechanical injuries. Mechanical injuries can be a consequence of grazing or insect and fungi attacks or they can be the result of impacts with snow, ice or rocks' fragments. In general traumatic resin ducts can be considered as a reaction of conifer trees to several kinds of environmental stress (Schweingruber 1996; Schweingruber 2001). As reported by Stoffel (2008), the presence of resin ducts should be considered as the result of a geomorphic process only when they form tangentially oriented rows with a compact and continuous arrangement of traumatic ducts.

The timing of the traumatic resin ducts formation is an important aspect to consider when they are used as a dating tool in geomorphic processes. In fact, it is important to understand if the resin duct formation is an immediate reaction to injuries or a delayed response.

Gärtner & Heinrich (2009) have demonstrated using wounding experiments imitating the impact of geomorphic processes, that wounding conducted before of the beginning of the vegetation period, in samples taken from the centre of the wound, produced an immediate reaction at least on one side of the lesion. The reaction to wounding in the zone adjacent to the wound tissue was characterised by the formation of epithelial cells as the first cells of the

annual ring (Fig.5a, b, c). Gärtner & Heinrich (2009) found that larch trees first formed traumatic resin ducts when treated before the beginning of the next growing season which was classified as an immediate reaction.

In the study here presented, samples taken from the side of the impact and in proximity of the scars are characterized by the formation of a line of traumatic resin ducts as the first cells of the annual ring. Resin ducts are tangentially oriented and form a continuous line with a compact arrangement of ducts.

Due to the presence in the injured trees of the traumatic resin ducts as a first line of cells in the 2007 rings and due to the dating of the last annual ring formed by the uprooted trees (2006), we can deduce, as a first rough dating, that the rockfall surely occurred during the dormancy period, that spans from the end of the growing season 2006 and the beginning of the growing season 2007. A useful indication to further restricting this dating window came from some oral evidences. Farm-workers that habitually use the valley floor to graze cows, suppose that the rockfall fell down during March 2007, before the beginning of the next growing season, that for larch at these altitude in the Alps starts in June. This evidence is consistent with the results of Gärtner & Heinrich's experiments and with our findings: the rock fall occurred before the beginning of the growing season 2007.

We can conclude that the results of our analysis confirm, in a natural and not artificially induced context, what demonstrated by these two authors. This work can be considered an example of successful use of traumatic resin ducts formation as a tool for dating a geomorphic event.

The analysis of meteorological data (Fig. 6 and 7), coming from a nearby meteorological station (Edolo), did not allow to relate the rockfall occurrence to any extreme climatic event.

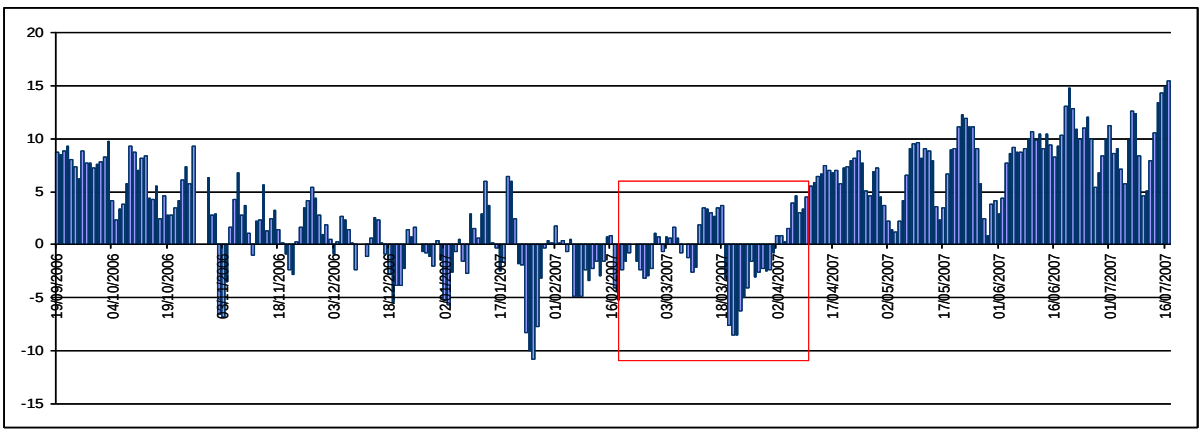

Fig. I-6 Daily mean temperatures (Edolo meteorological station, Lombardy), the red square indicates the period in with the event probably occurred.

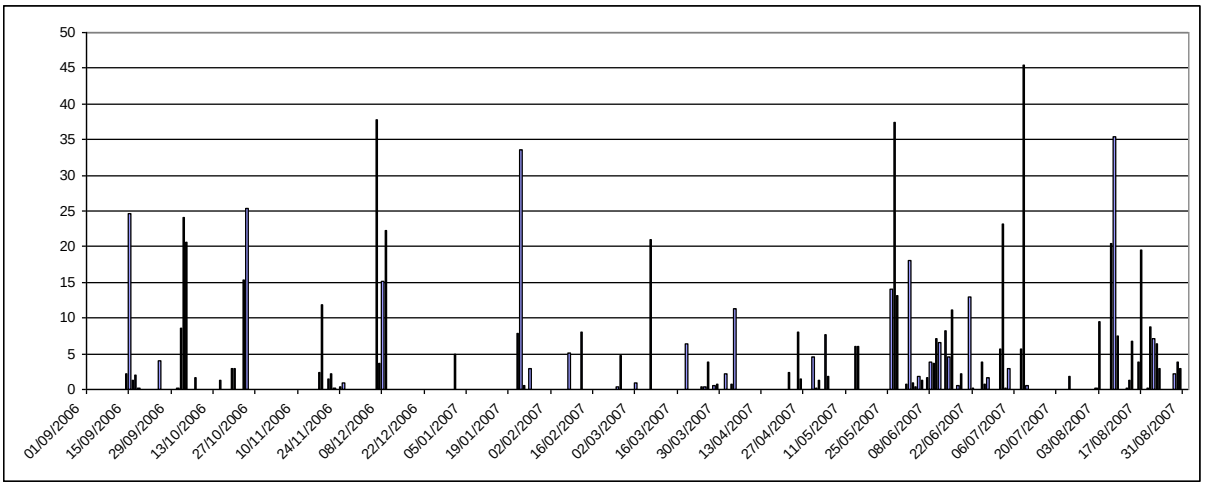

Fig. I-7 Daily cumulative precipitation (Edolo meteorological station).

Bibliography

Alestalo, J. 1971. Dendrochronological interpretation of geomorphic processes. Fennia 105: 1–140.

Baier, P., E. Führer, T. Kirisits & S. Rosner. 2002. Defence reactions of Norway spruce against bark beetles and the associated fungus Ceratocystis polonica in secondary pure and mixed species stands. Forest Ecol. Manag. 159: 73–86.

Baillie, M.G.L., Pilcher, J.R. 1973. A simple crossdating program for tree-ring research. Tree-Ring Bull. 33: 7–14.

Bianchi, A., Callegari, E., Jobstraibizer P., G., 1970. I tipi petrografici fondamentali del plutone dell'Adamello. Tonaliti-quarzodioriti-granodioriti e loro varietà leucocratiche. Mem. Ist. Geol, e Mi Univ. Padova, 27: 1-148 (con schizzi geologico 1:200.000).

Bianchi A. e Dal Piaz G.B., 1940 - Il settore nord-occidentale del massiccio dell'Adamello. Relazione preliminare sul rilevamento e sugli studi geologico-petrografici compiuti durante l'anno 1939 nell'alta VaI Camonica. Boll. R. Uff. Geol. It., 65: 1-18. Roma.

Braam, R.R., Weiss, E.E.J., Burrough, P.A., 1987. Spatial and temporal analysis of movement using dendrochronology. Catena 14: 573–584.

Callegari, E., 1983. Note introduttive alla geologia del massiccio dell'Adamello. In: «Il magmatismo tardo-alpino nelle Alpi. Escursione Adamello-Bregaglia». Soc. Geol. It. - Soc. It. Miner. Petr.: 14-18. Luglio 1983. Padova.

Callegari, E. 1985. Geological and petrological aspects of the magmatic activity at Adamello (northern Italy). Mem. Soc. Geol. It., 26 (1983): 83-103. Roma.

Cook ER, Kairiukstis LA. 1990. Methods of Dendrochronology – Applications in the Environmental Sciences. Kluwer: London.

Ferguson, C., W., 1970: Concept and techniques of Dendrochronology in Scientific Methods in medieval Archaeology. Rainer Berger, Editor. University of California Press.

Fantucci, R., Sorriso-Valvo, M., 1999. Dendrogeomorphological analysis of a slope near Lago, Calabria (Italy). Geomorphology30 (1–2): 165–174.

Franceschi, V.R., P. Krokene, T. Krekling & E. Christiansen. 2000. Phloem parenchyma cells are involved in local and distant defence responses to fungal inoculation or bark-beetle attack in Norway spruces (Pinaceae). Am. J. Bot. 87: 314–326.

Gärtner H., Heinrich I. The Formation of Traumatic Rows of Resin Ducts in *Larix decidua* and *Picea abies* (Pinaceae) as a Result of Wounding Experiments in the Dormant Season. IAWA Journal, Vol. 30 (2), 2009: 199–215.

Harris, C.,. Davies M.C.R,. Etzelmüller B, 2001.The assessment of potential geotechnical hazards associated with mountain permafrost in a warming global climate. Permafrost and Periglacial Processes 12: 145–156

Leonelli G., Pelfini, M., Morra di Cella, U., Garavaglia, V. 2010. Climate Warming and the Recent Treeline Shift in the European Alps: The Role of Geomorphological Factors in High-Altitude Sites. AMBIO. DOI 10.1007/s13280-010-0096-2

Luckman, B.H., 2004. Rockfall. In: Goudie, A. (Ed.), International Association of Geomorphology, Dictionary of Geomorphology. Routledge, London, p. 882.

Nagy, N.E., P. Krokene & H. Solheim. 2005. Anatomical-based defense responses of Scots pine (*Pinus sylvestris*) stems to two fungal pathogens. Tree Physiol. 26: 159–167.

O'Connor, J. E., and J. E. Costa, 1993. Geologic and hydrologic hazards in glacierized basins in North America resulting from 19th and 20th century global warming, Nat. Hazards, 8: 121–140, doi:10.1007/BF00605437.

Pilcher, J.,R., 1990 Sample preparation, cross-dating and measurement. In: Cook ER, Kairiukstis L (eds) Methods of dendrochronology: applications in the environmental sciences. Kluwer, Dordrecht, pp 40–51.

Rinn, F., 1996. TSAP (Time series Analysis and Presentation), Version 3.0. Heidelberg, Germany.

Schweingruber, F.H., 1988. Tree Rings. Basics and Applications of Dendrochronology. Kluwer, Dordrecht, 276 pp.

Schweingruber, F.H. 1996. Tree rings and environment. Dendroecology. Swiss Federal Institute for Forests, Snow and Landscape Research Birmensdorf and Paul Haupt-Verlag, Bern, Stuttgart, Vienna.

Schweingruber, F.H., 2001. Dendroökologische Holzanatomie. Paul Haupt, Bern.

Selby, M.J., 1993. Hillslope Materials and Processes. Oxford University Press, Oxford.

Shroder, J.F., 1978. Dendrogeomorphologic analysis of mass movement on Table Cliffs Plateau, Utah. Quat. Res. 9, 168–185. Shroder, J.F., 1980. Dendrogeomorphology; review and new techniques of tree-ring dating and geomorphology. Prog. Phys. Geogr. 4 (2): 161–188.

Stefanini, M.C., 2004. Spatio-temporal analysis of a complex landslide in the Northern Apennines (Italy) by means of dendrochronology. Geomorphology 63 (3–4): 191–202.

Stoffel, M., 2006. A review of studies dealing with tree rings and rockfall activity: the role of dendrogeomorphology in natural hazard research. Natural Hazards 39: 51–70.

Stoffel, M., 2008. Dating past geomorphic processes with tangential rows of traumatic resin ducts. Dendrochronologia 25(1): 53-60.

Stoffel, M., Perret, S., 2006. Reconstructing past rockfall activity with tree rings: some methodological considerations. Dendrochronologia 24 (1): 1–15.

Stoffel, M., Lièvre, I., Conus, D., Grichting, M.A., Raetzo, H., Gärtner, H.W., Monbaron, M., 2005a. 400 years of debris flow activity and triggering weather conditions: Ritigraben VS. Switzerland. Arctic Antarctic and Alpine Research 37: 387–395.

Stoffel, M., Schneuwly, D., Bollschweiler, M., Lie`vre, I., Delaloye, R., Myint, M., Monbaron, M., 2005b. Analyzing rockfall activity (1600–2002) in a protection forest – a case study using dendrogeomorphology. Geomorphology 68: 224–24.

Strunk, H., 1997. Dating of geomorphological processes using dendrogeomorphological methods. Catena 31: 137–151.

Wiles, G.C., P. E. Calkin & G.C. Jacoby. 1996. Tree-ring analysis and Quaternary geology: Principles and recent applications. Geomorphology 16: 259–272.

II. Appendix 2. List of sampled trees

SAMPLE	SPECIES	LAT.	LONG.	ELEVATION (m)
AVIO 1	PiCe	0,000000	0,000000	2100
AVIO 2	PiCe	46,179306	10,479444	2185
AVIO 3	LaDe	46,179306	10,476611	2135
AVIO 4	LaDe	46,179389	10,476750	2145
AVIO 5	PiCe	46,179583	10,475556	2125
AVIO 6	PiCe	46,179444	10,475444	2115
AVIO 7	PiCe	46,180167	10,474972	2136
AVIO 8	LaDe	46,179194	10,473111	2065
AVIO 9	LaDe	46,178000	10,471556	2082
AVIO 10	PiCe	46,177194	10,473361	2105
AVIO 11	LaDe	46,176833	10,473583	2115
AVIO 12	LaDe	46,177056	10,474083	2112
AVIO 13	LaDe	46,176222	10,474083	2138
AVIO 14	LaDe	46,176111	10,474333	2140
AVIO 15	LaDe	46,175083	10,474056	2182
AVIO 16	LaDe	46,174389	10,474056	2198
AVIO 17	LaDe	46,174389	10,474056	2200
AVIO 18	LaDe	46,174028	10,490694	2195
AVIO 19	LaDe	46,173722	10,473944	2215
AVIO 20	LaDe	46,174389	10,477056	2187
AVIO 21	LaDe	46,174472	10,476972	2186
AVIO 22	PiCe	46,174167	10,477639	2205
AVIO 23	PiCe	46,174167	10,477639	2198

Tab. II-1 Val d'Avio. List of samples.

SAMPLE	SPECIES	LAT.	LONG.	ELEVATION (m)
VF1	LaDe	46°05'27,1''	10°33'50,7''	1911
VF2	LaDe	46°05'30,5'	10°33'48,6''	1926
VF3	LaDe	46°05'55,7'	10°33'51,7''	1963
VF4	LaDe	46°05'55,7'	10°33'51,7''	2051
VF5	LaDe	46°05'55,7'	10°33'51,7''	2080
VF6	LaDe	46°05'20,3'	10°34'10,9''	2075
VF7	LaDe	46°05'20,3'	10°34'10,9''	2065
VF8	PiCe	46°05'19,6''	10°34'11,8''	2065
VF9	LaDe	46°05'19,6''	10°34'11,8''	2071
VF10	LaDe	46°05'19,6''	10°34'11,8''	2114
VF11	LaDe	46°05'19,6''	10°34'11,8''	2114
VF12	LaDe	46°05'210,5''	10°34'08,9''	2084
VF13	LaDe	46°05'210,5''	10°34'08,9''	2044
VF14	LaDe	46°05'210,5''	10°34'08,9''	2010
VF15	LaDe	46°05'22,1''	10°34'6,0''	1980
VF16	LaDe	46°05'21,3''	10°34'03''	1978
VF17	LaDe	46°05'02,7''	10°33'47,3''	1937
VF18	PiCe	46°05'03,3''	10°33'47,8''	1926
VF19	LaDe	46°05'10,1''	10°33'57,1''	1962
VF20	LaDe	46°05'39,7''	10°33'59,7''	1998

SAMPLE	SPECIES	LAT.	LONG.	ELEVATION (m)
VF21	LaDe	46°05'39,7"	10°33'59,7"	2002
VF22	PiCe	46°05'39,7"	10°33'59,7"	2002
VF23	PiCe	46°05'39,7"	10°33'59,7"	2035
VF24	LaDe	46°05'39,7"	10°33'59,7"	2035
VF25	LaDe	46°05'39,7"	10°33'59,7"	2035

Tab. II-2 Val di Fumo. List of samples

SAMPLE	SPECIES	LAT.	LONG.	ELEVATION (m)
MAL1	PcAb	46,140417	10,367028	0
MAL3	PcAb	46,139694	10,369000	1098
MAL4	PcAb	46,138917	10,368694	1131
MAL5	PcAb	46,139194	10,368778	1141
MAL6	PcAb	46,138056	10,373167	1111
MAL7	PcAb	46,139056	10,372667	1104
MAL8	PcAb	46,139056	10,372667	1104
MAL9	PcAb	46,128694	10,426611	1700
MAL10	PcAb	46,128667	10,426583	1701
MAL11	PcAb	46,128639	10,427417	1720
MAL12	PcAb	46,128667	10,427278	1720
MAL14	PcAb	46,128806	10,426111	1690
MAL33	PcAb	46,130583	10,422361	1823
MAL35	PcAb	46,130639	10,422417	1820
MAL63	PcAb	46,129528	10,426306	1725
MAL65	PcAb	46,130944	10,429972	1729
MAL66	PcAb	46,130944	10,429972	1733
MAL67	PcAb	46,131139	10,429500	1729
MAL68	PcAb	46,131139	10,429500	1730
MAL2	LaDe	46,139944	10,367972	1110
MAL13	LaDe	46,128611	10,427000	1710
MAL15	LaDe	46,131944	10,418278	1740
MAL16	LaDe	46,132000	10,432694	1720
MAL17	LaDe	46,131889	10,432389	1750
MAL18	LaDe	46,131944	10,433306	1690
MAL19	LaDe	46,131972	10,432417	1690
MAL20	LaDe	46,130667	10,433028	1750
MAL21	LaDe	46,130667	10,433028	2080
MAL21	LaDe	46,130667	10,433028	2080
MAL22	LaDe	46,134917	10,424944	2080
MAL23	LaDe	46,134861	10,424917	2080
MAL24	LaDe	46,129972	10,422833	2080
MAL25	LaDe	46,130639	10,422889	2080
MAL26	LaDe	46,130556	10,422917	1709
MAL27	LaDe	46,130389	10,422833	1728
MAL28	LaDe	46,130417	10,422833	1717
MAL29	LaDe	46,130500	10,422694	1728
MAL30	LaDe	46,130361	10,422694	1743
MAL31	LaDe	46,130333	10,422444	1732
MAL32	LaDe	46,130361	10,422417	1745
MAL34	LaDe	46,130639	10,422417	1750

SAMPLE	SPECIES	LAT.	LONG.	ELEVATION (m)
MAL36	LaDe	46,128278	10,425639	1690
MAL37	LaDe	46,128083	10,425750	1694
MAL38	LaDe	46,128361	10,425306	1694
MAL39	LaDe	46,128194	10,425917	1696
MAL40	LaDe	46,128167	10,426389	1715
MAL41	LaDe	46,128222	10,426556	1713
MAL42	LaDe	46,127639	10,426722	1735
MAL43	LaDe	46,127639	10,426722	1735
MAL44	LaDe	46,127639	10,426722	1735
MAL45	LaDe	46,127306	10,428194	1735
MAL46	LaDe	46,127306	10,428194	1795
MAL47	LaDe	46,127278	10,428167	1796
MAL48	LaDe	46,127111	10,428194	1810
MAL49	LaDe	46,127083	10,428194	1818
MAL50	LaDe	46,126917	10,428472	1832
MAL51	LaDe	46,126694	10,428500	1855
MAL52	LaDe	46,126500	10,428167	1855
MAL53	LaDe	46,126556	10,428028	1843
MAL54	LaDe	46,126553	10,428031	1845
MAL55	LaDe	46,126556	10,428033	1840
MAL56	LaDe	46,126667	10,427889	1840
MAL57	LaDe	46,126553	10,427889	1836
MAL58	LaDe	46,126778	10,427722	1815
MAL59	LaDe	46,126806	10,427583	1805
MAL60	LaDe	46,127139	10,427139	1756
MAL61	LaDe	46,127167	10,427278	1756
MAL62	LaDe	46,127361	10,427222	1764
MAL64	LaDe	46,130944	10,429972	1735
MAL69	LaDe	46,131278	10,429778	1738
MAL70	LaDe	46,131417	10,429722	1736

Tab. II-3 Val Malga. List of samples

SAMPLE	SPECIES	LAT.	LONG.	ELEVATION (m)
VP 1	PcAb	46,259444	10,659417	1745
VP 4	PcAb	46,259500	10,659667	1750
VP 5	PcAb	46,259333	10,660333	1770
VP 6	PcAb	46,259306	10,660333	1785
VP 7	PcAb	46,259306	10,660333	1780
VP 8	PcAb	46,259167	10,660028	11770
VP 12	LaDe	46,258778	10,659667	1790
VP 13	LaDe	46,258500	10,660833	1835
VP 15	LaDe	46,258306	10,660667	1840
VP 16	LaDe	46,257111	10,661167	1900
VP 17	PcAb	46,255250	10,659444	1900
VP 18	PcAb	46,253444	10,658194	1925
VP 19	PcAb	46,253611	10,656028	1940
VP 20	PcAb	46,252806	10,657500	1950
VP 21	PcAb	46,253028	10,657056	1830
VP 22	LaDe	46,250306	10,654472	2110

SAMPLE	SPECIES	LAT.	LONG.	ELEVATION (m)
VP 23	LaDe	46,253389	10,655972	2025
VP 25	LaDe	46,255722	10,654500	1950
VP 27	LaDe	46,256944	10,660333	1917
VP 28	LaDe	46,257444	10,660361	1890
VP 29	LaDe	46,257833	10,660944	1870
VP 30	LaDe	46,257833	10,660944	1870
PA 1	PcAb	46,263889	10,645083	1845
PA 2	LaDe	46,263528	10,646694	1825
PA 3	LaDe	46,264389	10,645417	1815
PA 4	PcAb	46,264389	10,645417	1815
PA 5	PcAb	46,263972	10,646750	1805
PA 7	PcAb	46,264417	10,646250	1785
PA 8	PcAb	46,264944	10,645694	1770
PA 9	LaDe	46,261444	10,665361	1870
PA 10	LaDe	46,266472	10,649583	1870
STAV 1	PcAb	46,274833	10,659944	1416
STAV 2	PcAb	46,261528	10,658139	1460
VP 2	PcAb			1745
VP 3	PiCe			1745
VP 24	LaDe			2025
VP 26	LaDe			1901

Tab. II-4 Val Presanella. List of samples.

SAMPLE	SPECIES	LAT.	LONG.	ELEVATION (m)
PRS 1	LaDe	46,239944	10,602417	2160,00
PRS 2	LaDe	46,239556	10,602472	2170,00
PRS 3	LaDe	46,238944	10,602472	2180,00
PRS 4	LaDe	46,238889	10,602778	2177,00
PRS 5	LaDe	46,238944	10,602889	2175,00
PRS 6	LaDe	46,239111	10,603333	2169,00
PRS 7	LaDe	46,241306	10,601500	2150,00
PRS 9	LaDe	46,241722	10,601583	2145,00
PRS 12	LaDe	46,242528	10,601278	2150,00
PRS 10	LaDe			
PRS 8	LaDe			
PRS 11	LaDe			
PRS 13	LaDe			

Tab. II-5 Val Presena. List of samples.

CODE	SITE	SPECIES	First ring date	Last ring date	BARK	PITH	RINGS
1	Val Presanella	LaDe	1568	1998	N	Y	431
2	Val Presanella	LaDe	1600	2004	N	Y	405
10	Val Presanella	LaDe	1723	1866	N	Y	164
13	Val Presanella	LaDe	1555	1963	N	Y	409
20	Val Presanella	LaDe	1597	2004	N	Y	408

CODE	SITE	SPECIES	First ring date	Last ring date	BARK	PITH	RINGS
21	Val Presanella	LaDe	1594	1999	N	Y	404
22	Val Presanella	LaDe	1603	2005	N	Y	403
16	Val Presanella-Tresati	LaDe	1741	1957	N	Y	217
17	Val Presanella	LaDe	1697	1982	N	Y	264
1071116.07	Val Presanella	LaDe	1738	1970	N	Y	233
1071116.08	Val Presanella	LaDe	1736	1983	N	Y	248
1071116.01	Coren di Boai	LaDe	1756	1984	N	Y	229
1071116.02	Coren di Boai	LaDe	1757	1979	N	Y	223
1071116.03	Coren di Boai	LaDe	1797	2007	Y	Y	211
1071116.04	Coren di Boai	LaDe	1797	2007	Y	Y	211
1071116.05	Val Presanella-Carbonere1	LaDe	X	X	N	Y	
1071116.06	Val Presanella-Carbonere2	LaDe	1832	2007	Y	Y	175
3	Val Presena	LaDe	X	X	N	Y	255
4	Val Presena	LaDe	1537	1914	N	Y	346
6	Val Presena	LaDe	?1710	?1916	N	Y	207
7	Val Presena	LaDe	?1712	?1875	N	Y	165
12	Val Presena	LaDe	X	X	N	N	396
18	Passo Cercen	LaDe	?1656	?1805	N	Y	150

Tab. II-6 List of samples coming from uprooted trees

Index of figures

Index of tables

Aknowledgements

At the end of this intense period of study my gratitude goes especially to my supervisor, Prof. Carlo Baroni, for constantly supporting and encouraging me in all phases of this research.

For his scientific support I wish to thank Dott. Giovani Leonelli, his valuable suggestions about data elaboration and his assistance during the writing of the manuscript have been crucial for the conclusion of this work.

I wish to express my gratitude to Prof. Maria Cristina Salvatore for the decisive support given during sampling field trips and for the realization of the GIS database.

My gratitude goes also to Dott.Maria Cleofe Stefanini for tree sampling in Val Presanella and in Val Presena and for introducing me to this fascinating Science.

I am also grateful to Dr. Gino Delpero for his help in tree sampling and for providing a part of the samples used in this project, and to Dr. Franco Angeli, responsible of the "Ufficio Forestale" of Malè (Trento).

I am very grateful to Prof. Manuela Pelfini and Prof. Alberto Carton for accepting to review this work contributing to improve the quality of the manuscript.

To my family and to my friends with two and four legs my eternal love and gratitude.